frontiers | Research Topics

Bone and joint infection: Past, present, and future

Edited by
Hongyi Shao, Guoli Hu, Chaofan Zhang and Chi Xu

Published in
Frontiers in Cellular and Infection Microbiology

ISSN 1664-8714
ISBN 978-2-8325-4745-8
DOI 10.3389/978-2-8325-4745-8

About Frontiers

Frontiers is more than just an open access publisher of scholarly articles: it is a pioneering approach to the world of academia, radically improving the way scholarly research is managed. The grand vision of Frontiers is a world where all people have an equal opportunity to seek, share and generate knowledge. Frontiers provides immediate and permanent online open access to all its publications, but this alone is not enough to realize our grand goals.

Frontiers journal series

The Frontiers journal series is a multi-tier and interdisciplinary set of open-access, online journals, promising a paradigm shift from the current review, selection and dissemination processes in academic publishing. All Frontiers journals are driven by researchers for researchers; therefore, they constitute a service to the scholarly community. At the same time, the *Frontiers journal series* operates on a revolutionary invention, the tiered publishing system, initially addressing specific communities of scholars, and gradually climbing up to broader public understanding, thus serving the interests of the lay society, too.

Dedication to quality

Each Frontiers article is a landmark of the highest quality, thanks to genuinely collaborative interactions between authors and review editors, who include some of the world's best academicians. Research must be certified by peers before entering a stream of knowledge that may eventually reach the public - and shape society; therefore, Frontiers only applies the most rigorous and unbiased reviews. Frontiers revolutionizes research publishing by freely delivering the most outstanding research, evaluated with no bias from both the academic and social point of view. By applying the most advanced information technologies, Frontiers is catapulting scholarly publishing into a new generation.

What are Frontiers Research Topics?

Frontiers Research Topics are very popular trademarks of the *Frontiers journals series*: they are collections of at least ten articles, all centered on a particular subject. With their unique mix of varied contributions from Original Research to Review Articles, Frontiers Research Topics unify the most influential researchers, the latest key findings and historical advances in a hot research area.

Find out more on how to host your own Frontiers Research Topic or contribute to one as an author by contacting the Frontiers editorial office: frontiersin.org/about/contact

Bone and joint infection: Past, present, and future

Topic editors

Hongyi Shao — Beijing Jishuitan Hospital, China

Guoli Hu — University of Texas Southwestern Medical Center, United States

Chaofan Zhang — First Affiliated Hospital of Fujian Medical University, China

Chi Xu — Department of Orthopaedics, Chinese PLA General Hospital, China

Citation

Shao, H., Hu, G., Zhang, C., Xu, C., eds. (2024). *Bone and joint infection: Past, present, and future*. Lausanne: Frontiers Media SA. doi: 10.3389/978-2-8325-4745-8

Table of contents

frontiers | Frontiers in Cellular and Infection Microbiology

TYPE Original Research
PUBLISHED 21 April 2023
DOI 10.3389/fcimb.2023.1182778

OPEN ACCESS

EDITED BY
Chaofan Zhang,
First Affiliated Hospital of Fujian Medical University, China

REVIEWED BY
Jianlin Xiao,
Department of Orthopaedics, Jilin University, China
Shuangfei Ni,
First Affiliated Hospital of Zhengzhou University, China

*CORRESPONDENCE
Yipeng Wang
ypwang@126.vip.com

SPECIALTY SECTION
This article was submitted to Clinical Microbiology, a section of the journal Frontiers in Cellular and Infection Microbiology

RECEIVED 09 March 2023
ACCEPTED 03 April 2023
PUBLISHED 21 April 2023

CITATION
Niu T, Zhang Y, Li Z, Bian Y, Zhang J and Wang Y (2023) The association between penicillin allergy and surgical site infection after orthopedic surgeries: a retrospective cohort study. *Front. Cell. Infect. Microbiol.* 13:1182778. doi: 10.3389/fcimb.2023.1182778

The association between penicillin allergy and surgical site infection after orthopedic surgeries: a retrospective cohort study

Tong Niu[1], Yuelun Zhang[2], Ziquan Li[1], Yanyan Bian[1], Jianguo Zhang[1] and Yipeng Wang[1]*

[1]Department of Orthopedics, Peking Union Medical College Hospital, Peking Union Medical College and Chinese Academy of Medical Sciences, Beijing, China, [2]Medical Research Centre, Peking Union Medical College Hospital, Peking Union Medical College and Chinese Academy of Medical Sciences, Beijing, China

Background: Cephalosporins are used as first-line antimicrobial prophylaxis for orthopedics surgeries. However, alternative antibiotics are usually used in the presence of penicillin allergy (PA), which might increase the risk of surgical site infection (SSI). This study aimed to analyze the relationship between SSI after orthopedic surgeries and PA among surgical candidates and related alternative antibiotic use.

Methods: In this single-center retrospective cohort study, we compared inpatients with and without PA from January 2015 to December 2021. The primary outcome was SSI, and the secondary outcomes were SSI sites and perioperative antibiotic use. Moreover, pathogen characteristics of all SSIs were also compared between the two cohorts.

Results: Among the 20,022 inpatient records, 1704 (8.51%) were identified with PA, and a total of 111 (0.55%) SSI incidents were reported. Compared to patients without PA, patients with PA had higher postoperative SSI risk (1.06%, 18/1704 vs. 0.51%, 93/18318), shown both in multivariable regression analysis (odds ratio [OR] 2.11; 95% confidence interval [CI], 1.26-3.50; p= 0.004) and propensity score matching (OR 1.84; 95% CI, 1.05-3.23; p= 0.034). PA was related to elevated deep SSI risk (OR 2.79; 95% CI, 1.47-5.30; p= 0.002) and had no significant impact on superficial SSI (OR 1.39; 95% CI, 0.59-3.29; p= 0.449). The PA group used significantly more alternative antibiotics. Complete mediation effect of alternative antibiotics on SSI among these patients was found in mediation analysis. Pathogen analysis revealed gram-positive cocci as the most common pathogen for SSI in our study cohort, while patients with PA had higher infection rate from gram-positive rods and gram-negative rods than non-PA group.

Conclusion: Compared to patients without PA, patients with PA developed more SSI after orthopedic surgeries, especially deep SSI. The elevated infection rate could be secondary to the use of alternative prophylactic antibiotics

KEYWORDS

alternative antibiotics, antimicrobial prophylaxis, orthopedics, penicillin allergy, surgical site infection

1 Introduction

Surgical site infection (SSI) is among the most lethal surgical complications both for surgeons and patients, leading to elevated postoperative morbidity and mortality rate (Beam and Osmon, 2018; Dagneaux et al., 2021; Sarfani et al., 2022). SSI is multifactorial, relating to patients' age, diabetic state, nutrition status, smoking history, etc. (Ban et al., 2017), and usually requires long-term antibiotics or even secondary operation. The SSI after orthopedic surgeries could be more complicated in nature as patients are usually older in age, with more comorbidities, and receive more surgeries with internal fixation/prosthesis implantation. A study published in 2014 showed an average of $11,876 increased cost within 30 postoperative days if the patient developed SSI. This additional cost would further rise to $15,243 for orthopedic patients, only secondary to that of the neurosurgical patients (Schweizer et al., 2014), making SSI a study focus in this field.

Reducing SSI requires multi-dimensional modalities. Surgical Care Improvement Project recommended appropriate antimicrobial prophylaxis (AMP), serum glucose control, proper skin preparation, early removal of foley tubes, and intraoperative body temperature control as key measures to reduce SSI (Rosenberger et al., 2011). The use of AMP is crucial and its efficacy has been proved in many studies. First- or second-generation cephalosporins are recommended as first-line AMP by most guidelines due to satisfying cost-effectiveness. For patients with penicillin allergy (PA), vancomycin and clindamycin are usually recommended as alternatives (Bratzler et al., 2013; Martin et al., 2019). Moreover, vancomycin is also considered for patients with methicillin-resistant Staphylococcus aureus (MRSA) colonization (Goyal et al., 2013; Wyles et al., 2019).

The efficacy of alternative antibiotic prophylaxis is still debatable compared to that of first-line cephalosporins. Studies showed elevated risk for adverse outcomes and various complications (Jeffres et al., 2016; MacFadden et al., 2016; Huang et al., 2018; Kaminsky et al., 2022), including SSI for surgical candidates (Blumenthal et al., 2018). Most of the relevant orthopedic studies analyzed patients after joint procedures with controversial outcomes (Ponce et al., 2014; Tan et al., 2016; Wyles et al., 2019). The impact of having PA is not otherwise reported in the literature regarding spine, trauma, or bone tumor surgeries. Moreover, the pathogenic differences have not been elucidated based on the presence of PA. Therefore, we performed a comprehensive analysis on PA and SSI based on the orthopedic patients in our center.

2 Method

2.1 Study population and inclusion criteria

This is a single-center retrospective cohort study. After obtaining approval from the Institutional Review Board in our center (Protocol number: K0385), we performed analysis on patients admitted to the orthopedics department in Peking Union Medical Collage Hospital during 1st January 2015 and 31st December 2021. All data was extracted from the Big Data Query and Analysis System in our hospital. Patients with existing history of penicillin allergy were included as the PA group, defined as penicillin allergy in medical records, regardless of the phenotype (i.e. self-reported allergy, positive penicillin skin testing, hypersensitivity reactions, etc.), with patients without penicillin allergy as the control group. The exclusion criteria included: 1) preoperative history of local or systemic infection; 2) admission due to open trauma; 3) postoperative infection from previous surgery in other centers; 4) delayed surgical site infection; 5) lack of antimicrobial prophylaxis preoperatively.

2.2 Perioperative protocol

In patients without PA, cefuroxime was the first-line antibiotics administered preoperatively at a dose of 1.5g intravenously 60 minutes before skin incision. In patients with PA, vancomycin or clindamycin were the preferred alternative antibiotic choice (vancomycin: 30mg/kg i.v. 120 minutes before skin incision, and clindamycin: 0.6-0.9g i.v. 60 minutes before skin incision, respectively). All patients received standardized perioperative infection prevention measures besides AMP, including but not limited to: hand hygiene, skin antiseptics, laminar airflow, maintaining normothermia, glucose control, etc.

2.3 Study outcomes

The primary outcome of this study was SSI after orthopedic surgeries. We first identified potential SSI based on following features: infection-related diagnosis, positive pathogen cultures, any debridement surgery, and any non-scheduled secondary surgery within 180 postoperative days. After thorough examination of their medical records, the diagnosis of SSI was established based on the 2021 CDC-NHSN criteria. The secondary outcomes of this study were the deep SSI, superficial SSI, and the AMP regimens between the two groups. Lastly, we described the common pathogens found in our SSI patients.

The primary exposure variable in this study was the presence of penicillin allergy. Based on literature review, the following SSI-related confounding factors were collected: 1) patient factors: age, hypertension, diabetes, hyperlipidemia/hypercholesterolemia, smoking history, alcohol intake, and American society of Anesthesiologists (ASA) class; 2) surgical factors: surgical history of the same site, emergency surgery, long operation duration (>3 hours), internal fixation, and implantation of joint prosthesis.

Eight orthopedic surgery types were included in this study: spine, joint replacement, trauma, arthroscopy, bone tumor, foot and ankle, hand surgery, and other surgeries (core decompression, limb deformity correction, and amputation, etc.).

2.4 Statistical analysis

Normally distributed quantitative data were presented as mean ± standard error, quantitative data without normal distribution were presented as quartiles, and count data were shown as numbers and its proportions [N, (%)]. Absolute standardized difference was used to compare the baseline characteristics, and <0.1 was considered to be balanced. Levene test was used to test for equal variance. For primary outcome, we utilized logistic regression and propensity score (PS) analysis to evaluate the correlation between PA and orthopedic SSI. Four models were used in the regression analysis: Model 1) univariable analysis; Model 2) incorporating confounding patient factors into the regression model; Model 3) incorporating confounding surgical factors into the regression model; and Model 4) including all confounding factors into the regression. SPSS PS matching tool (Version 3.04) was used for PS analysis to match patients with and without PA in a 1:4 ratio, with a caliper width of 0.1. All confounding factors were included into the propensity score matching (PSM) as covariates. In the regression analysis model, the ASA score was dichotomized as ≤ Class II and >Class II, and operation duration as >3h and ≤3h.

We performed mediation analysis using bootstrap methods based on both Model 4 and PSM Model to evaluate if the correlation between PA and SSI was mediated by the choice of AMP regimens. AMP regimens were further divided into cephalosporin and non-cephalosporin ones to see the potential mediation effect of the latter in the statistical analysis.

Statistical analysis was completed on SPSS 23.0, and a two-sided p-value < 0.05 was considered as statistically significant.

3 Results

3.1 Patient characteristics

From January 2015 to December 2021, a total of 26730 surgical admission records were identified, and 20022 records met our inclusion criteria (Figure 1). Among them, 1704 records were with PA (8.51%, 1704/20022). Patients in PA group were generally older in age, predominantly female, and with less smoking history and alcohol intake. The patients in PA group also had higher prevalence of multiple comorbidities and higher ASA classes compared to non-PA group. Differences were also found in surgery types and the percentage of secondary surgery. After PS Matching, the baseline characteristics were balanced between the two groups (Table 1).

3.2 Primary outcome

3.2.1 Correlation between PA and orthopedic SSI

A total of 111 (0.55%) SSI were identified after 20022 operations, 18 (1.05%) after 1704 operations in PA group, and 93 (0.51%) after 18,318 operations in the control group. Correlation between PA and orthopedic SSI was seen in both univariable analysis (OR 2.09; 95%CI, 1.26-3.47; p= .004) and multivariable logistic regression after including all confounding factors (OR 2.11; 95% CI, 1.26-3.50; p=0.004) (Table 2).

After performing PSM, a total of 6786 surgical records were matched to the 1,704 records in PA group. Similarly, 39 (0.57%) SSI were found in the matched control group, compared to 18 (1.05%) in the PA group. The potential confounding factors were distributed evenly in the PA and control group after PSM. Regression analysis still showed correlation between PA and SSI (OR 1.84; 95% CI, 1.05-3.23; p= 0.034).

Mediation analysis based on Model 4 revealed no statistical significance in the direct effect of PA on SSI incidence (OR -0.002; 95% CI -0.008-0.003 p= 0.330), but elevated OR in the indirect effect of AMP choice (OR 0.008; 95% CI, 0.004-0.012; p= 0.002). Meantime, mediation analysis based on PSM Model also revealed no statistical significance in the direct effect of PA on SSI incidence (OR -0.004; 95% CI -0.011-0.003 p= 0.264), but elevated OR in the indirect effect of AMP choice (OR 0.009; 95% CI, 0.004-0.015; p<

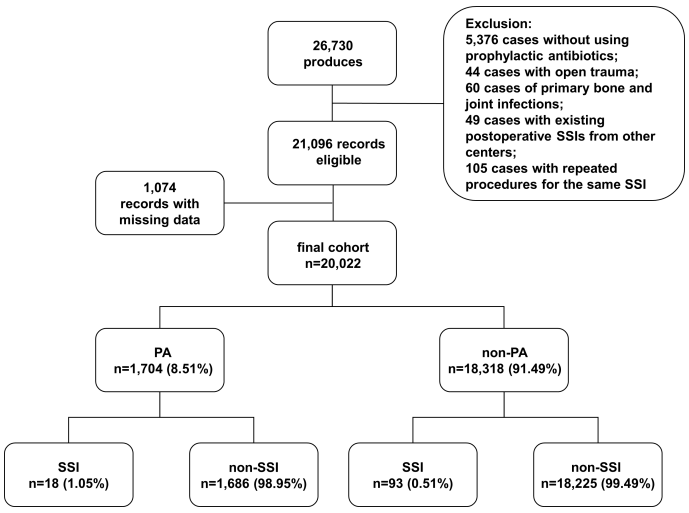

FIGURE 1
Flow diagram shows the study cohorts.

10.3389/fcimb.2023.1182778

TABLE 1 Baseline Characteristics before and after propensity score matching.

Characteristic	Before Matching			After Matching		
	Penicillin Allergy Group (n=1704)	Non-Penicillin Allergy Group (n=18318)	Standardized Difference	Penicillin Allergy Group (n=1704)	Non-Penicillin Allergy Group (n=6786)	Standardized Difference
Age	56.3 (19.8)	50.6 (21.8)	0.274	56.3 (19.8)	56.3 (20.1)	0.000
Sex (Female)	1251 (73.4)	10855 (59.3)	0.302	1251 (73.4)	4945 (72.9)	0.011
Hypertension	689 (40.4)	5542(30.3)	0.212	689 (40.4)	2762 (40.7)	0.006
Diabetes	235 (13.8)	1973 (10.8)	0.091	235 (13.8)	942 (13.9)	0.003
Hyperlipidemia	108(6.3)	737 (4.0)	0.104	108(6.3)	431 (6.4)	0.004
Smoking	218(12.8)	2914 (15.9)	0.089	218(12.8)	804 (11.8)	0.032
Alcohol intake	21 (1.2)	488 (2.7)	0.108	21 (1.2)	138 (2.0)	0.064
ASA Class						
1	310 (18.2)	4781 (26.1)	0.191	310 (18.2)	1372 (20.2)	0.051
2	1148 (67.4)	11706 (63.9)	0.074	1148 (67.4)	4450 (65.6)	0.038
3	244 (14.3)	1794 (9.8)	0.138	244 (14.3)	948 (14.0)	0.009
4	2 (0.1)	37 (0.2)	0.026	2 (0.1)	15 (0.2)	0.082
Surgery type						
Spine	753 (44.2)	9397 (51.3)	0.065	753 (44.2)	2942 (43.3)	0.018
Joint replacement	526 (30.9)	4557 (24.9)	0.127	526 (30.9)	2046 (30.2)	0.011
Trauma	190 (11.2)	2016 (11.0)	0.006	190 (11.2)	896 (13.2)	0.058
Arthroscopy	73 (4.3)	662 (3.6)	0.036	73 (4.3)	275 (4.1)	0.010
Bone tumor	70 (4.1)	902 (4.9)	0.044	70 (4.1)	315 (4.6)	0.030
Foot and ankle	67 (3.9)	582 (3.2)	0.043	67 (3.9)	235 (3.5)	0.026
Hand	16 (0.9)	104 (0.6)	0.035	16 (0.9)	42 (0.6)	0.035
Others	9 (0.5)	98 (0.5)	0.000	9 (0.5)	34 (0.5)	0.000
Multiple surgical history of the same site	53 (3.1)	457 (2.5)	0.036	53 (3.1)	204 (3.0)	0.006
Emergency surgery	17 (1.0)	170 (0.9)	0.010	17 (1.0)	66 (1.0)	0.000
Internal fixation/joint prosthesis	1507 (88.4)	16005 (87.4)	0.031	1507 (88.4)	5965 (87.9)	0.015
Operation duration>3h	434 (25.5)	5639 (30.8)	0.118	434 (25.5)	1714 (25.3)	0.005

0.001). Therefore, using non-cephalosporins as AMP has complete mediation effect on elevated SSI rate in PA patients.

3.3 Secondary outcomes

3.3.1 Correlation between PA and SSI type

We then performed analysis on deep and superficial infections. Among the 20022 operations included, there were 52 (0.26%) superficial SSI, 6 (0.35%) in PA group, and 46 (0.25%) in non-PA group. Uni- and multi-variable analysis both demonstrated no relationship between PA and superficial SSI (OR 1.44; 95%Cl, 0.61-3.37; p= 0.404; adjusted OR 1.39; 95% CI, 0.59-3.29; p= 0.449).

Among the 59 (0.29%) deep SSI in our cohort, 12 (0.71%) were in PA group, and 47 (0.26%) in control group. Strong correlation between PA and deep SSI after orthopedic surgeries was seen both in univariable analysis (OR 2.70; 95%Cl, 1.43-5.09; p= 0.001) and multi-variable logistic regression with all confounders incorporated (OR 2.79; 95% CI, 1.47-5.30; p= 0.002).

3.3.2 Preoperative AMP regimens

Cefuroxime was the most commonly prescribed AMP in our cohort (n=17562, 87.71%), followed by clindamycin (n=2376, 11.87%). Patients with PA used significantly less cefuroxime (12.61%, 215/1704 vs. 94.69%, 17347/18318; p< 0.001), and more clindamycin (85.79%, 1462/1704 vs. 4.98%, 914/18318; p< 0.001)

TABLE 2 Logistic regression and propensity score analysis of the association between penicillin allergy and orthopedics surgical site infection.

Logistic regression models (n=20022)	OR	95% CI	p-value
Model 1 (Unadjusted)	2.09	1.26-3.47	0.004
Model 2 (patient-related confounders adjusted)	2.06	1.23-3.43	0.006
Model 3 (surgery-related confounders adjusted)	2.13	1.28-3.55	0.003
Model 4 (fully adjusted)	2.11	1.26-3.50	0.004
Propensity score analysis (n=8490)			
PS matching	1.84	1.05-3.23	0.034

OR, odds ratio; CI, confidence interval; PS, propensity score.
Model 1 was a univariable crude model;
Model 2 included age, hypertension, diabetes mellitus, hyperlipidemia, smoking history, drinking history, ASA classification;
Model 3 included multiple surgical history of the same site, emergency surgery, operation duration>3h, implantation-related surgery;
Model 4 includes all the above confounders.

and quinolones (1.23%, 21/1704 vs. 0.15%, 27/18318; p< 0.001). Due to limited sample size, other alternative antibiotics, including vancomycin, were not further analyzed (Figure 2).

3.4 Pathogen characteristics

Among the 111 SSI found in our study, 69 (62.16%) was caused by single-pathogen infection, 9 (8.11%) by multi-pathogen infection, and 33 (29.73%) had negative culture. Gram-positive cocci (GPC) were the leading pathogen for SSI, accounting for 69 (88.46%) cases among the 78 positive cultures. Gram-negative rods (GNR) and Gram-positive rods (GPR) accounted for 15 (19.23%) and 6 (7.69%) infections, respectively. Fungal and actinomycotic infection were found in 3 (3.85%) cases. Patients with and without PA had different pathogen profiles for deep SSI. Though GPC remained to be most commonly seen in deep SSI, patients with PA had higher infection rate from GPR and GNR than non-PA group (Figure 3).

4 Discussion

In this cohort study that included 20,022 patients undergoing various orthopedic surgeries, we found a higher proportion of postoperative SSI among patients with PA. Mediation analysis demonstrated possible effect of alternative antibiotic use on the SSI among PA patients. While previous studies mainly focused on arthroplasty, ours covers the spectrum of spine, joint, trauma, arthroscopy, bone tumor, foot and ankle, and hand surgeries. Our result suggests that the impact of having PA on SSI exists for various orthopedic procedures.

We also advanced our study by performing further analysis on infection type and pathogens. In our study, the influence of PA mainly caused increase in deep SSI instead of superficial SSI. This could be related to a higher proportion of internal fixation among orthopedic patients, where it inevitably affects peripheral blood supply, and the disadvantages of using alternative antibiotics would be magnified when dealing with microbes adhering to deep tissue or fixation device. Previous study reported higher SSI after alternative

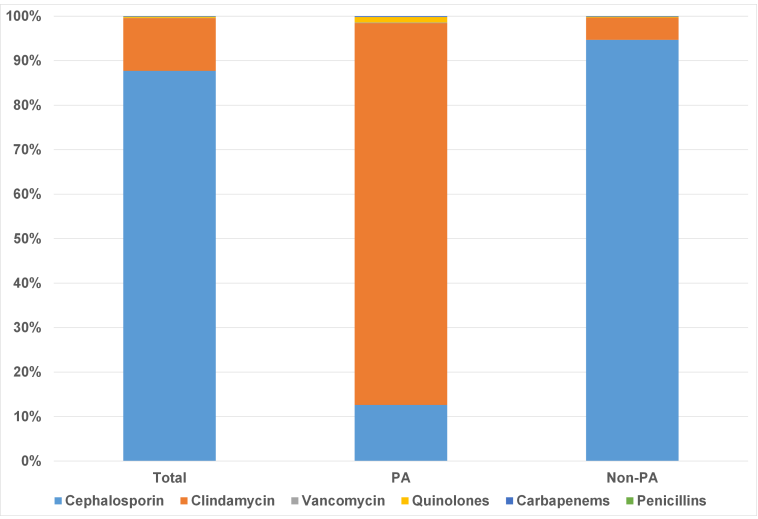

FIGURE 2
Preoperative prophylactic antibiotic regimens in patients with and without penicillin allergy.

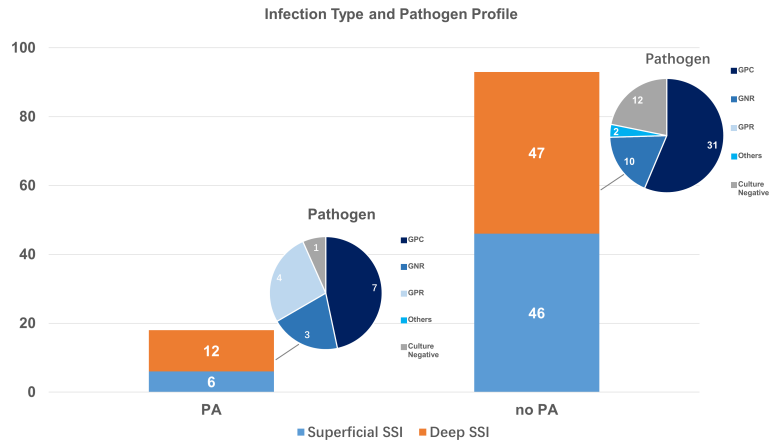

FIGURE 3
Pathogen profile of deep SSI in PA and Non-PA group.

vancomycin prophylaxis due to its narrow spectrum mainly against Gram-positive microbes (Kheir et al., 2017). Our PA cohort mainly used clindamycin as alternative antibiotics, which has a broader spectrum compared to vancomycin. But the resistance to clindamycin from Staphylococcus aureus and Cutibacterium acnes was reported to elevate in recent years (Achermann et al., 2014; Wang et al., 2021). Other GNRs may have inherent resistance by limiting permeability of clindamycin through outer membranes, like the families of Pseudomonas, Enterobacillus, and Acinetobacter (Leclercq and Courvalin, 1991). These pathogens were all common culprits for deep SSI in our PA cohort. Additionally, as a bacteriostatic antibiotic, clindamycin requires much higher concentration to be bactericidal (Spížek and Řezanka, 2004). Despite its comparable bacteriostatic outcome with bactericidal antibiotics in therapeutic use (Wald-Dickler et al., 2018), the role of clindamycin is still to be studied when used prophylactically.

Some previous studies reported correlation between elevated SSI risk and PA with alternative antibiotic use. A study by Blumenthal et al. (Blumenthal et al., 2018) enrolled 8,385 patients from obstetrics and gynecology, general surgery, and orthopedics departments and showed an 50% elevated risk of SSI in PA patients compared to general population due to the use of alternative antibiotics. Reports in orthopedics mainly focused on patients after arthroplasty. Ponce et al. (Ponce et al., 2014) analyzed more than 18,000 patients and concluded that patients on vancomycin AMP developed significantly more SSI than patients on cefazolin. Regarding the argument of under-dosing and untimely use of vancomycin, Kheir et al. (Kheir et al., 2017) launched a study on AMP use and still revealed an elevated SSI rate in vancomycin group than in cefazolin group despite timely and full-dose administration. Other studies, however, found no correlation between PA and SSI. A study by Tan et al. (Tan et al., 2016) analyzed 10,391 patients receiving joint replacement, and showed no difference in infection between patients with and without PA, as well as reduced MRSA infection rate in patients receiving vancomycin AMP. Another study on joint replacement by Stone et al. (Stone A. et al., 2019) demonstrated similar SSI rate after arthroplasty in patients with and without PA. But this study had limited statistical power with a small sample size of 5,000 patients, given a low SSI rate (0.6% in PA group and 0.4% in general population). This conclusion has also been derived in other surgical fields, for example after colorectal surgeries as described by Khan et al. (Khan et al., 2021). Despite controversy on the correlation, surgeons should still prioritize cephalosporins as AMP due to its cost-effectiveness and relatively definite prophylactic efficacy.

The prevalence of PA is reported to be 5-25% in general population (Li et al., 2019; Stone C. et al., 2019). Recent study showed a lower cross-reactivity rate between penicillin and cephalosporins than previously perceived, with limited cases of true IgE-mediated reaction (Shenoy et al., 2019). A meta-analysis on 6,001 patients from 30 studies calculated a mere 0.7% of cross-allergy rate in patients who received cephalosporins despite their PA (Sousa-Pinto et al., 2021). Based on this result, multiple efforts have been developed to rule out unreliable PA labels, mainly through skin tests or provocation tests. But for surgical candidates, skin test and oral provocation could inevitably prolong hospital stay and incur medical costs, and our end goal here is simply safe administration of cephalosporins. Based on this clinical demand, Kuruvilla et al. (Kuruvilla et al., 2020) developed a streamlined history-based screening stratification without potential anaphylactic exposure to increase the cephalosporin use, and successfully resulted in 80% use among PA patients. Compared with additional or repeated skin testing, history-based screening might be more friendly for surgical departments to adopt to safeguard the use of β-lactam antibiotics.

There are several limitations to our study. First, around 5% of all admission records were excluded from this study due to missing data (mainly the ASA classification and operation time) of unknown mechanism. We did not compensate by filling in the missing data, which could result in impaired statistical power. Notably, however, the missing data was equally distributed in two groups and we had relatively large sample size. Hence the missing data should not cause deviation to the conclusion. Second, subgroup analysis was not

performed based on different surgical types due to low SSI rate in our cohort. Studies focusing on different orthopedic surgical types and their SSI relation to PA history are warranted in the future. Third, as SSI is multi-factorial, the retrospective design of this study cannot incorporate all SSI-related confounding factors, for example the use of corticosteroids, immunosuppressants, or the presence of neoplasia, to exclude their influence on the result. Additionally, we were not able to obtain detailed labeling information due to limited database to perform subgroup analysis on the relationship between PA types and SSIs. Study of this kind could be further carried on in the future. The definition of our choice is based on clinical practice, where surgeons would predominantly base their antibiotic choice on the existence of previous PA labels, regardless of specific types. Therefore PA subtype variance should have little impact on the conclusion of our study. Moreover, the baseline characteristics were not fully balanced in this cohort study. To reduce the impact of this limitation, we have used 4 logistic regression models to include categorized patient factors and surgical factors separately into the analysis, and used PSM to further reduce the confounding effects. Therefore, prospective study of high quality is in need to further validate this conclusion.

5 Conclusion

In this study, we found an elevated SSI risk in patients with PA when compared to those without, especially deep SSI. This could potentially be related to the alternative antibiotics used in this population instead of cephalosporins. Based on the low incidence of cross-reactivity between penicillin and cephalosporins reported and the observed safety of using cephalosporins in patients with PA, we recommend detailed history-taking and skin tests when necessary, to remove inappropriate PA label and to reduce SSI risk.

Data availability statement

The raw data supporting the conclusions of this article will be made available by the authors, without undue reservation.

Ethics statement

The studies involving human participants were reviewed and approved by Peking Union Medical College Hospital Institutional Review Board. Written informed consent for participation was not required for this study in accordance with the national legislation and the institutional requirements.

Author contributions

TN, JZ, and YW contributed to conception and design of the study. TN, YB, and ZL collected the related data and wrote the manuscript. TN, YZ, and ZL analyzed the data. All authors contributed to the article and approved the submitted version.

Funding

This study was supported by the National Natural Science Foundation of China (82172517).

Conflict of interest

The authors declare that the research was conducted in the absence of any commercial or financial relationships that could be construed as a potential conflict of interest.

Publisher's note

References

Achermann, Y., Goldstein, E. J. C., Coenye, T., and Shirtliff, M. E. (2014). Propionibacterium acnes: from commensal to opportunistic biofilm-associated implant pathogen. *Clin. Microbiol. Rev.* 27 (3), 419–440. doi: 10.1128/CMR.00092-13

Ban, K. A., Minei, J. P., Laronga, C., Harbrecht, B. G., Jensen, E. H., Fry, D. E., et al. (2017). American College of surgeons and surgical infection society: surgical site infection guidelines 2016 update. *J. Am. Coll. Surg.* 224 (1), 59–74. doi: 10.1016/j.jamcollsurg.2016.10.029

Beam, E., and Osmon, D. (2018). Prosthetic joint infection update. *Infect. Dis. Clinics North America* 32 (4), 843–859. doi: 10.1016/j.idc.2018.06.005

Blumenthal, K. G., Ryan, E. E., Li, Y., Lee, H., Kuhlen, J. L., and Shenoy, E. S. (2018). The impact of a reported penicillin allergy on surgical site infection risk. *Clin. Infect. Dis.* 66 (3), 329–336. doi: 10.1093/cid/cix794

Bratzler, D. W., Dellinger, E. P., Olsen, K. M., Perl, T. M., Auwaerter, P. G., Bolon, M. K., et al. (2013). Clinical practice guidelines for antimicrobial prophylaxis in surgery. *Am. J. Health Syst. Pharm.* 70 (3), 195–283. doi: 10.2146/ajhp120568

Dagneaux, L., Limberg, A. K., Osmon, D. R., Leung, N., Berry, D. J., and Abdel, M. P. (2021). Acute kidney injury when treating periprosthetic joint infections after total knee arthroplasties with antibiotic-loaded spacers. *J. Bone Joint Surg.* 103 (9), 754–760. doi: 10.2106/JBJS.20.01825

Goyal, N., Miller, A., Tripathi, M., and Parvizi, J. (2013). Methicillin-resistant staphylococcus aureus (MRSA): colonisation and pre-operative screening. *Bone Joint J.* 95-B (1), 4–9. doi: 10.1302/0301-620X.95B1.27973

Huang, K. G., Cluzet, V., Hamilton, K., and Fadugba, O. (2018). The impact of reported beta-lactam allergy in hospitalized patients with hematologic malignancies requiring antibiotics. *Clin. Infect. Dis.* 67 (1), 27–33. doi: 10.1093/cid/ciy037

Jeffres, M. N., Narayanan, P. P., Shuster, J. E., and Schramm, G. E. (2016). Consequences of avoiding beta-lactams in patients with beta-lactam allergies. *J. Allergy Clin. Immunol.* 137 (4), 1148–1153. doi: 10.1016/j.jaci.2015.10.026

Kaminsky, L. W., Ghahramani, A., Hussein, R., and Al-Shaikhly, T. (2022). Penicillin allergy label is associated with worse clinical outcomes in bacterial pneumonia. *J. Allergy Clin. Immunology: In Pract.* 10 (12), 3262–3269. doi: 10.1016/j.jaip.2022.08.027

Khan, A., Wolford, D., Ogola, G., Thompson, R., Daher, P., Stringfield, S. B., et al (2021). Impact of patient-reported penicillin allergy on antibiotic prophylaxis and

surgical site infection among colorectal surgery patients. *Dis. Colon Rectum*. 65 (11), 1397–1404. doi: 10.1097/DCR.0000000000002190

Kheir, M. M., Tan, T. L., Azboy, I., Tan, D. D., and Parvizi, J. (2017). Vancomycin prophylaxis for total joint arthroplasty: incorrectly dosed and has a higher rate of periprosthetic infection than cefazolin. *Clin. Orthopaedics Related Res.* 475 (7), 1767–1774. doi: 10.1007/s11999-017-5302-0

Kuruvilla, M., Sexton, M., Wiley, Z., Langfitt, T., Lynde, G. C., and Wolf, F. (2020). A streamlined approach to optimize perioperative antibiotic prophylaxis in the setting of penicillin allergy labels. *J. Allergy Clin. Immunology: In Pract.* 8 (4), 1316–1322. doi: 10.1016/j.jaip.2019.12.016

Leclercq, R., and Courvalin, P. (1991). Intrinsic and unusual resistance to macrolide, lincosamide, and streptogramin antibiotics in bacteria. *Antimicrob. Agents Chemother.* 35 (7), 1273–1276. doi: 10.1128/AAC.35.7.1273

Li, P. H., Siew, L. Q. C., Thomas, I., Watts, T. J., Ue, K. L., Rutkowski, K., et al. (2019). Beta-lactam allergy in Chinese patients and factors predicting genuine allergy. *World Allergy Organ. J.* 12 (8), 100048. doi: 10.1016/j.waojou.2019.100048

MacFadden, D. R., LaDelfa, A., Leen, J., Gold, W. L., Daneman, N., Weber, E., et al. (2016). Impact of reported beta-lactam allergy on inpatient outcomes: a multicenter prospective cohort study. *Clin. Infect. Dis.* 63 (7), 904–910. doi: 10.1093/cid/ciw462

Martin, C., Auboyer, C., Boisson, M., Dupont, H., Gauzit, R., Kitzis, M., et al. (2019). Antibioprophylaxis in surgery and interventional medicine (adult patients). update 2017. *Anaesth Crit. Care Pain Med.* 38 (5), 549–562. doi: 10.1016/j.accpm.2019.02.017

Ponce, B., Raines, B. T., Reed, R. D., Vick, C., Richman, J., and Hawn, M. (2014). Surgical site infection after arthroplasty: comparative effectiveness of prophylactic antibiotics. *J. Bone Joint Surg.* 96 (12), 970–977. doi: 10.2106/JBJS.M.00663

Rosenberger, L. H., Politano, A. D., and Sawyer, R. G. (2011). The surgical care improvement project and prevention of post-operative infection, including surgical site infection. *Surg. Infec* 12 (3), 163–168. doi: 10.1089/sur.2010.083

Sarfani, S., Stone, C. A., Murphy, G. A., and Richardson, D. R. (2022). Understanding penicillin allergy, cross-reactivity, and antibiotic selection in the preoperative setting. *J. Am. Acad. Orthopaedic Surgeons* 30 (1), e1–e5. doi: 10.5435/JAAOS-D-21-00422

Schweizer, M. L., Cullen, J. J., Perencevich, E. N., and Vaughan Sarrazin, M. S. (2014). Costs associated with surgical site infections in veterans affairs hospitals. *JAMA Surg.* 149 (6), 575. doi: 10.1001/jamasurg.2013.4663

Shenoy, E. S., Macy, E., Rowe, T., and Blumenthal, K. G. (2019). Evaluation and management of penicillin allergy. *JAMA* 321 (2), 188. doi: 10.1001/jama.2018.19283

Sousa-Pinto, B., Blumenthal, K. G., Courtney, L., Mancini, C. M., and Jeffres, M. N. (2021). Assessment of the frequency of dual allergy to penicillins and cefazolin. *JAMA Surg.* 156 (4), e210021. doi: 10.1001/jamasurg.2021.0021

Spížek, J., and Řezanka, T. (2004). Lincomycin, clindamycin and their applications. *Appl. Microbiol. Biotechnol.* 64 (4), 455–464. doi: 10.1007/s00253-003-1545-7

Stone, A. H., Kelmer, G., MacDonald, J. H., Clance, M. R., and King, P. J. (2019). The impact of patient-reported penicillin allergy on risk for surgical site infection in total joint arthroplasty. *J. Am. Acad. Orthopaedic Surgeons* 27 (22), 854–860. doi: 10.5435/JAAOS-D-18-00709

Stone, C. A., Trubiano, J., Coleman, D. T., Rukasin, C. R. F., and Phillips, E. J. (2019). The challenge of de-labeling penicillin allergy. *Allergy* 75 (2), 273–288. doi: 10.1111/all.13848

Tan, T. L., Springer, B. D., Ruder, J. A., Ruffolo, M. R., and Chen, A. F. (2016). Is vancomycin-only prophylaxis for patients with penicillin allergy associated with increased risk of infection after arthroplasty? *Clin. Orthopaedics Related Res.* 474 (7), 1601–1606. doi: 10.1007/s11999-015-4672-4

Wald-Dickler, N., Holtom, P., and Spellberg, B. (2018). Busting the myth of "Static vs cidal": a systemic literature review. *Clin. Infect. Dis.* 66 (9), 1470–1474. doi: 10.1093/cid/cix1127

Wang, H., Zhuang, H., Ji, S., Sun, L., Zhao, F., Wu, D., et al. (2021). Distribution of erm genes among MRSA isolates with resistance to clindamycin in a Chinese teaching hospital. *Infec Genet. Evol.* 96, 105127. doi: 10.1016/j.meegid.2021.105127

Wyles, C. C., Hevesi, M., Osmon, D. R., Park, M. A., Habermann, E. B., Lewallen, D. G., et al. (2019). 2019 John charnley award: increased risk of prosthetic joint infection following primary total knee and hip arthroplasty with the use of alternative antibiotics to cefazolin: the value of allergy testing for antibiotic prophylaxis. *Bone Joint J.* 101-B (6_Supple_B), 9–15. doi: 10.1302/0301-620X.101B6.BJJ-2018-1407.R1

frontiers | Frontiers in Cellular and Infection Microbiology

TYPE Original Research
PUBLISHED 28 April 2023
DOI 10.3389/fcimb.2023.1129072

OPEN ACCESS

EDITED BY
Hongyi Shao,
Beijing Jishuitan Hospital, China

REVIEWED BY
Denghui Xie,
Southern Medical University, China
Minwei Zhao,
Peking University Third Hospital, China

*CORRESPONDENCE
Ning Hu
huncqjoint@yeah.net
Wei Huang
huangwei68@263.net

†These authors have contributed equally to this work

RECEIVED 11 January 2023
ACCEPTED 18 April 2023
PUBLISHED 28 April 2023

CITATION
Qin L, Zhao C, Wang H, Yang J, Chen L, Su X, Wei L, Zhang T, Li J, Jian C, Hu N and Huang W (2023) Detection of inguinal lymph nodes is promising for the diagnosis of periprosthetic joint infection. *Front. Cell. Infect. Microbiol.* 13:1129072. doi: 10.3389/fcimb.2023.1129072

Detection of inguinal lymph nodes is promising for the diagnosis of periprosthetic joint infection

Leilei Qin[1,2†], Chen Zhao[1,2†], Hai Wang[1,3], Jianye Yang[1,2], Li Chen[1,2], Xudong Su[1,2], Li Wei[1,2], Tao Zhang[1,2], Jia Li[4], Changchun Jian[1,5], Ning Hu[1,2*] and Wei Huang[1,2*]

[1]Department of Orthopaedics, The First Affiliated Hospital of Chongqing Medical University, Chongqing, China, [2]Orthopedic Laboratory, Chongqing Medical University, Chongqing, China, [3]Department of Orthopaedics, Fuling Central Hospital Affiliated of Chongqing University, Chongqing, China, [4]Department of Radiology, The First Affiliated Hospital of Chongqing Medical University, Chongqing, China, [5]Department of Orthopedics, Affiliated Hospital of North Sichuan Medical College, Sichuan, China

Background: Localized inguinal lymphadenopathy often represents lower extremity pathogen infection, while normalized lymphadenopathy is associated with infection regression. We hypothesized that inguinal lymph nodes (LNs) were enlarged in Periprosthetic Joint Infection (PJI) patients and that normalized inguinal LNs would be a promising way to determine the timing of reimplantation.

Methods: We prospectively enrolled 176 patients undergoing primary and revision hip or knee arthroplasty. All patients underwent ultrasound examination of inguinal LNs preoperatively. The diagnostic value of inguinal LNs in PJI was evaluated by the receiver operating characteristic (ROC) curve.

Results: The median level of inguinal LNs was 26mm in the revision for PJI group compared with 12 mm in the aseptic revision group ($p< 0.0001$). The size of the inguinal LNs well distinguishes PJI from aseptic failure (AUC= 0.978) compare with ESR (AUC= 0.707) and CRP (AUC= 0.760). A size of 19mm was determined as the optimal threshold value of the inguinal LNs for the diagnosis of PJI, with a sensitivity of 92% and specificity of 96%.

Conclusion: Ultrasonic analysis of inguinal LNs is a valuable piece of evidence for the diagnosis of PJI and evaluation of persistent infection.

KEYWORDS

prosthetic joint infection, lymph nodes, lymphadenopathy, ultrasound, diagnosis

Introduction

Periprosthetic joint infection (PJI) after total joint arthroplasty is still one of the catastrophic complications that clinicians must overcome (Kurtz et al., 2012; Parvizi et al., 2018). Accurate diagnosis of PJI is related to the surgical method of prosthesis revision and the optimal timing of two-stage exchange arthroplasty. However, timely and accurate diagnosis of PJI remains a challenge, as PJI are often caused by low-virulence pathogens and are associated with mature prosthetic biofilms (Qin et al., 2020). Currently, the diagnosis of PJI relies on molecular biomarkers derived from serum and synovial fluid in addition to conventional etiological tests (Cheok et al., 2022; Goud et al., 2022). Meanwhile, with the development of molecular biology research, the application of some new technologies, such as fluorescence *in situ* hybridization and next-generation sequencing technology, has significantly reduced the difficulty of PJI diagnosis (Lippmann et al., 2019; Kildow et al., 2021). The use of novel biomarkers and specific testing techniques remains controversial, considering the availability of tests in different healthcare facilities and the cost-effectiveness of these tests. Therefore, it is a common goal of clinicians to find a noninvasive test with a high recognition effect for PJI.

The lymphatic system is part of the body's immune system. Of these, lymph nodes are accessory structures to the entire lymphatic system and play a crucial role in the body's ability to fight infection, acting as filters for foreign bodies such as cancer cells and infections (Zhang et al., 2021). The cells in the lymph nodes are lymphocytes, which produce antibodies (protein particles that bind to foreign substances, including infectious particles), and macrophages that digest debris, which act as the body's "cleaning" cells (Girard and Springer, 1995). Swollen lymph nodes usually occur as a result of infection from bacteria or viruses (Shimono et al., 2017). Among them, inguinal lymph nodes serve as guardians of lower limb immunity, and their pathological enlargement may indicate an infection in the lower body (Bui and Bordoni, 2022). Inguinal lymph nodes in asymptomatic patients have a mean short axis of 5.4 mm, usually no more than 10mm, and a short axis diameter greater than 15 mm is considered abnormal (Bontumasi et al., 2014). Notably, lymph nodes rapidly increase in size in response to infection in adjacent tissues and organs within 2 to 3 days and return to normal size within 2 to 4 weeks after the infection is fully controlled (Indelicato et al., 2006; Shimono et al., 2017).

We hypothesized that the severity of inguinal lymphadenopathy is different from pathogen-induced PJI and sterile inflammatory induced prosthetic aseptic failure, and such difference is beneficial for differentiating between different disease types. Therefore, our purpose was to explore whether ultrasound assessment of inguinal lymph node size can be used for diagnosing PJI. Additionally, we also investigated the performance of inguinal lymph nodes in patients undergoing reimplantation, which is of interest in determining whether infection persists before reimplantation.

Materials and methods

Patient cohort and characteristics

From January 2020 to June 2022, we prospectively included patients who underwent primary total hip/knee arthroplasty (TJA) or hip/knee revision procedures. Patients with any type of skin ulcers, hematoma, sexually transmitted diseases (STDs), a recent history of trauma or dislocation (within 2 weeks), extra-articular infections of the lower extremities, co-existing immune system diseases such as rheumatoid arthritis, tumors (lymphoma, skin cancer of the lower extremities, prostate cancer, bladder cancer, and gynecological tumors), and those receiving immunotherapy were excluded. Patients included in this study were divided into group A: patients receiving primary arthroplasty; Group B: patients who underwent revision arthroplasty due to aseptic failure; Group C: patients undergoing the first stage of a 2-stage exchange revision protocol for the treatment of PJI; Group D: patients treated with PJI undergoing reimplantation protocol. For the reimplantation group, we first confirmed that every patient had no pain or discomfort regarding to clinical signs. Then we conducted MSIS standards and synovial fluid culture to exclude the possibility of infection. During the operation, two surgeons with more than 20 years of experience took different tissues for microbial culture. The cohort was included in the study after a series of methods failed to detect signs of infection. A total of 23 patients were excluded for reasons including rheumatoid arthritis (8 patients), a history of trauma within 14 days (6 patients), leg ulcers (3 patients), tinea pedis (3 patients), prostatitis (1 patient), and voluntary withdrawal from the cohort (2 patients). The number of exclusions and the specific reasons are recorded in Figure 1.

Aseptic revision refers to the failure of primary arthroplasty due to loosening, wear, instability, and dislocation of the prosthesis, excluding infection (Qin et al., 2020; Qin et al., 2022). The procedure is based on history, physical examination, imaging,

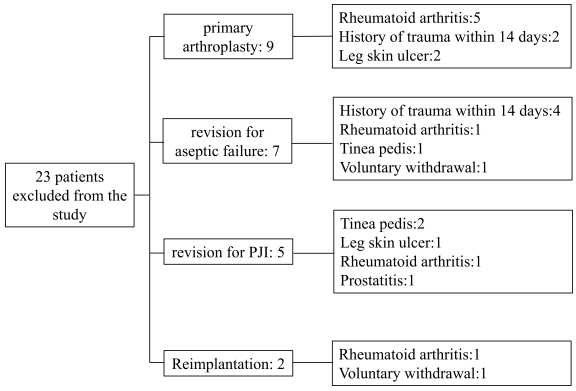

FIGURE 1
The number and reasons of excluded patients, by group.

serum inflammatory markers, intraarticular synovial fluid sampling, and intraoperative visual evaluation of the prosthesis with pain during movement and presence of the bone-cement interface around the prosthesis. Indications of implant loosening including 2mm opacity, osteolysis, implant displacement, and heterotopic ossification (Chalmers et al., 2017; Anil et al., 2022). PJI is defined by the Musculoskeletal Infection Society (MSIS) criteria (Parvizi and Gehrke, 2014). We recorded gender, age, the involved joint and BMI of the patients. At least 3 tissue samples were collected for microbiological culture and extended culture for 14 days during revision arthroplasty.

Procedure for detecting inguinal lymph nodes by ultrasound

On the second day after admission, all included patients underwent an ultrasound examination of the inguinal lymph nodes, prior to planned surgery. Preoperative ultrasonography was performed using APLIO i800 TUS-AI800 (Canon Medical Systems, USA) equipment with Ultra-Wideband Linear i18LX5 sensor by two ultrasound physicians with more than 5 years of experience. During the ultrasound, the patient was placed in a supine position and outward rotation and extension of the limbs were checked. Sufficient pressure was applied with the probe and the frequency was changed according to the patient's body habits. Normal scanning of the vascular axis was performed first, and at least a second longitudinal scan was performed in all cases, in order to measure the two main orthogonal planes of the lymph nodes (Solivetti et al., 2012; Jacobson et al., 2015). The long and short axes of the most suspected reactive lymph nodes were measured using sonographer and the long axis was taken as a parameter to assess lymph node size (Figure 2).

Statistical analysis

Statistical analysis of the data was performed using GraphPad Prism 9.0 (GraphPad Software, San Diego, California, USA). Chi-square test was used for categorical variables and Mann-Whitney analysis was used for continuous variables. Youden J statistic was used to determine the optimal threshold of inguinal lymph node size between PJI and aseptic loosening (J = sensitivity 1 specificity 1). The sensitivity and specificity of this threshold in differentiating aseptic loosening from PJI were further calculated by the following formula: Sensitivity= (true positive + true negative)/(true positive + true negative + false positive + false negative), Specificity= (true negative + false positive)/(true positive + true negative + false positive + false negative). The feasibility of inguinal lymph node size in the identification of PJI is determined by the Receiver Operator Characteristic (ROC) curves. A p-value less than 0.05 was considered statistically significant.

Results

A total of 176 patients were enrolled, including 58 patients with primary arthroplasty, 47 patients with revision for aseptic failure, 38 patients with revision for PJI and 33 patients with reimplantation. The characteristics of each group are shown in Table 1. No statistically significant differences were noted between the four groups concerning age, BMI, gender and involved joint. And the median time of antibiotic holiday in reimplantation group was 56 days. We then compared the size of bilateral (affected side and normal side) inguinal lymph nodes in each group and drew a histogram, as shown in Figure 3. It can be seen that the inguinal lymph nodes of the uninvolved lower limbs were consistent in each group, while the inguinal lymph nodes of the affected side were significantly enlarged (except for group A). The median level of inguinal lymph nodes was 26mm (range, 24 to 30mm) in the group C compared with 12 mm (range, 10 to 15mm) in the group B ($p< 0.0001$) (Table 2). The median level of inguinal lymph nodes was 4mm (range, 3.5 to 4mm) in the primary arthroplasty cohort and 9mm (range, 8 to 10mm) in the reimplantation group (Figure 3).

We compared the median levels of ESR and CRP in groups B and C in Table 2. As can be seen, the median levels of both ESR and CRP were significantly higher in group C. The median level of ESR was 35 mm/h (range, 18 to 47 mm/h) in the group C compared with 21 mm/h (range, 19 to 34 mm/h) in the group B ($p=0.0053$), and the median level of CRP was 19 mg/L (range, 14.4 to 25mg/L) in group C compared with 15mg/L (range, 5.9 to 23mg/L) in group B ($p=0.0025$).

To further confirm the importance of inguinal lymph node size in differentiating PJI from aseptic failure, ROC curves were drawn

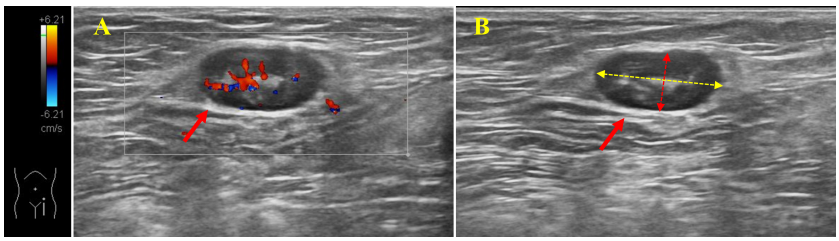

FIGURE 2
Ultrasonography of inguinal lymph nodes. **(A)**: Color Doppler shows enlarged blood supply in lymph nodes in the inguinal region. **(B)**: Measurements of the long and short axes of the lymph nodes. Solid red arrows: lymph nodes; Yellow dotted arrow: long axis of lymph node; Red dotted arrow: short axis of lymph node.

10.3389/fcimb.2023.1129072

TABLE 1 Demographic data for the study population.

Characteristic	Group A (N=58)	Group B (N=47)	Group C (N=38)	Group D (N=33)	P value
Age (years)	58.5 ± 6.1	60.4 ± 5.3	61.6 ± 6.3	61.9 ± 6.4	>0.05#
BMI (kg/m2)	24.7 ± 2.8	24.3 ± 2.7	23.5 ± 1.9	23.9 ± 2.6	>0.05#
Gender					>0.05*
Male	27	24	17	14	
Female	31	23	21	19	
Involved Joint					>0.05*
Knee	32	27	21	19	
Hip	26	20	17	17	
Antibiotic Holiday (Days) median	NA	NA	NA	56	
P25, P75				(42, 84)	

Group A = primary arthroplasty, Group B = aseptic revision, Group C = first stage of a 2-stage exchange revision protocol, Group D = second stage of a 2-stage exchange protocol (reimplantation), Variables are expressed as mean ± SD (standard deviation), BMI (Body Mass Index), * Chi squared test, # Mann-Whitney U test.

with the PJI group as a positive reference and the aseptic loosening group as a negative control, and optimal truncation value of inguinal lymph nodes for diagnosing PJI was calculated. As shown in Figure 4 and Table 3, the area under the curve (AUC) for inguinal lymph node was 0.978 (95% CI 0.946 to 1.000), and was more accurate than serum ESR 0.707 (95% CI 0.567 to 0.853) and serum CRP 0.760 (95% CI 0.628 to 0.892). The optimal threshold of inguinal lymph node size for PJI detection was 19mm, and the sensitivity, specificity and accuracy were 92%, 96% and 94%, respectively.

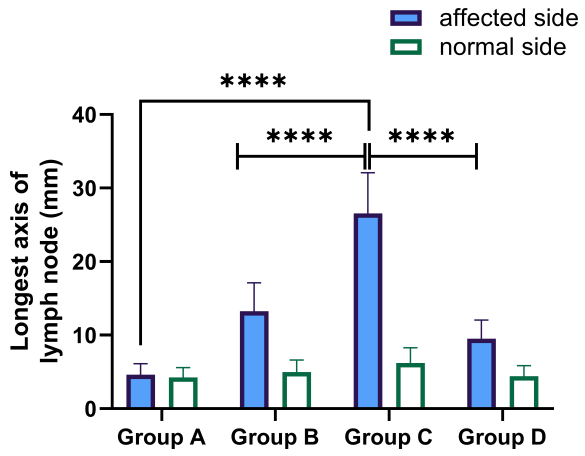

FIGURE 3
Performance of longest axis of the inguinal lymph node in the affected and normal lower limbs in each group. Group (A) = primary arthroplasty, Group (B) = aseptic revision, Group (C) = first stage of a 2-stage exchange revision protocol, Group (D) = second stage of a 2-stage exchange protocol (reimplantation), **** p-value< 0.0001.

Discussion

To our knowledge, this was the first study to evaluate the size of the inguinal lymph nodes by ultrasound as a diagnostic method for PJI, and also to analyze the appearance of the inguinal lymph nodes in reimplantation patients. In our cohort, inguinal lymph nodes were more accurate than ESR and CRP in diagnosing PJI. Notably, in patients with the second stage of a 2-stage exchange protocol for PJI, the size of the groin lymph nodes had largely returned to normal. This is of concern to us because there is no diagnostic gold standard for determining persistence of the infection during replantation, and often the surgeon must make a decision according to clinical symptoms and laboratory parameters (Fu et al., 2018). Besides, clinical experience has to be referred to in some cases. Previous studies have shown that serological markers such as C-reactive protein (CRP) and erythrocyte sedimentation (ESR) are unreliable markers for evaluating the persistence of reimplantation infection (George et al., 2016; Fu et al., 2018). More recently, it has been proposed that the LE strip test can be used as a reliable tool for diagnosing the persistence of infection and outperforming the serum CRP and ESR assays (Logoluso et al., 2022). However, patients in the cohort of this study were followed for less than two years after replantation which is the same as in our study, justifying the necessity of long-term. Due to the lack of long-term clinical follow-up in these patients, it is not possible to accurately determine whether the recovery of inguinal lymph node size represents the disappearance of pathogen infection. In any event, no recurrence of infection in this cohort was noticed during follow-up of fewer than 6 months.

Lymph nodes contain monocytes, macrophages, lymphatic vessels and lymph fluid, are part of the reticuloendothelial system (Mohseni et al., 2014). Lymph nodes were central to the body's defenses against foreign antigens and function as filters, removing foreign particles from fluids that run through the lymphatic vessels (Gowing, 1974). When the pathogen is captured in the lymph

TABLE 2 Comparison of parameters between each group.

Parameters	Group A	Group B	Group C	Group D	P1 value	P2 value
ESR (mm/h)						
median	11.0	21.0	35.0	12.0	0.0053	<0.0001
P25, P75	(8.0, 14.0)	(19.0, 34.0)	(18.0, 47.0)	(9.0, 16.0)		
CRP (mg/L)						
median	5	15.0	19.0	9	0.0025	<0.0001
P25, P75	(3.3, 5.9)	(5.9, 23.0)	(14.4, 25.0)	(5.1,11)		
Inguinal lymph nodes (mm)						
median	4	12.0	26.0	9	<0.001	<0.0001
P25, P75	(3.5, 4)	(10.0, 15.0)	(24.0, 30.0)	(8, 10)		

P1: group B vs group C; P2: group C vs group D; CRP, C-reactive protein; ESR, erythrocyte sedimentation rate, Group B = aseptic revision, Group C = first stage of a 2-stage exchange revision protocol.

nodes, it can lead to lymphocyte proliferation and enlargement, often presenting as focal lymph node enlargement in the lymphatic drainage area (Darnal et al., 2005; Mohseni et al., 2014). Inguinal lymph nodes, located in the upper part of the femoral triangle, receive lymphatic reflux material from the anterior tibial and popliteal lymph nodes, and are the first destination of lymphatic reflux of the whole lower limb (Hong et al., 2013). Localized inguinal lymphadenopathy is usually caused by infection, including STDs and pathogens in lower limb tissue (Twist and Link, 2002; Mohseni et al., 2014). In the present study, significant swelling of the inguinal lymph nodes was observed in all PJI patients. We found that when the inguinal lymph node size reached 19mm, the sensitivity and specificity of PJI were 0.92 (95%CI, 75.03 to 98.58) and 0.96 (95%CI, 80.46 to 99.79) respectively.

The current study had several strengths. First, color Doppler ultrasound has been used as a useful imaging tool to assess lymph node enlargement since the early 1970s, and ultrasound assessment of groin lymph node size is available in most medical institutions (Mountford and Atkinson, 1979; Choi et al., 1995). For patients, non-invasive and economical ultrasound testing is more acceptable. The second advantage of this study is that we prospectively compared the size of inguinal lymph nodes in patients with different disease types, reducing experimental heterogeneity. We then applied statistical methods to determine the appropriate threshold for inguinal lymph node diagnosis of PJI. While this threshold may change as data from different institutions increases, it is a good starting point and a guide for clinicians wishing to use this test. Finally, there is no doubt that the study of the timing of reimplantation in two-stage revision surgery is the most concerned topic in orthopedic infections (Shahi et al., 2017; Logoluso et al., 2022). We evaluated the appearance of inguinal lymph nodes in patients undergoing reimplantation for treatment of PJI, and there were no recurrent cases of infection in existing follow-up, although long-term follow-up results were lacking. The satisfactory results of the inguinal lymph nodes provide a possibility for decision-making on the timing of the two-stage revision, as well as a potential reference for evaluating the effectiveness of antibiotic therapy.

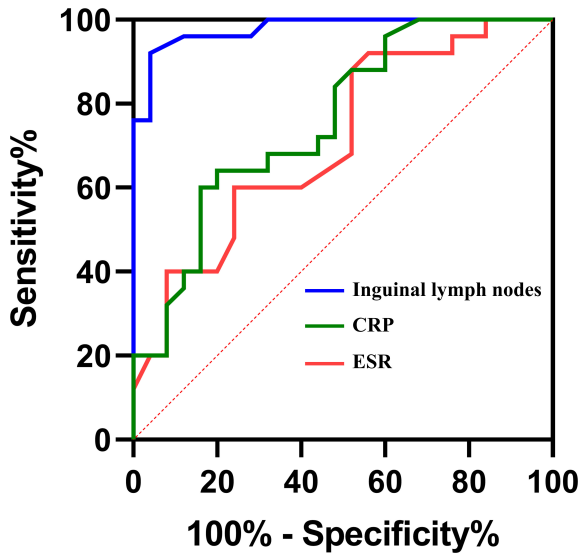

FIGURE 4
Receiver Operating Characteristic curves (ROCs) and area under curves (AUC) of the three tests in diagnosing PJI.

This study also had some limitations. First, although ultrasound is the most commonly used technique to detect inguinal lymph nodes, the operator's operation and judgment will affect the results. The ultrasound examiners in this study were all experienced technicians with systematic training. Therefore, we believe that the results of this study are highly reliable. Second, we all know that there is no "gold standard" for diagnosing PJI, so some patients assigned to the sterile revision group may actually have PJI. Our use of the Society of Musculoskeletal Infections (MSIS) criteria to define PJI may have skewed the results, even though the MSIS criteria are generally accepted as the best definition of PJI (Parvizi and Gehrke, 2014). Finally, this study excluded patients with autoimmune inflammatory diseases such as RA, which reduced the scope of application of the findings of this study. Previous studies have shown that rheumatoid arthritis causes enlarged lymph nodes in patients (Habermann and Steensma, 2000; Mohseni et al., 2014). Therefore, inguinal lymph node examination is of reference value in patients with suspected infection of the related nodes, but in cases such as associated lower limb infection or systemic immune system

TABLE 3 Performance of these parameters for diagnosing PJI.

Parameters	AUC (95% CI)	Best threshold	Sensitivity (95% CI)	Specificity (95% CI)	PPV (%)	NPV (%)	Accuracy (%)
Inguinal lymph nodes	0.978 (0.946 to 1.000)	19 (mm)	92.0 (75.03 to 98.58)	96.0 (80.46 to 99.79)	95.8	92.3	94.0
CRP	0.760 (0.628 to 0.892)	18.1 (mg/L)	64.0 (44.52 to 79.75)	80.0 (60.87 to 91.14)	68.2	70.1	72.5
ESR	0.707 (0.567 to 0.853)	34.5 (mm/h)	60.0 (40.74 to 76.60)	76.0 (56.57 to 88.50)	66.7	68.0	66.0

PJI, periprosthetic joint infection, CRP, C-reactive protein; ESR, erythrocyte sedimentation rate, CI, confidence interval; PPV, positive predictive value; NPV, negative predictive value.

disorders, the accuracy of ultrasound diagnosis may be interfered. Therefore, in future studies, we hope to explore the specific manifestations of inguinal lymph nodes in patients with inflammatory diseases.

In conclusion, the clinical application of inguinal lymph node detection adds a new powerful tool for the diagnosis of PJI. Based on our preliminary findings, we believe that ultrasound testing of inguinal lymph node size is an inexpensive, immediate, and universally available test that should be added to patient screening for PJI. In patients undergoing reimplantation, swollen lymph nodes may signal persistent pathogen infections, and of course, the interpretation of the inguinal lymph nodes in two-stage revision still requires further long-term follow-up research.

Data availability statement

The raw data supporting the conclusions of this article will be made available by the authors, without undue reservation.

Ethics statement

The studies involving human participants were reviewed and approved by Institutional Review Committee of the First Affiliated Hospital of Chongqing Medical University. The patients/participants provided their written informed consent to participate in this study. Written informed consent was obtained from the individual(s) for the publication of any potentially identifiable images or data included in this article.

Author contributions

WH and NH conceived the manuscript. LQ and CZ wrote the first draft. JY and XS revised the first draft. LQ and HW performed the experiments. LC, LW, JL and CJ provided grouping suggestions and grammar modifications. All authors contributed to the article and approved the submitted version.

Funding

This work was supported by the National Natural Science Foundation of China (Grant number: 82072443 and 81972069) and The Youth Excellence Program of the First Affiliated Hospital of Chongqing Medical University (Grant number: ZYRC2020-03).

Conflict of interest

The authors declare that the research was conducted in the absence of any commercial or financial relationships that could be construed as a potential conflict of interest.

Publisher's note

References

Anil, U., Singh, V., and Schwarzkopf, R. (2022). Diagnosis and detection of subtle aseptic loosening in total hip arthroplasty. *J. Arthroplasty.* (2022) Aug; 37(8):1494-1500 doi: 10.1016/j.arth.2022.02.060

Bontumasi, N., Jacobson, J. A., Caoili, E., Brandon, C., Kim, S. M., and Jamadar, D. (2014). Inguinal lymph nodes: size, number, and other characteristics in asymptomatic patients by CT. *Surg. Radiol. Anat* 36, 1051–1055. doi: 10.1007/s00276-014-1255-0

Bui, T., and Bordoni, B. (2022). "Anatomy, abdomen and pelvis, inguinal lymph node," in *StatPearls* (Treasure Island (FL: StatPearls Publishing LLC).

Chalmers, B. P., Sculco, P. K., Fehring, K. A., Trousdale, R. T., and Taunton, M. J. (2017). A novel percentage-based system for determining aseptic loosening of total knee arthroplasty tibial components. *J. Arthroplasty* 32, 2274–2278. doi: 10.1016/j.arth.2017.02.020

Cheok, T., Smith, T., Siddiquee, S., Jennings, M. P., Jayasekera, N., and Jaarsma, R. L. (2022). Synovial fluid calprotectin performs better than synovial fluid polymerase chain reaction and interleukin-6 in the diagnosis of periprosthetic joint infection : a systematic review and meta-analysis. *Bone Joint J.* 104-b, 311–320. doi: 10.1302/0301-620X.104B3.BJJ-2021-1320.R1

Choi, M. Y., Lee, J. W., and Jang, K. J. (1995). Distinction between benign and malignant causes of cervical, axillary, and inguinal lymphadenopathy: value of Doppler spectral waveform analysis. *AJR Am. J. Roentgenol* 165, 981–984. doi: 10.2214/ajr.165.4.7677005

Darnal, H. K., Karim, N., Kamini, K., and Angela, K. (2005). The profile of lymphadenopathy in adults and children. *Med. J. Malaysia* 60, 590–598.

Fu, J., Ni, M., Li, H., Li, X., Chai, W., Zhou, Y., et al. (2018). The proper timing of second-stage revision in treating periprosthetic knee infection: reliable indicators and risk factors. *J. Orthop Surg. Res.* 13, 214. doi: 10.1186/s13018-018-0885-z

George, J., Kwiecien, G., Klika, A. K., Ramanathan, D., Bauer, T. W., Barsoum, W. K., et al. (2016). Are frozen sections and MSIS criteria reliable at the time of reimplantation of two-stage revision arthroplasty? *Clin. Orthop Relat. Res.* 474, 1619–1626.

Girard, J. P., and Springer, T. A. (1995). High endothelial venules (HEVs): specialized endothelium for lymphocyte migration. *Immunol. Today* 16, 449–457. doi: 10.1016/0167-5699(95)80023-9

Goud, A., Nützinger, D., van der Bij, A., Jenniskens, K., Groenewold, J., De Gast, A., et al. (2022). Synovial-based tests outperform serum markers to rule out infection in total knee arthroplasty and total hip arthroplasty: a systematic review and meta-analysis. *J. Arthroplasty* 37, 802–808.e805. doi: 10.1016/j.arth.2021.12.020

Gowing, N. F. (1974). Tumours of the lymphoreticular system: nomenclature, histogenesis, and behaviour. *J. Clin. Pathol. Suppl. (R Coll. Pathol)* 7, 103–107. doi: 10.1136/jcp.27.Suppl_7.103

Habermann, T. M., and Steensma, D. P. (2000). Lymphadenopathy. *Mayo Clin. Proc.* 75, 723–732. doi: 10.1016/S0025-6196(11)64620-X

Hong, J. P., Sun, S. H., and Ben-Nakhi, M. (2013). Modified superficial circumflex iliac artery perforator flap and supermicrosurgery technique for lower extremity reconstruction: a new approach for moderate-sized defects. *Ann. Plast. Surg.* 71, 380–383. doi: 10.1097/SAP.0b013e3182503ac5

Indelicato, D. J., Grobmyer, S. R., Newlin, H., Morris, C. G., Haigh, L. S., Copeland, E. M.3rd, et al. (2006). Delayed breast cellulitis: an evolving complication of breast conservation. *Int. J. Radiat. Oncol. Biol. Phys.* 66, 1339–1346. doi: 10.1016/j.ijrobp.2006.07.1388

Jacobson, J. A., Khoury, V., and Brandon, C. J. (2015). Ultrasound of the groin: techniques, pathology, and pitfalls. *AJR Am. J. Roentgenol* 205, 513–523. doi: 10.2214/AJR.15.14523

Kildow, B. J., Ryan, S. P., Danilkowicz, R., Lazarides, A. L., Penrose, C., Bolognesi, M. P., et al. (2021). Next-generation sequencing not superior to culture in periprosthetic joint infection diagnosis. *Bone Joint J.* 103-b, 26–31. doi: 10.1302/0301-620X.103B1.BJJ-2020-0017.R3

Kurtz, S. M., Lau, E., Watson, H., Schmier, J. K., and Parvizi, J. (2012). Economic burden of periprosthetic joint infection in the united states. *J. Arthroplasty* 27, 61–65.e61. doi: 10.1016/j.arth.2012.02.022

Lippmann, T., Braubach, P., Ettinger, M., Kuehnel, M., Laenger, F., and Jonigk, D. (2019). Fluorescence in situ hybridization (FISH) for the diagnosis of periprosthetic joint infection in formalin-fixed paraffin-embedded surgical tissues. *J. Bone Joint Surg. Am.* 101, e5. doi: 10.2106/JBJS.18.00243

Logoluso, N., Pellegrini, A., Suardi, V., Morelli, I., Battaglia, A. G., D'anchise, R., et al. (2022). Can the leukocyte esterase strip test predict persistence of periprosthetic joint infection at second-stage reimplantation? *J. Arthroplasty* 37, 565–573. doi: 10.1016/j.arth.2021.11.022

Mohseni, S., Shojaiefard, A., Khorgami, Z., Alinejad, S., Ghorbani, A., and Ghafouri, A. (2014). Peripheral lymphadenopathy: approach and diagnostic tools. *Iran J. Med. Sci.* 39, 158–170.

Mountford, R. A., and Atkinson, P. (1979). Doppler Ultrasound examination of pathologically enlarged lymph nodes. *Br. J. Radiol.* 52, 464–467. doi: 10.1259/0007-1285-52-618-464

Parvizi, J., and Gehrke, T. (2014). Definition of periprosthetic joint infection. *J. Arthroplasty* 29, 1331. doi: 10.1016/j.arth.2014.03.009

Parvizi, J., Tan, T. L., Goswami, K., Higuera, C., Della Valle, C., Chen, A. F., et al. (2018). The 2018 definition of periprosthetic hip and knee infection: an evidence-based and validated criteria. *J. Arthroplasty* 33, 1309–1314.e1302. doi: 10.1016/j.arth.2018.02.078

Qin, L., Du, C., Yang, J., Wang, H., Su, X., Wei, L., et al. (2022). Synovial fluid interleukin levels cannot distinguish between prosthetic joint infection and active rheumatoid arthritis after hip or knee arthroplasty. *Diagnostics* 12, 1196. doi: 10.3390/diagnostics12051196

Qin, L., Li, X., Wang, J., Gong, X., Hu, N., and Huang, W. (2020). Improved diagnosis of chronic hip and knee prosthetic joint infection using combined serum and synovial IL-6 tests. *Bone Joint Res.* 9, 587–592. doi: 10.1302/2046-3758.99.BJR-2020-0095.R1

Shahi, A., Kheir, M. M., Tarabichi, M., Hosseinzadeh, H. R. S., Tan, T. L., and Parvizi, J. (2017). Serum d-dimer test is promising for the diagnosis of periprosthetic joint infection and timing of reimplantation. *J. Bone Joint Surg. Am.* 99, 1419–1427. doi: 10.2106/JBJS.16.01395

Shimono, J., Miyoshi, H., Kamimura, T., Eto, T., Miyagishima, T., Sasaki, Y., et al. (2017). Clinicopathological features of primary splenic follicular lymphoma. *Ann. Hematol.* 96, 2063–2070. doi: 10.1007/s00277-017-3139-y

Solivetti, F. M., Elia, F., Graceffa, D., and Di Carlo, A. (2012). Ultrasound morphology of inguinal lymph nodes may not herald an associated pathology. *J. Exp. Clin. Cancer Res.* 31, 88. doi: 10.1186/1756-9966-31-88

Twist, C. J., and Link, M. P. (2002). Assessment of lymphadenopathy in children. *Pediatr. Clin. North Am.* 49, 1009–1025. doi: 10.1016/S0031-3955(02)00038-X

Zhang, J., Guo, J. R., Huang, Z. S., Fu, W. L., Wu, X. L., Wu, N., et al. (2021). Transbronchial mediastinal cryobiopsy in the diagnosis of mediastinal lesions: a randomised trial. *Eur. Respir. J.* 2021 Dec 9; 58(6):2100055. doi: 10.1183/13993003.00055-2021

frontiers | Frontiers in Cellular and Infection Microbiology

TYPE Review
PUBLISHED 02 May 2023
DOI 10.3389/fcimb.2023.1193645

OPEN ACCESS

EDITED BY
Chaofan Zhang,
First Affiliated Hospital of Fujian Medical University, China

REVIEWED BY
Anna Benini,
University of Verona, Italy
Chengzhen Liang,
Zhejiang University, China

*CORRESPONDENCE
Bangbao Lu
14182832@qq.com
Fangjie Zhang
zhangfj@csu.edu.cn

†These authors have contributed equally to this work and share first authorship

RECEIVED 25 March 2023
ACCEPTED 20 April 2023
PUBLISHED 02 May 2023

CITATION
He M, Arthur Vithran DT, Pan L, Zeng H, Yang G, Lu B and Zhang F (2023) An update on recent progress of the epidemiology, etiology, diagnosis, and treatment of acute septic arthritis: a review. *Front. Cell. Infect. Microbiol.* 13:1193645. doi: 10.3389/fcimb.2023.1193645

An update on recent progress of the epidemiology, etiology, diagnosis, and treatment of acute septic arthritis: a review

Miao He[1,2†], Djandan Tadum Arthur Vithran[1,2†], Linyuan Pan[1†], Haijin Zeng[1], Guang Yang[1], Bangbao Lu[1,2*] and Fangjie Zhang[2,3*]

[1]Department of Orthopaedics, Xiangya Hospital, Central South University, Changsha, Hunan, China, [2]National Clinical Research Center for Geriatric Disorders, Xiangya Hospital, Central South University, Changsha, Hunan, China, [3]Department of Emergency Medicine, Xiangya Hospital, Central South University, Changsha, Hunan, China

Acute septic arthritis is on the rise among all patients. Acute septic arthritis must be extensively assessed, identified, and treated to prevent fatal consequences. Antimicrobial therapy administered intravenously has long been considered the gold standard for treating acute osteoarticular infections. According to clinical research, parenteral antibiotics for a few days, followed by oral antibiotics, are safe and effective for treating infections without complications. This article focuses on bringing physicians up-to-date on the most recent findings and discussions about the epidemiology, etiology, diagnosis, and treatment of acute septic arthritis. In recent years, the emergence of antibiotic-resistant, particularly aggressive bacterial species has highlighted the need for more research to enhance treatment approaches and develop innovative diagnosis methods and drugs that might combat better in all patients. This article aims to furnish radiologists, orthopaedic surgeons, and other medical practitioners with contemporary insights on the subject matter and foster collaborative efforts to improve patient outcomes. This review represents the initial comprehensive update encompassing patients across all age groups.

KEYWORDS

septic arthritis, Pathogenic microorganism, antibiotics, arthroscopy, epidemiology

1 Introduction

Acute Septic arthritis(ASA) is a rare and serious orthopedic emergency mainly affecting a single joint (5-10% of multiple joints) that, if left untreated, can lead to systemic sepsis and has a 16.3 percent death rate (Forlin and Milani, 2008; Ilharreborde, 2015; Montgomery and Epps, 2017; Tretiakov et al., 2019; Abram et al., 2020; Chan et al., 2020; Erkilinc et al., 2021; Momodu and Savaliya, 2022). The prevalence changes with age (Geirsson et al., 2008; Mathews et al., 2010; Kennedy et al., 2015; Maneiro et al., 2015),

ethnicity (Morgan et al., 1996), and socioeconomic status (Gupta et al., 2001). In most circumstances, males are more likely to be affected than females (Al Saadi et al., 2009; Pääkkönen, 2017; Momodu and Savaliya, 2022).Although any joint is vulnerable to infection (Shirtlif and Mader, 2002), the knee is the most common site of infection (affecting almost half of all cases), followed by the hip, shoulder, elbow, and ankle. Rheumatoid arthritis, neonates, diabetes, heavy drinking, and old age are possible risk factors of ASA (Kaandorp et al., 1995; Mathews et al., 2010).

Hematogenous spread is the most common route for these infections to reach the joint space, while penetrating trauma or inoculation are potential triggers (Mathews et al., 2010; Ross, 2017).In addition to a patient's medical history and physical examination, confirmation of a clinical diagnosis of septic arthritis needs the isolation of an infectious agent from synovial fluid. In cases when repeated joint aspiration has been unsuccessful, surgery is advised over medical treatment (Lane et al., 1990; Balabaud et al., 2007). Improper or delayed diagnosis and treatment may result in permanent joint damage and disability (Peters et al., 1992). *Staphylococcus aureus* is the most commonly cultured organism. It is followed by *Kingella kingae*, *Streptococcus pyogenes*, and *Streptococcus pneumonia*, depending on the patient age (Moumile et al., 2005). Antibiotic coverage should start in suspected cases when blood cultures and a serologic test and microscopic analysis of synovial fluid collected from the affected joint are the initial steps in diagnosing septic arthritis. White blood cell (WBC) count, C-reactive protein (CRP) level evaluation, erythrocyte sedimentation rate (ESR), and aerobic and anaerobic blood cultures comprise the serologic testing battery. Using arthrocentesis, it is also feasible to get a WBC count, neutrophil percentage, Gram stain, and culture from synovial fluid. In fifty percent of instances with septic arthritis, arthrocentesis yields positive culture results; nevertheless, this is insufficient to establish a diagnosis (Weston et al., 1991; Kocher et al., 2003; Quick et al., 2018).Standard treatment consists of irrigation and debridement of the affected joint, followed by intravenous antibiotics. This can be accomplished using either an open surgery technique (arthrotomy) or a minimally invasive minimally invasive technique (arthroscopy) (Perry, 1999). Arthroscopic management has supplanted open management as the treatment for septic arthritis (Butt et al., 2011).

However open management is still widely utilized and remains the preferred option for many hospitals. In order to limit the risk of lifelong disability, making a fast diagnosis and treatment plan for ASA patients is crucial. To provide the best possible care for these patients, doctors must have a comprehensive awareness of the patient's medical history, the results of the physical exam, the diagnostic testing, and the available treatment options. These topics continue to be the subject of debate among experts, and Unfortunately, the literature has no consensus about the etiology, the best treatment, and the diagnosis method available for ASA patients. Therefore, in the current review study, we aim to provide an up-to-date on the recent epidemiology, etiology, diagnosis, and best treatment option for acute septic arthritis for physicians constantly facing these conditions in their daily work at the hospital.

2 Epidemiology

Many factors prevent us from having a complete picture of acute septic arthritis's epidemiology. The rarity of the illness makes future research challenging due to their high overhead costs and other obstacles. Patients in whom septic arthritis is strongly suspected clinically may or may not have the diagnosis established microbiologically, historically leading to difficulties in disease categorization.

The annual incidence of ASA varies from 1 to 35 cases per 100,000 individuals in different countries (Gafur et al., 2008; Riise et al., 2008; Horowitz et al., 2011; Montgomery and Epps, 2017; Okubo et al., 2017; Welling et al., 2018; Safdieh et al., 2019; Cohen et al., 2020; Nossent et al., 2021; Momodu and Savaliya, 2022), with the United States having a rate of 4 to 10 cases per 100,000 individuals (Montgomery and Epps, 2017; Okubo et al., 2017; Okubo et al., 2017; Swarup et al., 2020; Erkilinc et al., 2021). The incidence of the large joint is higher than small joints for septic arthritis and raised with age; the most commonly involved large joint was the knee and hand interphalangeal in the small joints (Mathews et al., 2010; Ilharreborde, 2015; Momodu and Savaliya, 2022). Staphylococcus aureus is the most common pathogen causing septic arthritis (Kennedy et al., 2015; Jung et al., 2018; McBride et al., 2020).

Children have a higher incidence of septic arthritis than adults (Donders et al., 2022). Individuals whose immune systems are compromised for whatever cause (sickle cell anemia, HIV/AIDS, chemotherapy patients). Individuals with diabetes mellitus, rheumatoid arthritis, recent joint surgery, a joint prosthesis, intra-articular injections in the past, a history of skin infections or cutaneous ulcers, HIV infection, or age over 80 are at increased risk (Margaretten et al., 2007; Horowitz et al., 2011).

Septic arthritis is on the rise, associated with an aging population, an increase in the number of invasive procedures performed, and an increase in the number of patients receiving immunosuppressive therapy. More research is needed on the topic to reach a consensus on the epidemiology of ASA.

3 Etiology

3.1 Pathogenic microorganisms

The prevalence and susceptibility of organisms that cause septic arthritis have not altered substantially during the past decades (Dubost et al., 2014). Staphylococcus aureus is the most prevalent organism for all age categories and risk groups, followed by Streptococcus (Kennedy et al., 2015).

The hip and knee are the joints most commonly affected by septic arthritis in children. As shown in Table 1, the most prevalent organism is *methicillin-sensitive Staphylococcus aureus* (MSSA), followed by methicillin-resistant Staphylococcus aureus (MRSA) and *Streptococcus pneumoniae* (Young et al., 2011). MSSA, MRSA, *group B streptococci*, *Klebsiella pneumoniae*, and gram-negative bacilli regularly infect infants younger than 3 months; *Neisseria gonorrhoeae* and *Candida* are rare pathogens in this age group

TABLE 1 Pathogenic microorganisms for septic arthritis in all age groups.

AGES GROUP	COMMON PATHOGENS	RARE PATHOGENS
Infants younger than 3 months old	Staphylococcus aureus(MSSA and MRSA) group B streptococci Klebsiella pneumoniae gram-negative bacilli.	Neisseria gonorrhoeae Candida
Young children from 3 months to 5 years old	Staphylococcus aureus(MSSA and MRSA) group A streptococcus Aureus Streptococcus pneumoniae	Haemophilus influenzae type B
Children older than 5 years	Staphylococcus aureus(MSSA and MRSA) group A streptococcus.	Streptococcus pneumoniae group A And Beta hemolytic streptococcus Salmonella Neisseria meningitidis Neisseria gonorrhoeae Pseudomonas aeruginosa Candida anaerobic bacteria other than group B
Adults	Staphylococcus aureus, coagulase-negative Staphylococcus, Streptococcus, and Pseudomonas, and other Gram-negative bacteria.	

(Ben-Zvi et al., 2019; Mooney and Murphy, 2019). Pathogens such as MSSA and MRSA, *group A streptococcus aureus*, and *Streptococcus pneumoniae* are common in infants and young children between 3 months and 5 years of age. *Haemophilus influenzae* type B and *Kingella kingae* are uncommon pathogens that commonly infect children aged 6 months to 4 years (Castellazzi et al., 2016; Villani et al., 2021). Pathogens such as *methicillin-resistant Staphylococcus aureus* (MRSA), *group A streptococcus, Streptococcus pneumoniae, Salmonella, Neisseria meningitidis, Neisseria gonorrhoeae, Pseudomonas aeruginosa, Candida, and anaerobic bacteria* other than group B are uncommon in children over 5 years old (Ben-Zvi et al., 2019). Children's septic elbow is most commonly caused by Staphylococcus aureus (Bowakim et al., 2010).

Pathogenic bacteria in adults may be directly tied to the patient's medical history, physical state, drug misuse, etc., but the most prevalent pathogens are still *Staphylococcus aureus, coagulase-negative Staphylococcus, Streptococcus, Pseudomonas, and other Gram-negative bacteria*. In 233 cases of septic arthritis over 10 years, MSSA was the primary causal infection, but MRSA arthritis was rarely diagnosed (Clerc et al., 2011). In the United States, MRSA has become the leading cause of septic arthritis (Ross, 2017). Infections caused by MRSA are common in the elderly, intravenous drug users, and after orthopedic surgery. *Streptococcus pyogenes* is typically connected with autoimmune diseases, persistent skin infections, and trauma, but group B streptococci are frequently seen in the elderly, especially with diabetes, cirrhosis, and neurological disorders. Gram-negative bacilli infections account for 10–20% of cases of septic arthritis, and they frequently affect patients with urinary tract and intestinal infections and those with long-term implants. In the United States, injection drug use has become the most prevalent risk factor for septic arthritis. Septic arthritis in injected drug users is more frequently caused by MRSA, MSSA, *Serratia sp, Escherichia coli, Proteus, Klebsiella*, and *Enterobacter* and is more likely to affect the sacroiliac, acromioclavicular, sternoclavicular, and facet joints (Ross et al., 2020). Infrequently, anaerobic microorganisms are seen in diabetic patients, those who have received joint prosthesis implantation, and those who have sustained penetrating trauma. Women who develop septic arthritis during menstruation or pregnancy or who are sexually active should be evaluated for *Neisseria gonorrhoeae* infection (Clerc et al., 2011). Infection of a joint by MRSA appears to be related to worse outcomes (Ross, 2017). *Beta-hemolytic streptococci* predominantly caused streptococcal septic arthritis in older, multimorbid patients (Lotz et al., 2019).

The primary pathogens of septic arthritis produced by animal bites are the oral flora of injured animals and the flora of human skin, which includes various pathogens. *Pasteurella, Staphylococcus, Streptococcus*, and anaerobic bacteria are typical pathogens. Other uncommon pathogens include *Capnocytophaga*, which is transmitted by dog bites. Cat bites can potentially spread *Bartonella hansenii*. Pathogens of human bites are often aerobic gram-positive *cocci* (such as group A *streptococcus*) and *anaerobic bacteria*; *Pasteurella multocida* and *Eikenella eros* are rare pathogens (Moro-Lago et al., 2017; Gjika et al., 2019). *Pantoea agglomerans, Nocardia stellate, Sporothrix schenckii*, and purulent joints induced by consuming unpasteurized dairy products are the most prevalent pathogens of septic arthritis caused by horticultural workers or plant puncture wounds. Brucella is the most prevalent cause of inflammation (Smith et al., 2006; Clerc et al., 2011).

3.2 Pathological processes

The primary routes of joint infection include: 1) Hematogenous spread: pathogenic bacteria of the infection *foci* in other parts of the body spread to the joint through the blood circulation; hematogenous spread of infection is the most common etiology of shoulder sepsi[s] (Sweet et al., 2019; Gramlich et al., 2020); 2) Adjacent infection: the pathogenic bacteria come from the skin and soft tissue infection around the joint or secondary intra-articular infection after osteomyelitis;3) iatrogenic: such as secondary

infection following joint cavity puncture or medicament injection, or secondary intra-articular infection following joint replacement and per-articular fracture internal fixation and implantation, 4) traumatic, including trauma, stab wounds, and animal bites, resulting in joint soft tissue or joint infection after articular sac injury (Gjika et al., 2019; Couderc et al., 2020).

There are three stages to the pathophysiology of septic arthritis: 1) serous exudation stage: after pathogenic bacteria enter the joints, synovial congestion and edema, leukocyte infiltration, and serous exudation, there is typically no obvious damage to articular cartilage at this stage; if active treatment is administered, the exudate can be completely absorbed, the articular cartilage will not be destroyed, and the joint function will not be compromised. 2) Serous fibrinous exudation stage: the disease progresses, the exudate becomes turbid, the number of white blood cells and pus cells increases dramatically, synovitis worsens, vascular permeability increases and fibrin deposition causes articular cartilage rupture, ulcers, and shedding. The cartilage is uneven, resulting in poor joint function. 3) Purulent exudation stage: Inflammation progresses, the articular cartilage is involved, the subchondral bone and synovium are also destroyed, the soft tissues surrounding the joints can also be involved in cellulitis, the exudate is purulent, and the process is irreversible and causes severe dysfunction (Mathews et al., 2010; Couderc et al., 2020).

4 Clinical symptoms

Clinical signs might be modest or severe, especially in newborns and children are commonly atypical. The main symptoms include abrupt onsets such as chill, high fever, delirium, coma, and convulsions. It is more prevalent in youngsters, and some severe instances might be expressed as sepsis or septic shock (Synger, 2016). The joint's local manifestations include heat, discomfort, dysfunction, mobility, and postural restriction. Very superficial joints, such as the knee and elbow, may exhibit noticeable redness and edema (Gottlieb et al., 2019). The patellar floating test may be positive. Deep joints, such as the hip and sacroiliac joint, may not exhibit visible swelling and fever, but joints may still be reluctant to move owing to pain, and a physical examination of diseased joints may be refused (Long et al., 2019; Couderc et al., 2020).

5 Laboratory test

Blood test: leucocytes are markedly elevated, generally greater than 10x109/L; leucocyte esterase for suspected septic arthritis in native joints has a high negative predictive value; for infection in a native knee, there should be few false-positive results (McNabb et al., 2017). Adopting leucocyte esterase may promote the quicker discharge of patients with negative results (Knapper et al., 2021). While erythrocyte sedimentation rate (ESR) and C-reactive protein (CRP) are also significantly elevated, elevated procalcitonin (PCT) is of greater diagnostic significance.

For knee, elbow, shoulder, hip, etc., if suspected of septic arthritis, an experienced physician should perform joint puncture and synovial fluid aspiration. Gram stain and culture of synovial fluid should be tested; genetic testing of pathogenic microorganisms should also be performed to rapidly identify the possible pathogenic bacteria in the synovial fluid or blood by polymerase chain reaction (PCR) or next-generation sequencing (NGS). WBC≥50,000/ml in a synovial fluid provides diagnostic significance for septic arthritis; however, only 5% of individuals with septic arthritis had WBC <50,000/ml in their synovial fluid (Coutlakis et al., 2002). Gram stains are positive in 40% to 70% of septic arthritis patients (Ross, 2017), although, in a study by McBride et al., 543 samples of septic arthritis in adults, only 40% had a positive synovial fluid culture (McBride et al., 2020). In another conducted by Daynes et al.,55% of 183 adult patients with native septic arthritis had positive synovial fluid cultures, while 54% of 65 patients with native septic arthritis had positive blood cultures; 91% of the blood culture results were identical to the joint fluid culture results. Other pathogens isolated from joint fluid cultures were MRSA, *Streptococcus* species, *Pseudomonas*, and others (Daynes et al., 2016). Automatic mPCR demonstrated at least equivalent performance to synovial fluid culture in diagnosing septic arthritis, with the tremendous advantage of a shorter time (Sigmund et al., 2019). Another study found that the PCR test for septic arthritis identified the bacterial etiology better (Coulin et al., 2021). In a single-center, cross-sectional investigation involving 95 patients, 16s rDNA PCR in synovial fluid did not improve the diagnostic performance of septic arthritis in native adult joints, particularly for Gram-positive cocci infections (Coiffier et al., 2019).

Because the pathogen culture has a high risk of false-negative results and is time-consuming, new timely diagnostic procedures are required. NGS has emerged as an enabling technological platform for detecting and taxonomic characterizing microorganisms in clinical samples from patients (Gu et al., 2019). Considering that almost all infectious agents contain DNA or RNA genomes, NGS has become an indispensable tool for detecting and classifying microorganisms in patient samples. NGS plays a crucial role in etiological discovery; the 2019-nCoV was initially discovered using NGS (Zhu et al., 2020). In patients with prosthetic joint infection, targeted antibiotic treatment for culture-negative infection based on metagenomic NGS (mNGS) results resulted in a favorable outcome. The mNGS test is reliable for identifying pathogens associated with culture-negative prosthetic joint infection (Tarabichi et al., 2018; Wang et al., 2020). Preoperative aspirated synovial fluid detected by mNGS provides more aetiological information than preoperative culture (Fang et al., 2021), and NGS is more accurate and sensitive than bacterial culture and serological indicators such as CRP, IL-6, and PCT for identifying prosthetic joint infection (Yin et al., 2021). In a study by Huang et al., a total of 130 samples from 92 patients with osteoarticular infections, the overall sensitivity of mNGS was 88.5%; however, the sensitivity of joint fluid samples was much greater, as shown in Figure 1. mNGS identified Coagulase-negative *Staphylococci*, Gram-negative Bacillus, Streptococci, Anaerobe, non-tuberculous *mycobacterium*, and *Mycoplasma* as pathogens. However, the sensitivity of mNGS was greater in antibiotic-treated samples than in microbiological cultures (Huang et al., 2020). NGS identified bacteria at a higher incidence in the skin, and deep tissue

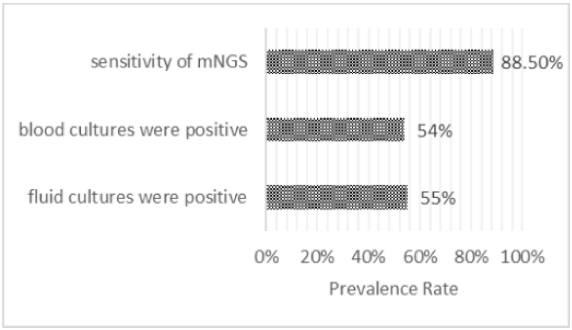

FIGURE 1
Compares the diagnostic value among mNGS, blood culture, and synovial fluid culture. (A total of 130 samples from 92 patients with osteoarticular infection account for the sensitivity of mNGS (Welling et al., 2018), while others were derived from another study altogether, 183 adult patients with septic arthritis (Kennedy et al., 2015)).

samples than conventional culture did in indigenous, non-infected subjects undergoing initial operations. Before NGS may be utilized reliably in orthopedic cases (Rao et al., 2020), it is necessary to evaluate which NGS data are clinically significant and which are false positives.

6 Imaging

Within one week of onset, X-ray and CT images of the articular structures are largely normal or reveal primarily soft tissue swelling, muscle space blurring, and joint space enlargement due to joint effusion. There is no obvious specificity, and with the improvement of economic living standards, there has been an increase in the number of patients seeking medical attention at the earliest stages of the disease, so X-rays and CT are limited in their ability to diagnose early septic arthritis. However, X-rays and CT are helpful in the differential diagnosis of acute osteomyelitis.

In patients with septic arthritis, MRI can detect the destruction of articular cartilage, characterized by rough, fuzzy, and shedding articular cartilage, and increased T2WI and PDWI signals at the damaged site, bone marrow edema. This is manifested as focal T2WI and PDWI signal increase of articular bones, and soft tissue edema is manifested as diffuse swelling of the soft tissue around the synovium, with increased T2WI and PDWI signals (Kang et al., 2020). In other cases, multiple abscess cavities can be seen in the surrounding soft tissue, which manifests as multiple cystic structures in the soft tissue around the joint. The enhanced scan shows a ring-enhanced lesion, purulent joints inflammatory synovial tissues that are hyperplasia, showing that the joint capsule synovium is thickened, the enhanced scan is enhanced, and even the intra-articular ligaments are wrapped. The joint cavity effusion manifests as the cavity's long T1WI and long T2WI signals. Pediatric septic arthritis can be accompanied by metaphyseal osteomyelitis, epiphyseal osteomyelitis, or abscess, manifested by a low signal on T1WI and a high signal on T2WI. A lamellar periosteal reaction can sometimes be seen at the metaphysis (Karchevsky et al., 2004). Synovial enhancement, peri synovial edema, and joint effusion are most commonly correlated with the clinical diagnosis of a septic joint (Karchevsky et al., 2004). Independent associations of risk for septic arthritis include synovial fluid WBC ≥ 30,000/ml, bacteria reported on synovial fluid gram stain, duration of pain >2 days, and history of septic arthritis at any joint (Holzmeister et al., 2021). MRI should be utilized to diagnose suspected septic arthritis (Monsalve et al., 2015). As demonstrated in Table 1, the differential diagnosis included joint tuberculosis, rheumatoid arthritis, rheumatoid arthritis, gouty arthritis, and osteoarthritis synovitis.

7 Antibiotics therapy

Early and appropriate administration of antibiotics (without waiting for bacteriological results) and immobilization of the afflicted limb are required. Antibiotics require thoroughly evaluating the patient's medical history and clinical symptoms. If there is sepsis or septic shock, antibiotics must be de-escalated empirically. *Staphylococcus aureus* has the highest resistance to penicillin, reaching 96%, and is sensitive to vancomycin, teicoplanin, linezolid, rifampicin, amikacin, Gentamicin, and ciprofloxacin; *Klebsiella pneumoniae* and *Escherichia coli* have a higher sensitivity to meropenem and imipenem, cephalosporin third generation, ciprofloxacin, and tetracycline. Nevertheless, rifampicin, amikacin, Gentamicin, tetracycline, and ciprofloxacin have relatively large side effects, and children are generally unsuitable for use (Clerc et al., 2011).

No substantial rise in resistance microorganisms causing septic arthritis was identified in a retrospective research period of 15 years involving 85 patients with septic arthritis; these results lend support to the use of narrow-spectrum antimicrobials on an empirical basis for septic arthritis (Ben-Chetrit et al., 2020).

For babies younger than three months, empiric therapy for septic arthritis should target *Staphylococcus aureus, Streptococcus, and Gram-negative bacilli*. The preferred treatment is nafcillin or vancomycin coupled with cefotaxime or ceftazidime (if *Pseudomonas* is suspected). *Staphylococcus aureus* and other gram-positive organisms should be the focus of empirical therapy for septic arthritis in children 3 months (for example, *Group A Streptococcus, Streptococcus pneumoniae*). Clindamycin, or a cephalosporin of the first generation, is a suitable treatment. If the youngster is not immunized against *Haemophilus influenzae*, ampicillin or amoxicillin should be administered. If just 10%-15% of the isolated bacteria are MRSA and the child is hemodynamically stable, cefazolin and nafcillin can be explored for treatment. If 10%-15% of the isolated bacteria are MRSA, it is advised to administer clindamycin and vancomycin. Consider *Streptococcus pneumoniae* resistant to penicillin, vancomycin, and clindamycin. If the infection is highly suspected to be Gram-negative *bacilli*, providing cephalosporins of the second or third generation is advisable. Cephalosporins (such as cefazolin, cefotaxime, and ceftriaxone) can typically be used to treat Chinchilla infections, although they are resistant to vancomycin and typically resistant to clindamycin and *staphylococcus* Resistant to a penicillin (nafcillin) (Erkilinc et al., 2021). Corticosteroids may enhance the proportion of patients without discomfort and the proportion of patients with the normal function of the afflicted joint at 12 months, as well as decrease the number of days children

require antibiotic treatment (Delgado-Noguera et al., 2018). Therefore, preoperative antibiotics should be avoided in children after septic arthritis was not proven to be diagnosed. Therefore, antibiotics should not be administered to children with an unconfirmed diagnosis of septic arthritis. Their prescription delays the diagnosis and ultimate surgery, causing extra problems and washouts (MacLean et al., 2015).

For empirical coverage of large-joint septic arthritis, Amoxicillin/clavulanate or cefuroxime would be sufficient for large-joint infections. Infections of tiny joints in diabetics would be much better treated with a broad-spectrum antibiotic. Systematic coverage of MRSA is not justified, although known carriers should be considered (Clerc et al., 2011).

Antibiotic courses of 3 to 4 weeks are usually adequate for uncomplicated bacterial arthritis. Treatment duration should be extended to 6 weeks if there is imaging evidence of accompanying osteomyelitis (Ross, 2017). In a prospective, unblinded, randomized, non-inferiority study comparing either 2 or 4 weeks of antibiotic therapy after surgical drainage of native joint bacterial arthritis in adults, 2 weeks of targeted antibiotic therapy is not inferior to 4 weeks regarding cure rate, adverse events, or sequelae. It leads to a significantly shorter hospital stay, as Figure 2 showed, at least for hand and wrist arthritis (Gjika et al., 2019). For uncomplicated native joints with septic arthritis of the hand, current evidence suggests that a 2-week course of antibiotic therapy following surgery cured septic arthritis (Sendi et al., 2020).

8 Surgical procedures

Once a patient is diagnosed with septic arthritis characterized by joint discomfort, reduced mobility, and inability to bear weight, he or she should have surgery or arthroscopy for irrigation and debridement to drain purulent fluid (Cargnelli, 2015; Memon et al., 2018). In the absence of clinical sepsis, early joint drainage does not appear to improve the risk of sequelae for native septic arthritis compared to delayed drainage (Lauper et al., 2018). Nevertheless, pathogen type and comorbid diseases did not affect the length of stay (Daynes et al., 2016). In a retrospective study of 79 patients with septic knee arthritis, effective treatment needed an average of 1.3 operations. With arthroscopic irrigation and debridement, most patients with septic knee arthritis need only one surgical surgery to eliminate the infection. From the symptom beginning to surgery, the necessity for several interventions increases (Dave et al., 2016).

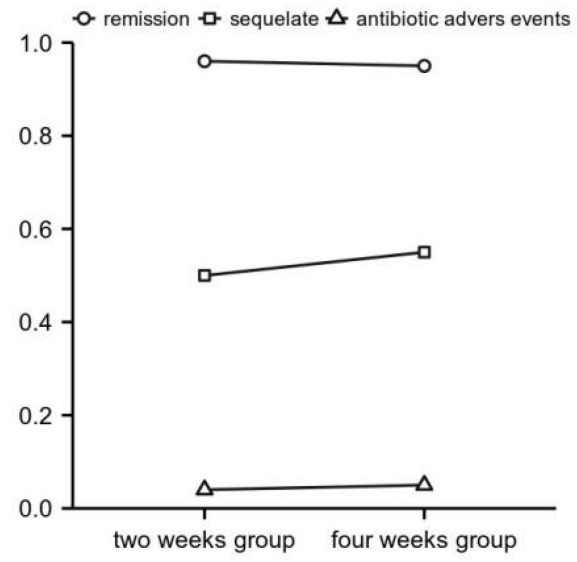

FIGURE 2
Outcomes of arthritis therapy of the hands and wrists (subgroup analysis). X-axis: study outcome parameters. Y-axis: number of corresponding episodes with proportions and absolute number of cases (Ross, 2017).

Arthroscopic surgery can treat joint cavity infections with debridement under the microscope, continuous closed lavage and drainage, harmful bacteria disappear rapidly, infection control is dependable, antibiotics are employed for a short period, and the efficacy is satisfactory. Arthroscopic treatment for acute native knee septic arthritis was a more successful index surgery, required fewer total irrigation procedures, and had a lower reinfection rate and low initial inflammatory response than existing treatment (Peres et al., 2016). After arthroscopic treatment, the patient's long-term range of motion was much greater (Johns et al., 2017). A Systematic Review concluded that arthroscopic native hip irrigation and debridement for septic arthritis appear to comprise a safe and effective treatment option for selected patients (Cargnelli, 2015). Arthroscopic management may be a safe option for treating hip septic arthritis with potentially limited morbidity (Lee et al., 2014; Khazi et al., 2020). For septic shoulder arthritis, most patients with septic arthritis of native shoulders were effectively treated with a single arthroscopic irrigation and debridement (Joo et al., 2020). However, systematic reviews showed that arthroscopic surgery and open Arthrotomy have similar efficacy, although arthroscopic native shoulder septic arthritis had the results of pain alleviation and joint movement recovery; unfortunately, there was a high reoperation rate (Memon et al., 2018; Bovonratwet et al., 2019).

Continuous irrigation of the joint cavity is an option for patients undergoing unconditional arthroscopic surgery or those with shallow joints. It is necessary to make two holes in the joints, one for the intake tube and one for the outlet tube. Daily perfusion of 2000-3000 ml antibiotic-containing saline through the catheter, the outlet tube has a clear liquid, and the lavage can be stopped after culture without bacterial growth, but drainage The tube still needs to be sucked for several days until the drainage volume is reduced to no fluid outflow, and the local symptoms and signs have disappeared (Johns et al., 2017). Surgical joint incision and drainage are required for intra-articular infection caused by the prosthesis around the joint (Smith et al., 2006).

9 Treatment outcomes and prognosis

A retrospective cohort analysis included 12132 patients with septic arthritis who underwent arthroscopic knee washing in England between 1997 and 2017. Among 10 195 (84%) patients with septic arthritis as the primary admission diagnosis, the 90-day

mortality rate was 7.05 percent, but 22.69% in 1842 patients older than 79. The 1-year rates for arthrodesis, amputation and arthroplasty were 0.13%, 0.40%, and 1.33%, respectively. Within 15 years of follow-up, 8.76% of patients had undergone arthroplasty, equating to a risk of arthroplasty six times that of the general population (Abram et al., 2020).

In contrast to the knee, it is envisaged that septic arthritis of the shoulder will result in a severe loss of function (Gramlich et al., 2020). Long-term recurrence of glenohumeral fractures following clinically effective therapy Joint septic arthritis is uncommon, and few patients get elective arthroplasty after septic shoulder arthritis (Sweet et al., 2019). If the therapies were ineffective, the death rate at 30 days was 2% and increased to 6% after 90 days (Kennedy et al., 2015). Treatment failure was independently linked with joint size, age, intra-articular non-arthroplasty prosthesis, and surgical procedures performed. Small-joint septic arthritis has a better prognosis than large-joint septic arthritis and may be treated safely with shorter antibiotic courses (McBride et al., 2020). Injection drug use is a growing cause of septic knee admissions and is related to greater rates of death, recurrent arthroscopic or open irrigation, and debridement (Oh et al., 2018). A retrospective single-center study of 186 patients with native septic arthritis revealed that Staphylococcus aureus infection, endocarditis, and the involvement of joints difficult to access with needle drainage predict treatment failure and that age, baseline leukocyte count, bacteremia, diabetes, and chronic renal failure predict mortality (Maneiro et al., 2015). In Old age, anginosus group streptococci, *enterococci*, and polymicrobial infections predicted poor outcomes, while antibiotic treatment duration can likely be shortened (Kaandorp et al., 1995). MRSA was identified as a risk factor for an unplanned return to the operating room after arthroscopic treatment (Jaffe et al., 2017). *Staphylococcus aureus* is an independent risk factor for the recurrence of infections after surgical treatment of shoulder septic arthritis (Böhler et al., 2017).

Patients with septic arthritis of the shoulder frequently experience substantial systemic complications regardless of the treatment method. Septicemia was a common complication among all treatment groups, with cultures most frequently indicating *Staphylococcus aureus* as the causative organism (Jiang et al., 2017). Adults with a history of inflammatory arthropathy, involvement of a large joint, a synovial-fluid nucleated cell count of >85.0 × 109 cells/L, infection with S. aureus, or a history of diabetes had a higher risk of failure of a single surgical debridement for acute septic arthritis and requiring additional surgical debridement (Hunter et al., 2015).

10 Conclusions

Notwithstanding the pressing need for prompt diagnosis and intervention, a dearth of comprehensive data pertaining to various facets of its management at an advanced level exists. Septic arthritis of an acute nature primarily impacts the joints of the hip and knee. Staphylococcus aureus and Streptococcus are the predominant pathogenic microorganisms. Diagnosis of septic arthritis is typically straightforward based on clinical manifestations, laboratory findings, and MRI. Early and appropriate administration of antibiotics for 2-4 weeks is imperative. Arthroscopic surgery is a minimally invasive approach that yields favorable outcomes for treating septic arthritis. In cases where the ordering providers encounter challenging scenarios, effective communication between the radiologist and the providers can be facilitated by the radiologist's up-to-date knowledge of the latest research. This can enable the radiologist to provide valuable insights and recommend a joint aspiration procedure. A cooperative effort among radiologists, orthopaedic surgeons, and other medical professionals is necessary to enhance patient outcomes.

Author contributions

MH, DTAV, and PL have contributed equally to this work and shared the first authorship did the writing—original draft preparation, Conceptualization, Writing - review & editing and Data curation and Software; HZ and GY did Methodology, Data curation and Investigation; BL and FZ did the Supervision, the Project administration and Validation. All authors contributed to the article and approved the submitted version.

Funding

This study was supported by the National Natural Science Foundation of China (81501023, 81874034, 81902303), the Rui E (Ruiyi) Emergency Medical Research Special Funding Project (No.R2019007) and the Natural Science Foundation of Changsha City (No.kq2208380).

Conflict of interest

The authors declare that the research was conducted in the absence of any commercial or financial relationships that could be construed as a potential conflict of interest.

Publisher's note

References

Abram, S. G. F., Alvand, A., Judge, A., Beard, D. J., and Price, A. J. (2020). Mortality and adverse joint outcomes following septic arthritis of the native knee: a longitudinal cohort study of patients receiving arthroscopic washout. *Lancet Infect. Dis.* 20 (3), 341–349. doi: 10.1016/S1473-3099(19)30419-0

Al Saadi, M. M., Al Zamil, F. A., Bokhary, N. A., Al Shamsan, L. A., Al Alola, S. A., and Al Eissa, Y. S. (2009). Acute septic arthritis in children. *Pediatr. Int.* 51, 377–380. doi: 10.1111/j.1442-200X.2008.02791.x

Balabaud, L., Gaudias, J., Boeri, C., Jenny, J.-Y., and Kehr, P. (2007). Results of treatment of septic knee arthritis: a retrospective series of 40 cases. *Knee Surg. Sports Traumatol Arthrosc* 15, 387–392. doi: 10.1007/s00167-006-0224-5

Ben-Chetrit, E., Zamir, A., Natsheh, A., Nesher, G., Wiener-Well, Y., and Breuer, G. S. (2020). Trends in antimicrobial resistance among bacteria causing septic arthritis in adults in a single center: A 15-years retrospective analysis. *Internal Emergency Med.* 15 (4), 655–661. doi: 10.1007/s11739-019-02244-8

Ben-Zvi, L., Sebag, D., Izhaki, G., Katz, E., and Bernfeld, B. (2019). Diagnosis and management of infectious arthritis in children. *Curr. Infect. Dis. Rep.* 21 (7), 1-12. doi: 10.1007/s11908-019-0678-5

Böhler, C., Pock, A., Waldstein, W., Staats, K., Puchner, S. E., Holinka, J., et al. (2017). Surgical treatment of shoulder infections: a comparison between arthroscopy and Arthrotomy. *J. Shoulder Elbow Surg.* 26 (11), 1915–1921. doi: 10.1016/j.jse.2017.04.001

Bovonratwet, P., Fu, M. C., Pathak, N., Ondeck, N. T., Bohl, D. D., Nho, S. J., et al. (2019). Surgical treatment of septic shoulders: A comparison between arthrotomy and arthroscopy. *Arthroscopy-the J. Arthroscopic Related Surg.* 35 (7), 1984–198+. doi: 10.1016/j.arthro.2019.02.036

Bowakim, J., Marti, R., and Curto, A. (2010). Elbow septic arthritis in children: clinical presentation and management. *J. Pediatr. Orthopaedics-Part B* 19 (3), 281–284. doi: 10.1097/BPB.0b013e3283387d2d

Butt, U., Amissah-Arthur, M., Khattak, F., and Elsworth, C. F. (2011). What are we doing about septic arthritis? a survey of UK-based rheumatologists and orthopedic surgeons. *Clin. Rheumatol* 30, 707–710. doi: 10.1007/s10067-010-1672-3

Cargnelli, S., Catapano, M., Peterson, D., Simunovic, N., Larson, C. M., Ayeni, O. R., et al. (2015). Efficacy of hip arthroscopy for the management of septic arthritis: A systematic review. *Arthroscopy-the J. Arthroscopic Related Surg.* 31 (7), 1358–1370. doi: 10.1016/j.arthro.2014.12.028

Castellazzi, L., Mantero, M., and Esposito, S. (2016). Update on the management of pediatric acute osteomyelitis and septic arthritis. *Int. J. Mol. Sci.* 17 (6), 855. doi: 10.3390/ijms17060855

Chan, B. Y., Crawford, A. M., Kobes, P. H., Allen, H., Leake, R. L., Hanrahan, C. J., et al. (2020). Septic arthritis: an evidence-based review of diagnosis and image-guided aspiration. *Am. J. Roentgenology* 215 (3), 568–581. doi: 10.2214/AJR.20.22773

Clerc, O., Prod'hom, G., Greub, G., Zanetti, G., and Senn, L. (2011). Adult native septic arthritis: a review of 10 years of experience and lessons for empirical antibiotic therapy. *J. Antimicrobial Chemotherapy* 66 (5), 1168–1173. doi: 10.1093/jac/dkr047

Cohen, E., Katz, T., Rahamim, E., Bulkowstein, S., Weisel, Y., and Leibovitz, R. (2020). Septic arthritis in children: updated epidemiologic, microbiologic, clinical and therapeutic correlations. *Pediatr. Neonatol.* 61, 325–330. doi: 10.1016/j.pedneo.2020.02.006

Coiffier, G., David, C., Gauthier, P., Le Bars, H., Guggenbuhl, P., Jolivet-Gougeon, A., et al. (2019). Broad-range 16 s rDNA PCR in synovial fluid does not improve the diagnostic performance of septic arthritis in native joints in adults: cross-sectional single-center study in 95 patients. *Clin. Rheumatol* 38 (7), 1985–1992. doi: 10.1007/s10067-019-04492-7

Couderc, M., Bart, G., Coiffier, G., Godot, S., Seror, R., Ziza, J. M, et al. (2020). French recommendations on the management of septic arthritis in an adult native joint. *Joint Bone Spine* 87 (6), 538–547. doi: 10.1016/j.jbspin.2020.07.012

Coulin, B., Demarco, G., Spyropoulou, V., Juchler, C., Vendeuvre, T., Habre, C., et al. (2021). Osteoarticular infection in children an update on the epidemiological, clinical, and biological features of kingella kingae. *Bone Joint J.* 103B (3), 578–583. doi: 10.1302/0301-620X.103B3.BJJ-2020-0936.R2

Coutlakis, P. J., Roberts, W. N., and Wise, C. M. (2002). Wise, Another look at synovial fluid leukocytosis and infection. *Jcr-Journal Clin. Rheumatol.* 8 (2), 67–71. doi: 10.1097/00124743-200204000-00001

Dave, O. H., Patel, K. A., Andersen, C. R., and Carmichael, K. D. (2016). Surgical procedures needed to eradicate infection in knee septic arthritis. *Orthopedics* 39 (1), 50–54. doi: 10.3928/01477447-20151222-05

Daynes, J., Roth, M. F., Zekaj, M., Hudson, I., Pearson, C., and Vaidya, R. (2016). Adult native septic arthritis in an inner city hospital: effects on length of stay. *Orthopedics* 39 (4), e674–e679. doi: 10.3928/01477447-20160419-01

Delgado-Noguera, M. F., Delgadillo, J. M.F., Franco, A. A., Vazquez, J. C., and Calvache, J. A. (2018). Corticosteroids for septic arthritis in children. *Cochrane Database Systematic Rev.* 11. doi: 10.1002/14651858.CD012125.pub2

Donders, C. M., Spaans, A. J., van Wering, H., and van Bergen, C. J. (2022). Developments in diagnosis and treatment of paediatric septic arthritis. *World J. Orthop.* 13 (2), 122–130. doi: 10.5312/wjo.v13.i2.122

Dubost, J.-J., Couderc, M., Tatar, Z., Tournadre, A., Lopez, J., Mathieu, S., et al. (2014). Three-decade trends in the distribution of organisms causing septic arthritis in native joints: Single-center study of 374 cases. *Joint Bone Spine* 81 (5), 438–440. doi: 10.1016/j.jbspin.2014.05.001

Erkilinc, M., Gilmore, A., Weber, M., and Mistovich, R. J. (2021). Current concepts in pediatric septic arthritis. *J. Am. Acad. Orthop Surg.* 29, 196–206. doi: 10.5435/JAAOS-D-20-00835

Fang, X., Cai, Y., Mei, J., Huang, Z., Zhang, C., Yang, B., et al. (2021). Optimizing culture methods according to preoperative mNGS results can improve joint infection diagnosis. *Bone Joint J.* 103B (1), 39–45. doi: 10.1302/0301-620X.103B1.BJJ-2020-0771.R2

Forlin, E., and Milani, C. (2008). Sequelae of septic arthritis of the hip in children: a new classification and a review of 41 hips. *J. Pediatr. Orthop.* 28, 524–528. doi: 10.1097/BPO.0b013e31817bb079

Gafur, O. A., Copley, L. A., Hollmig, S. T., Browne, R. H., Thornton, L. A., Crawford, S. E., et al. (2008). The impact of the current epidemiology of pediatric musculoskeletal infection on evaluation and treatment guidelines. *J. Pediatr. Orthop.* 28, 777–785. doi: 10.1097/BPO.0b013e318186eb4b

Geirsson, A., Statkevicius, S., and Vikingsson, A. (2008). Septic arthritis in Iceland 1990–2002: increasing incidence due to iatrogenic infections. *Ann. Rheum Dis.* 67 (5), 638–643. doi: 10.1136/ard.2007.077131

Gjika, E., Beaulieu, J. Y., Vakalopoulos, K., Gauthier, M., Bouvet, C., Gonzalez, A., et al. (2019). Two weeks versus four weeks of antibiotic therapy after surgical drainage for native joint bacterial arthritis: a prospective, randomised, non-inferiority trial. *Ann. Rheumatic Dis.* 78 (8), 1114–1121. doi: 10.1136/annrheumdis-2019-215116

Gottlieb, M., Holladay, D., and Rice, M. (2019). Current approach to the evaluation and management of septic arthritis. *Pediatr. Emergency Care* 35 (7), 509–513. doi: 10.1097/PEC.0000000000001874

Gramlich, Y., Klug, A., Walter, G., Kremer, M., Hoffmann, R., and Kemmerer, M. (2020). Septic arthritis of native shoulder and knee joint: What are the differences in bacterial spectrum, treatment, and outcome? *Surg. Infections* 21 (4), 391–397. doi: 10.1089/sur.2019.245

Gu, W., Miller, S., and Chiu, C. Y. (2019). Clinical metagenomic next-generation sequencing for pathogen detection. In A. K. Abbas, K. C. Aster and M. B. and Feany, editors. *Annu. Rev. Pathol.*. 14, 319–338. doi: 10.1146/annurev-pathmechdis-012418-012751

Gupta, M. N., Sturrock, R. D., and Field, M. (2001). A prospective 2 year study of 75 patients with adultonset septic arthritis. *Rheumatology* 40 (1), 24–30. doi: 10.1093/rheumatology/40.1.24

Holzmeister, A., Frazzetta, J., Yuan, F. F.N., Cherones, A., Summers, H., Cohen, J., et al. (2021). Evaluation for septic arthritis of the native adult knee is aided by multivariable assessment. *Am. J. Emergency Med.* 46, 614–618. doi: 10.1016/j.ajem.2020.11.048

Horowitz, D. L., Katzap, E., Horowitz, S., and Barilla-LaBarca, M. L. (2011). Approach to septic arthritis. *Am. Fam Physician.* 84, 653–660.

Huang, Z.-d., Zhang, Z. J., Yang, B., Li, W. B., Zhang, C. J., Fang, X. Y., et al. (2020). Pathogenic detection by metagenomic next-generation sequencing in osteoarticular infections. *Front. Cell. Infect. Microbiol.* 10, 471. doi: 10.3389/fcimb.2020.00471

Hunter, J. G., Gross, J. M., Dahl, J. D., Amsdell, S. L., and Gorczyca, J. T. (2015). Risk factors for failure of a single surgical debridement in adults with acute septic arthritis. *J. Bone Joint Surg.* 97A (7), 558–564. doi: 10.2106/JBJS.N.00593

Ilharreborde, B. (2015). Sequelae of pediatric osteoarticular infection. *Orthop Traumatol Surg. Res.* 101 (suppl 1), S129–S137. doi: 10.1016/j.otsr.2014.07.029

Jaffe, D., Costales, T., Greenwell, P., Christian, M., Henn, III, and , R. F. (2017). Methicillin-Resistant Staphylococcus aureus Infection Is a Risk Factor for Unplanned Return to the Operating Room in the Surgical Treatment of a Septic Knee. *J. Knee Surg.* 30 (9), 872–878. doi: 10.1055/s-0037-1598079

Jiang, J. J., Piponov, H. I., Mass, D. P., Angeles, J. G., and Shi, L. L. (2017). Septic arthritis of the shoulder: A comparison of treatment methods. *J. Am. Acad. Orthopaedic Surgeons* 25 (8), E175–E184. doi: 10.5435/JAAOS-D-16-00103

Johns, B. P., Loewenthal, M. R., and Dewar, D. C. (2017). Open compared with arthroscopic treatment of acute septic arthritis of the native knee. *J. Bone Joint Surg.* 99 (6), 499–505. doi: 10.2106/JBJS.16.00110

Joo, Y.-B., Lee, W. Y., Shin, H. D., Kim, K. C., and Kim, Y. K. (2020). Risk factors for failure of eradicating infection in a single arthroscopic surgical procedure for septic arthritis of the adult native shoulder with a focus on the volume of irrigation. *J. Shoulder Elbow Surg.* 29 (3), 497–501. doi: 10.1016/j.jse.2019.07.014

Jung, S. W., Kim, D. H., Shin, S. J., Kang, B. Y., Eho, Y. J., and Yang, S. W. (2018). Septic arthritis associated with systemic sepsis. *International Orthopaedics* 42 (1), 1–7. doi: 10.1007/s00264-017-3565-4

Kaandorp, C. J. E., Schaardenburg, D. V., Krijnen, P., Habbema, J. D. F., and Van de Laar, M. S. F. J. (1995). Risk factors for septic arthritis in patients with joint disease. *Arthritis Rheum* 38, 1819–1825. doi: 10.1002/art.1780381215

Kang, M. S., Jeon, J. Y., and Park, S.-S. (2020). Differential MRI findings of transient synovitis of the hip in children when septic arthritis is suspected according to symptom

duration. *J. Pediatr. Orthopaedics-Part B* 29 (3), 297–303. doi: 10.1097/BPB.0000000000000671

Karchevsky, M., Schweitzer, M. E., Morrison, W. B., and Parellada, J. A. (2004). MRI findings of septic arthritis and associated osteomyelitis in adults. *Am. J. Roentgenology* 182 (1), 119–122. doi: 10.2214/ajr.182.1.1820119

Kennedy, N., Chambers, S. T., Nolan, I., Gallagher, K., Werno, A., Browne, M., et al. (2015). Native joint septic arthritis: epidemiology, clinical features, and microbiological causes in a new zealand population. *J. Rheumatol.* 42 (12), 2392–2937. doi: 10.3899/jrheum.150434

Khazi, Z. M., Cates, W. T., An, Q., Duchman, K. R., Wolf, B. R., Westermann, R. W., et al. (2020). Arthroscopy Versus Open Arthrotomy for Treatment of Native Hip Septic Arthritis: An Analysis of 30-Day Complications. *Arthroscopy-the J. Arthroscopic Related Surg.* 36 (4), 1048–1052. doi: 10.1016/j.arthro.2019.10.008

Knapper, T., Murphy, R. J., Rocos, B., Fagg, J., Murray, N., and Whitehouse, M. R. (2021). Utility of bedside leucocyte esterase testing to rule out septic arthritis. *Emergency Med. J.* 38 (9), 707–710. doi: 10.1136/emermed-2020-209842

Kocher, M. S., Mandiga, R., Murphy, J. M., Goldmann, D., Harper, M., Sundel, R., et al. (2003). A clinical practice guideline for treatment of septic arthritis in children: efficacy in improving process of care and effect on outcome of septic arthritis of the hip. *J. Bone Joint Surg.* 85 (6), 994–999. doi: 10.2106/00004623-200306000-00002

Lane, J. G., Falahee, M. H., Wojtys, E. M., Hankin, F. M., and Kaufer, H. (1990). Pyarthrosis of the knee. treatment considerations. *Clin. Orthop Relat. Res.* 252, 198–204. doi: 10.1097/00003086-199003000-00029

Lauper, N., Davat, M., Gjika, E., Müller, C., Belaieff, W., Pittet, D., et al. (2018). Native septic arthritis is not an immediate surgical emergency. *J. Infect.* 77 (1), 47–53. doi: 10.1016/j.jinf.2018.02.015

Lee, Y.-K., Park, K. S., Ha, Y. C., and Koo, K. H. (2014). Arthroscopic treatment for acute septic arthritis of the hip joint in adults. *Knee Surg. Sports Traumatology Arthroscopy* 22 (4), 942–945. doi: 10.1007/s00167-012-2283-0

Long, B., Koyfman, A., and Gottlieb, M. (2019). Evaluation and management of septic arthritis and its mimics in the emergency department. *Western J. Emergency Med.* 20 (2), 331–341. doi: 10.1007/s00167-012-2283-0

Lotz, H., Strahm, C., Zdravkovic, V., Jost, B., and Albrich, W. C. (2019). Septic arthritis due to streptococci and enterococci in native joints: a 13 year retrospective study. *Infection* 47 (5), 761–770. doi: 10.1007/s15010-019-01301-w

MacLean, S. B. M., Timmis, C., Evans, S., Lawniczak, D., Nijran, A., and Bache, E. (2015). Preoperative antibiotics for septic arthritis in children: delay in diagnosis. *J. Orthopaedic Surg.* 23 (1), 80–83. doi: 10.1177/230949901502300119

Maneiro, J., Souto, A., Cervantes, E., Mera, A., Carmona, L., and Gomez-Reino, J. (2015). Predictors of treatment failure and mortality in native septic arthritis. *Clin. Rheumatol.* 34 (11), 1961–1967. doi: 10.1007/s10067-014-2844-3

Margaretten, M. E., Kohlwes, J., Moore, D., and Bent, S. (2007). Does this adult patient have septic arthritis? *JAMA* 297 (13), 1478–1488. doi: 10.1001/jama.297.13.1478

Mathews, C. J., Weston, V. C., Jone, A., Filed, M., and Coakley, G. (2010). Bacterial septic arthritis in adults. *Lancet* 375, 846–855. doi: 10.1016/S0140-6736(09)61595-6

McBride, S., Mowbray, J., Caughey, W., Wong, E., Luey, C., Siddiqui, A., et al. (2020). Epidemiology, management, and outcomes of large and small native joint septic arthritis in adults. *Clin. Infect. Dis.* 70 (2), 271–279. doi: 10.1093/cid/ciz265

McNabb, D. C., Dennis, D. A., Kim, R. H., Miner, T. M., Yang, C. C., and Jennings, J. M. (2017). Determining false positive rates of leukocyte esterase reagent strip when used as a detection tool for joint infection. *The Journal of Arthroplasty* 32 (1), 220–222. doi: 10.1016/j.arth.2016.05.065

Memon, M., Kay, J., Ginsberg, L., de Sa, D., Simunovic, N., Samuelsson, K., et al. (2018). Arthroscopic management, and outcomes of large and small native joint septic arthritis in adults. *Arthroscopy-the J. Arthroscopic Related Surg.* 34 (2), 625. doi: 10.1016/j.arthro.2017.07.038

Momodu, I. I., and Savaliya, V. (2022). *Septic arthritis StatPearls* (StatPearls Publishing).

Monsalve, J., Kan, J. H., Schallert, E. K., Bisset, G. S., Zhang, W., and Rosenfeld, S. B. (2015). Septic arthritis in children: Frequency of coexisting unsuspected osteomyelitis and implications on imaging work-up and management. *Am. J. Roentgenology* 204 (6), 1289–1295. doi: 10.2214/AJR.14.12891

Montgomery, N. I., and Epps, H. R. (2017). Pediatric septic arthritis. *Orthop Clin. North Am.* 48, 209–216. doi: 10.1016/j.ocl.2016.12.008

Mooney, J. F. III, and Murphy, R. F. (2019). Septic arthritis of the pediatric hip: update on diagnosis and treatment. *Curr. Opin. Pediatr.* 31 (1), 79–85. doi: 10.1097/MOP.0000000000000703

Morgan, D. S., Fisher, D., Merianos, A., and Currie, B. J. (1996). An 18 year clinical review of septic arthritis from tropical Australia. *Epidemiol. Infect.* 117 (3), 423–428. doi: 10.1017/S0950268800059070

Moro-Lago, I., Talavera, G., Moraleda, L., and González-Morán, G. (2017). Clinical presentation and treatment of septic arthritis in children. *Rev. espanola cirugia ortopedica y traumatologia* 61 (3), 170–175. doi: 10.1016/j.recot.2017.02.002

Moumile, K., Merckx, J., Glorion, C., et al. (2005). Bacterial aetiology of acute osteoarticular infections in children. *Acta Paediatr.* 94, 419–422. doi: 10.1080/08035250410023278

Nossent, J. C., Raymond, W. D., Keen, H. I., Raymond, W. D., Keen, H. I., and Inderjeeth, C. A. (2021). Septic arthritis in children: a longitudinal population-based study in Western Australia. *Rheumatol Ther.* 8, 877–888. doi: 10.1007/s40744-021-00307-x

Oh, D. H. W., Wurcel, A. G., Tybor, D. J., Burke, D., Menendez, M. E., and Salzler, M. J. (2018). Increased Mortality and Reoperation Rates After Treatment for Septic Arthritis of the Knee in People Who Inject Drugs: Nationwide Inpatient Sample, 2000-2013. *Clin. Orthopaedics Related Res.* 476 (8), 1557–1565. doi: 10.1097/01.blo.0000534682.68856.d8

Okubo, Y., Nochioka, K., and Marcia, T. (2017). Nationwide survey of pediatric septic arthritis in the united states. *J. Orthop.* 14, 342–346. doi: 10.1016/j.jor.2017.06.004

Pääkkönen, M. (2017). Septic arthritis in children: diagnosis and treatment. *Pediatr. Health Med. Ther.* 8, 65–68. doi: 10.2147/PHMT.S115429

Peres, L. R., Marchitto, R. O., Pereira, G. S., Yoshino, F. S., de Castro Fernandes, M., and Matsumoto, M. H. (2016). Arthrotomy versus arthroscopy in the treatment of septic arthritis of the knee in adults: a randomized clinical trial. *Knee Surg. Sports Traumatology Arthroscopy* 24 (10), 3155–3162. doi: 10.1007/s00167-015-3918-8

Perry, C. R. (1999). Septic arthritis. *Am. J. Orthop* 28, 168–178.

Peters, W., Irving, J., and Letts, M. (1992). Long-term effects of neonatal bone and joint infection on adjacent growth plates. *J. Pediatr. Orthop.* 12, 806–810. doi: 10.1097/01241398-199211000-00020

Quick, R. D., Williams, J., Fernandez, M., Gottschalk, H., Cosgrove, P., Kahlden, K., et al. (2018). Improved diagnosis and treatment of bone and joint infections using an evidence-based treatment guideline. *J. Pediatr. Orthop.* 38, e354–e359. doi: 10.1097/BPO.0000000000001187

Rao, A. J., MacLean, I. S., Naylor, A. J., Garrigues, G. E., Verma, N. N., and Nicholson, G. P. (2020). Next-generation sequencing for diagnosis of infection: is more sensitive really better? *J. Shoulder Elbow Surg.* 29 (1), 20–26. doi: 10.1016/j.jse.2019.07.039

Riise, ØR, Handeland, K. S., Cvancarova, M., Wathne, K. O., Nakstad, B., Abrahamsen, T. G., et al. (2008). Incidence and characteristics of arthritis in Norwegian children: a population-based study. *Pediatrics.* 121, e299–e306. doi: 10.1542/peds.2007-0291

Ross, J. J. (2017). Septic arthritis of native joints. *Infect. Dis. Clin. N Am.* 3, 203–218. doi: 10.1016/j.idc.2017.01.001

Ross, J. J., Ard, K. L., and Carlile, N. (2020). Septic Arthritis and the Opioid Epidemic: 1465 Cases of Culture-Positive Native Joint Septic Arthritis From 1990-2018. *Open Forum Infect. Dis.* 7 (3), ofaa089. doi: 10.1093/ofid/ofaa089

Safdieh, G., Silberman, J., Nguyen, J., Doyle, S. M., Blanco, J. S., Scher, D. M., et al. (2019). Pediatric septic arthritis and osteomyelitis in the USA: a national KID database analysis. *HSS J.* 15, 159–166. doi: 10.1007/s11420-018-9644-2

Sendi, P., Kaempfen, A., Uçkay, I., and Meier, R. (2020). Bone and joint infections of the hand. *Clin. Microbiol. Infection* 26 (7), 848–856. doi: 10.1016/j.cmi.2019.12.007

Shirtlif, M. E., and Mader, J. T. (2002). Acute septic arthritis. *Clin. Microbiol. Rev.* 15, 527–544. doi: 10.1128/cmr.15.4.527-544

Sigmund, I. K., Holinka, J., Sevelda, F., Staats, K., Heisinger, S., Kubista, B., et al. (2019). Performance of automated multiplex polymerase chain reaction (mPCR) using synovial fluid in the diagnosis of native joint septic arthritis in adults. *Bone Joint J.* 101B (3), 288–296. doi: 10.1302/0301-620X.101B3.BJJ-2018-0868.R1

Synger, M.. (2016). The third international consensus definitions for sepsis and septic shock. *Jama* 315 (8), 801–810. doi: 10.1001/jama.2016.0287

Smith, J. W., Chalupa, P., and Hasan, M. S. (2006). Infectious arthritis: clinical features, laboratory findings and treatment. *Clin. Microbiol. Infection* 12 (4), 309–314. doi: 10.1111/j.1469-0691.2006.01366.x

Swarup, I., Meza, B. C., Weltsch, D., Jina, A. A., Lawrence, J. T., and Baldwin, K. D. (2020). Septic arthritis of the knee in children: a critical analysis review. *JBJS Rev.* 8, e0069. doi: 10.2106/JBJS.RVW.19.00069

Sweet, M. C., Sheena, G. J., Liu, S., Fisk, F. E., Lynch, J. R., and Muh, S. J. (2019). Clinical characteristics and long-term outcomes after septic arthritis of the native glenohumeral joint: A 20-year retrospective review. *Orthopedics* 42 (1), e118–e123. doi: 10.3928/01477447-20181227-01

Tarabichi, M. , Shohat, N., Goswami, K., and Parvizi, J. (2018). Can next generation sequencing play a role in detecting pathogens in synovial fluid? *Bone Joint J.* 100B (2), 127–133. doi: 10.1302/0301-620X.100B2.BJJ-2017-0531.R2

Tretiakov, M., Cautela, F. S., Walker, S. E., Dekis, J. C., Beyer, G. A., Newman, J. M., et al. (2019). Septic arthritis of the hip and knee treated surgically in pediatric patients: analysis of the kids' inpatient database. *J. Orthop.* 16, 97–100. doi: 10.1016/j.jor.2018.12.017

Villani, M. C., Hamilton, E. C., Klosterman, M. M., Jo, C., Kang, L. H., Copley, L. A., et al. (2021). Primary septic arthritis among children 6 to 48 months of age: Implications for pcr acquisition and empiric antimicrobial selection. *J. Pediatr. Orthopaedics* 41 (3), 190–196. doi: 10.1097/BPO.0000000000001744

Wang, C., et al. (2020). Can metagenomic next-generation sequencing identify the pathogens responsible for culture-negative prosthetic joint infection? *BMC Infect. Dis.* 20 (1).

Welling, B. D., Haruno, L. S., and Rosenfeld, S. B. (2018). Validating an algorithm to predict adjacent musculoskeletal infections in pediatric patients with septic arthritis. *Clin. Orthop Relat. Res.* 476, 153–159. doi: 10.1007/s11999.0000000000000019

Weston, V. C., Jones, A. C., Bradbury, N., Fawthrop, F., and Doherty, M. (1991). Clinical features and outcome of septic arthritis in a single UK health district 1982–1991. *Ann. Rheum Dis.* 58, 214–219. doi: 10.1136/ard.58.4.214

Yin, H., Xu, D., and Wang, D. (2021). Diagnostic value of next-generation sequencing to detect periprosthetic joint infection. *BMC Musculoskeletal Disord.* 22 (1), 1-9. doi: 10.1186/s12891-021-04116-9

Young, T. P., Maas, L., Thorp, A. W., and Brown, L. (2011). Etiology of septic arthritis in children: an update for the new millennium. *Am. J. Emergency Med.* 29 (8), 899–902.

Zhu, N., Zhang, D., Wang, W., Li, X., Yang, B., Song, J., et al. (2020). A Novel coronavirus from patients with pneumonia in China, 2019. *New Engl. J. Med.* 382 (8), 727–733. doi: 10.1056/NEJMoa2001017

frontiers | Frontiers in Cellular and Infection Microbiology

TYPE Original Research
PUBLISHED 24 May 2023
DOI 10.3389/fcimb.2023.1182480

OPEN ACCESS

EDITED BY
Chaofan Zhang,
First Affiliated Hospital of Fujian Medical University, China

REVIEWED BY
Rafael Franco-Cendejas,
National Institute of Rehabilitation Luis Guillermo Ibarra Ibarra, Mexico
Shaobo Yao,
First Affiliated Hospital of Fujian Medical University, China

*CORRESPONDENCE
Gang-Hua Tang
gtang0224@smu.edu.cn
Bin Yu
yubin@smu.edu.cn

RECEIVED 08 March 2023
ACCEPTED 11 May 2023
PUBLISHED 24 May 2023

CITATION
Ren S-Q, Ma Y, Fu L-L, Hu K-Z, Liang H-R, Yu B and Tang G-H (2023) A comparative ^{18}F-FDG and an anti-PD-L1 probe PET/CT imaging of implant-associated *Staphylococcus aureus* osteomyelitis. *Front. Cell. Infect. Microbiol.* 13:1182480. doi: 10.3389/fcimb.2023.1182480

A comparative ^{18}F-FDG and an anti-PD-L1 probe PET/CT imaging of implant-associated *Staphylococcus aureus* osteomyelitis

Shu-Qi Ren[1], Yuan Ma[2], Li-Lan Fu[1], Kong-Zhen Hu[1], Hao-Ran Liang[1], Bin Yu[2]* and Gang-Hua Tang[1]*

[1]GuangDong Medical Products Administration (GDMPA) Key Laboratory for Quality Control and Evaluation of Radiopharmaceuticals, Department of Nuclear Medicine, Nanfang Hospital, Southern Medical University, Guangzhou, China, [2]Guangdong Provincial Key Laboratory of Bone and Cartilage Regenerative Medicine, Division of Orthopedics and Traumatology, Department of Orthopedics, Nanfang Hospital, Southern Medical University, Guangzhou, China

Background: Early and accurate diagnosis of infection-induced osteomyelitis, which often involves increased PD-L1 expression, is crucial for better treatment outcomes. Radiolabeled anti-PD-L1 nuclear imaging allows for sensitive and non-invasive whole-body assessments of PD-L1 expression. This study aimed to compare the efficacy of ^{18}F-FDG and an ^{18}F-labeled PD-L1-binding peptide probe (^{18}F-PD-L1P) in PET imaging of implant-associated Staphylococcus aureus osteomyelitis (IAOM).

Methods: In this study, we synthesized an anti-PD-L1 probe and compared its efficacy with ^{18}F-FDG and ^{18}F-PD-L1P in PET imaging of implant-associated Staphylococcus aureus osteomyelitis (IAOM). The %ID/g ratios (i.e., radioactivity ratios between the infected and non-infected sides) of both probes were evaluated for sensitivity and accuracy in post-infected 7-day tibias and post-infected 21 days, and the intensity of ^{18}F-PD-L1P uptake was compared with pathological changes measured by PD-L1 immunohistochemistry (IHC).

Results: Compared with ^{18}F-FDG, ^{18}F-PDL1P demonstrated higher %ID/g ratios for both post-infected 7-day tibias (P=0.001) and post-infected 21 days (P=0.028). The intensity of ^{18}F-PD-L1P uptake reflected the pathological changes of osteomyelitic bones. In comparison to ^{18}F-FDG, ^{18}F-PDL1P provides earlier and more sensitive detection of osteomyelitis caused by S. aureus.

Conclusion: Our findings suggest that the ^{18}F-PDL1P probe is a promising tool for the early and accurate detection of osteomyelitis caused by S. aureus.

KEYWORDS

osteomyelitis, PET imaging, PD-L1, implant-associated *Staphylococcus aureus* osteomyelitis, ^{18}F-FDG

1 Introduction

Posttraumatic and postoperative osteomyelitis continue to be among the most serious complications following bone trauma or surgery (Odekerken et al., 2014a) Improper treatment of acute osteomyelitis and recurrent episodes of chronic osteomyelitis can lead to limb disability and high amputation rates (Gratz et al., 2001; Conterno and Turchi, 2013). In the early postoperative period, detecting deep orthopedic implant infections can be challenging, making early diagnosis critical for effective treatment and implant survival (Odekerken et al., 2014b). Therefore, having a specific diagnostic tool to monitor implant infections is imperative.

Currently, the early diagnosis of osteomyelitis poses a significant challenge. Among various imaging modalities, such as CT, MRI, labeled leukocyte imaging, and gallium imaging, ^{18}F-FDG-PET imaging may play a role in confirming or excluding the diagnosis of peripheral bone osteomyelitis (Makinen et al., 2005; Termaat et al., 2005; van der Bruggen et al., 2010; Lankinen et al., 2012; Chatziioannou et al., 2015; Llewellyn et al., 2019). However, ^{18}F-FDG PET has potential limitations as a tool for diagnosing bone infection. This method relies on the intensive glucose consumption of mononuclear cells and granulocytes, which can lead to increased ^{18}F-FDG uptake in both bacterial infections and aseptic inflammatory processes (Koort et al., 2004). Because ^{18}F-FDG uptake is mediated by metabolism, increased ^{18}F-FDG uptake is also associated with acute fractures, normally healing bone and degenerative changes (Koort et al., 2004). Therefore, while ^{18}F-FDG-PET imaging may aid in the diagnosis of peripheral bone osteomyelitis, its diagnostic accuracy must be interpreted with caution.

Some studies have indicated that there is a persistent elevation of IFN-γ in bones of mice infected with *S. aureus* by days 3 and 14 post-infection, indicating activation of the immune system and potential bone destruction by these inflammatory factors (Syedbasha and Egli, 2017; Lin et al., 2021). In response to infection, increased levels of proinflammatory cytokines such as IFN-γ and TNF-α can upregulate PD-1/PD-L1 expression locally or systemically (Patil et al., 2018; Curran et al., 2021; Sandker et al., 2022). Furthermore, the detection of increased PD-1/PD-L1 expression in both animal models of *S. aureus* osteomyelitis and human patients with the disease suggests its relevance in the pathogenesis, and at the cellular level, *S. aureus* infection has been demonstrated to induce the expression of PD-1/PD-L1 in bone marrow macrophages (Li et al., 2023). Nuclear imaging, which employs a radiolabeled anti-PD-L1 probe, enables non-invasive, sensitive, and quantitative assessments of PD-L1 expression on a whole-body scale (Niemeijer et al., 2018; Zhou M. et al., 2022). Various preclinical studies in onco-immunology have demonstrated the feasibility of this approach in immunocompetent mouse models (Sun et al., 2022). Moreover, recent clinical studies using a radiolabeled anti-PD-L1 antibody (Bensch et al., 2018), peptide (Zhou X. et al., 2022) demonstrated that nuclear imaging using PD-L1 targeting tracers can assess PD-L1 expression *in vivo*. However, there have been no studies that have conducted an in-depth investigation of PD-L1 expression or imaging in osteomyelitis disease models.

In this study, we have shown that the expression of PD-L1 is upregulated in bone tissues infected with Implant-Associated *S. aureus* osteomyelitis (IAOM) in mouse models. Furthermore, we have identified PET imaging with an ^{18}F-labeled PD-L1-Binding Peptide probe (^{18}F-PDL1P) as a promising technique for the early detection of bone infections.

2 Results

2.1 Establishment of IAOM mouse model

To establish a mouse model of IAOM, the hind leg was shaved followed by disinfection with iodine (Figure 1A). A 5-mm incision was made on the ventral side of the leg (Figure 1B). After the tibia was exposed, a pinhole was drilled by a 26-gauge syringe needle. (Figure 1C) Next, a 9-mm ster-ile stainless pin (0.5 mm in diameter) was inserted into the bone marrow cavity through the canal.(For the right side's infected tibia, implants were soaked in 1 *ml* of *S. aureus* solution at 1 × 105 CFU/ml, while the left side's control received an equal amount of sterile PBS) (Figure 1D). The incision was then closed with a 5-0 suture (Figure 1E).

2.2 Radiographic evaluation and htopathological characteristics of the bone with IAOM

Radiographic signs of osteomyelitis were not observed in the uncontaminated control tibia. By day 7 postinfection, there was no discernible change between the infected side and control side in terms of bone shape or intramedullary bone mineral density (BMD) (Figure 2A). However, by day 21 post-infection, the infected tibia of IAOM mice exhibited an obvious periosteal reaction, altered bone morphology, increased bone mineral density, and osteolysis around the infected implant, indicating osteonecrosis. Conversely, the implanted bone in the uninfected tibia showed no signs of alteration (Figure 2A). Moreover, by day 21 following surgery, the radiographic values for the infected tibia were significantly higher than those for the control tibia ($p=0.013$) (Figure 2B).

To observe the histopathological changes in infected bone, hematoxylin and eosin (H&E) staining was performed in the control and infected tibia on days 21 postoperation. No significant alterations were detected in the bone morphology or histology of the control group. However, as the IAOM progressed to the chronic stage on day 21 post-infection, the *infected* tibia exhibited clear signs of bone destruction, including extensive infiltration of neutrophils in the medullary cavity, the formation of necrotic abscesses in the medullary cavity, deformity of the entire tibia, and sequestrum formation (Figure 2C).

In the 3-week follow-up, the severity of radiographic signs of osteomyelitis (periosteal elevation, *cortical* thickening, and osteolysis) was increased in the group of contaminated implants. When the infection occurred 21 days later, the infected tibia showed the typical signs of chronic osteomyelitis. Collectively, the above data demonstrated that the IAOM mouse model showed typical

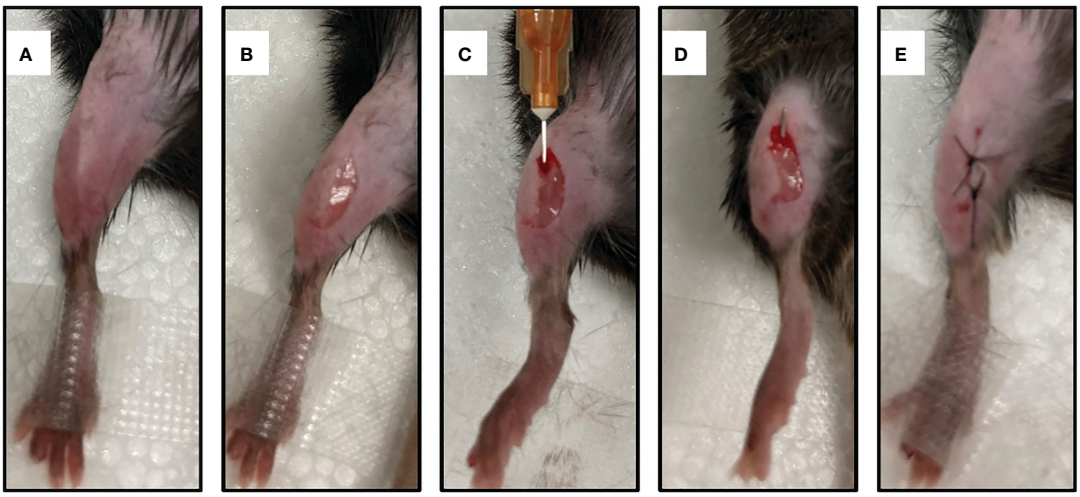

FIGURE 1
Establishment of a mouse model of implant-associated osteomyelitis. **(A)** skin preparation and disinfection. **(B)** A midline 5mm incision was made with a 15-blade scalpel through the skin at the area of mouse's leg. **(C)** A unicortical defect was made using the needle of a 26-gauge syringe. **(D)** A 9-mm sterile stainless pin (0.5 mm in diameter) was implanted into the medullary cavity. **(E)** The incision was closed with 5-0 silk suture.

radiologic pathological changes of acute and chronic osteomyelitis along with the time of infection.

2.3 Location of *S. aureus* in the bone with IAOM

To confirm the location of *S. aureus* in infected tibia, immunohistochemical staining was performed. In the infected right tibia, colonization of the bone marrow (Figure 3A) and bone cortex (Figure 3B) by *S. aureus* was observed at both 7 and 21 days. No colonization of the bone marrow and bone cortex of the left leg tibia by *S. aureus* was observed in the non-*S. aureus*-infected metal graft (Figure 3A).

2.4 Comparative study of ^{18}F-FDG and ^{18}F-PDL1P micro-PET imaging

PET/CT imaging results revealed a significantly increased uptake of ^{18}F-PDL1P in *the infected bone compared to the uninfected tibia during the first week post-surgery* (Figure 4A), with no notable increase in ^{18}F-FDG uptake (Figure 4C). In the subsequent three weeks after surgery, both ^{18}F-PDL1P (Figure 4B) and ^{18}F-FDG (Figure 4D) showed an *in*creased uptake in the osteomyelitic tibia when compared to the opposite uninfected ti*b*ia, as demonstrated by PET imaging.

To quantify the ^{18}F-FDG and ^{18}F-PDL1P uptake in both groups and investigate whether ^{18}F-FDG and^{18}F-PDL1P PET enables differentiation between control and infected implants, the uptake of both tracers by the uptake of the bone tissue around the implants was determined. The PET quantitative data demonstrated that during the first week after surgery, there was no significant difference in ^{18}F-FDG PET findings between the right and left tibias. Specifically, the %ID/g of the left bone was 5.38 ± 1.66, while that of the right bone was 6.9 ± 0.1 (P=0.117) (Figure 4G). However, as osteomyelitis progressed to the third week, the uptake of ^{18}F-FDG in the infected bone increased significantly when compared to the contralateral bones (P<0.001) (Figure 4H). Notably, the activity of ^{18}F-PDL1P was significantly higher in the infected region than in the contralateral bones at both 7 (P<0.003) (Figure 4E) and 21 days (P<0.001) (Figure 4F).

We found that compared to ^{18}F-FDG, ^{18}F-PDL1P showed significantly higher %ID/g ratios in the right (R) and left (L) tibias at both 7 days (P=0.001) and 21 days (P=0.028) post-infection (Figure 5).

2.5 Locoregional upregulation of PD-L1 in *Staphylococcus aureus* infected bone

To further demonstrate that the accumulation observed in *S. aureus*-infected tibias was predominantly PD-L1 specific, we performed immunohistochemical analysis of the infected tibias.

We observed a significant number of PD-L1-positive cells in and around the infection foci in the bone marrow after 7 and 21 days of *S. aureus* infection, but only a few PD-L1-expressing cells were found in the control site (Figure 6A). On day 7 post-infection by *S. aureus*, no PD-L1-positive cells were observed in the bone cortex (Figure 6B). However, as the infection progressed and worsened at day 21 following infection, we also discovered an expression of PD-L1-positive cells in the bone cortex.

The immunohistochemical analyses show that the uptake of ^{18}F-PDL1P in *S. aureus*-infected bone was PD-L1-mediated.

3 Discussion

In this experimental study, ^{18}F-FDG and ^{18}F-PDL1P for PET imaging of bone infection were compared.^{18}F-FDG has been adopted as a tracer in PET imaging of bone infections (Koort

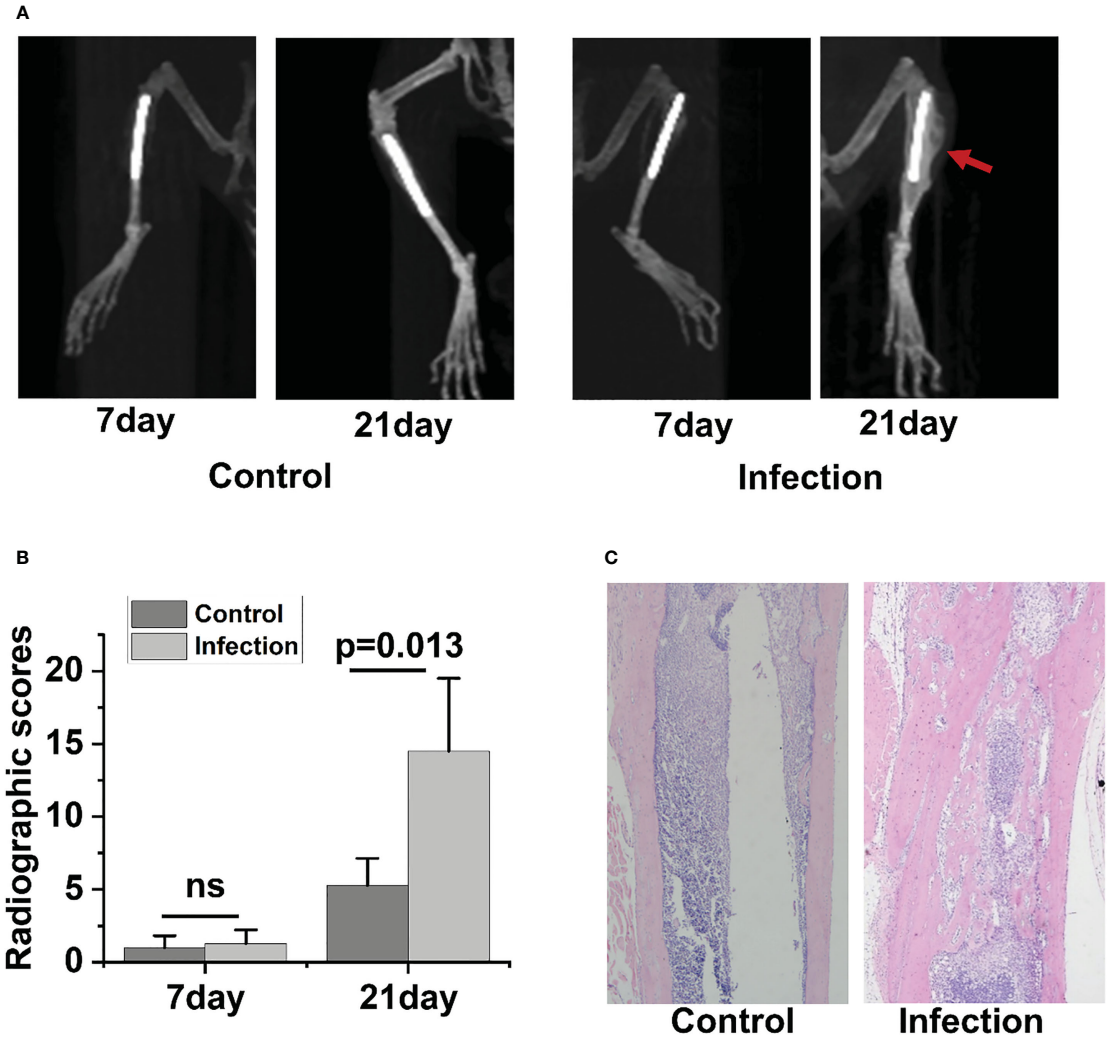

FIGURE 2
Radiographic and histopathological evidence of bone destruction in infected tibia. Representative radiographic images of tibia bones from control and implant-associated osteomyelitis (IAOM) mice **(A)**. Quantification of bone destruction using a radiographic scoring method **(B)**. Histopathological analysis of tibia in control and infected mice **(C)**. ns, no statistical difference between the two groups at the same time point (n = 4 per group).

et al., 2004; Makinen et al., 2005; Lankinen et al., 2012; Odekerken et al., 2014a; Chatziioannou et al., 2015), but the applicability of ^{18}F-PDL1P has not been reported for the same indication. By day 7 postinfection, ^{18}F-FDG revealed a substantial uptake in uninfected healing-deficient bone and was comparable to infected bone, according to the vivo PET imaging. This led to a false-positive result because it was impossible to discern between infected and uninfected bone. However, during this same time, ^{18}F-PDL1P proved useful for distinguishing between infected and uninfected bone. By day 21 postinfection, compared to bones with healing defects, bones with persistent osteomyelitis showed considerably higher uptake of both ^{18}F-FDG and ^{18}F-PDL1P, according to *in vivo* PET imaging. Furthermore, compared to ^{18}F-FDG, ^{18}F-PDL1P had a greater rate of increased uptake. The results of our experimental design are consistent with earlier study (Odekerken et al., 2014b) in that the third postoperative week was the earliest time at which it was possible to distinguish between ^{18}F-FDG uptake from uninfected healing-deficient bone and infected bone.

Staphylococcus aureus remains by far the more common pathogen in osteomyelitis (Chen et al., 2022; Zhang et al., 2022). Clinical data in Nanfang hospital shows that *Staphylococcus aureus* covers 15% of the pathogenic bacteria in osteomyelitis. (*Staphylococcus aureus* covers 15% of the pathogenic bacteria in all surgical site infections (Saadatian-Elahi et al., 2008)). So *Staphylococcus aureus* has the characteristics of stable infection and tissue characteristics close to clinicopathological features (Hidaka, 1985; Liu et al., 2022). Both stainless steel and titanium alloys are the most commonly used materials in orthopedics. There is no significant difference between stainless steel and titanium (Metsemakers et al., 2016), stainless steel implant as infection vectors was used in this study. A well-liked animal model for studying osteomyelitis is the IAOM model of tibial osteomyelitis (Koort et al., 2004; Sun et al., 2022). The model's great reproducibility in the induction of infection was confirmed by bacteriology. On conventional radiographs and CT scans, as well as histopathologically, the generated bone infection resembled chronic human post-traumatic osteomyelitis. In the current study, the ID/g

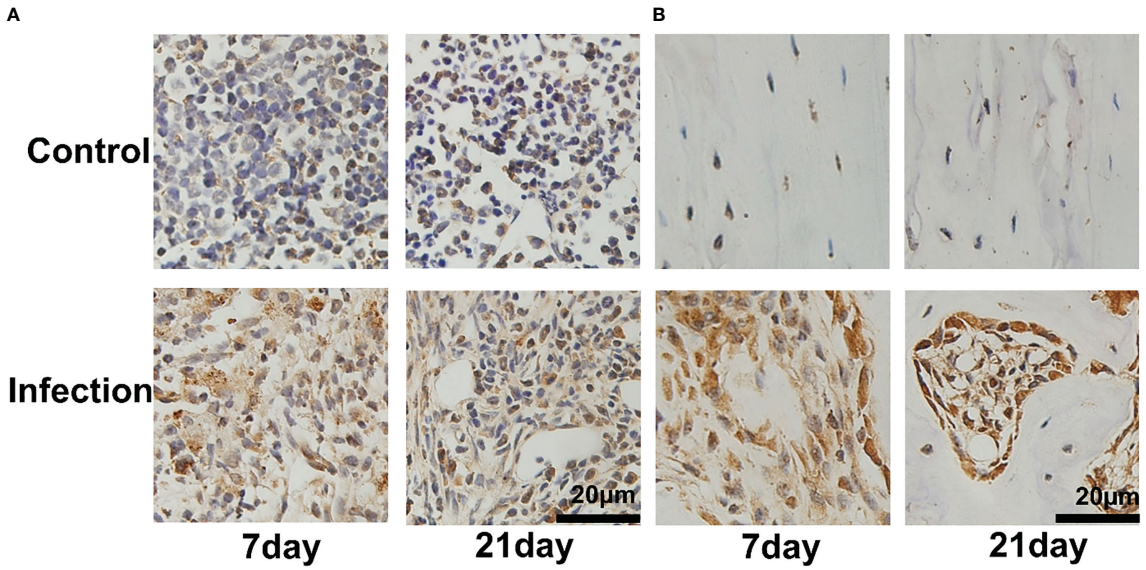

FIGURE 3
Bacterial colonization of tibial tissue in IAOM mice. Immunohistochemistry images of S. aureus invading and propagating in canaliculi of murine tibiae **(A)** and bone cortex **(B)**. (n = 2 per group). Scale bar =20μm.

ratios between the infected and contralateral bones ranged from 1.22 to 1.68 for ^{18}F-FDG and from 2.18 to 2.38 for ^{18}F-PDL1P, where bacterial osteomyelitis of the mouse tibia was microbiologically verified. Additional studies are necessary to address the following issues: (1) the lack of investigation into the correlation between bacterial load, bacterial activity, and imaging, which could be an essential area for future exploration and may become a focus of our future research direction; and (2) the validation of the diagnostic potential of ^{18}F-PDL1P for osteomyelitis using IAOM, as suggested by the findings of this preclinical study, necessitates confirmation through experimentation involving human subjects.

The delicate balancing act between efficient antimicrobial immune defenses and immune-mediated tissue damage appears to be regulated by the PD-1:PD-L1 pathway, which is thought to be a major factor in how an infection will progress (Dyck and Mills, 2017; Qin et al., 2019; Wang et al., 2021; Sandker et al., 2022). Notably, PET imaging of PD-L1 expression has shown to be a reliable predictor of response to immunotherapy and well-correlated with immunohistochemistry (Bensch et al., 2018; Vento et al., 2019; Kelly et al., 2021).Therefore, PET imaging of osteomyelitic using anti-PD-L1P probes is a promising imaging modality. Given that cytokine-induced inflammation can cause a rapid and transient increase in PD-L1 expression levels (Sandker et al., 2022), PD-L1 targeting peptides with shorter circulation times may provide an advantage. With the aid of nuclear imaging, a more strategic design of studies involving immune checkpoint inhibition to treat chronic infectious illnesses complicated by immune dysfunction is now possible. This imaging modality can help assess potential therapeutic synergy between PD-L1 blocking and current antimicrobial immune-activating medications, such as prednisone, TNF-alpha antagonists, and IL-6 blockers, by monitoring changes in PD-L1 expression levels.

Taken together, our findings indicate that^{18}F-FDG and ^{18}F-PDL1P accumulated in *S. aureus* osteomyelitis. ^{18}F-PDL1P in contrast to^{18}F-FDG, provides earlier and more sensitive detection of osteomyelitis caused by *S. aureus*. ^{18}F-PDL1P was shown to be a potentially effective tracer for the detection of acute osteomyelitic and chronic osteomyelitic with higher T/N(target to nontarget ratio) than ^{18}F-FDG.Further studies are needed to clarify the value of ^{18}F-PDL1P PET for clinical purposes. Furthermore, our results indicate that ^{18}F-PDL1P PET may provide a tool in human clinical diagnostics and for the evaluation of antimicrobial strategies in animal models of orthopedic implant infection.

4 Methods

4.1 *Staphylococcus aureus* strains and pathogenic challenge

S. aureus was isolated from a patient with chronic osteomyelitis, and methicillin-sensitive *S. aureus* was identified using PHOENIX 100 (Becton, Dickinson Microbiology Systems, USA). A frozen stock of *S. aureus* strains was routinely grown on tryptic soy broth (TSB) with shaking at 180 rpm at 37°C for 16 h and collected by centrifugation at 3,000 rpm for 10 min. The bacterial pellets were washed and resuspended in phosphate-buffered saline (PBS). The concentration of *S. aureus* was adjusted to an optical density (OD) of 0.5 at 600 nm, approximately equal to 1×10^8 CFU/ml, and further adjusted to 1×10^5 CFU/ml for soaking implants for IAOM mice.

4.2 Implant-associated *S. aureus* osteomyelitis mice model

Protocols for animal experiments were approved by the Animal Care and Use Committee at Nanfang Hospital, Southern

10.3389/fcimb.2023.1182480

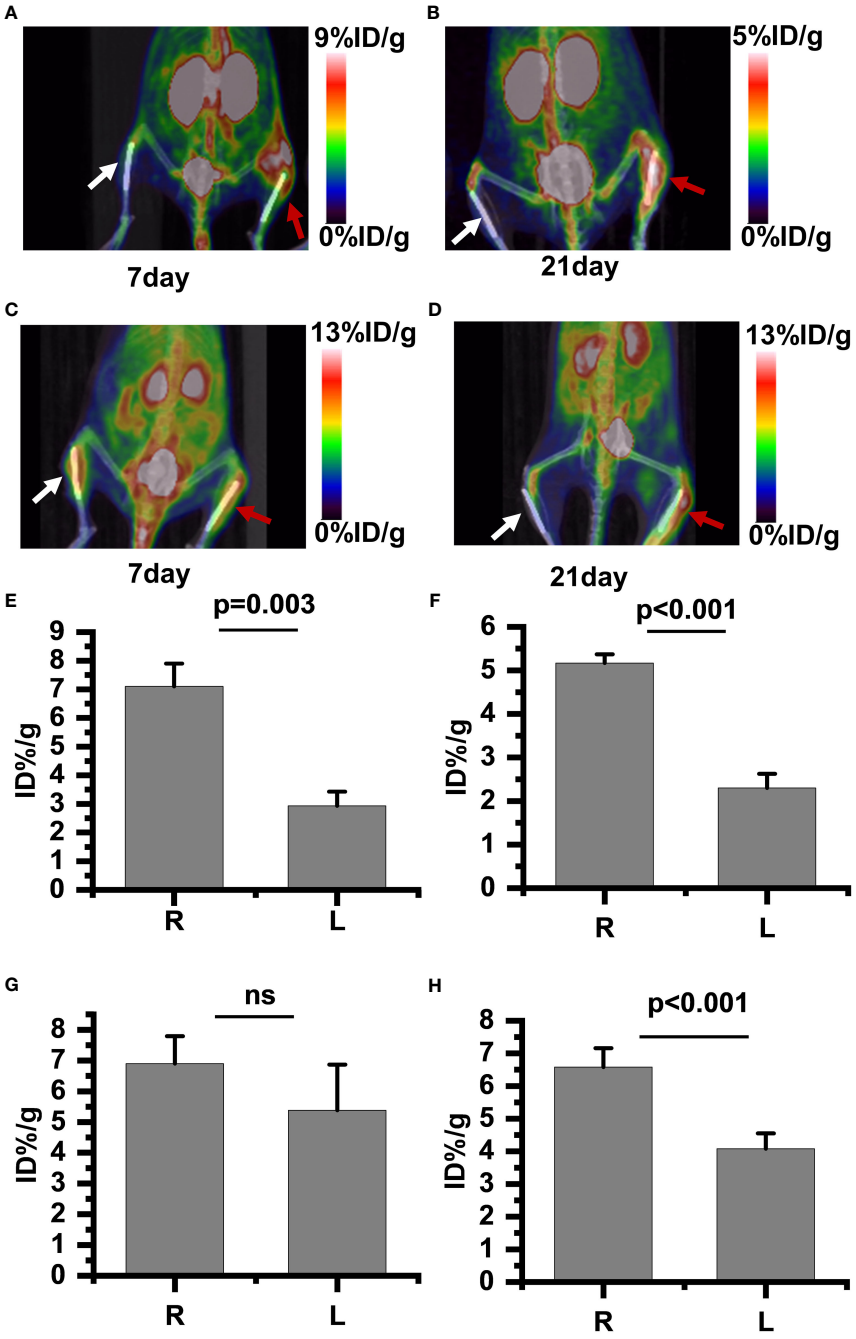

FIGURE 4
^{18}F-PDL1P PET maximal intensity projection (MIP) images of the lower body were taken on post-infection days 7 **(A)** and 21 **(B)**. ^{18}F-FDG PET MIP images of the lower body were taken on post-infection days 7 **(C)** and 21 **(D)**. Intake value of ^{18}F-PDL1P PET of the post infection on 7 days **(E)** and 21 days **(F)**. Intake value of ^{18}F-FDG PET of the post infection on 7 days **(G)** and 21 days **(H)**. The right infected tibia (red arrow) and the left uninfected tibia (white arrow) are shown. ns, no statistical difference between the two groups at the same time point.

Medical University. Male C57BL/6 mice aged 10 to 12 weeks were housed in a facility with a 12-h light/dark cycle, 24 ± 2°C room temperature, and provided with ad libitum access to water and food. The left and right legs of the mice were separately assigned to a self-control group and an IAOM group. Prior to surgery, mice were anesthetized by intraperitoneal injection of tribromoethanol (125 mg/kg of body weight). Implants were soaked in 1 ml of *S. aureus* solution at 1×10^5 CFU/ml for IAOM mice, while an equal volume of sterile PBS was used for the controls. After the hind leg was shaved and disinfected with iodine, a 5-mm incision was made on the ventral side of the leg. The tibia was then exposed, and a pinhole was drilled using a 26-gauge syringe needle. Next, a 9-mm sterile stainless pin (0.5 mm in diameter) was inserted into the bone marrow cavity through the canal. The incision was closed with a 5-0 suture. Both tibiae were collected on days 7 and 21 after the operation for further analysis.

10.3389/fcimb.2023.1182480

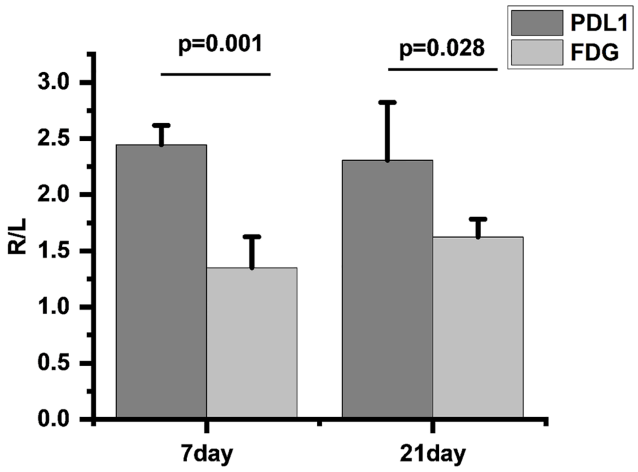

FIGURE 5
Comparison of ^{18}F-FDG and ^{18}F-PDL1P uptake rates on infected and uninfected Sides at 7 and 21 Days Post-Infection, R/L(radioactivity ratios between the right infected and left non-infected sides).

4.3 Radiosynthesis

[^{18}F]Fluoride was created by bombarding a high pressure [^{18}O]H_2O target with 18 MeV proton beams using a PET trace biomedical cyclotron (PET 800, General Electric, Boston, MA, USA). Radioactivity was measured using a Capintec CAPRAC-R dosage calibrator (NJ, USA). [^{18}F]FDG was produced with a specific radioactivity of >76 GBq/mol and a radiochemical purity of >98% using a fully automated FDG synthesis module (IBA). For radiosynthesis of ^{18}F-PDL1P, the method described previously was used (Tang et al., 2021; Sun et al., 2022), with manual execution.

4.4 PET/CT imaging of IAOM mouse model

Comparative ^{18}F-FDG and ^{18}F-PDL1P PET/CT imaging was performed at 1 and 3 weeks after a 4-hour fasting period prior to tracer injection. Mice were anesthetized and placed in a micro-PET scanner (Siemens, Erlangen, Germany) in the prone position, followed by tail vein injection of a range of 7.4 MBq to 11.1 MBq of ^{18}F-FDG and ^{18}F-PDL1P. Three-dimensional ordered-subset expectation maximum (OSEM) algorithm (Siemens, Erlangen, Germany) was used for image reconstruction with attenuation correction and for anatomical reference with CT data. Images and regions of interest (ROIs) were generated using Inevon Research

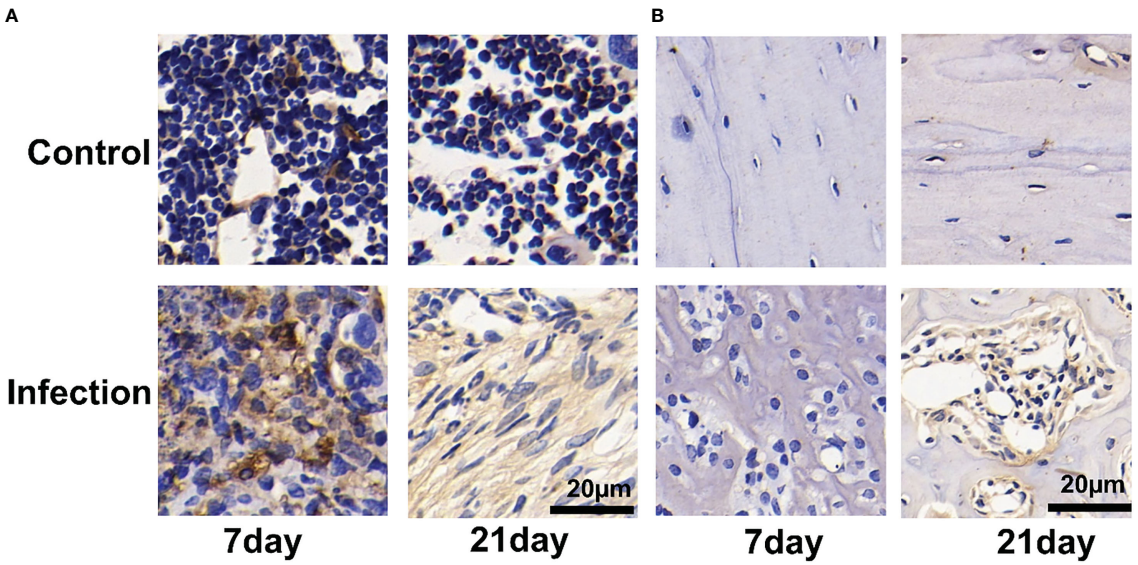

FIGURE 6
Immunohistochemistry for PD-L1 expression of Staphylococcus aureus-infected and vehicle control implanted bone marrow **(A)** and bone **(B)**. Representative images of immunohistochemistry for PD-L1 in bone and bone marrow (n = 2 per group). Scale bar = 20 μm.

Workplace 4.1 software (Siemens, Erlangen, Germany). The standardized circular ROI (radius 3.8 mm) of the right operated tibia and the corresponding region of the left contralateral tibia were quantitatively analyzed for ^{18}F-FDG and ^{18}F-PDL1P uptake, expressed as mean %ID/g. The mean %ID/g was calculated as the mean radioactivity of the ROI divided by the relative injected dose of radioactivity per kilogram of body weight.

4.5 Radiographic evaluation and histological analysis

Quantitative evaluation of the IAOM was performed using a modified scale based on previously reported radiographic parameters (Smeltzer et al., 1997). These parameters include periosteal elevation, architectural deformation, widening of the bone shaft, production of new bone, and deformation of soft tissue, which were evaluated as radiographic indicators of disease. Each parameter was scored between 0 and 4, with a score of 4 indicating the most severe evidence of illness. The same researcher (Y.M.), who was blinded to the infection status of each mouse, scored each radiograph. The total score for each sample was calculated as the sum of the scores for the five parameters.

Following infection on day 21, mice were sedated and intracardially given 4% paraformaldehyde. Proximal and middle bone segments of the harvested tibias were preserved in 4% paraformaldehyde overnight at 4°C. The samples were then demineralized in 10% EDTA for ten days, processed, and paraffin-embedded. Subsequently, 4 μm coronal sections were cut and stained with hematoxylin-eosin (H&E)

4.6 Immunohistochemistry

After deparaffinization and rehydration, antigen retrieval for immunohistochemical analysis was carried out by incubating the section in a protease K solution (1 mg/ml) at 37°C for 15 min. Endogenous peroxidase activity was then quenched in 3% H_2O_2 for 15 min. Sections were treated with the rabbit anti-*S* antibody after being blocked for 1 hour at room temperature with 10% goat serum. Sections were then incubated with mouse anti-PD-L1 antibody (catalog no. MH68942; Abmart, Shanghai, China) or *S. aureus* antibody (catalog no. ab20920; Abcam) for 1 hour at room temperature. Finally, sections were incubated with avidin-conjugated horseradish peroxidase (HRP) complex in accordance with the manufacturer's protocol (Vectastain ABC HRP kit; Vector Laboratories, USA). In the end, sections' peroxidase activities were discovered using a kit for 3,3'-diaminobenzidine (DAB) substrate (Vector Laboratories).

4.7 Statistical analysis

The standard deviation (SD) and mean were used to express the data. Statistical analysis was performed using SPSS version 22.0 (IBM Corp, Armonk, NY, USA) to assess the significance of differences between two datasets. A p-value less than 0.05 was considered statistically significant.

5 Conclusions

In this work, we find that the expression of PD-L1 was increased in the infected bone in mouse models. And PET using an anti-PD-L1 probe is a promising imaging modality for early bone infections.

Data availability statement

The raw data supporting the conclusions of this article will be made available by the authors, without undue reservation.

Ethics statement

The animal study was reviewed and approved by Nanfang Hospital animal ethic committee.

Author contributions

S-QR and YM contribute equally to the work. S-QR: Validation, Formal analysis, Data Analysis, Writing-Review and Editing; YM: Validation, Formal analysis, Resources; L-LF: Writing - Review and Editing; K-ZH: Resources; H-RL: Validation; BY: Project administration; G-HT: Supervision, Funding acquisition, Project administration, Writing - Review and Editing. All authors contributed to the article and approved the submitted version.

Funding

This study was funded by the Guangdong Basic and Applied Basic Research Foundation (2022A1515010072, 2022A1515110051, 2020A1515011399), Guangzhou Science and Technology Plan (2023B03J0529), Medical Products Administration of Guangdong Province (2021ZDB02), Nanfang Hospital Talent Introduction Fundation of Southern Medical University (123456), and the National Natural Science Foundation of China (91949121).

Conflict of interest

The authors declare that the research was conducted in the absence of any commercial or financial relationships that could be construed as a potential conflict of interest.

Publisher's note

References

Bensch, F., van der Veen, E. L., Lub-de Hooge, M. N., Jorritsma-Smit, A., Boellaard, R., Kok, I. C., et al. (2018). (89)Zr-atezolizumab imaging as a non-invasive approach to assess clinical response to PD-L1 blockade in cancer. *Nat. Med.* 24 (12), 1852–1858. doi: 10.1038/s41591-018-0255-8

Chatziioannou, S., Papamichos, O., Gamaletsou, M. N., Georgakopoulos, A., Kostomitsopoulos, N. G., Tseleni-Balafouta, S., et al. (2015). 18-Fluoro-2-deoxy-D-glucose positron emission tomography/computed tomography scan for monitoring the therapeutic response in experimental *staphylococcus aureus* foreign-body osteomyelitis. *J. Orthop Surg. Res.* 10, 132. doi: 10.1186/s13018-015-0274-9

Chen, P., Lin, Q. R., Huang, M. Z., Zhang, X., Hu, Y. J., Chen, J., et al. (2022). Devascularized bone surface culture: a novel strategy for identifying osteomyelitis-related pathogens. *J. Pers. Med.* 12 (12), 2050. doi: 10.3390/jpm12122050

Conterno, L. O., and Turchi, M. D. (2013). Antibiotics for treating chronic osteomyelitis in adults. *Cochrane Database Syst. Rev.* 9), Cd004439. doi: 10.1002/14651858.CD004439.pub3

Curran, C. S., Busch, L. M., Li, Y., Xizhong, C., Sun, J., Eichacker, P. Q., et al. (2021). Anti-PD-L1 therapy does not improve survival in a murine model of lethal *staphylococcus aureus* pneumonia. *J. Infect. Dis.* 224 (12), 2073–2084. doi: 10.1093/infdis/jiab274

Dyck, L., and Mills, K. H. G. (2017). Immune checkpoints and their inhibition in cancer and infectious diseases. *Eur. J. Immunol.* 47 (5), 765–779. doi: 10.1002/eji.201646875

Gratz, S., Rennen, H. J., Boerman, O. C., Oyen, W. J., Burma, P., Corstens, F. H., et al. (2001). (99m)Tc-interleukin-8 for imaging acute osteomyelitis. *J. Nucl. Med.* 42 (8), 1257–1264.

Hidaka, S. (1985). [An experimental study on pyogenic osteomyelitis with special reference to polymicrobial infections]. *Nihon Seikeigeka Gakkai Zasshi* 59 (4), 429–441.

Kelly, M. P., Makonnen, S., Hickey, C., Arnold, T. C., Giurleo, J. T., Tavaré, R., et al. (2021). Preclinical PET imaging with the novel human antibody (89)Zr-DFO-REGN3504 sensitively detects PD-L1 expression in tumors and normal tissues. *J. Immunother. Cancer* 9 (1), e002025. doi: 10.1136/jitc-2020-002025

Koort, J. K., Mäkinen, T. J., Knuuti, J., Jalava, J., and Aro, H. T. (2004). Comparative ^{18}F-FDG PET of experimental *staphylococcus aureus* osteomyelitis and normal bone healing. *J. Nucl. Med.* 45 (8), 1406–1411.

Lankinen, P., Lehtimäki, K., Hakanen, A. J., Roivainen, A., and Aro, H. T. (2012). A comparative ^{18}F-FDG PET/CT imaging of experimental *staphylococcus aureus* osteomyelitis and staphylococcus epidermidis foreign-body-associated infection in the rabbit tibia. *EJNMMI Res.* 2 (1), 41. doi: 10.1186/2191-219X-2-41

Li, K., Chen, Y., Lin, Y., Zhang, G., Su, J., Wu, X., et al. (2023). PD-1/PD-L1 blockade is a potent adjuvant in treatment of *staphylococcus aureus* osteomyelitis in mice. *Mol. Ther.* 31 (1), 174–192. doi: 10.1016/j.ymthe.2022.09.006

Lin, Y., Su, J., Wang, Y., Xu, D., Zhang, X., and Yu, B. (2021). mRNA transcriptome analysis of bone in a mouse model of implant-associated *staphylococcus aureus* osteomyelitis. *Infect. Immun.* 89 (5), e00814-20 doi: 10.1128/IAI.00814-20

Liu, H., Xu, D., Ma, Y., Qian, J., Yang, Y., Yu, B., et al. (2022). Mechanisms of hierarchical topographies tuning bacteria and cell biological responses to the surfaces of pure titanium and Cu-bearing titanium alloy. *ACS Appl. Mater Interfaces* 14 (17), 19226–19240. doi: 10.1021/acsami.2c02802

Llewellyn, A., Jones-Diette, J., Kraft, J., Holton, C, Harden, M., and Simmonds, M. (2019). Imaging tests for the detection of osteomyelitis: a systematic review. *Health Technol. Assess.* 23 (61), 1–128. doi: 10.3310/hta23610

Makinen, T. J., Lankinen, P., Pöyhönen, T., Jalava, J., Aro, H. T., and Roivainen, A. (2005). Comparison of ^{18}F-FDG and 68Ga PET imaging in the assessment of experimental osteomyelitis due to *staphylococcus aureus*. *Eur. J. Nucl. Med. Mol. Imaging* 32 (11), 1259–1268. doi: 10.1007/s00259-005-1841-9

Metsemakers, W. J., et al. (2016). Titanium and steel fracture fixation plates with different surface topographies: influence on infection rate in a rabbit fracture model. *Injury* 47 (3), 633–639. doi: 10.1016/j.injury.2016.01.011

Niemeijer, A. N., Leung, D., Huisman, M. C., Bahce, I., Hoekstra, O. S., van Dongen, G. A. M. S., et al. (2018). Whole body PD-1 and PD-L1 positron emission tomography in patients with non-small-cell lung cancer. *Nat. Commun.* 9 (1), 4664. doi: 10.1038/s41467-018-07131-y

Odekerken, J. C., Walenkamp, G. H., Brans, B. T., Welting, T. J., and Arts, J. J. (2014a). The longitudinal assessment of osteomyelitis development by molecular imaging in a rabbit model. *BioMed. Res. Int.* 2014, 424652. doi: 10.1155/2014/424652

Odekerken, J. C., Brans, B. T., Welting, T. J., and Walenkamp, G. H. (2014b). (18)F-FDG microPET imaging differentiates between septic and aseptic wound healing after orthopedic implant placement: a longitudinal study of an implant osteomyelitis in the rabbit tibia. *Acta Orthop* 85 (3), 305–313. doi: 10.3109/17453674.2014.900894

Patil, N. K., Luan, L., Bohannon, J. K., Hernandez, A., Guo, Y., and Sherwood, E. R. (2018). Frontline science: anti-PD-L1 protects against infection with common bacterial pathogens after burn injury. *J. Leukoc. Biol.* 103 (1), 23–33. doi: 10.1002/JLB.5HI0917-360R

Qin, W., Hu, L., Zhang, X., Jiang, S., Li, J., Zhang, Z., et al. (2019). The diverse function of PD-1/PD-L pathway beyond cancer. *Front. Immunol.* 10, 2298. doi: 10.3389/fimmu.2019.02298

Saadatian-Elahi, M., Teyssou, R., and Vanhems, P. (2008). *Staphylococcus aureus*, the major pathogen in orthopaedic and cardiac surgical site infections: a literature review. *Int. J. Surg.* 6 (3), 238–245. doi: 10.1016/j.ijsu.2007.05.001

Sandker, G. G. W., Adema, G., Molkenboer-Kuenen, J., Wierstra, P., Bussink, J., Heskamp, S., et al. (2022). PD-L1 antibody pharmacokinetics and tumor targeting in mouse models for infectious diseases. *Front. Immunol.* 13, 837370. doi: 10.3389/fimmu.2022.837370

Smeltzer, M. S., Thomas, J. R., Hickmon, S. G., Skinner, R. A., Nelson, C. L., Griffith, D., et al. (1997). Characterization of a rabbit model of staphylococcal osteomyelitis. *J. Orthop Res.* 15 (3), 414–421. doi: 10.1002/jor.1100150314

Sun, P., Han, Y., Hu, K., Huang, S., Wang, M., Zhou, K., et al. (2022). Synthesis and biological evaluation of Al[(18)F]-NOTA-IPB-PDL1P as a molecular probe for PET imaging of PD-L1 positive tumors. *Bioorg Chem.* 122, 105682. doi: 10.1016/j.bioorg.2022.105682

Syedbasha, M., and Egli, A. (2017). Interferon lambda: modulating immunity in infectious diseases. *Front. Immunol.* 8, 119. doi: 10.3389/fimmu.2017.00119

Tang, G., Sun, P., and Chen, H. (2021). *Targeting PD-L1 peptide probes and their usage in the synthesis of PET imaging probes, S.M.U* (China: Nanfang Hospital).

Termaat, M. F., Raijmakers, P. G., Scholten, H. J., Bakker, F. C., Patka, P., and Haarman, H. J. (2005). The accuracy of diagnostic imaging for the assessment of chronic osteomyelitis: a systematic review and meta-analysis. *J. Bone Joint surgery. Am. volume* 87 (11), 2464–2471. doi: 10.2106/00004623-200511000-00013

van der Bruggen, W., Bleeker-Rovers, C. P., Boerman, O. C., Gotthardt, M., and Oyen, W. J. (2010). PET and SPECT in osteomyelitis and prosthetic bone and joint infections: a systematic review. *Semin. Nucl. Med.* 40 (1), 3–15. doi: 10.1053/j.semnuclmed.2009.08.005

Vento, J., Mulgaonkar, A., Woolford, L., Nham, K., Christie, A., and Bagrodia, A. (2019). PD-L1 detection using (89)Zr-atezolizumab immuno-PET in renal cell carcinoma tumorgrafts from a patient with favorable nivolumab response. *J. Immunother. Cancer* 7 (1), 144. doi: 10.1186/s40425-019-0607-z

Wang, J. F., Wang, Y. P., Xie, J., Zhao, Z. Z., Gupta, S., Guo, Y., et al. (2021). Upregulated PD-L1 delays human neutrophil apoptosis and promotes lung injury in an experimental mouse model of sepsis. *Blood* 138 (9), 806–810. doi: 10.1182/blood.2020009417

Zhang, X., Chen, P., Wan, H. Y., Zhu, R. J., Zhou, Y., Song, M. R., et al. (2022). Antimicrobial potency, prevention ability, and killing efficacy of daptomycin-loaded versus vancomycin-loaded β-tricalcium phosphate/calcium sulfate for methicillin-resistant *staphylococcus aureus* biofilms. *Front. Microbiol.* 13, 1029261. doi: 10.3389/fmicb.2022.1029261

Zhou, M., Wang, X., Chen, B., Xiang, S., Rao, W., Zhang, Z., et al. (2022). Preclinical and first-in-human evaluation of (18)F-labeled d-peptide antagonist for PD-L1 status imaging with PET. *Eur. J. Nucl. Med. Mol. Imaging* 49 (13), 4312–4324. doi: 10.1007/s00259-022-05876-9

Zhou, X., Jiang, J., Yang, X., Liu, T., Ding, J., Nimmagadda, S., et al. (2022). First-in-Humans evaluation of a PD-L1–binding peptide PET radiotracer in non–small cell lung cancer patients. *J. Nucl. Med.* 63 (4), 536–542. doi: 10.2967/jnumed.121.262045

frontiers | Frontiers in Cellular and Infection Microbiology

TYPE Original Research
PUBLISHED 28 June 2023
DOI 10.3389/fcimb.2023.1206393

OPEN ACCESS

EDITED BY
Chaofan Zhang,
First Affiliated Hospital of Fujian Medical University, China

REVIEWED BY
İlhami Çelik,
University of Health Sciences, Türkiye
Hongye Peng,
China Academy of Chinese Medical Sciences, China
Jinxiang Wang,
Sun Yat-sen University, China
Jiaheng Xie,
Nanjing Medical University, China

*CORRESPONDENCE
Hong-Fa Zhong
zhonghongfa88@sina.com
Wen-Cai Liu
liuwencaincu@163.com

RECEIVED 15 April 2023
ACCEPTED 13 June 2023
PUBLISHED 28 June 2023

CITATION
Ying H, Guo B-W, Wu H-J, Zhu R-P, Liu W-C and Zhong H-F (2023) Using multiple indicators to predict the risk of surgical site infection after ORIF of tibia fractures: a machine learning based study. *Front. Cell. Infect. Microbiol.* 13:1206393. doi: 10.3389/fcimb.2023.1206393

Using multiple indicators to predict the risk of surgical site infection after ORIF of tibia fractures: a machine learning based study

Hui Ying[1], Bo-Wen Guo[1], Hai-Jian Wu[1], Rong-Ping Zhu[1], Wen-Cai Liu[2*] and Hong-Fa Zhong[1*]

[1]Department of Emergency Trauma Surgery, Ganzhou People's Hospital, Ganzhou, China, [2]Department of Orthopaedics, Shanghai Jiao Tong University Affiliated Sixth People's Hospital, Shanghai, China

Objective: Surgical site infection (SSI) are a serious complication that can occur after open reduction and internal fixation (ORIF) of tibial fractures, leading to severe consequences. This study aimed to develop a machine learning (ML)-based predictive model to screen high-risk patients of SSI following ORIF of tibial fractures, thereby aiding in personalized prevention and treatment.

Methods: Patients who underwent ORIF of tibial fractures between January 2018 and October 2022 at the Department of Emergency Trauma Surgery at Ganzhou People's Hospital were retrospectively included. The demographic characteristics, surgery-related variables and laboratory indicators of patients were collected in the inpatient electronic medical records. Ten different machine learning algorithms were employed to develop the prediction model, and the performance of the models was evaluated to select the best predictive model. Ten-fold cross validation for the training set and ROC curves for the test set were used to evaluate model performance. The decision curve and calibration curve analysis were used to verify the clinical value of the model, and the relative importance of features in the model was analyzed.

Results: A total of 351 patients who underwent ORIF of tibia fractures were included in this study, among whom 51 (14.53%) had SSI and 300 (85.47%) did not. Of the patients with SSI, 15 cases were of deep infection, and 36 cases were of superficial infection. Given the initial parameters, the ET, LR and RF are the top three algorithms with excellent performance. Ten-fold cross-validation on the training set and ROC curves on the test set revealed that the ET model had the best performance, with AUC values of 0.853 and 0.866, respectively. The decision curve analysis and calibration curves also showed that the ET model had the best clinical utility. Finally, the performance of the ET model was further tested, and the relative importance of features in the model was analyzed.

Conclusion: In this study, we constructed a multivariate prediction model for SSI after ORIF of tibial fracture through ML, and the strength of this study was the use of multiple indicators to establish an infection prediction model, which can better reflect the real situation of patients, and the model show great clinical prediction performance.

KEYWORDS

machine learning, risk factors, surgical site infection, tibia fractures, predictive model

Introduction

The incidence of tibia fractures has gradually increased in tandem with the development of the economy and transportation industry. As a serious complication that can occur after open reduction and internal fixation (ORIF) of tibial fractures, surgical site infections (SSI) can lead to serious consequences such as prolonged hospitalization, increased hospital costs, readmissions, osteomyelitis, pseudoarthrosis and even sepsis or death (Henkelmann et al., 2017; Petrosyan et al., 2021; Ying et al., 2021; Barrés-Carsí et al., 2022), which poses a substantial burden to patients and their families. Another noteworthy problem is that the number of patients who develop SSI after discharge from hospital increases with shorter hospitalization times. As preventing SSI is more critical than secondary treatment, clinicians should balance the relationship between infection prevention and shortening hospitalization time. Consequently, it is essential to identify high-risk patients of SSI after tibia fracture and personalize prevention strategies accordingly.

There are many studies that have reported recognized risk factors for SSI, such as diabetes mellitus, obesity, prolonged surgical duration, smoking, elevated inflammatory indicators, etc (Ma et al., 2018; Norris et al., 2019; Ballhause et al., 2021). Additionally, some studies have also highlighted unexpected risk factors such as urinary tract infection (UTI) and bleeding disorders (Yoon and King, 2020; Saiz et al., 2022). To analyze postoperative infections ideally, it is necessary to consider adequate variables. However, most studies' risk factors are not comprehensive, and simple risk factor analysis has limited clinical application. The use of multiple indicators to develop a prediction model for SSI can be more clinically valuable.

Machine learning (ML) is a form of artificial intelligence that focuses on the use of data and algorithms to predict outcomes, identify patterns and trends within the data and learn from previous experience (Handelman et al., 2018; Liu WC. et al., 2022). ML has demonstrated robust predictive capabilities and is suitable for preoperative medical risk stratification and resource allocation (Ngiam and Khor, 2019; Yeo et al., 2022). In recent years, ML is widely used in the field of medicine, such as for early detection and diagnosis of cancer (Jones et al., 2022), as well as for coronavirus disease 2019 (COVID-19) diagnosis (Pfaff et al., 2022). Although ML has been demonstrated to have greater accuracy than conventional methods, few studies have established ML-based predictive models to identify high-risk patients of SSI, especially in patients with tibia fractures. The purpose of this study was to develop a ML-based predictive model to identify high-risk patients of SSI after ORIF of tibial fractures, which contributes to providing guidance for surgeons to develop personalized prevention and treatment.

Materials and methods

Study population

Patients who underwent ORIF of tibial fractures in the Department of Emergency Trauma Surgery at Ganzhou People's Hospital from January 2018 to October 2022 were retrospectively collected. This study was approved by the Ethics Committee of Ganzhou People's Hospital. The inclusion criteria were as follows: (1) patients were diagnosed as closed tibial fractures; (2) patients underwent ORIF surgery. The exclusion criteria were as follows: (1) patients with Open injury; (2) patients with multiple site damage; (3) patients with pathological fracture or fracture nonunion; (4) Patients with acute inflammation and infection in other areas of the body; (5) Patients with incomplete data.

Diagnosis of surgical site infection

The diagnosis of SSI for this study was based on the criteria developed by the Centers for Disease Control in the United States (Horan et al., 1992). In this study, SSI was defined as acute infection within 30 days after ORIF. Patients who met one of the following criteria would be diagnosed as SSI: (1) the wound presented the symptoms or signs of redness, swelling, fever, pain, tenderness to palpation and/or purulent drainage; (2) there was abscess aspirated from the wound and the culture was positive; (3) Fluid or tissue harvested from revision surgery was cultured positively; (4) evidences of SSI was confirmed by histopathologic and radiologic examinations; (5) SSI was diagnosed by the surgeons and definitely noted in the medical records. According to the location of SSI, it was divided into superficial infection and deep infection.

Data selection

We collected the demographic characteristics, surgery-related variables and laboratory parameters of patients from inpatient electronic medical records, while these variables have been shown to be associated with SSI according to relevant studies (Liu et al., 2018; Norris et al., 2019). Demographic characteristics including Gender, Age, Smoking, Hypertension, Diabetes. Surgery-related variables including Estimated blood loss, Procedure duration, ASA score, Blood transfusion history. Preoperative laboratory parameters including White blood cell (WBC), Neutrophil percentage (%), Lymphocyte percentage (%), Neutrophil count, Lymphocyte count, Red blood cell (RBC), Hemoglobin, Platelet (PLT), Prothrombin time (PT), Activated partial thromboplastin time (APTT), D-Dimer, Total Protein, Albumin, Globulin, Serum glucose, Urinary leukocyte count, Urinary bacterial count. Information on all variables was complete for these patients.

Statistical analyses

The statistical analyses in this study were all performed by Python (version 3.8, Python Software Foundation). Categorical variables were expressed as frequency or proportions and compared by the chi-square test or Fisher's exact test. K-S-L test was used to test the normality of continuous data. Continuous non-normally distributed variables were evaluated using the Wilcoxon rank-sum test and shown as median and the first quartile (Q1) and the third quartile (Q3). A significant difference was set as $P<0.05$.

Data preprocessing, model establishment and performance evaluation

Data of patients were randomly sliced into training and test set in a ratio of 7:3 using a stratified random sampling method in python. Categorical variables such as smoking and diabetes status were processed using label encoding methods. The training set was used to construct the models, and the test set was used to evaluate the prediction performance of models. To address the imbalance of data distribution, random oversampling methods were used. The key of this method is to oversampling the data samples of small classes to increase the number of data samples of small classes to improve the accuracy of the model.

In this study, ten different ML algorithms were constructed with scikit-learn, xgboost and lightgbm modules: Logistic regression (LR), K Neighbors Classifier (KNN), Decision Tree Classifier (DT), Extra Trees Classifier (ET), Random Forest Classifier (RF), Extreme Gradient Boosting (XGBoost), Light Gradient Boosting Machine (Lightgbm), naïve Bayes (NB), Gradient Boosting Classifier (GBC), and Ada Boost Classifier (ADA). The performance of these algorithms was compared without hyper-parameter optimization and the accuracy and area under the receiver operating characteristic curve (AUC) were calculated to select the top three algorithms for further development. The models were then optimized by adjusting the hyper-parameters using the randomized search method, followed by internal and external validation.

Ten-fold cross-validation was used for internal verification, which the training set was split into 10 sets, and nine of them were used for model training and one for model evaluation. The corresponding correct rate was obtained for each trial and the average of the correct rate of the results of 10 times was used as an estimate of the accuracy of the algorithm. AUC and ROC curve were calculated in the test set to externally validate the predictive performance of the ML models. To further evaluate the clinical value of the models, decision curve analyses (DCA) were calculated to show the net benefit of using a model at different thresholds. Calibration was assessed graphically between the predicted and observed outcomes for the training and validation samples. Calibration curve was plotted to assess the calibration of different ML models. Calibration curves depict the calibration of each model in terms of the agreement between the predicted risks of SSI and observed outcomes. Comparing the evaluation indexes of the three model to select the best-performing model.

For the best model, the Youden index, which maximizes the sum of the sensitivity and specificity, was defined to calculate the appropriate cut-off values. External validation was performed using cumulative lift measures to calculate the multiple of the model's prediction ability compared with the random selection. The confusion matrix intuitively showed prediction performance and the difference between the model prediction result and the real situation. The feature importance and impact of each input variable on the model output was assessed by computing Shapley Additive Explanations (SHAP) values. SHAP was a game-theoretic approach to interpreting the output of ML models. It used the classical Shapley values from game theory and their associated extensions to relate optimal credit allocation to local explanations.

Results

Data baseline

According to the inclusion and exclusion criteria, a total of 351 patients underwent ORIF of tibial fractures were included in this study and 242 patients were excluded. Among the patients included, 51 (14.53%) had SSI and 300 (85.47%) without. In 51 patients with SSI, there were 15 cases of deep infection and 36 cases of superficial infection. The detailed characteristics are shown in Table 1. The total cohort was split into a training set (n=245) and a test set (n=106) in a ratio of 7:3, while the differences in variables between two groups were not statistically significant (Table 2).

Candidate algorithms screening

245 samples were randomly selected for model training. Of these samples, 36 (14.69%) had SSI and 209 (85.31%) without. And, all features were used to construct predictive models in this study. The prediction performances of the various models are exhibited in Figure 1. In the initial selection, accuracy and AUC were defined as the main parameters to evaluate the models' performance. The top three algorithms with excellent performance were selected for the next step experiment, including Extra Trees Classifier (ET) (accuracy: 0.841; AUC: 0.805), Logistic regression (LR) (accuracy: 0.734; AUC: 0.789) and Random Forest Classifier (RF) (accuracy: 0.820; AUC: 0.786).

Model development and selection

Internal and external validation after adjusting the optimal hyper-parameter configuration of the models. The final hyperparameters setting of the three models are listed in Supplementary Table 1. The performance of the machine learning models was verified by 10-fold cross-validation in the training set, and the results are shown in Figure 2A. It can be seen that the ET (AUC: 0.853) model had better performance than LR (AUC: 0.832) and RF (AUC: 0.781) model in internal verification. The ROC curves of three constructed models using the test set are shown in Figure 2B. The results also show that the ET model has the best prediction performance with an AUC of 0.866. Both internal validation and external validation show that ET model has the best performance.

Clinical utility

The Decision curve analysis (DCA) of the three model is presented in Figure 3A. DCA demonstrated that the ET model added more net benefit compared with RF model or LR model, indicating that it had better clinical impact at a wide range of probability thresholds. Calibration curves depict the calibration of each model in terms of the agreement between the predicted risks of

10.3389/fcimb.2023.1206393

TABLE 1 Baseline characteristics of study population.

Variables		Overall	No	Yes	P-Value
n		351	300	51	
Gender, n (%)	Female	161 (45.9)	139 (46.3)	22 (43.1)	0.672
	Male	190 (54.1)	161 (53.7)	29 (56.9)	
Age, median [Q1,Q3]		44.0 [27.5,56.0]	43.0 [27.0,55.0]	50.0 [34.0,56.5]	0.055
Smoking, n (%)	No	314 (89.5)	270 (90.0)	44 (86.3)	0.423
	Yes	37 (10.5)	30 (10.0)	7 (13.7)	
Hypertension, n (%)	No	285 (81.2)	248 (82.7)	37 (72.5)	0.087
	Yes	66 (18.8)	52 (17.3)	14 (27.5)	
Diabetes , n (%)	No	322 (91.7)	285 (95.0)	37 (72.5)	<0.001
	Yes	29 (8.3)	15 (5.0)	14 (27.5)	
Estimated blood loss, median [Q1,Q3]		50.0 [30.0,150.0]	50.0 [27.5,100.0]	100.0 [100.0,300.0]	<0.001
Procedure duration, median [Q1,Q3]		150.0 [105.0,200.0]	150.0 [99.8,180.0]	220.0 [157.5,292.5]	<0.001
ASA, n (%)	1	29 (8.3)	27 (9.0)	2 (3.9)	0.061
	2	311 (88.6)	266 (88.7)	45 (88.2)	
	3	11 (3.1)	7 (2.3)	4 (7.8)	
Blood transfusion history, n (%)	No	333 (94.9)	294 (98.0)	39 (76.5)	<0.001
	Yes	18 (5.1)	6 (2.0)	12 (23.5)	
WBC, median [Q1,Q3]		9.1 [7.5,11.1]	9.1 [7.4,11.0]	9.8 [8.4,11.6]	0.095
Neutrophils%, median [Q1,Q3]		74.5 [68.6,79.8]	73.4 [68.1,79.0]	79.0 [73.3,84.3]	<0.001
Lymphocyte%, median [Q1,Q3]		16.9 [12.6,21.7]	17.4 [13.4,22.3]	14.0 [9.3,17.0]	<0.001
Neutrophil count, median [Q1,Q3]		6.7 [5.1,8.4]	6.5 [5.1,8.3]	7.5 [6.2,9.2]	0.012
Lymphocyte count, median [Q1,Q3]		1.5 [1.2,1.9]	1.5 [1.2,1.9]	1.2 [1.0,1.5]	<0.001
RBC, median [Q1,Q3]		4.4 [4.0,4.8]	4.4 [4.0,4.8]	4.2 [3.7,4.6]	0.036
HB, median [Q1,Q3]		130.0 [117.0,141.0]	131.0 [118.0,141.0]	129.0 [112.0,138.5]	0.263
PLT, median [Q1,Q3]		234.0 [201.0,280.0]	234.0 [202.0,279.2]	234.0 [182.0,282.5]	0.568
PT, median [Q1,Q3]		11.2 [10.6,11.8]	11.2 [10.7,11.8]	11.1 [10.4,11.9]	0.631
APTT, median [Q1,Q3]		26.2 [24.8,28.3]	26.3 [24.8,28.3]	25.9 [24.4,28.4]	0.619
D_Dimer, median [Q1,Q3]		3.9 [1.9,9.4]	3.4 [1.6,8.1]	7.3 [3.5,16.2]	<0.001
Total Protein, median [Q1,Q3]		65.9 [63.1,69.7]	65.8 [63.4,69.7]	66.4 [62.0,69.8]	0.364
Albumin, median [Q1,Q3]		41.2 [39.2,43.1]	41.4 [39.2,43.2]	40.7 [38.5,42.6]	0.203
Globulin, median [Q1,Q3]		24.9 [22.2,27.5]	24.8 [22.2,27.5]	25.1 [22.5,27.4]	0.784
Glucose, median [Q1,Q3]		5.5 [5.0,6.2]	5.5 [5.0,6.0]	6.2 [5.5,6.9]	<0.001
Urinary leukocyte, median [Q1,Q3]		4.0 [0.0,13.9]	3.7 [0.0,13.7]	5.0 [1.2,19.3]	0.195
Urinary bacterial, median [Q1,Q3]		7.2 [0.0,105.5]	7.0 [0.0,95.1]	9.1 [0.0,123.5]	0.471

infection and observed outcomes of infection. As shown in Figure 3B, the calibration curve of ET model demonstrated good agreement between prediction and observation. The above results show that the ET model has the best clinical performance, so we choose the ET model as the final prediction model to identify high-risk patients of SSI after ORIF of tibial fractures.

Model performance and feature importance

As illustrated in Figure 4A, decreasing sensitivity and increasing specificity are shown for an increasing probability of infection, with a histogram for the distribution of the predicted probability. We

10.3389/fcimb.2023.1206393

TABLE 2 Baseline characteristics of training set and test set.

Variables		Overall	Train	Test	P-Value
n		351	245	106	
Infection, n (%)	No	300 (85.5)	209 (85.3)	91 (85.8)	1
	Yes	51 (14.5)	36 (14.7)	15 (14.2)	
Gender, n (%)	Female	161 (45.9)	113 (46.1)	48 (45.3)	0.977
	Male	190 (54.1)	132 (53.9)	58 (54.7)	
Age, median [Q1,Q3]		44.0 [27.5,56.0]	44.0 [27.0,55.0]	46.0 [28.2,57.8]	0.369
Smoking, n (%)	No	314 (89.5)	218 (89.0)	96 (90.6)	0.799
	Yes	37 (10.5)	27 (11.0)	10 (9.4)	
Hypertension, n (%)	No	285 (81.2)	200 (81.6)	85 (80.2)	0.866
	Yes	66 (18.8)	45 (18.4)	21 (19.8)	
Diabetes , n (%)	No	322 (91.7)	228 (93.1)	94 (88.7)	0.247
	Yes	29 (8.3)	17 (6.9)	12 (11.3)	
Estimated blood_loss, median [Q1,Q3]		50.0 [30.0,150.0]	100.0 [30.0,150.0]	50.0 [30.0,150.0]	0.751
Procedure duration, median [Q1,Q3]		150.0 [105.0,200.0]	155.0 [106.0,210.0]	150.0 [96.2,180.0]	0.114
ASA, n (%)	1	29 (8.3)	18 (7.3)	11 (10.4)	0.562
	2	311 (88.6)	220 (89.8)	91 (85.8)	
	3	11 (3.1)	7 (2.9)	4 (3.8)	
Blood transfusion history, n (%)	No	333 (94.9)	232 (94.7)	101 (95.3)	1
	Yes	18 (5.1)	13 (5.3)	5 (4.7)	
WBC, median [Q1,Q3]		9.1 [7.5,11.1]	9.1 [7.5,11.1]	9.1 [7.6,11.0]	0.883
Neutrophils%, median [Q1,Q3]		74.5 [68.6,79.8]	74.1 [68.5,79.3]	74.8 [68.8,81.3]	0.487
Lymphocyte%, median [Q1,Q3]		16.9 [12.7,21.7]	17.0 [13.2,21.9]	16.8 [11.2,21.3]	0.591
Neutrophil count, median [Q1,Q3]		6.7 [5.1,8.4]	6.7 [5.1,8.4]	6.7 [5.3,8.3]	0.809
Lymphocyte count, median [Q1,Q3]		1.5 [1.2,1.9]	1.5 [1.2,1.9]	1.5 [1.1,1.8]	0.716
RBC, median [Q1,Q3]		4.4 [4.0,4.8]	4.4 [4.0,4.8]	4.3 [3.9,4.8]	0.638
HB, median [Q1,Q3]		130.0 [117.0,141.0]	131.0 [117.0,141.0]	129.0 [117.0,140.0]	0.521
PLT, median [Q1,Q3]		234.0 [201.0,280.0]	234.0 [203.0,279.0]	239.5 [193.8,282.8]	0.732
PT, median [Q1,Q3]		11.2 [10.6,11.8]	11.2 [10.6,11.8]	11.2 [10.6,11.8]	0.581
APTT, median [Q1,Q3]		26.2 [24.8,28.3]	26.2 [24.8,28.3]	26.3 [24.7,28.3]	0.76
D_Dimer, median [Q1,Q3]		3.9 [1.9,9.4]	3.9 [1.8,9.5]	3.7 [1.9,8.9]	0.822
Total Protein, median [Q1,Q3]		65.9 [63.1,69.7]	65.9 [63.2,69.8]	66.1 [63.0,69.7]	0.931
Albumin, median [Q1,Q3]		41.2 [39.2,43.1]	41.5 [39.3,43.3]	40.8 [38.8,43.0]	0.173
Globulin, median [Q1,Q3]		24.9 [22.2,27.5]	24.8 [22.2,27.5]	25.2 [22.4,27.7]	0.422
Glucose, median [Q1,Q3]		5.6 [5.0,6.2]	5.5 [5.0,6.1]	5.7 [5.1,6.5]	0.165
Urinary leukocyte, median [Q1,Q3]		4.0 [0.0,13.9]	4.6 [0.4,15.3]	2.3 [0.0,8.9]	0.054
Urinary bacterial, median [Q1,Q3]		7.2 [0.0,105.5]	8.1 [0.0,110.5]	5.4 [0.0,93.6]	0.262

defined an optimal cut-off probability of 0.18 for the ET model according to the Youden index and the sensitivity and specificity were 0.867, 0.769 respectively. Figure 4B demonstrates the cumulative gains of ET model, which showed the rate of SSI events captured by ET model over a given number of samples. The cumulative lift demonstrates a snapshot of the ratio of the percentage of patients with infection to the percentage of patients without. We used it to compare ET model vs a theoretically ideal

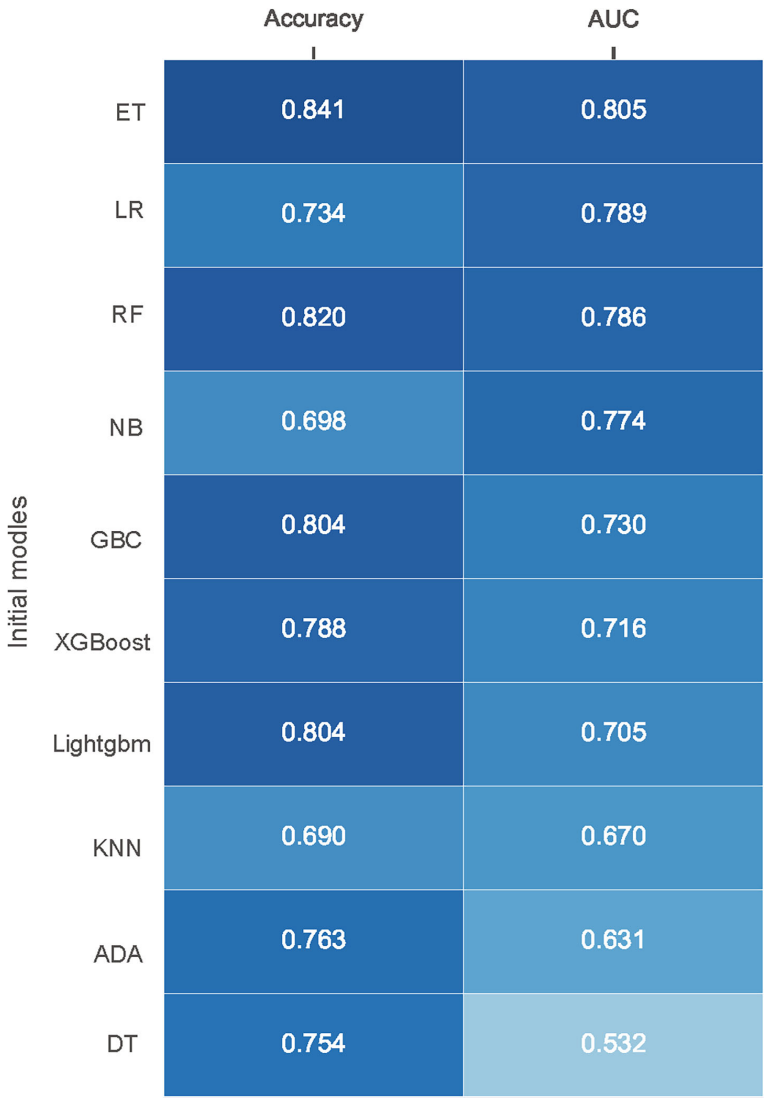

FIGURE 1
Performance of different models in internal validation without initial parameters. Models are ordered according to their AUC. AUC, area under receiver operating characteristic curve; ET, Extra Trees Classifier; LR, Logistic regression; RF, Random Forest Classifier; NB, Naive Bayes; GBC, Gradient Boosting Classifier; XGBoost, Extreme Gradient Boosting; Lightgbm, Light Gradient Boosting Machine; KNN, K Neighbors Classifier; ADA, Ada Boost Classifier; DT, Decision Tree Classifier.

model (perfectly predicts SSI given a sample) and a model that is no better than random guessing. When cut-off value was 0.18, the lift value was 2.7 for the ET model. The confusion matrix (Figure 4C) of the ET model in the test set indicated its great prediction performance. To reveal the relative importance of features in ET model, SHAP values were calculated and are plotted in Figure 5. As shown, Diabetes, Estimated blood loss, Procedure duration, Blood transfusion history are the most important features for distinguishing the SSI and non-SSI groups.

Discussion

Tibial fractures are a frequent and complicated injury for orthopedic surgeons, typically resulting from high-energy trauma and often leading to complications (Choo and Morshed, 2014; Henkelmann et al., 2017). Identification high-risk patients for surgical site infection (SSI) and providing personalized prevention and treatment are important considerations. This study included 351 patients, of whom 51 developed postoperative infections. Previous literature reported a wide range of the rate of SSI between 2.6–45% for tibial fractures (Henkelmann et al., 2017), while our results show that the overall incidence of SSI is 15%, and 4.1% for deep SSI, falling within the previously reported range. Compared to other types of fractures, there is a higher incidence rate of SSI after ORIF of tibial fractures (Shen et al., 2021), and the possible cause for this difference is that tibia is covered with sparse soft tissue and usually suffers from severe injuries (Norris et al., 2019).

ML has been widely used in the medical field, and a ML-based multivariate prediction model was constructed to screen out high-risk patients of SSI in this study. Ten algorithms including LR, KNN, DT, ET, RF, XGBoost, Lightgbm, NB, GBC and ADA were

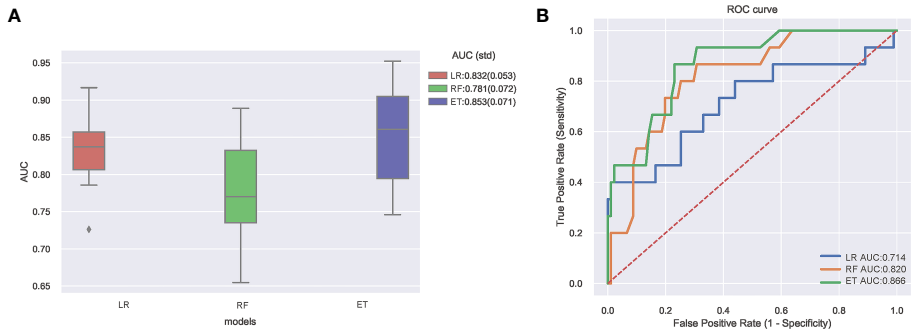

FIGURE 2
(A) Ten-fold cross-validation results of different machine learning models. **(B)** The ROC curves of different machine learning models in external test set. AUC, area under receiver operating characteristic curve; ROC, receiver operating characteristic; ET, Extra Trees Classifier; LR, Logistic regression; RF, Random Forest Classifier.

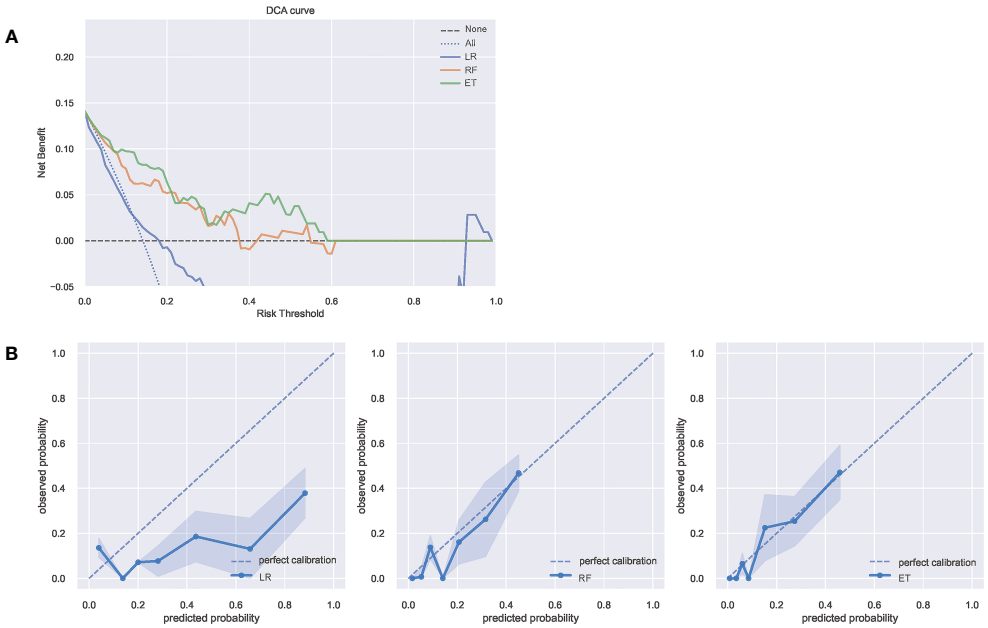

FIGURE 3
(A) The DCA curves of the three model. The net benefit was calculated by adding the true positives and subtracting the false positives. The y-axis represents the net benefit, and the x-axis represents the threshold probability. The Oblique line represents the assumption that all patients will infection, and the horizontal line represents the assumption that no patients with infection. **(B)** The calibration curves of the three models. The y-axis represents the actual infection rate. The diagonal dotted line represents an ideal model and the blue solid line represents the performance of the model, while the model closer fit to the diagonal dotted line represents a better prediction. DCA, decision curve analysis; ET, Extra Trees Classifier; LR, Logistic regression; RF, Random Forest Classifier.

used to predict SSI risk after ORIF of tibial fractures. Through internal and external validation, it is found that ET model has the best prediction performance, and the test set AUC of ET model is 0.896, moreover, the prediction model also shows great clinical performance.

In the models we constructed, all the included indicators are the possible risk factors for SSI according to previous literature (Liu et al., 2018; Norris et al., 2019) and these indicators mainly fall into three categories: demographic characteristics, surgery-related variables and laboratory parameters. Predictor variables should be included as much as possible to better reflect the actual situation of patients, but some risk factors for SSI are excluded because they cannot be collected or difficult to measure, for instance, it is difficult to weigh fracture patients, so BMI cannot be calculated, and wound dressing is greatly affected by the experience and habits of the clinician and cannot be measured. To our knowledge, this is the first to include almost all collectable indicators to develop a ML-based prediction model for SSI after ORIF of tibia fractures. Through the feature importance experiment, we identified several indicators that have the greatest impact on the model, and diabetes, estimated blood loss, procedure duration, blood transfusion history, lymphocyte count and PLT are the top six.

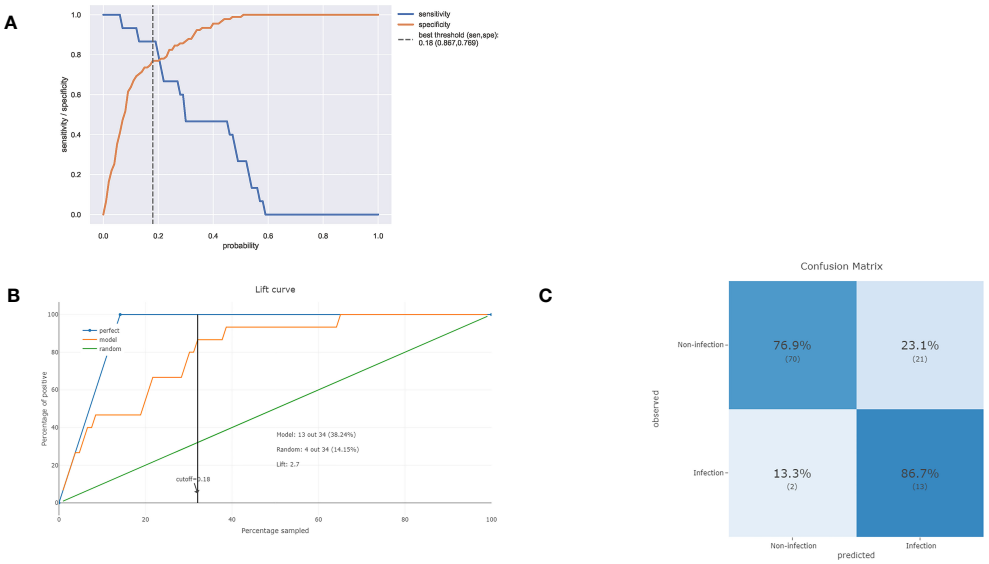

FIGURE 4
(A) Sensitivity and specificity versus cut-off probability plot of the ET model. Decreasing sensitivity and increasing specificity are shown for increasing probability thresholds for infection. **(B)** The cumulative lift demonstrates a snapshot of the ratio of the percentage of patients with infection events reached during a treatment campaign to the percentage of patients targeted. It showed the rate of positive events captured by a model over a given number of samples. **(C)** The confusion matrix of the ET model in the test set.

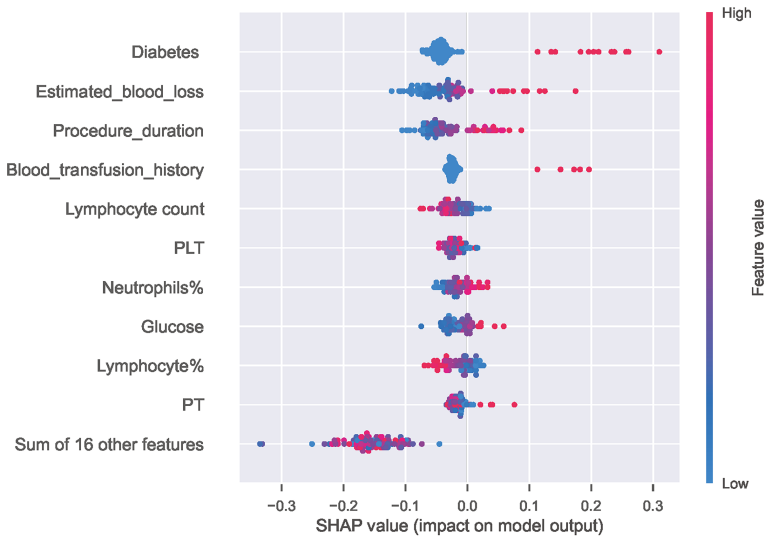

FIGURE 5
Distribution of the impact of each feature on the output of ET model estimated using the SHAP values. The plot sorts features by the sum of SHAP value magnitudes over all samples and shows the order of feature importance. This figure described data from the test cohort, with each point representing one patient. The color represents the feature value (red high, blue low). The x axis measures the impact on the model output (right positive, left negative). A positive value indicate a SSI risk and a negative value indicate a good outcome. SHAP, SHapley Additive explanation; PLT, Platelet; PT, Prothrombin time.

Our results show that the diabetes was the most important variable in the model, and lots of research have indicated diabetes is an independent risk factor for SSI. Such as, Bachoura et al. found that diabetes is the nonmodifiable risk factors for SSIs after skeletal trauma (Bachoura et al., 2011), and Oladeji et al. show that diabetic patients were 2.7 times more likely to develop a deep infection than ordinary patients after pilon fracture fixation (Oladeji et al., 2021). The microvascular blood flow of patients with diabetes is usually damaged, which decreased the ability to deliver antibiotics or inflammatory cells to the injured area to resist infection, resulting in the higher risk of SSI. Diabetic status was identified by the medical records, and we noticed that glucose control in patients with diabetes was different, which may have different effects on the occurrence of infection. Similar study has been reported by

Anderson et al. that glucose ≥200 mg/dL was a significant independent risk factor for 90-day deep surgical site infections in orthopaedic trauma patients (Anderson et al., 2021). In addition, Andres et al. indicated that stress-induced hyperglycemia also increased the risk of infection in orthopedic trauma patients without a history of diabetes (Rodriguez-Buitrago et al., 2019). Therefore, diabetes alone cannot well reflect its impact on infection, while the combination of serum glucose and diabetes can produce a better predictive value.

Prolonged operative time is a well-accepted risk factor for SSI after tibia fractures. A retrospective analysis of 309 tibial plateau fractures found operative times approaching 3 hours was related to an increased risk for SSI (Colman et al., 2013). Li et al. also showed that patients who developed SSI after surgery had a longer operative time (200.5 ± 82.5 min) than those without infection (142.8 ± 54.1 minutes) (Li et al., 2018). Prolonged operative time not only results in more extensive soft-tissue stripping and extended exposure of the wound but also leads to higher estimated blood loss (EBL). EBL, as an independent predictor of SSI after orthopedic surgery, has been widely reported in the previous literature (Li et al., 2015; Liu WC. et al., 2022), and our results also show that the EBL plays an important role in infection prediction. Moreover, our study found that patients with SSIs had a higher proportion of blood transfusion history compared with patients without SSIs. Similar evidence was also found in Panteli et al.'s study, and it show post-operative transfusion associations with deep infection (Panteli et al., 2021). Additionally, some studies believe that Immunosuppression as the consequence of blood transfusion is related to the increase of SSI rate (Hill et al., 2003; Guerado et al., 2016). From a clinical perspective, patients who need blood transfusion after surgery are associated with more blood loss or poor physical condition, and all these factors may increase the rate of SSI. Operation time, EBL, and blood transfusion history influence each other to varying degrees, and they should not be considered in isolation.

In contrast to patient and intraoperative factors, which are sometimes subjective and unclear in showing body status, serum biomarkers are more sensitive and objective (Wu et al., 2022). The abnormal preoperative inflammatory indicators is not only the reflection of the acute inflammatory response but also the stress response of body to injury, which may contribute to the prediction of infection. Zhao et al. reported that the increase in preoperative inflammatory markers such as WBC count is significantly associated with SSI (Zhao et al., 2022), and Lu et al. showed that NLR (the values of ratio of neutrophil to lymphocyte) ≥6.4 is independently associated with SSI (Lu et al., 2022). Some scholars believed that lymphocytes represent the immune function of patients and thus are associated with infection (Iwata et al., 2016). Consistent with the previous literature, we also found that some inflammatory indicators had statistically significant differences between SSI and non-SSI patients and played an important role in model construction in this study, such as neutrophil and lymphocyte. As Imabayashi et al. found that the combination of neutrophil count, lymphocyte ratio, and C-reactive protein ratio, may be a strong tool for detecting SSI (Imabayashi et al., 2022), Thus, it may be a better choice to use a combination of inflammation indicators to predict infection.

Although the univariate analysis did not suggest a significant correlation between the PLT and SSI, we cannot completely ignore its importance in infection prediction. Liu et al. reported that the temporal changes of the PLT count in immunocompromised patients who have undergone femoral neck fracture repair can serve as an early warning of SSI (Liu J. et al., 2022). Zhang et al. posit that platelet count were significantly higher in the Deep surgical site infection (DSSI) group than in the non-DSSI group PLT after ORIF for traumatic limb fractures (Zhang et al., 2018). On the other hand, Hu et al.'s study found that PLT<288 × 10^9 is an independent risk factor for wound infection after surgical treatment of open fractures (Hu et al., 2020). Saiz et al. found that patients with bleeding disorder are more likely to develop SSI than patients without (Saiz et al., 2022). The lack of statistical difference in PLT indicators may be due to the limited sample size in our study. However, it is important to note that PLT has a significant impact on the ML-based predictive model for SSI, which highlights the potential benefits of using ML methods to detect subtle associations that may not be apparent with traditional statistical approaches.

It is worth noting that the prediction model in this study was established for clinical purposes, and the ET model demonstrated good clinical performance. The confusion matrix showed that 13 out of the 15 infected patients were correctly predicted in the external test. Further prospective clinical prediction tests are needed to verify the actual effectiveness of the model. According to the risk assessment results generated by the prediction model, clinicians should pay more attention to high-risk patients of SSI and develop personalized treatment. Furthermore, this screening approach help to strike a balance between shortening the average hospital stay and minimizing post-discharge infection rates; screening high-risk patients allows for selective extension of hospitalization for those at high risk, while potentially reducing the hospitalization duration for low-risk patients.

Limitations

This study has several limitations. First, this is a retrospective study, which limits the source of data to medical records and reduces the credibility of the evidence. Additionally, the retrospective study design may introduce selection bias, and patients with confirmed SSI in other institutions were excluded. Furthermore, the number of cases in this study was relatively small, and it was a single-center research. Future studies should be conducted in multiple centers with larger sample sizes.

Conclusions

In summary, this study constructed a multivariate prediction model for SSI after ORIF of tibial fracture using ML. The use of multiple indicators to establish the infection prediction model was a significant strength of this study, which can better reflect the real situation of patients. The model demonstrated good clinical prediction performance, which contributes to the screening and personalized treatment of high-risk patients of SSI.

Data availability statement

The raw data supporting the conclusions of this article will be made available by the authors, without undue reservation.

Ethics statement

The studies involving human participants were reviewed and approved by the Ethics Committee of Ganzhou People's Hospital. The patients/participants provided their written informed consent to participate in this study.

Author contributions

HY, W-CL and H-FZ conceived of and designed the study. HY, W-CL, B-WG, H-JW and R-PZ performed analysis and generated the figures and tables. HY and W-CL wrote the manuscript and HY, W-CL and H-FZ critically reviewed the manuscript. All authors have read and approved the manuscript.

Conflict of interest

The authors declare that the research was conducted in the absence of any commercial or financial relationships that could be construed as a potential conflict of interest.

Publisher's note

Supplementary material

The Supplementary Material for this article can be found online at: https://www.frontiersin.org/articles/10.3389/fcimb.2023.1206393/full#supplementary-material

References

Anderson, B. M., Wise, B. T., Joshi, M., Castillo, R., O'Toole, R. V., and Richards, J. E. (2021). Admission hyperglycemia is a risk factor for deep surgical-site infection in orthopaedic trauma patients. *J. Orthop Trauma* 35 (12), e451–e457.

Bachoura, A., Guitton, T. G., Smith, R. M., Vrahas, M. S., Zurakowski, D., and Ring, D. (2011). Infirmity and injury complexity are risk factors for surgical-site infection after operative fracture care. *Clin. Orthop Relat. Res.* 469 (9), 2621–2630.

Ballhause, T. M., Krause, M., Roß, J., Rueger, J. M., Frosch, K. H., Klatte, T. O., et al. (2021). Third day laboratory follow-up: mandatory for surgical site infections of tibial plateau fractures. *Eur. J. Trauma Emerg. Surg.* 47 (2), 581–587.

Barrés-Carsí, M., Navarrete-Dualde, J., Quintana Plaza, J., Escalona, E., Muehlendyck, C., Galvain, T., et al. (2022). Healthcare resource use and costs related to surgical infections of tibial fractures in a Spanish cohort. *PloS One* 17 (11), e0277482.

Choo, K. J., and Morshed, S. (2014). Postoperative complications after repair of tibial plateau fractures. *J. Knee Surg.* 27 (1), 11–19.

Colman, M., Wright, A., Gruen, G., Siska, P., Pape, H. C., Tarkin, I., et al. (2013). Prolonged operative time increases infection rate in tibial plateau fractures. *Injury* 44 (2), 249–252.

Guerado, E., Medina, A., Mata, M. I., Galvan, J. M., and Bertrand, M. L. (2016). Protocols for massive blood transfusion: when and why, and potential complications. *Eur. J. Trauma Emerg. Surg.* 42 (3), 283–295.

Handelman, G. S., Kok, H. K., Chandra, R. V., Razavi, A. H., Lee, M. J., and Asadi, H. (2018). eDoctor: machine learning and the future of medicine. *J. Intern. Med.* 284 (6), 603–619.

Henkelmann, R., Frosch, K. H., Glaab, R., Lill, H., Schoepp, C., Seybold, D., et al. (2017). Infection following fractures of the proximal tibia - a systematic review of incidence and outcome. *BMC Musculoskelet Disord.* 18 (1), 481.

Hill, G. E., Frawley, W. H., Griffith, K. E., Forestner, J. E., and Minei, J. P. (2003). Allogeneic blood transfusion increases the risk of postoperative bacterial infection: a meta-analysis. *J. Trauma* 54 (5), 908–914.

Horan, T. C., Gaynes, R. P., Martone, W. J., Jarvis, W. R., and Emori, T. G. (1992). CDC Definitions of nosocomial surgical site infections, 1992: a modification of CDC definitions of surgical wound infections. *Am. J. Infect. Control* 20 (5), 271–274.

Hu, Q., Zhao, Y., Sun, B., Qi, W., and Shi, P. (2020). Surgical site infection following operative treatment of open fracture: incidence and prognostic risk factors. *Int. Wound J.* 17 (3), 708–715.

Imabayashi, H., Miyake, A., and Chiba, K. (2022). Establishment of a suitable combination of serological markers to diagnose surgical site infection following spine surgery: a novel surgical site infection scoring system. *J. Orthop Sci.* 27 (3), 569–573.

Iwata, E., Shigematsu, H., Koizumi, M., Nakajima, H., Okuda, A., Morimoto, Y., et al. (2016). Lymphocyte count at 4 days postoperatively and CRP level at 7 days postoperatively: reliable and useful markers for surgical site infection following instrumented spinal fusion. *Spine (Phila Pa 1976)* 41 (14), 1173–1178.

Jones, O. T., Matin, R. N., van der Schaar, M., Prathivadi Bhayankaram, K., Ranmuthu, C. K.I., Islam, M. S., et al. (2022). Artificial intelligence and machine learning algorithms for early detection of skin cancer in community and primary care settings: a systematic review. *Lancet Digit Health* 4 (6), e466–e476.

Li, Q., Liu, P., Wang, G., Dong, T., Chen, W., Zhang, Y., et al. (2015). Risk factors of surgical site infection after acetabular fracture surgery. *Surg. Infect. (Larchmt)* 16 (5), 577–582.

Li, J., Zhu, Y., Liu, B., Dong, T., Chen, W., Zhang, Y., et al. (2018). Incidence and risk factors for surgical site infection following open reduction and internal fixation of adult tibial plateau fractures. *Int. Orthop* 42 (6), 1397–1403.

Li, Q., Liu, P., Wang, G., Yang, Y., Dong, J., Wang, Y., Zhou, D., et al. (2018). Risk factors for surgical site infection after posterior lumbar spinal surgery. *Spine (Phila Pa 1976)* 43 (10), 732–737.

Liu, J., Xu, X., Lv, X., and Shen, G. (2022). Correlation between surgical site infection and time-dependent blood platelet count in immunocompromised patients after femoral neck fracture. *J. Int. Med. Res.* 50 (1), 3000605211068689.

Liu, W. C., Ying, H., Liao, W. J., Zhou, Y., Yang, D., Duan, M. S., et al. (2022). Using preoperative and intraoperative factors to predict the risk of surgical site infections after lumbar spinal surgery: a machine learning-based study. *World Neurosurg.* 162, e553–e560.

Lu, K., Ma, T., Yang, C., Qu, Q., and Liu, H. (2022). Risk prediction model for deep surgical site infection (DSSI) following open reduction and internal fixation of displaced intra-articular calcaneal fracture. *Int. Wound J.* 19 (3), 656–665.

Ma, Q., Aierxiding, A., Wang, G., Wang, C., Yu, L., and Shen, Z. (2018). Incidence and risk factors for deep surgical site infection after open reduction and internal fixation of closed tibial plateau fractures in adults. *Int. Wound J.* 15 (2), 237–242.

Ngiam, K. Y., and Khor, I. W. (2019). Big data and machine learning algorithms for health-care delivery. *Lancet Oncol.* 20 (5), e262–e273.

Norris, G. R., Checketts, J. X., Scott, J. T., Vassar, M., Norris, B. L., and Giannoudis, P. V. (2019). Prevalence of deep surgical site infection after repair of periarticular knee fractures: a systematic review and meta-analysis. *JAMA Netw. Open* 2 (8), e199951.

Oladeji, L. O., Platt, B., and Crist, B. D. (2021). Diabetic pilon factures: are they as bad as we think? *J. Orthop Trauma* 35 (3), 149–153.

Panteli, M., Vun, J. S. H., West, R. M., Howard, A., Pountos, I., and Giannoudis, P. V. (2021). Surgical site infection following intramedullary nailing of subtrochanteric femoral fractures. *J. Clin. Med.* 10 (15), 3331.

Petrosyan, Y., Thavorn, K., Maclure, M., Smith, G., McIsaac, D. I., Schramm, D., et al. (2021). Long-term health outcomes and health system costs associated with surgical site infections: a retrospective cohort study. *Ann. Surg.* 273 (5), 917–923.

Pfaff, E. R., Girvin, A. T., Bennett, T. D., Bhatia, A., Brooks, I. M., Deer, R. R., et al. (2022). Identifying who has long COVID in the USA: a machine learning approach using N3C data. *Lancet Digit Health* 4 (7), e532–e541.

Rodriguez-Buitrago, A., Basem, A., Okwumabua, E., Enata, N., Evans, A., Pennings, J., et al. (2019). Hyperglycemia as a risk factor for postoperative early wound infection after bicondylar tibial plateau fractures: determining a predictive model based on four methods. *Injury* 50 (11), 2097–2102.

Saiz, A. M.Jr., Stwalley, D., Wolinsky, P., and Miller, A. N. (2022). Patient comorbidities associated with acute infection after open tibial fractures. *J. Am. Acad. Orthop Surg. Glob Res. Rev.* 6 (9), e22.

Shen, J., Sun, D., Fu, J., Wang, S., Wang, X., and Xie, Z. (2021). Management of surgical site infection post-open reduction and internal fixation for tibial plateau fractures. *Bone Joint Res.* 10 (7), 380–387.

Wu, X., Ma, X., Zhu, J., and Chen, C. (2022). C-reactive protein to lymphocyte ratio as a new biomarker in predicting surgical site infection after posterior lumbar interbody fusion and instrumentation. *Front. Surg.* 9, 910222.

Yeo, I., Klemt, C., Robinson, M. G., Esposito, J. G., Uzosike, A. C., and Kwon, Y. M. (2022). The use of artificial neural networks for the prediction of surgical site infection following TKA. *J. Knee Surg* 36 (06), 637–643.

Ying, H., Luo, Z. W., Peng, A. F., Yang, Q. K., Wu, X., and Chen, X. Y. (2021). Incidences and reasons of postoperative surgical site infection after lumbar spinal surgery: a large population study. *Eur. Spine J* 31 (2), 482–488.

Yoon, J. S., and King, J. T. Jr. (2020). Preoperative urinary tract infection increases postoperative morbidity in spine patients. *Spine (Phila Pa 1976)* 45 (11), 747–754.

Zhang, Z., Ji, Y., Wang, Z., and Chen, Y. (2018). The association between platelet indices and deep surgical site infection after open induction internal fixation for traumatic limb fractures. *Infect. Drug Resist.* 11, 2533–2538.

Zhao, S., Ye, Z., Zeng, C., Huang, J., Zhang, W., and Li, R. (2022). Retrospective analysis of infection factors in secondary internal fixation after external fixation for open fracture of a long bone: a cohort of 117 patients in a two-center clinical study. *BioMed. Res. Int.* 2022, 7284068.

frontiers | Frontiers in Cellular and Infection Microbiology

TYPE Original Research
PUBLISHED 03 July 2023
DOI 10.3389/fcimb.2023.1177830

OPEN ACCESS

EDITED BY
Hongyi Shao,
Beijing Jishuitan Hospital, China

REVIEWED BY
Anna Benini,
University of Verona, Italy
Minwei Zhao,
Peking University Third Hospital, China

*CORRESPONDENCE
Nan Jiang
hnxyjn@smu.edu.cn
Yan-jun Hu
huyanjun4750@smu.edu.cn

†These authors have contributed equally to this work

RECEIVED 02 March 2023
ACCEPTED 12 June 2023
PUBLISHED 03 July 2023

CITATION
Song C-s, Zhang P, Lin Q-r, Hu Y-y, Pan C-q, Jiang N and Hu Y-j (2023) Nitric oxide synthase 2 genetic variation rs2297514 associates with a decreased susceptibility to extremity post-traumatic osteomyelitis in a Chinese Han population. *Front. Cell. Infect. Microbiol.* 13:1177830. doi: 10.3389/fcimb.2023.1177830

Nitric oxide synthase 2 genetic variation rs2297514 associates with a decreased susceptibility to extremity post-traumatic osteomyelitis in a Chinese Han population

Chen-sheng Song[1,2†], Ping Zhang[1†], Qing-rong Lin[1], Ying-yu Hu[1,3], Chun-qiu Pan[4], Nan Jiang[1,2*] and Yan-jun Hu[1*]

[1]Division of Orthopaedics and Traumatology, Department of Orthopaedics, Nanfang Hospital, Southern Medical University, Guangzhou, China, [2]Guangdong Provincial Key Laboratory of Bone and Cartilage Regenerative Medicine, Nanfang Hospital, Southern Medical University, Guangzhou, China, [3]Department of Hospital Management, Southern Medical University, Guangzhou, China, [4]Department of Emergency Trauma Center, Nanfang Hospital, Southern Medical University, Guangzhou, China

Background: Previous studies have indicated that nitric oxide synthase 2 (*NOS2*) genetic variations are involved in delayed fracture healing and fracture non-union. Whether these genetic variants associate with the development of osteomyelitis (OM) remains unclear. Here, we analyzed the potential relationships between *NOS2* genetic variations and the risk of developing post-traumatic OM (PTOM) in a Chinese Han population.

Methods: Altogether 704 participants, including 336 PTOM patients and 368 healthy controls, were genotyped of rs2297514 and rs2248814 of the *NOS2* gene using the SNaPshot genotyping method.

Results: Outcomes showed that the frequency of allele C of rs2297514 in the patient group was significantly lower than that in the control group (48.7% *vs.* 54.5%, P = 0.029, OR = 0.792, 95% CI 0.642 – 0.976). In addition, significant associations were found between rs2297514 and susceptibility to PTOM by the recessive model (P = 0.007, OR = 0.633, 95% CI 0.453 – 0.884), and the homozygous model (P = 0.039, OR = 0.648, 95% CI 0.429 – 0.979). Moreover, patients with the CC genotype of rs2297514 had lower inflammatory biomarkers levels than the TT genotype, especially for the C-reactive protein (CRP) level (median: 4.1 mg/L *vs.* 8.9 mg/L, P = 0.027). However, no significant relationship was noted between rs2248814 and the risk of developing PTOM.

Conclusion: In this Chinese cohort, rs2297514 is correlated with a decreased risk of PTOM development, with genotype CC as a protective factor.

KEYWORDS

post-traumatic osteomyelitis, fracture-related infection, Nos2, single nucleotide polymorphisms, rs2297514, case-control study

1 Introduction

Osteomyelitis (OM), a hard-to-treat, deep-bone infection, remains a significant healthcare problem worldwide (Muthukrishnan et al., 2019). According to the infection route, OM can occur following perioperative and contiguous conditions, hematogenous spread, and vascular insufficiency-related disorders (e.g., diabetic foot) (Lew and Waldvogel, 1997). Post-traumatic OM (PTOM) remains one primary cause of OM, the incidence of which ranges from 0% to 55%, depending on multiple systematic and local factors of the individuals (Hogan et al., 2013). Despite great advances in surgical techniques, PTOM still poses challenges to orthopaedic surgeons, which primarily attributed to its characteristic of high heterogeneity (Jiang et al., 2020). Early and accurate diagnosis is sometimes difficult, and treatment is always tricky, with high risks of limb deformity and infection recurrence (Panteli and Giannoudis, 2016). Thus, how to reduce the incidence and increase the cure rate is of great clinical significance, which is built on comprehensive understanding of its pathogenesis.

PTOM pathogenesis is complex and associated with both extrinsic and intrinsic factors (Beck-Broichsitter et al., 2015). Most of the previous studies focused on the environmental factors, ignoring the potential role of host factors in developing PTOM. Recently, increasing evidence has suggested that as a representative of host factors, single nucleotide variations (SNVs) were also linked to PTOM development. Such SNVs included but were not limited to rs689466 in cyclooxygenase-2 (COX-2) gene (Wang et al., 2017), rs16944, rs2234663, rs1143627, rs4251961, rs1800796, and rs2234663 in interleukin (IL) genes (Alves De Souza et al., 2017; Jiang et al., 2020). These findings demonstrated that SNVs might play essential roles in PTOM development.

The nitric oxide synthase 2 (NOS2) enzyme, encoded by the *NOS2* gene, is responsible for synthesizing nitric oxide (NO) in the human body. As a reactive free radical, NO mediates multiple biological processes, such as neurotransmission, antitumoral and antimicrobial activities (Huang et al., 2018). In addition, a previous study (Zhu et al., 2001) reported that NOS2 might also participate in the bone fracture healing process, implying that NOS2 plays a role in bone metabolism. Moreover, two recent studies reported *NOS2* SNVs associated with the susceptibility to delayed fracture-healing (Sathyendra et al., 2014) and even fracture non-union (Huang et al., 2018), which confirmed the important role of NOS2 in the fracture healing process.

It is known that PTOM is a bone metabolism-related disorder, characterized by inflammatory bone destruction with or without new bone formation. We speculated that *NOS2* genetic SNVs might also participate in the occurrence of PTOM. Therefore, in the present study, we investigated the potential relationships between *NOS2* genetic SNVs, rs2297514 and rs2248814, and susceptibility to PTOM in a Chinese Han population.

2 Materials and methods

2.1 Study design, setting, definition, inclusion, and exclusion criteria

The present study was designed as a case-control analysis, with comparison conducted between PTOM patients and healthy controls. Included patients were those who had sought medical attention for PTOM in our hospital between January 2016 and December 2019. Participants in the control group were healthy adults. PTOM is defined as a chronic and persistent inflammatory bone disease by infecting microorganisms, characterized by progressive bone destruction and sequestrum formation following trauma and/or orthopaedic surgery, with infection duration exceeding ten weeks (Metsemakers et al., 2018). PTOM was diagnosed concerning any of the confirmatory criteria outlined by the International Fracture-Related Infection (FRI) Consensus Group (Govaert et al., 2020), including wound breakdown to the bone or the implant, sinus or fistula connecting the bone or the implant, positive pathogen culture outcomes, and positive histopathology test outcomes. Patients with OM following diabetic foot or hematogenous spread, and those who refused to participate were excluded. All the included participants or their legal guardians had signed the informed consent form. This study, conducted following the tenets of the 1964 Helsinki declaration, was approved by the medical ethical committee of Nanfang Hospital, Southern Medical University (NFEC-2019-087).

2.2 DNA extraction and SNV genotyping

Peripheral blood samples (5ml each) were collected in the ethylene diamine tetraacetic acid (EDTA) and stored at –80° C. Then, the genomic DNA of each sample was extracted from leukocytes according to the instructions of the Flexi Gene-DNA Kit (Qiagen, Valencia, CA). Two tag SNVs in the *NOS2* gene (rs2297514 and rs2248814) were genotyped using the Multiplex SNaPshot system (Applied Biosystems, Foster City, USA). The forward (F), reverse (R), and extension primers used for polymerase chain reactions (PCR) and extension reactions were as follows: For rs2297514: F: 5'-GCACAGATCA ATGAAACCTGC-3', R: 5'-CGTCTACTCTTGGTTAACCAC-3', extension primer: 5'-CTGAGAGAGGAAGTGGAGCAGATGCT-3'. For rs2248814: F: 5'-GTCTCCGCTTCTCGTCCT-3', R: 5'-GG GTGTGAAGGGTCCTCTAC-3', extension primer: 5'-AG CGGGGTCCTGGCTTGGCTC-3'. The detailed procedure of the SNaPshot genotyping method was described previously (Jiang et al., 2016).

2.3 Outcome parameters

Primary outcome measures were comparisons between PTOM patients and healthy controls regarding genotype distribution,

mutant allele frequency, and four genetic models (dominant, recessive, homozygous, and heterozygous models) of the two *NOS2* SNVs (rs2297514 and rs2248814). Secondary outcomes were the preoperative serological levels of white blood cell (WBC) count, percentage of polymorphonuclear leukocytes (PMN%), erythrocyte sedimentation rate (ESR), C-reactive protein (CRP), procalcitonin (PCT), interleukin-6 (IL-6), tumor necrosis factor-α (TNF-α), and serum amyloid A (SAA), among different genotypes of the two *NOS2* SNVs. In addition, clinical characteristics of the PTOM cohort were summarized.

2.4 Statistical analysis

Statistical analysis was conducted using the Statistical Product and Service Solutions software (version 17.0, SPSS Inc., Chicago, IL, USA). Data distribution was first evaluated for normality by the Kolmogorov-Smirnov test. Continuous variables were presented as mean ± standard deviation (SD) or median with interquartile range (IQR) based on data distribution. For normally distributed data, Student's t-test or one-way analysis of variance (ANOVA) was used to compare differences between two groups or among three groups. Otherwise, the Mann-Whitney U or Kruskal-Wallis H tests were applied. *Post-hoc* multiple comparisons were conducted using LSD/Dunnett's T3 following one-way ANOVA or the Mann-Whitney U test following the Kruskal-Wallis H test.

The genotype distributions of the healthy controls were tested to confirm the Hardy-Weinberg Equilibrium (HWE) using the chi-square test. The chi-square test or Fisher's exact test was used to compare genotype distribution, mutant allele frequency, and the four genetic models, with corresponding odds ratios (ORs) and 95% confidence intervals (CIs) between the patients and healthy controls. All reported values were 2-sided with a P value of less than 0.05, which was considered statistically significant.

3 Results

3.1 Demographics and clinical characteristics

Altogether 468 patients diagnosed with chronic OM (COM) and 368 healthy controls were screened for inclusion, with no statistical differences in sex ratio (0.31 *vs.* 0.37, P = 0.25) or median age [48 (IQR 33, 59) years *vs.* 46 (IQR 37, 52) years, P = 0.08] between the patients and controls. Of the 468 COM patients, 132 were categorized as non-PTOM (70 having diabetic-foot related OM and 62 having hematogenous spread-related OM), with the remaining 336 patients included for analysis. Among the 336 PTOM patients, traffic accidents accounted for 40% of all injury types, with the tibia (59%) as the most frequent infection site. The positive rate of intraoperative sample culture was 57%, with *Staphylococcus aureus* (46%) being the most frequently detected one.

3.2 HWE test outcomes

The *NOS2* genetic variation rs2297514 genotype distribution of the healthy controls failed in the HWE (P = 0.04), while the distribution of rs2248814 of the healthy controls was in the HWE (P = 0.248).

3.3 Potential links between NOS2 gene SNVs and the susceptibility to PTOM

Regarding rs2297514, outcomes revealed a significant difference in genotype distribution between the patients and healthy controls (P = 0.026). Further comparison outcome showed that the allele C frequency in the patient group was significantly lower than that in the control group (48.7% *vs.* 54.5%, P = 0.029, OR = 0.792, 95% CI 0.642-0.976), demonstrating such a mutant allele may be protective. Additionally, significant links were found between rs2297514 and susceptibility to PTOM by recessive (P = 0.007, OR = 0.633, 95% CI 0.453 – 0.884) and homozygous (P = 0.039, OR = 0.648, 95% CI 0.429 – 0.979) models (Table 1). These suggest that the CC genotype of rs2297514 may be a protective factor against PTOM.

As for rs2248814, no significant relationships were found between this SNP site and the risk of developing PTOM in this Chinese cohort, neither by outcomes of genotype distribution and allele frequency nor by results of the four genetic models (Table 1).

3.4 Preoperative serological levels of inflammatory biomarkers among different genotypes of the two NOS2 SNV Sites among the PTOM patients

Significant differences were identified regarding the medial levels of ESR (P = 0.042) and CRP (P < 0.001) among the three genotypes of rs2297514. Outcomes of *post hoc* multiple comparisons by Mann-Whitney U test demonstrated that the medial CRP level of patients with the CC genotype was relatively lower than that of the TT genotype (4.1 mg/L *vs.* 8.9 mg/L, P = 0.027). In addition, patients with the CT genotype had significantly lower levels of ESR (P = 0.012) and CRP (P < 0.001) and a relatively lower IL-6 (P = 0.038) level than those of the TT genotype (Table 2). Concerning rs2248814, the only positive result was that patients with AG genotype had a relatively higher level of TNF-α than that of the GG genotype (P = 0.037) (Table 2).

4 Discussion

As mentioned previously, successful management of PTOM still represents significant challenges, as early and accurate diagnosis is sometimes difficult. Treatment is often tricky, with infection recurrence risk as high as 20 to 30% (Panteli and Giannoudis, 2016). In addition, such a disorder also brings socioeconomic problems. According to a recent survey of a group of Belgian

TABLE 1 Relationships between the two *NOS2* genetic variations and susceptibility to PTOM.

SNPs	Items		Patients (n = 336)	Controls (n = 368)	*P* values	OR (95% CI)
rs2297514	Genotype (n, %)	CC	78 (23.2)	119 (32.3)	0.026	
		CT	171 (50.9)	163 (44.3)		
		TT	87 (25.9)	86 (23.4)		
	Allele frequency	C *vs.* T	327/345	401/335	0.029	0.792 (0.642 – 0.976)
	Dominant model	CC+CT *vs.* TT	249/87	282/86	0.437	0.873 (0.619 – 1.230)
	Recessive model	CC *vs.* CT+TT	78/258	119/249	0.007	0.633 (0.453 – 0.884)
	Homozygous model	CC *vs.* TT	78/87	119/86	0.039	0.648 (0.429 – 0.979)
	Heterzygous model	CT *vs.* TT	171/87	163/86	0.846	1.037 (0.718 – 1.497)
rs2248814	Genotype (n, %)	GG	145 (43.2)	172 (46.7)	0.525	
		AG	153 (45.5)	152 (41.3)		
		AA	38 (11.3)	44 (12.0)		
	Allele frequency	G *vs.* A	443/229	496/240	0.559	0.936 (0.750 – 1.168)
	Dominant model	GG+AG *vs.* AA	298/38	324/44	0.789	1.065 (0.671 – 1.690)
	Recessive model	GG *vs.* AG+AA	145/191	172/196	0.340	0.865 (0.642 – 1.165)
	Homozygous model	GG *vs.* AA	145/38	172/44	0.923	0.976 (0.600 – 1.589)
	Heterzygous model	AG *vs.* AA	153/38	152/44	0.539	1.166 (0.715 – 1.900)

SNP, Single nucleotide polymorphism; OR, Odds Ratio; CI, Confidence Interval.

patients (Iliaens et al., 2021), the direct hospital-related medical care costs of FRI are eight times that of non-FRI of long bone fractures. While in the USA, treatment of bone infection can be up to $150,000 per patient and up to 1.62 billion a year by 2020 (Muthukrishnan et al., 2019). Thus, such heavy economic burdens aggravate the negative influences of PTOM on patients, both physically and psychologically (Walter et al., 2022). Therefore, how to decrease the morbidity and increase the cure rate is clinical significance, built on a comprehensive understanding of PTOM pathogenesis.

Whether PTOM occurs depends on the complex interactions between extrinsic and intrinsic factors, while previous studies primarily focused on extrinsic factors. As a typical representative of intrinsic factors, growing evidence has shown that SNVs also involve in the development of PTOM. Here, we analyzed potential relationships between *NOS2* gene SNVs and susceptibility to PTOM in a Chinese Han population. Outcomes of 704 subjects demonstrated that rs2297514 might be correlated with a reduced risk of PTOM development, with genotype CC as a protective factor. In contrast, the present failed to find a positive link between rs2248814 and the risk of PTOM development in this Chinese cohort. Our findings can be discussed with the following aspects.

First, we found that rs2297514 was associated with a decreased susceptibility to PTOM in this population, with mutant allele C and genotype CC as protective factors. Aside from the current study, two previous studies (Sathyendra et al., 2014; Huang et al., 2018) reported that this SNV was related to the fracture healing process. In 2014, Sathyendra et al. (2014) included 62 participants from the USA and screened 144 SNVs in potentially osteogenic genes. They observed that rs2297514 was linked to an elevated risk of developing atrophic delayed fracture-healing (P = 0.015, OR = 3.98), with CT genotype and allele T as risk factors. Later in 2018, Huang et al. (2018) also analyzed this SNV in the development of fracture non-union among a Chinese Han population. Similarly, they also noted that rs2297514 was correlated to an increased susceptibility to fracture non-union, with the T allele as a risk factor. Our present study shared similarities with the two investigations; the mutant allele C as a protective factor in the present study means that the wild-type allele T may be a risk factor for PTOM. However, we found it is the genotype TT, instead of CT, that was identified as a risk factor. Several possible factors might account for the differences, such as different orthopaedic disorders, different ethnicities, and even different numbers of participants.

Second, we failed to find any significant correlations between rs2248814 and the risk of PTOM development in this Chinese cohort, which was in accordance with the study by Huang et al. (2018). However, Sathyendra et al. (2014) reported that such an SNV also increased the risk of delayed fracture healing in an American population. In addition to PTOM, rs2248814 was also reported to be related to several different disorders. Hancock et al. (2008) found that this SNV was a genetic risk factor for Parkinson's disease. While Velez et al. (2009) observed that rs2248814, interacting with rs1327474, contributed to pulmonary tuberculosis susceptibility in African-Americans. Lim et al. (2013) indicated *NOS2* genetic SNVs (rs2248814 and rs2072324) associated with a sustained virological response to peginterferon plus ribavirin therapy for chronic hepatitis C in Taiwanese Chinese. However, in a recent study (Brookes et al., 2020) focusing on

TABLE 2 Preoperative serological levels of inflammatory biomarkers among different genotypes of rs2297514 and rs2248814 in the PTOM patients.

Items	WBC ($\times10^9$/L)	PMN% (%)	ESR (mm/1h)	CRP (mg/L)	PCT (ng/ml)	IL-6 (pg/ml)	TNF-α (pg/ml)	SAA (mg/L)
rs2297514								
CC	6.9 (5.6, 8.1)	61.7 (51.8, 68.2)	16 (7, 33.5)	4.1 (1.8, 10.3)	0.042 (0.029, 0.057)	6.2 (4.1, 10.5)	8.8 (7.5, 11.9)	11.5 (6.2, 22.7)
CT	6.8 (5.7, 8.1)	59.1 (51.7, 65.8)	13 (6, 29.8)	3.7 (1.2, 7.6)	0.043 (0.030, 0.069)	4.7 (3.2, 11.0)	9.4 (7.6, 12.0)	10.5 (6.2, 18.1)
TT	7.5 (5.8, 9.2)	58.5 (51.2, 65.9)	20 (10, 60.8)	8.9 (3.0, 22.4)	0.046 (0.032, 0.083)	8.1 (3.5, 14.6)	9.3 (7.6, 11.4)	12.1 (5.6, 64.5)
P values #	0.295	0.259	**0.042**	**0.000**	0.614	0.085	0.821	0.280
Post hoc multiple comparisons ^								
CC *vs.* CT	0.774	0.103	0.311	0.094	0.523	0.234	0.685	0.359
CC *vs.* TT	0.285	0.242	0.223	0.027	0.380	0.258	0.961	0.479
CT *vs.* TT	0.123	0.844	**0.012**	**0.000**	0.534	0.038	0.545	0.138
rs2248814								
AA	7.5 (5.6, 9.3)	59.4 (51.6, 65.4)	20 (10, 48)	5.8 (2.6, 16.0)	0.043 (0.035, 0.074)	5.8 (3.0, 13.2)	9.4 (7.6, 12.2)	11.1 (6.2, 34.6)
AG	6.9 (5.7, 8.3)	59 (51.1, 65.9)	14 (7, 40)	4.1 (1.3, 12.2)	0.041 (0.030, 0.070)	5.9 (3.6, 11.1)	9.5 (7.9, 11.9)	10.2 (6.0, 18.7)
GG	6.8 (5.7, 8.0)	60.2 (51.9, 67.6)	15 (6, 32)	4.6 (1.6, 10.1)	0.045 (0.031, 0.072)	6.1 (3.4, 12.7)	8.3 (7.2, 11.8)	11.6 (6.3, 23.2)
P values #	0.472	0.499	0.547	0.228	0.740	0.989	0.104	0.407
Post hoc multiple comparisons ^								
AA *vs.* AG	0.276	0.608	0.343	0.097	0.781	0.917	0.936	0.364
AA *vs.* GG	0.228	0.806	0.289	0.250	0.757	0.936	0.232	0.963
AG *vs.* GG	0.850	0.243	0.762	0.381	0.452	0.893	0.037	0.219

PTOM, Post-traumatic osteomyelitis; WBC, white blood cell count; PMN%, percentage of polymorphonuclear; ESR, erythrocyte sedimentation rate; CRP, C-reactive protein; PCT, procalcitonin; IL-6, interleukin-6; TNF-α, tumor necrosis factor-α; SAA, serum amyloid A. # These P values were obtained by the Kruskal-Wallis H test. ^ These P values were received by the Mann-Whitney U test. Bold values mean statistical significance.

potential relationships between *NOS2* genetic SNVs and susceptibility to the Achilles tendon injuries, the rs2248814 variant might not be linked to the risk of developing Achilles tendinopathy or Achilles tendon rupture. Nonetheless, considering these findings were derived from a single study, more investigations should be conducted to certify these outcomes.

Third, we found PTOM patients with the CC genotype of rs2297514 had relatively lower inflammatory biomarkers (apart from PMN%) levels than those with TT genotype, implying that such an SNV participating in the development of PTOM may partly via its influences on peripheral levels of inflammatory indicators. Interestingly, patients with the CT genotype had significantly lower levels of ESR and CRP and a relatively lower IL-6 than those with the TT genotype, though the heterozygous model found no significant association. Thus, whether the CT genotype is a risk or a protective factor requires further investigations with a larger sample size.

Although we compared serological levels of eight different inflammatory biomarkers among different genotypes of rs2297514 and rs2248814, it is not enough to uncover the underlying mechanisms. It is known that NO, the synthesis of which is regulated by NOS2, is a reactive free radical that plays as an important mediator in neurotransmission, antimicrobial and antitumoral activities (Huang et al., 2018). In addition, previous studies (Zhu et al., 2001; Sathyendra et al., 2014; Huang et al., 2018) had indicated the important role of NOS2 in bone metabolism. Based on these, we speculate that one potential mechanism of *NOS2* SNVs involving in the pathogenesis of PTOM is *NOS2* SNVs may influence expression levels of the NOS2 protein, the latter of which not only affect antimicrobial abilities of the human body, but also affect the bone metabolism process. Of course, future in-depth research is necessary to uncover the detailed mechanisms.

Our study also has several limitations. First, the sample size of the current research remains limited. More eligible patients and controls should be recruited for analysis to obtain more accurate conclusions. Second, the genotype distribution of rs2297514 among the healthy controls was not in HWE; thus, a cautious attitude should be taken, and future studies should testify to such outcomes. Third, we only focused on PTOM; whether such SNVs involve in the occurrence of other OM types, including hematogenous-related OM, and diabetic foot OM, requires further studies. Meanwhile, only two SNVs of the *NOS2* gene were analyzed; whether another SNVs in this gene play a role in the development of PTOM also needs investigation.

5 Conclusions

In summary, we found that *NOS2* genetic SNV rs2297514 is associated with a decreased susceptibility to PTOM in this Chinese

Han population, with the genotype of CC as a protective factor. Also, such an SNV may play a role partly via its influences on peripheral blood levels of inflammatory biomarkers. Furthermore, the current study failed to find enough evidence to support the hypothesis that rs2248814 is related to PTOM occurrence, which needs to be certified by future studies.

Data availability statement

The original contributions presented in the study are included in the article/supplementary materials, further inquiries can be directed to the corresponding author/s.

Ethics statement

The studies involving human participants were reviewed and approved by Southern Medical University Nanfang Hospital. The patients/participants provided their written informed consent to participate in this study.

Author contributions

C-SS and PZ contributed equally to this study. NJ and Y-JH designed the study. C-SS, Q-RL, Y-YH, and C-QP conducted the experiment. C-SS and NJ performed the statistical analysis. C-SS, PZ, and Q-RL participated in the sample collections. C-SS and PZ drafted the manuscript. NJ and Y-JH contributed to the manuscript revision. All authors contributed to the article approved the submitted version.

Funding

This research was funded by Guangdong Provincial Science and Technology Project, grant number: 2020A0505100039, Guangzhou Science and Technology Project, grant number 202002020001, and Xinjiang Uygur Autonomous Region Science and Technology Support Project, grant number: 2022E02040.

Conflict of interest

The authors declare that the research was conducted in the absence of any commercial or financial relationships that could be construed as a potential conflict of interest.

Publisher's note

References

Alves De Souza, C., Queiroz Alves De Souza, A., Queiroz Alves De Souza, M. D. S., Dias Leite, J. A., Silva De Morais, M., and Barem Rabenhorst, S. H. (2017). A link between osteomyelitis and IL1RN and IL1B polymorphisms-a study in patients from northeast Brazil. *Acta orthop* 88 (5), 556–561. doi: 10.1080/17453674.2017.1348439

Beck-Broichsitter, B. E., Smeets, R., and Heiland, M. (2015). Current concepts in pathogenesis of acute and chronic osteomyelitis. *Curr. Opin. Infect. Dis.* 28 (3), 240–245. doi: 10.1097/QCO.0000000000000155

Brookes, C., Ribbans, W. J., El Khoury, L. Y., and Raleigh, S. M. (2020). Variability within the human iNOS gene and Achilles tendon injuries: evidence for a heterozygous advantage effect. *J. Sci. Med. Sport* 23 (4), 342–346. doi: 10.1016/j.jsams.2019.11.001

Govaert, G. A. M., Kuehl, R., Atkins, B. L., Trampuz, A., Morgenstern, M., Obremskey, W. T., et al. (2020). Fracture-related infection consensus G: diagnosing fracture-related infection: current concepts and recommendations. *J. orthop Trauma* 34 (1), 8–17. doi: 10.1097/BOT.0000000000001614

Hancock, D. B., Martin, E. R., Vance, J. M., and Scott, W. K. (2008). Nitric oxide synthase genes and their interactions with environmental factors in parkinson's disease. *Neurogenetics* 9 (4), 249–262. doi: 10.1007/s10048-008-0137-1

Hogan, A., Heppert, V. G., and Suda, A. J. (2013). Osteomyelitis. *Arch. Orthop Trauma Surg.* 133 (9), 1183–1196. doi: 10.1007/s00402-013-1785-7

Huang, W., Zhang, K., Zhu, Y., Wang, Z., Li, Z., and Zhang, J. (2018). Genetic polymorphisms of NOS2 and predisposition to fracture non-union: a case control study based on han Chinese population. *PloS One* 13 (3), e0193673. doi: 10.1371/journal.pone.0193673

Iliaens, J., Onsea, J., Hoekstra, H., Nijs, S., Peetermans, W. E., and Metsemakers, W. J. (2021). Fracture-related infection in long bone fractures: a comprehensive analysis of the economic impact and influence on quality of life. *Injury* 52 (11), 3344–3349. doi: 10.1016/j.injury.2021.08.023

Jiang, N., Li, S. Y., Ma, Y. F., Hu, Y. J., Lin, Q. R., and Yu, B. (2020). Associations between interleukin gene polymorphisms and risks of developing extremity posttraumatic osteomyelitis in Chinese han population. *Mediators Inflammation* 2020, 3278081. doi: 10.1155/2020/3278081

Jiang, N., Zhao, X. Q., Qin, C. H., Hu, Y. J., Wang, L., Xie, G. P., et al. (2016). Association of vitamin d receptor gene TaqI, BsmI, FokI and ApaI polymorphisms and susceptibility to extremity chronic osteomyelitis in Chinese population. *Injury* 47 (8), 1655–1660. doi: 10.1016/j.injury.2016.06.005

Lew, D. P., and Waldvogel, F. A. (1997). Osteomyelitis. *N Engl. J. Med.* 336 (14), 999–1007. doi: 10.1056/NEJM199704033361406

Lim, Y. P., Peng, C. Y., Liao, W. L., Hung, D. Z., Tien, N., Chen, C. Y., et al. (2013). Genetic variation in NOS2A is associated with a sustained virological response to peginterferon plus ribavirin therapy for chronic hepatitis c in Taiwanese Chinese. *J. Med. Virol.* 85 (7), 1206–1214. doi: 10.1002/jmv.23598

Metsemakers, W. J., Kuehl, R., Moriarty, T. F., Richards, R. G., Verhofstad, M. H. J., Borens, O., et al. (2018). Infection after fracture fixation: current surgical and microbiological concepts. *Injury* 49 (3), 511–522. doi: 10.1016/j.injury.2016.09.019

Muthukrishnan, G., Masters, E. A., Daiss, J. L., and Schwarz, E. M. (2019). Mechanisms of immune evasion and bone tissue colonization that make staphylococcus aureus the primary pathogen in osteomyelitis. *Curr. Osteoporos Rep.* 17 (6), 395–404. doi: 10.1007/s11914-019-00548-4

Panteli, M., and Giannoudis, P. V. (2016). Chronic osteomyelitis: what the surgeon needs to know. *EFORT Open Rev.* 1 (5), 128–135. doi: 10.1302/2058-5241.1.000017

Sathyendra, V., Donahue, H. J., Vrana, K. E., Berg, A., Fryzel, D., Gandhi, J., et al. (2014). Single nucleotide polymorphisms in osteogenic genes in atrophic delayed fracture-healing: a preliminary investigation. *J. Bone Joint Surg. Am. volume* 96 (15), 1242–1248. doi: 10.2106/JBJS.M.00453

Velez, D. R., Hulme, W. F., Myers, J. L., Weinberg, J. B., Levesque, M. C., Stryjewski, M. E., et al. (2009). Gilbert JR et al: NOS2A, TLR4, and IFNGR1 interactions influence pulmonary tuberculosis susceptibility in African-americans. *Hum. Genet.* 126 (5), 643–653. doi: 10.1007/s00439-009-0713-y

Walter, N., Rupp, M., Baertl, S., Hinterberger, T., and Alt, V. (2022). Prevalence of psychological comorbidities in bone infection. *J. Psychosom Res.* 157, 110806. doi: 10.1016/j.jpsychores.2022.110806

Wang, L., Jiang, N., Lin, Q. R., Qin, C. H., Hu, Y. J., and Yu, B. (2017). Cyclooxygenase-2 (COX-2) polymorphism rs689466 may contribute to the increased susceptibility to post-traumatic osteomyelitis in Chinese population. *Infect. Dis.* 49 (11-12), 817–823. doi: 10.1080/23744235.2017.1347816

Zhu, W., Diwan, A. D., Lin, J. H., and Murrell, G. A. (2001). Nitric oxide synthase isoforms during fracture healing. *J. Bone Miner Res.* 16 (3), 535–540. doi: 10.1359/jbmr.2001.16.3.535

frontiers | Frontiers in Cellular and Infection Microbiology

TYPE Review
PUBLISHED 17 July 2023
DOI 10.3389/fcimb.2023.1210345

OPEN ACCESS

EDITED BY
Hongyi Shao,
Beijing Jishuitan Hospital, China

REVIEWED BY
Vittorio Sambri,
The Greater Romagna Hub Laboratory - DIMES Unibo, Italy
Christoph Biehl,
University Medical Center Giessen, Germany
Marc Hanschen,
Technical University of Munich, Germany

*CORRESPONDENCE
Markus Rupp
Markus.rupp@ukr.de

RECEIVED 24 April 2023
ACCEPTED 23 June 2023
PUBLISHED 17 July 2023

CITATION
Schindler M, Walter N, Maderbacher G, Sigmund IK, Alt V and Rupp M (2023) Novel diagnostic markers for periprosthetic joint infection: a systematic review.
Front. Cell. Infect. Microbiol. 13:1210345.
doi: 10.3389/fcimb.2023.1210345

Novel diagnostic markers for periprosthetic joint infection: a systematic review

Melanie Schindler[1], Nike Walter[1], Guenther Maderbacher[2], Irene K. Sigmund[3], Volker Alt[1] and Markus Rupp[1*]

[1]Department of Trauma Surgery, University Hospital Regensburg, Regensburg, Germany, [2]Department of Orthopaedic Surgery, University Hospital of Regensburg, Asklepios Klinikum Bad Abbach, Bad Abbach, Germany, [3]Nuffield Orthopaedic Centre, Oxford University Hospitals National Health Service (NHS) Foundation Trust, Oxford, United Kingdom

Background: Identifying novel biomarkers that are both specific and sensitive to periprosthetic joint infection (PJI) has the potential to improve diagnostic accuracy and ultimately enhance patient outcomes. Therefore, the aim of this systematic review is to identify and evaluate the effectiveness of novel biomarkers for the diagnosis of PJI.

Methods: We searched the MEDLINE, EMBASE, PubMed, and Cochrane Library databases from January 1, 2018, to September 30, 2022, using the search terms "periprosthetic joint infection," "prosthetic joint infection," or "periprosthetic infection" as the diagnosis of interest and the target index, combined with the term "marker." We excluded articles that mentioned established biomarkers such as CRP, ESR, Interleukin 6, Alpha defensin, PCT (procalcitonin), and LC (leucocyte cell count). We used the MSIS, ICM, or EBJS criteria for PJI as the reference standard during quality assessment.

Results: We collected 19 studies that analyzed fourteen different novel biomarkers. Proteins were the most commonly analyzed biomarkers (nine studies), followed by molecules (three studies), exosomes (two studies), DNA (two studies), interleukins (one study), and lysosomes (one study). Calprotectin was a frequently analyzed and promising marker. In the scenario where the threshold was set at ≥50-mg/mL, the calprotectin point-of-care (POC) performance showed a high sensitivity of 98.1% and a specificity of 95.7%.

Conclusion: None of the analyzed biomarkers demonstrated outstanding performance compared to the established parameters used for standardized treatment based on established PJI definitions. Further studies are needed to determine the benefit and usefulness of implementing new biomarkers in diagnostic PJI settings.

KEYWORDS

periprosthetic joint infection, PJI, diagnostic marker, diagnostics, synovial fluid

1 Introduction

Periprosthetic joint infection (PJI) is a devastating complication that can occur after total joint arthroplasty (TJA). It often requires long-term antibiotic therapy and multiple revision surgeries, and even with optimal treatment, it can significantly decrease a patient's quality of life. Additionally, the risk of mortality is high for those affected by PJI (Wildeman et al., 2021). In addition to the significant impact on individual patients, the socioeconomic burden of PJI is substantial and expected to increase in the future (Peel et al., 2013) The one-year and five-year risk of PJI after total hip arthroplasty (THA) is 0.7% and 1.1%, respectively, while for total knee arthroplasty (TKA), the corresponding figures are 0.7% and 1.4% (Kurtz et al., 2018). The overall one-year and five-year survival rates after PJI diagnosis were 88.7% and 67.2% for THA and 91.7% and 71.7% for TKA, respectively (Kurtz et al., 2018). In Germany, the total number of total joint arthroplasty (TJA) procedures is projected to increase by 45% for TKA and 23% for THA between now and 2040 (Rupp et al., 2020). Similarly, in the US, the incidence rate of primary TKAs is projected to increase by 43% from 2020 to 2050 (Klug et al., 2021). Among these revision surgeries, the biggest share is performed due to PJI (25%), followed by mechanical loosening (19%) as the second most common reason for TKA revisions (Bozic et al., 2015).

The treatment of infected and aseptic failures after TJA differs significantly and can impose a significant burden on patients (Andersson et al., 2010). Therefore, it is essential to avoid treating a non-infected joint as an infected one, and vice versa, as this can lead to increased morbidity, unnecessary costs, and avoidable surgical interventions (Moojen et al., 2014). Accurate diagnostics are thus of paramount importance in clinical practice to ensure appropriate treatment and avoid these adverse outcomes (Kurtz et al., 2022). In some cases, diagnosing PJI is straightforward, as clear clinical findings such as the presence of a sinus tract or pus around the implanted prosthesis are considered confirming diagnostic criteria (Parvizi et al., 2018; McNally et al., 2021). However, in many cases, these confirming criteria are not present, making PJI diagnostics challenging (Balato et al., 2020). Diagnosis typically relies on laboratory tests such as serology or synovial fluid analysis, microbiological analysis of tissue specimens or synovial fluid, as well as histological and radiographic findings. In recent years, efforts have been made to improve diagnostic accuracy. In 2011, the Musculoskeletal Infection Society (MSIS) published PJI criteria that classify "major" criteria, including the presence of a communicating sinus tract and two positive periprosthetic cultures, and "minor" criteria, such as elevated ESR/CRP, elevated synovial leukocyte count, elevated synovial polymorphonuclear (PMN)%, purulent material, isolated organism in one culture, and intraoperative frozen sections with histology (Parvizi et al., 2011). In 2013, the Infectious Diseases Society of America (IDSA) provided its own PJI diagnostic criteria with the aim of standardizing diagnostics (Osmon et al., 2013). Unlike the MSIS criteria, the IDSA criteria do not include elevated inflammatory markers but consider other factors such as the growth of a virulent organism from a single culture or the presence of acute inflammation from histopathology of the periprosthetic tissue. In 2013, the International Consensus Meeting (ICM) introduced a new minor criterion - the leukocyte esterase in synovial fluid measured by a urine strip test. Later, Parvizi et al. updated the ICM concept by introducing a scoring system based on the different sensitivity and specificity of the markers in 2018 (Parvizi et al., 2018). This updated system included promising new markers such as alpha-defensin in synovial fluid and D-dimer in serum. In 2021, the European Bone and Joint Infection Society (EBJIS) criteria were introduced, classifying cases as "unlikely," "likely," and "confirmed" All these criteria rely on various clinical, laboratory, microbiological, and histological analyses, as well as intraoperative findings, to establish a diagnosis (see Table 1).

Despite the improvements made in recent decades that have made correct diagnosis of PJI more likely through the introduction of different PJI criteria, the identification of a novel biomarker that is highly specific and sensitive for PJI could enable easier and more accurate diagnosis of this devastating disease, ultimately improving patient outcomes. Therefore, the objective of this systematic review is to identify and evaluate novel biomarkers for preoperative PJI diagnostics.

2 Materials and methods

2.1 Search strategy

This systematic review of the literature was performed according to the preferred Reporting Items for Systematic Reviews and Meta-Analyses guidelines (Page et al., 2021).We searched in the electronic databases MEDLINE, EMBASE, PubMed and Cochrane Library. The following search terms were used to screen literature that utilized new marker for PJI diagnosis: We used "periprosthetic joint infection" OR "prosthetic joint infection" OR "periprosthetic infection" as the diagnosis of interest and the target index applied AND "marker". To focus on novel biomarkers already used biomarkers of the established PJI diagnostic criteria of MSIS, ICM and EBJIS were not included in the analysis. Therefore, the search terms included NOT "CRP", NOT "ESR", NOT "Interleukin 6", NOT "Alpha defensin", NOT "PCT" (Procalcitonin), NOT "LC" (leucocyte cell count). A second approach to only include novel biomarkers was setting the time frame for study inclusion from January 1, 2018 to September 30, 2022. After identification, all records were screened by two independent reviewers for the diagnostic markers either determined from blood samples or synovial fluid. All included articles had to be published in English. Animal studies, and studies investigating histological diagnostics were excluded from the analysis.

2.2 Data extraction and quality assessment

Two reviewers performed data extraction independently, and divergences was discussed with a third reviewer. Data were extracted from the eligible studies including the author names, year of publication, country, total number of participants (PJI/control group), mean age of the patients, level of evidence, study design,

TABLE 1 Commonly used PJI criteria and clinical and diagnostic markers included.

	MSIS (Parvizi et al., 2011) (2011)	IDSA (Osmon et al., 2013) (2013)	ICM (Parvizi and Gehrke, 2014) (2013)	ICM (Parvizi et al., 2018) (2018)	EBJIS (McNally et al., 2021) (2021)
Clinical					
Communicating sinus tract	✓	✓	✓	✓	✓
Purulent material	✓	✓	X	✓	✓
Blood					
CRP (mg/L)	↑	X	10	10	>10
ESR (mm/hr)	↑	X	30	30	X
D-Dimer (µg/L)	X	X	X	30	X
Synovial fluid cytological analysis					
Synovial leukocyte count (cells/µL)	✓	X	3.000	3.000	>1.500
Synovial PMN (%)	↑	X	90	70	>65%
Synovial fluid biomarkers					
Alpha Defensin	X	X	X	1.0	✓
Leukocyte esterase	X	X	+/++*	++*	X
Microbiology					
Culture	≥ 1	≥ 1	✓	✓	≥ 1
Sonication (CFU/ml)	X	X	X	X	>1
Histology					
High-power field (400 x magnificantion)	>5 neutrophils per hpf in 5 phf	✓	>5 neutrophils per hpf in 5 phf	✓	>5 neutrophils in single hpf
Others					
Nuclear imaging (WBC scintigraphy)	X	X	X	X	✓

(CRP- C-reactive protein, ESR- erythrocyte sedimentation rate, PMN- polymorphonuclear neutrophils, WBC- white blood cell count).
* The leukocyte concentration is evaluated using test strips on the basis of the color scale from left - to right +++.

biomarker, sample type, sample part, sample collection, reference standard and sensitivity, specificity or cut-off of the new marker.

The Quality Assessment of Diagnostic Accuracy Studies-2 (QUADAS-2) tool was used to determine the potential risk of bias of each study following the full-text assessment (Whiting et al., 2011). MSIS, ICM or EBJS criteria for PJI were considered the reference standard during quality assessment.

An application to register this review in the International Prospective Register of Systematic Reviews (PROSPERO) was submitted but rejected because of study prioritization focusing on SARS- CoV-2 infections.

3 Results

3.1 Search results

The electronic database and bibliography search identified 149 studies, of which 130 were excluded after title/abstract and full text evaluation (see Figure 1 and Table 2). Therefore, 19 studies met the inclusion criteria. Of these, fifteen studies (79%) had prospective designs, and the remaining four (22%) were retrospective studies. Six studies (33%) focused solely on periprosthetic knee infections, while thirteen (67%) included both periprosthetic knee and hip infections. All studies provided diagnostic data for periprosthetic hip and knee infections based on the MSIS, EBJIS, or ICM criteria. The number of patients in the selected studies ranged from 23 to 224. Among the selected studies, 15 (79%) analyzed synovial fluid, three (16%) analyzed blood, and one (5%) analyzed urine (Table 3). The different biomarker analyses are shown in Tables 4 and 5.

The quality of all selected studies was evaluated using the QUADAS-2 tool, and the results are presented in Table 6.

Proteins were primarily analyzed as potential markers, with calprotectin being a frequently studied novel marker (Warren et al., 2021; Grassi et al., 2022; Warren et al., 2022) (Table 2). In one study, the calprotectin point-of-care (POC) performance showed a sensitivity of 98.1% and a specificity of 95.7% in a scenario with a threshold of ‡50-mg/mL (Figures 2, 3) (Warren et al., 2021).

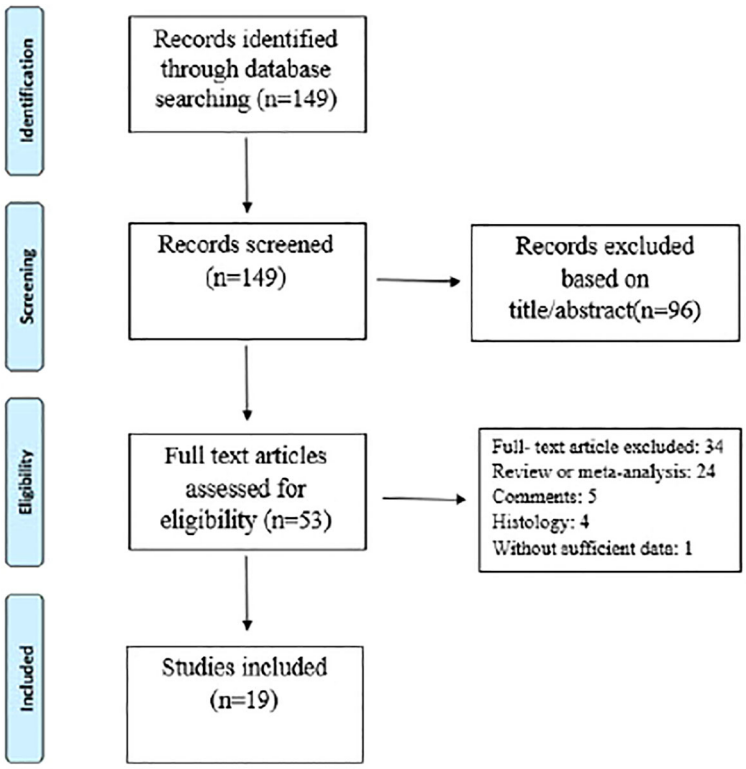

FIGURE 1
Flow diagram of study selection.

Wang et al. collected 50 synovial fluid aspirates from hips and knees and verified the most promising proteins using ELISA (enzyme-linked immunosorbent assay) (Wang et al., 2019). The study identified that lactoferrin (LTF), myeloid nuclear differentiation antigen (MNDA), and polymorphonuclear leukocyte serine protease 3 (PRTN3) were sensitive, while LTF and MNDA were specific for diagnosing PJI. A retrospective cohort study analyzed only TKA synovial fluid and when applying the MSIS criteria, neutrophil gelatinase-associated lipocalin (NGAL) revealed 92% sensitivity and 83% specificity (Dijkman et al., 2020) (Figures 2, 3).

An additional novel approach to diagnose PJI involves analyzing the pattern of urinary peptide excretion. In a study analyzing urinary samples from 30 patients prior to surgery, a marker model consisting of 83 peptides demonstrated the best diagnostic performance with a sensitivity of 95% and specificity of 90% for diagnosing PJI (Omar et al., 2021) (Figures 2, 3). In a study by Vergara et al., synovial fluid was collected from 30.6% of patients with proven infections, 30.6% with aseptic implant failures, and 38.8% controls. Lipocalin-2 (LCN2) was found to discriminate nearly perfectly between controls and confirmed infections (Vergara et al., 2019) (Figure 2, 3). Soluble Pecam 1 (sPecam-1) is an immunologically reactive molecule that is removed from the surface of T cells upon activation by proinflammatory signals. Synovial samples were taken intraoperatively from 16 native knees, 20 aseptic knee revisions, and 22 knees with PJI. The amount of sPecam-1 was significantly greater in knees with PJI compared to aseptic TKA revision procedures ($p \leq 0.001$) (Fuchs et al., 2021) (Table 5). In a prospective cohort study, Zonulin, soluble CD14 (sCD14), and lipopolysaccharide (LPS) were tested in blood samples before antibiotic administration. The study included 134 patients, of which 44 had PJI, 64 had aseptic failure, and 26 underwent primary TKA. Zonulin (7.642 ± 6.077 ng/mL vs 4.560 ± 3.833 ng/mL; $p < 0.001$) and sCD14 levels (555.721 ± 216.659 ng/mL vs 396.872 ± 247.920 ng/mL; $p = 0.003$) were significantly increased in PJI compared to non-infected cases (Chisari et al., 2022) (Table 5). Jubel et al. analyzed fourteen soluble immunoregulatory markers using bead-based multiplex assays and showed significant differences for nine markers when comparing PJI and control groups (Jubel et al., 2021) (Table 5). Extracellular vesicles (EVs) represent another group of the novel markers analyzed (Rüwald et al., 2020; Sallai et al., 2022). The concentration of EVs was significantly higher in the septic samples ($p = 0.0105$) and showed a different size pattern as compared to the aseptic ones (Table 4). Fröschen et al. evaluated a combination of six cytokines (IL-2, IL-4, IL-5, IL-6, lL-12 and GM-CSF) performed better in diagnosing chronic PJI than any cytokine alone. Regression analysis for this combination revealed a sensitivity of 100% and a specificity of 88.9% for a cut-of value of 0.41 (Fröschen et al., 2020). Myeloperoxidase (MPO) is a bactericidal enzyme that acts against pathogenic microorganisms, such as in PJI. In a small cohort study of 37 patients, MPO levels were significantly higher in the chronic PJI group than in the aseptic failure group ($p < 0.001$) ($p < 0.001$) (Ikeda et al., 2020) (Table 5). Another marker is cell-free deoxyribonucleic acid (cf-DNA) in synovial fluid and peripheral

TABLE 2 Summary of *subgroups* in the *diagnosis* marker.

Marker	Number of studies
Protein	9
Calprotectin	Grassi et al. (2022), Warren et al. (2022), Warren et al. (2021) (3)
LTF, MNDA, PRTN3	Wang et al. (2019) (1)
NGAL	Dijkman et al. (2020) (1)
Urinary peptide markers	Omar et al. (2021) (1)
Lipocalin-2	Vergara et al. (2019) (1)
Soluble Pecam-1	Fuchs et al. (2021) (1)
Zonulin, LPS, sCD14	Chisari et al. (2022) (1)
sCD28, sCD80, sCTLA-4, sBTLA	Jubel et al. (2021) (1)
Exosomes	2
EVs	Rüwald et al. (2020), Sallai et al. (2022) (2)
Interleukins	1
Cytokines (IL-1b, IL-2, IL-4, IL-5, IL-6, IL-8, IL-10, IL-12, IL-17, GM-CSF, TNF-α, INF-γ)	Fröschen et al. (2020) (1)
Lysosomes	1
MPO	Ikeda et al. (2020) (1)
DNA	2
Cf-DNA	Echeverria et al. (2021), Cobra et al. (2022) (2)
Molecule	3
BJI InoPlexT	Dartus et al. (2021) (1)
D-lactate	Karbysheva et al. (2020), Yermak et al. (2019) (2)

blood (Echeverria et al., 2021; Cobra et al., 2022). The sensitivity and specificity in synovial fluid were 96.2% and 100%, respectively (Figures 2, 3). BJI InoPlex is a multiplex ELISA that measures the immune response to certain bacterial species from *Staphylococcus epidermidis, aureus* and *lugdunensis, Streptococcus B* and *Cutibacterium acnes*. Dartus et al. included eleven hip and thirteen knee arthroplasty cases. The sensitivity for diagnosing a chronic PJI based on the 2018 ICM criteria was 50% and the specificity was 56% (Dartus et al., 2021) (Figure 2, 3).

D-lactate was studied in the largest cohort of patients (148 and 224) by Karbysheva et al. and Yermak et al. who used different PJI criteria. The sensitivity ranged from 86.4% to 94.3% and the specificity ranged from 78.4% to 80.8% with similar cutoffs (Yermak et al., 2019; Karbysheva et al., 2020) (Figures 2, 3).

4 Discussion

Over the last five years, 19 studies have reported on new biomarkers for PJI, with 15 of these studies specifically focused on parameters in the synovial fluid. Most of the studies analyzed proteins (nine studies), followed by molecules (three studies), exosomes (two studies), DNA (two studies), interleukins (one study), and lysosomes (one study). Calprotectin is a promising and frequently analyzed marker (Table 1) (Warren et al., 2021; Grassi et al., 2022; Warren et al., 2022). In scenarios with a threshold of ≥50 mg/mL, the calprotectin point-of-care performance showed a high sensitivity of 98.1% and specificity of 95.7% (Figures 2, 3). LCN2 is another hopeful marker that nearly perfectly discriminates between controls and confirmed infections in a small cohort of patients (72 patients/22 PJI) (Figures 2, 3) (Vergara et al., 2019). D-lactate, which has been analyzed in a large cohort of patients, is also noteworthy, revealing 94% sensitivity and 78% specificity (Figures 2, 3) (Yermak et al., 2019; Karbysheva et al., 2020). The sensitivity and specificity of these markers are comparable to those of established markers. A review by Sigmund et al. presented the performance of established and novel serum inflammatory biomarkers. The sensitivity and specificity of established markers such as erythrocyte sedimentation rate (ESR) or white blood cell count (WBC) demonstrated similar sensitivity and specificity in comparison to new markers. C-reactive protein (CRP) with a cut-off of 3-32mg/L showed a sensitivity of 62-100% and specificity of 64-96%, while procalcitonin demonstrated a maximum sensitivity of 90% and specificity of 100% (Sigmund et al., 2021).

More than two-thirds of the studies analyzed biomarkers from synovial fluid, but it's important to note that diagnostic hip aspirations are unsuccessful in up to one-third of patients (Christensen et al., 2022). Five of the 19 studies analyzed only preoperative aspirates. Furthermore, there is a discordance of approximately 20% between preoperative aspirate culture and intraoperative synovial fluid culture, which makes relying solely on synovial fluid in the preoperative setting for diagnosing PJI challenging (Li et al., 2021). A meta-analysis of 14 studies that pooled preoperative aspiration culture data revealed an average sensitivity of 67.6% (range 28% to 100%) and an average specificity of 98.4% (range 96% to 100%) (Rodriguez-Merchan, 2018).

Inflammation triggers a series of signaling cascades, and different markers investigated in PJI are linked to these cascades, either up or down. For instance, calprotectin is secreted by neutrophils (Stríz and Trebichavský, 2004) which play a vital role in PJI diagnostics as PMN%. Likewise, the measurement of calprotectin in synovial fluid is significantly associated with PMN % and is an important marker for diagnosing PJI (Burri et al., 2013; Lisowska-Myjak et al., 2016; Honar et al., 2022). Similarly, D-lactate concentration is linked to microbial load. The concentration of D-lactate seems to depend on the number of bacteria, as higher levels of D-lactate were observed in culture-positive PJI compared to culture-negative PJI (Yermak et al., 2019). Given the interdependence of markers in the inflammation signaling cascades, it is not surprising that relying on a single new marker alone may not revolutionize PJI diagnostics.

Alpha defensin, which is a diagnostic marker included in the ICM 2018 criteria (Table 1), was initially hailed as a game-changing diagnostic marker. However, as it became known that alpha

TABLE 3 Characteristics of the studies involved in the current study.

Study	Country	Patient Number (PJI)	Control group	Mean Age (y)	Level of evidence	Study design	Biomarker	Sample type	Sample Part	Sample collection	Ref Standard
Chisari et al. (Chisari et al., 2022)	USA	134 (44)	AIF 90 TJA 26	68	II	Prospective	Zonulin sCD14	Blood	Hip Knee	Before antibiotics	ICM criteria
Cobra et al. (Cobra et al., 2022)	Bra	66 (40- chronic)	AIF 26	71/70	I	Prospective	cf-DNA	Synovial fluid	Knee	Intraoperative	ICM criteria
Dartus et al. (Dartus et al., 2021)	Fra	24 (8-chronic)	AIF 16	63	IV	Retrospective	BJI InoPlexT	Blood	Hip Knee	Preoperative	MSIS criteria
Dijkman et al. (Dijkman et al., 2020)	Nld	76 (13)	AIF 89	69	III	Retrospective	NGAL LE WBC	Synovial fluid	Knee	Pre-/ intraoperative	MSIS/ Pro implantat criteria
Echeverria et al. (Echeverria et al., 2021)	USA	53 (53)	0	68	II	Prospective	cf DNA	Blood	Hip Knee	Preoperative	MSIS criteria
Fröschen et al. (Fröschen et al., 2020)	Ger	32 (14)	AIF 18	68	IV	Retrospective	Cytokine	Synovial fluid	Hip Knee	Pre-/ intraoperativ	MSIS criteria
Fuchs et al. (Fuchs et al., 2021)	Ger	58 (22)	AIF 20 TJA 16	71	II	Prospective	Soluble Pecam-1	Synovial fluid	Knee	Intraoperative	EBJIS criteria
Grassi et al. (Grassi et al., 2022)	Ita	93 (39)	AIF 50	77	II	Prospective	Calprotectin rapid test, Calprotectin ELISA immunoassay	Synovial fluid	Knee	Preoperative	ICM criteria
Ikeda et al. (Ikeda et al., 2020)	Jpn	37 (19- chronic)	AIF 18	75	II	Prospective	MPO	Synovial fluid	Hip, Knee	Intraoperative	ICM criteria
Jubel et al. (Jubel et al., 2021)	Ger	99 (39)	AIF 24 TJA 23 Native 13	67	II	Prospective	Soluble immunregulartory markers	Synovial fluid	Hip, Knee	Preoperative/ intraoperative	MSIS criteria
Karbysheya et al. (Karbysheva et al., 2020)	Ger	224 (71)	AIF 153	66	I	Prospective	D-lactate	Synovial fluid	Hip, Knee	Preoperative	MSIS criteria/ Institutional Criteria
Omar et al. (Omar et al., 2021)	Ger	30 (20)	AIF 10	70	I	Prospective	Urinary peptide markers	Urine	Hip, Knee	Preoperative	MSIS criteria
Rüwald et al. (Rüwald et al., 2020)	Ger	23 (12)	AIF 11	71	II	Prospective	EVs	Synovial fluid	Hip, Knee	Intraoperativ	MSIS criteria
Sallai et al. (Sallai et al., 2022)	Hun	34 (17)	AIF 17	72	II	Prospective	EVs	Synovial fluid	Hip, Knee	Intraoperativ	MSIS criteria
Vergara et al. (Vergara et al., 2019)	Esp	72 (22)	AIF 22 TJA 28	74	II	Prospective	Lipocalin-2	Synovial fluid	Hip Knee	Intraoperative	MSIS criteria

(Continued)

10.3389/fcimb.2023.1210345

10.3389/fcimb.2023.1210345

TABLE 3 Continued

Study	Country	Patient Number (PJI)	Control group	Mean Age (y)	Level of evidence	Study design	Biomarker	Sample type	Sample Part	Sample collection	Ref Standard
Wang et al. (Wang et al., 2019)	Chn	50 (25)	AIF 25	64/69	III	Retrospective	LTF, PRTN3, MNDA	Synovial fluid	Hip Knee	Intraoperative	MSIS criteria
Warren et al. (Warren et al., 2021)	USA	123 (53)	AIF 70	66	I	Prospective	Calprotectin POC test	Synovial fluid	Knee	Intraoperative	MSIS criteria
Warren et al. (Warren et al., 2022)	USA	123 (53)	AIF 70	66	I	Prospective	Calprotectin POC test	Synovial fluid	Knee	Intraoperative	EBJIS/MSIS/ICM criteria
Yermak et al. (Yermak et al., 2019)	Ger	148 (44)	AIF 104	70	I	Prospective	D-lactate	Synovial fluid	Hip, Knee, Shoulder	Preoperative/ intraoperative	EBJIS criteria

NGAL, Neutrophil Gelatinase-Associated Lipocalin; LE, Leukocyte Esterase; WBC, White Blood Count; cf, DNA; Cell-Free Deoxyribonucleic; MPO, Myeloperoxidase; EVs, Extracellular Vesicles; LTF, Lactoferrin; PRTN3, Polymorphonuclear leukocyte serine protease 3; MNDA, Myeloid Nuclear Differentiation Antigen.

defensin is released by neutrophilic granulocytes and acts as part of the non-specific immune system, it was not surprising that the hoped-for diagnostic breakthrough was followed by disappointment. In the literature, the sensitivity of alpha-defensin for the diagnosis of PJI has been reported to range from 67% to 100%, and the specificity from 89% to 99% (Kasparek et al., 2016; Wyatt et al., 2016; Balato et al., 2020). Renz et al. calculated a sensitivity of 84% using the MSIS criteria, 67% using the IDSA criteria, and 54% using the PRO-IMPLANT/EBJIS criteria (Renz et al., 2018). Such variation according to the various criteria presents a challenge in clinical application. Therefore, the routine use of alpha-defensin testing is not recommended in the literature and should only be performed as an additional diagnostic test. Costs also have to be taken into account when using alpha-defensin for diagnostics. ELISA for alpha-defensin is much more expensive than the leukocyte esterase test strip (£0.11 [US$0.17] per test), costing around £500 [US$760] per test (Wyatt et al., 2016).

Besides cost, availability is a major concern for implementing new biomarkers in clinical practice. Established markers like CRP and synovial WBC are commonly used in medical centers, whereas newer markers like alpha defensin are rarely used for routine diagnosis of PJI. Alpha defensin is only collected in 19.4% of cases, while microbiological (97.7%), leukocyte count (74.8%), and PMN% (65.8%) are the most frequently measured parameters in diagnostic setting (Ahmad et al., 2016). Furthermore, storage of specimens poses a challenge as certain markers, such as cytokines and s-Pecam1, require specific temperatures during transportation, which can complicate logistics. As a result, introducing these markers in clinical practice can be difficult.

Modern genomic sequencing diagnostics may offer a solution to the challenges associated with biomarkers and conventional microbial diagnostics. While culture-based detection methods remain the gold standard, they are plagued by several limitations, including low sensitivity. Microbiological culture only detects the pathogen in 44-80% of cases (Malhotra and Morgan, 2004; Williams et al., 2004). One major factor that significantly affects the probability of detecting a pathogen through culture-based methods is the duration of the culture (Saleh et al., 2003; Schäfer et al., 2008). Additionally, contamination and resulting false positive findings can also be problematic (Yee et al., 2013). To overcome these limitations, culture-independent, molecular biology-based methods can be employed as an alternative diagnostic tool. In particular, plasmatic detection of circulating free DNA through Next Generation Sequencing (NGS) has shown promise as a diagnostic method for patients with bloodstream infections. Metagenomic NGS (mNGS) offers the ability to identify multiple organisms in a single sample (Gu et al., 2019). Early studies have suggested that NGS-based diagnostics are more effective than conventional culture-based methods for detecting bloodstream infections (Grumaz et al., 2016; Decker et al., 2017; Grumaz et al., 2019). In the case of PJI, Echeverria et al. identified the pathogen in 35 cases, including four cases that were deemed culture-negative (57%) (Echeverria et al., 2021). Having a pathogenic marker such as circulating free DNA could be beneficial as it specifically identifies present bacteria compared

10.3389/fcimb.2023.1210345

TABLE 4 Analysis of biomarker for PJI diagnosis.

Study	Biomarker Cut-off	Sensitivity (95% CI)	Specificity (95% CI)	AUC (95% CI)	Accuracy (95%CI)	PLN (95% CI)	NLR (95% CI)	PPV	NPV
Cobra et al. (Cobra et al., 2022)	Cf-DNA 15 ng/mL	96.2 (80.4-99.9)	100 (91.2-100)	1.0 (0.9-1.0)					
Dartus et al. (Dartus et al., 2021)	BJI InoPlexT Positive	50	56	–		36	69		
Dijkman et al. (Dijkman et al., 2020)	LE ++	39	88						
MSIS									
MSIS	WBC count 2575 cells/µL	92	84						
MSIS	NGAL 0.7355 µg/mL	92	83						
Pro-Implant	LE ++	39	92						
Pro-Implant	WBC count 1865 cells/µL	100	97						
Pro-Implant	NGAL 0.7355 µg/mL	95	95						
Fröschen.et al. (Fröschen et al., 2020)	IL Ib >29.08 pg/mL	92.9 (66.1–99.8)	83.3 (58.6–96.4)	0.9 (0.9–1.0)		–	–		
	IL 2 >9.065	92.9 (68.5–99.6)	61.1 (38.6–79.7)	0.8 (0.7–1.0)					
	IL 4 >1.890	92.9 (66.1–99.8)	72.2 (46.5–90.3)	0.9 (0.8–1.0)					
	IL 5 >4.720	71.4 (41.9–91.6)	77.8 (52.4–93.6)	0.8 (0.6–1.0)					
	IL 6 >1975	92.9 (66.1–99.8)	88.9 (65.3–98.6)	1.0 (0.9–1.0)					
	IL 8 >2748	85.7 (57.2–98.2)	72.2 (46.5–90.3)	0.9 (0.7–1.0)					
	IL10 >10.38	92.9 (66.1–99.8)	83.3 (58.6–96.4)	0.9 (0.8–1.0)					
	IL12 >14.10	100.0 (76.8–100.0)	66.7 (41.0–86.7)	0.8 (0.6–0.9)					
	IL17 >124.6	92.9 (66.1–99.8)	83.3 (58.6–96.4)	0.9 (0.8–1.0)					
	GM-CSF >1.895	78.6 (49.2–95.3)	66.7 (41.0–86.7)	0.7 (0.6–0.9)					
	TNF-α >29.39	71.4 (41.9–91.6)	77.8 (52.3–93.6)	0.8 (0.6–1.0)					
	IFN-γ >6.215	92.9 (66.1-99.8)	61.1 (35.8–82.7)	0.8 (0.7–1.0)					
Grassi et al. (Grassi et al., 2022)	Calprotectin ELISA immunoassay	92.3 (79.1-98.4)	100 (92.8-100)	1.0 (0.9-1.0)		–	0.1 (0.0-0.2)	100	94.3 (84.9-98)
	Calprotectin rapid test	97.4 (86.5-99.9)	94 (83.5-98.7)	1.0 (0.9-1.0)		16.2 (5.4-48.7)	0.0 (0.0-0.2)	92.7 (80.9-97.4)	97.9 (87.1-99.7)

(Continued)

TABLE 4 Continued

Study	Biomarker Cut-off	Sensitivity (95% CI)	Specificity (95% CI)	AUC (95% CI)	Accuracy (95%CI)	PLN (95% CI)	NLR (95% CI)	PPV	NPV
	LE test	46.1 (30.1-62.8)	94 (83.5-98.7)	0.7 (0.6-0.8)		7.7 (2.4-24.3)	0.6 (0.4-0.8)	85.7 (65.6-95)	73 (62.6-81.9)
Ikeda et al. (Ikeda et al., 2020)	MPO 40.000 ng/mL	84	100	–		1	0.9		
	30.000 ng/mL	95	100	–		1	0.9		
	20.000 ng/mL	95	94	–		0.9	0.9		
	10.000 ng/mL	100	94	–		1	1		
	1000 ng/mL	100	72	–		0.8	1		
	Ideal 1487- 16,463 ng/mL	100	94	1.0 (1.0–1)		95	10		
Karbysheva et al. (Karbysheva et al., 2020)	D-lactate 1.3 mmol/L MSIS	94.3 (86.2-98.4)	78.4 (66.8-81.2)	0.9 (0.9-1.0)				67 (56.9-76.1)	96.8 (91.9-99.1)
	Institutional Criteria	92.4 (84.9-96.9)	88.6 (81.9-93.5)	1.0 (0.9-1.0)				85 (76.5-91.3)	94.4 (88.7-97.7)
Omar et al. (Omar et al., 2021)	Urinary peptide markers	95	90	1.0 (0.8-1.0)				65	
Vergara et al. (Vergara et al., 2019)	Lipocalin-2 152 ng/mL	100 (88-100)	100 (94-100)	1.0 (1.0-1.00)					
Wang et al. (Wang et al., 2019)	LTF 221.19 ng/mL	97.1	90	1		–	–		
	MNDA 13.12 ng/mL	77.1	97.5	1		–	–		
	PRTN3 7.30 ng/mL	88.6	45	1		–	–		
Warren et al. (Warren et al., 2022)	Calprotectin POC test ≥50 mg/L	98.1	95.7	1		94.5	98.5		
	≥14-mg/L	98.1	87.1	0.9		85.2	98.4		
Warren et al. (Warren et al., 2021)	Calprotectin POC test MSIS >50 mg/L	98.1	95.7	1		94.5	98.5		
	ICM	98.2	98.5	0.984		98.2	98.5		
	EBJIS	93.2	100	0.966		100	94.2		
Yermak et al. (Yermak et al., 2019)	D-lactate 1.263 mmol/l	86.4 (75-95)	80.8 (73-88)	0.93 (86-95)					

to nonspecific markers. Thus, NGS could be utilized to identify the pathogen in cases where culture-based methods are ineffective.

Several limitations of this systematic review must be acknowledged. First, the study compared three different PJI criteria, which are the most commonly used ones. The MSIS and ICM criteria were used in six studies. Sigmund et al. conducted a retrospective study of 206 PJI patients, of which 101 (49%) were diagnosed with PJI using the EBJIS definition, 99 (48%) with the IDSA definition, and 86 (42%) with the ICM definition. A total of 84 cases (41%) had an infection based on all three criteria. The novel

TABLE 5 Analysis of biomarker for PJI diagnosis.

Study	Subject	Biomarker	PJI	Non PJI	Sig.
Chisari et al. (Chisari et al., 2022)	PJI 44 AIF 90	Zonulin (ng/mL)	7.6± 6.1	4.6± 3.8	p < 0.001
		sCD14 (ng/mL)	555.7± 216.7	396.9± 247.9	p < 0.003
	Acute (n=14) vs. Chronic (n=30)	Zonulin (ng/mL)	11.6± 6.7	5.8± 4.8	p < 0.005
Echeverria et al. (Echeverria et al., 2021)	Pathogen identified by blood cfDNA-seq (n=35)	Species identified by surgical joint culture	23		–
		Genus identified by surgical joint culture	8		–
		Pathogen not identified by surgical joint culture	4		–
	Pathogen not identified by blood cfDNA-seq (n=15)	Species identified by surgical joint culture	12		–
		Genus identified by surgical joint culture	3		–
Fuchs et al. (Fuchs et al., 2021)	PJI vs. AIF	Soluble Pecam-1 (ng/mL)	73.0± 22.9	44.0 ± 11.8	p < 0.001
	PJI- TJA		73.0± 22.9	26.02± 6.48	p < 0.001
Jubel et al., (Jubel et al., 2021)	Soluble immunregulartory markers –	sLAG-3 (pg/ml)	319.7± 38.4	6534.3± 753.3	p < 0.001
	PJI vs. CO	sCTLA-4 (pg/ml)	450.0± 58.5	59.3± 16.9	p < 0.001
		sCD27 (pg/ml)	32088.4± 5436.8	5610.2± 2444.6	p < 0.001
		sCD80 (pg/ml)	1671.9± 184.8	238.2± 66.2	p < 0.001
		sTIM-3 (pg/ml)	319.7± 38.4	6534.3± 753.3	p < 0.001
		sPD-1 (pg/ml)	253.7± 59.4	32.8± 15.3	p < 0.001
		IDO (pg/ml)	1892.8± 519.1	38.5± 16.1	p < 0.001
		sBTLA (pg/ml)	3716.6± 674.9	594.9± 199.1	p < 0.001
Rüwald et al. (Rüwald et al., 2020)	EVs	Nanovesicles Size (nm)	224.8 ± 90.7	156.5 ± 64.4	p = 0.001
			Higher particle concentrations in PJI than AIF		p = 0.032
			High fluorescence intensities of CD 9 in AIF than PJI		p < 0.001
			High fluorescence intensities of CD 81 in AIF than PJI		p = 0.037
Sallai et al. (Sallai et al., 2022)	Polymorphonuclear derived EVs	Concentration	Higher in PJI than AIF		p = 0.0105

(Continued)

TABLE 5 Continued

Study	Subject	Biomarker	PJI	Non PJI	Sig.
		Annexin V	Increased Eventnumber in PJI than AIF		p = 0.046
		Annexin V and anti-CD177	Increased Eventnumber in PJI than AIF		p = 0.0105
		Lactotransferrin	Significant difference in the abundance in PJA than AIF		p = 0.00646
		Myeloperoxidase	Significant difference in the abundance in PJA than AIF		p = 0.01061
		Lysozyme C	Significant difference in the abundance in PJA than AIF		p = 0.04687
		Annexin A6	Significant difference in the abundance in PJA than AIF		p = 0.03921
		Alpha-2-HS-glycoprotein	Significant difference in the abundance in PJA than AIF		p = 0.03146

TABLE 6 Quality evaluation of selected studies.

Study	Risk of bias				Applicability concerns		
	Patient selection	Index test	Reference standard	Flow and timing	Patient selection	Index test	Reference standard
Chisari et al. (Chisari et al., 2022)	High	Low	Low	Low	High	Low	Low
Cobra et al. (Cobra et al., 2022)	Low	Low	Low	Low	Low	Low	Low
Dartus et al. (Dartus et al., 2021)	High	High	Low	Low	High	High	Low
Dijkman et al. (Dijkman et al., 2020)	High	High	Low	Low	High	Low	Low
Echeverria et al., (Echeverria et al., 2021)	Low	Low	Low	Low	Low	Low	Low
Fröschen.et al. (Fröschen et al., 2020)	High	Low	Low	Low	High	Low	High
Fuchs et al. (Fuchs et al., 2021)	High	Low	Low	Low	High	Low	Low
Grassi et al. (Grassi et al., 2022)	High	High	Low	Low	High	Low	Low
Ikeda et al. (Ikeda et al., 2020)	High	High	Low	Low	High	High	Low
Jubel et al. (Jubel et al., 2021)	High	Low	Low	Low	High	Low	Low
Karbysheva et al. (Karbysheva et al., 2020)	Low	High	Low	Low	Low	Low	Low
Omar et al. (Omar et al., 2021)	Low	Low	Low	Low	Low	Low	Low
Rüwald et al. (Rüwald et al., 2020)	High	Low	Low	Low	High	Low	Low

(Continued)

TABLE 6 Continued

Study	Risk of bias				Applicability concerns		
	Patient selection	Index test	Reference standard	Flow and timing	Patient selection	Index test	Reference standard
Sallai et al. (Sallai et al., 2022)	High	Low	Low	Low	High	Low	Low
Vergara et al. (Vergara et al., 2019)	High	High	Low	Low	High	Low	Low
Wang et al. (Wang et al., 2019)	Low	Low	Low	Low	Low	Low	Low
Warren et al. (Warren et al., 2022)	Low	Low	Low	Low	Low	Low	Low
Warren et al. (Warren et al., 2021)	Low	Low	Low	Low	Low	Low	Low
Yermak et al. (Yermak et al., 2019)	High	Low	Low	Low	High	Low	Low

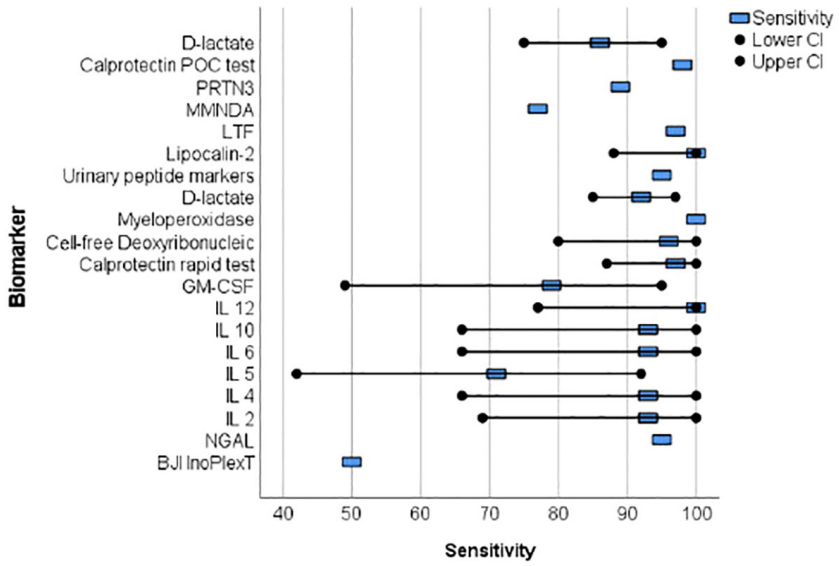

FIGURE 2
The forest plots of the sensitivity for novel diagnosis marker of periprosthetic joint infection.

EBJIS definition appears to be more sensitive for PJI diagnosis compared to the IDSA and ICM definitions. All infections classified by the IDSA or ICM criteria were identified by the EBJIS definition, indicating that the EBJIS definition is superior to the IDSA and ICM criteria for PJI diagnostics. However, only two studies in this systematic review used the EBJIS definition, which was introduced recently in 2021 (Sigmund et al., 2022). However, the present systematic review is limited by several factors. Secondly, only two studies in our review employed the recently introduced EBJIS definition, which limits the generalizability of our findings. Thirdly, the use of different cut-off values for biomarkers across studies makes comparison challenging. Finally, the limited availability of information on the time elapsed since the arthroplasty procedure may affect the accuracy of some biomarkers, as their diagnostic performance may vary in the early postoperative period (Yi et al., 2014).

5 Conclusion

Based on the current analysis, no novel biomarker investigated in the past five years for diagnosing PJI has been

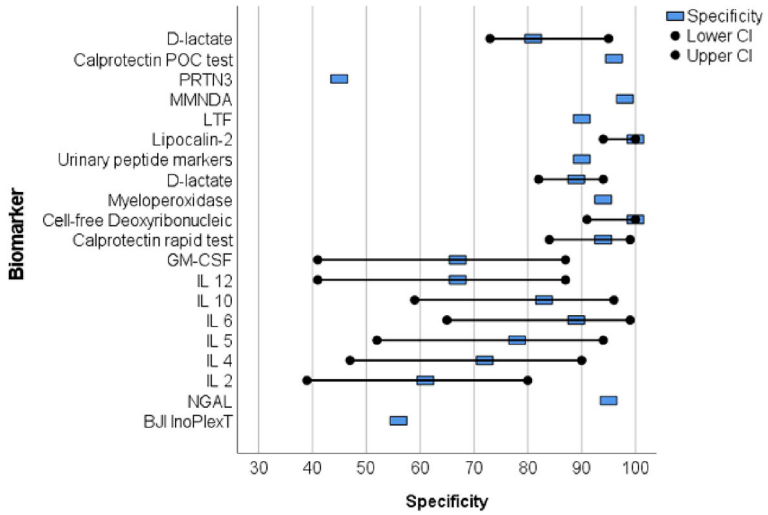

FIGURE 3
The forest plots of the specificity for novel diagnostic marker of periprosthetic joint infection.

proven to outperform the already established diagnostic parameters. Further studies may demonstrate the usefulness of additional markers, such as calprotectin, in the established PJI diagnostic criteria.

Author contributions

SM, NW, and MR contributed to conception and design of the study. SM and NW organized the database. SM and NW performed the statistical analysis. SM wrote the first draft of the manuscript. NW and MR wrote sections of the manuscript. All authors contributed to the article and approved the submitted version.

Conflict of interest

The authors declare that the research was conducted in the absence of any commercial or financial relationships that could be construed as a potential conflict of interest.

Publisher's note

References

Ahmad, S. S., Becker, R., Chen, A. F., and Kohl, S. (2016). EKA survey: diagnosis of prosthetic knee joint infection. *Knee Surg. Sports Traumatol Arthrosc* 24, 3050–3055. doi: 10.1007/s00167-016-4303-y

Andersson, A. E., Bergh, I., Karlsson, J., and Nilsson, K. (2010). Patients' experiences of acquiring a deep surgical site infection: an interview study. *Am. J. Infect. Control* 38, 711–717. doi: 10.1016/j.ajic.2010.03.017

Balato, G., Matteo, V., Ascione, T., Di Donato, S.L., Franco, C., Smeraglia, F., et al. (2020). Laboratory-based versus qualitative assessment of α-defensin in periprosthetic hip and knee infections: a systematic review and meta-analysis. *Arch. Orthop Trauma Surg.* 140, 293–301. doi: 10.1007/s00402-019-03232-5

Bozic, K. J., Kamath, A. F., Ong, K., Lau, E., Kurtz, S., Chan, V., et al. (2015). Comparative epidemiology of revision arthroplasty: failed THA poses greater clinical and economic burdens than failed TKA. *Clin. Orthop Relat. Res.* 473, 2131–2138. doi: 10.1007/s11999-014-4078-8

Burri, E., Schulte, F., Muser, J., Meier, R., and Beglinger, C. (2013). Measurement of calprotectin in ascitic fluid to identify elevated polymorphonuclear cell count. *World J. Gastroenterol.* 19, 2028–2036. doi: 10.3748/wjg.v19.i13.2028

Chisari, E., Cho, J., Wouthuyzen-Bakker, M., and Parvizi, J. (2022). Gut permeability may be associated with periprosthetic joint infection after total hip and knee arthroplasty. *Sci. Rep.* 12, 15094. doi: 10.1038/s41598-022-19034-6

Christensen, T. H., Ong, J., Lin, D., Aggarwal, V. K., Schwarzkopf, R., Rozell, J. C., et al. (2022). How does a "Dry tap" impact the accuracy of preoperative aspiration results in predicting chronic periprosthetic joint infection? *J. Arthroplasty* 37, 925–929. doi: 10.1016/j.arth.2022.01.066

Cobra, H., Mozella, A. P., Da Palma, I. M., Salim, R., and Leal, A. C. (2022). Cell-free deoxyribonucleic acid: a potential biomarker of chronic periprosthetic knee joint infection. *J. Arthroplasty* 37, 2455–2459. doi: 10.1016/j.arth.2022.07.002

Dartus, J., Martinot, P., Leclerc, J.-T., Senneville, E., Wallet, F., Putman, S., et al. (2021). Diagnostic accuracy of the BJI InoPlex™ (Diaxonhit) immunoassay on blood samples for periprosthetic joint infection in complex microbiological situations. preliminary results of 24 cases in a French reference center for complex bone and joint infection (CRIOAC). *Orthop Traumatol Surg. Res.* 107, 102909. doi: 10.1016/j.otsr.2021.102909

Decker, S. O., Sigl, A., Grumaz, C., Stevens, P., Vainshtein, Y., Zimmermann, S., et al. (2017). Immune-response patterns and next generation sequencing diagnostics for the detection of mycoses in patients with septic shock-results of a combined clinical and experimental investigation. *Int. J. Mol. Sci.* 8, 18. doi: 10.3390/ijms18081796

Dijkman, C., Thomas, A. R., Koenraadt, K. L. M., Ermens, A. A. M., and van Geenen, R. C. I. (2020). Synovial neutrophilic gelatinase-associated lipocalin in the diagnosis of periprosthetic joint infection after total knee arthroplasty. *Arch. Orthop Trauma Surg.* 140, 941–947. doi: 10.1007/s00402-020-03427-1

Echeverria, A. P., Cohn, I. S., Danko, D. C., Shanaj, S., Blair, L., Hollemon, D., et al. (2021). Sequencing of circulating microbial cell-free DNA can identify pathogens in periprosthetic joint infections. *J. Bone Joint Surg. Am.* 103, 1705–1712. doi: 10.2106/JBJS.20.02229

Fröschen, F. S., Schell, S., Schildberg, F. A., Klausing, A., Kohlhof, H., Gravius, S., et al. (2020). Analysis of synovial biomarkers with a multiplex protein microarray in patients with PJI undergoing revision arthroplasty of the hip or knee joint. *Arch. Orthop Trauma Surg.* 140, 1883–1890. doi: 10.1007/s00402-020-03388-5

Fuchs, M., Trampuz, A., Kirschbaum, S., Winkler, T., and Sass, F. A. (2021). Soluble pecam-1 as a biomarker in periprosthetic joint infection. *J. Clin. Med.* 10 (4), 612. doi: 10.3390/jcm10040612

Grassi, M., Salari, P., Farinelli, L., D'Anzeo, M., Onori, N., and Gigante, A. (2022). Synovial biomarkers to detect chronic periprosthetic joint infection: a pilot study to compare calprotectin rapid test, calprotectin ELISA immunoassay and leukocyte esterase test. *J. Arthroplasty* 37, 781–786. doi: 10.1016/j.arth.2021.12.040

Grumaz, S., Grumaz, C., Vainshtein, Y., Stevens, P., Glanz, K., Decker, S. O., et al. (2019). Enhanced performance of next-generation sequencing diagnostics compared with standard of care microbiological diagnostics in patients suffering from septic shock. *Crit. Care Med.* 47, e394–e402. doi: 10.1097/CCM.0000000000003658

Grumaz, S., Stevens, P., Grumaz, C., Decker, S. O., Weigand, M. A., Hofer, S., et al. (2016). Next-generation sequencing diagnostics of bacteremia in septic patients. *Genome Med.* 8, 73. doi: 10.1186/s13073-016-0326-8

Gu, W., Miller, S., and Chiu, C. Y. (2019). Clinical metagenomic next-generation sequencing for pathogen detection. *Annu. Rev. Pathol.* 14, 319–338. doi: 10.1146/annurev-pathmechdis-012418-012751

Honar, N., Nezamabadipour, N., Dehghani, S. M., Haghighat, M., Imanieh, M. H., Ataollahi, M., et al. (2022). An evaluation of ascitic calprotectin for diagnosis of ascitic fluid infection in children with cirrhosis. *BMC Pediatr.* 22, 382. doi: 10.1186/s12887-022-03433-9

Ikeda, S., Uchiyama, K., Minegishi, Y., Nakamura, M., and Takaso, M. (2020). Evaluation of myeloperoxidase in synovial fluid as a biomarker for chronic periprosthetic joint infection. *Int. Orthop* 44, 1915–1920. doi: 10.1007/s00264-020-04753-0

Jubel, J. M., Randau, T. M., Becker-Gotot, J., Scheidt, S., Wimmer, M. D., and Kohlhof, H. (2021). sCD28, sCD80, sCTLA-4, and sBTLA are promising markers in diagnostic and therapeutic approaches for aseptic loosening and periprosthetic joint infection. *Front. Immunol.* 12, 687065. doi: 10.3389/fimmu.2021.687065

Karbysheva, S., Yermak, K., Grigoricheva, L., Renz, N., Perka, C., and Trampuz, A. (2020). Synovial fluid d-Lactate-A novel pathogen-specific biomarker for the diagnosis of periprosthetic joint infection. *J. Arthroplasty* 35, 2223–2229.e2. doi: 10.1016/j.arth.2020.03.016

Kasparek, M. F., Kasparek, M., Boettner, F., Faschingbauer, M., Hahne, J., and Dominkus, M. (2016). Intraoperative diagnosis of periprosthetic joint infection using a novel alpha-defensin lateral flow assay. *J. Arthroplasty* 31, 2871–2874. doi: 10.1016/j.arth.2016.05.033

Klug, A., Gramlich, Y., Rudert, M., Drees, P., Hoffmann, R., Weißenberger, M., et al. (2021). The projected volume of primary and revision total knee arthroplasty will place an immense burden on future health care systems over the next 30 years. *Knee Surg. Sports Traumatol Arthrosc* 29, 3287–3298. doi: 10.1007/s00167-020-06154-7

Kurtz, S. M., Higgs, G. B., Lau, E., Iorio, R. R., Courtney, P. M., and Parvizi, J. (2022). Hospital costs for unsuccessful two-stage revisions for periprosthetic joint infection. *J. Arthroplasty* 37, 205–212. doi: 10.1016/j.arth.2021.10.018

Kurtz, S. M., Lau, E. C., Son, M.-S., Chang, E. T., Zimmerli, W., and Parvizi, J. (2018). Are we winning or losing the battle with periprosthetic joint infection: trends in periprosthetic joint infection and mortality risk for the Medicare population. *J. Arthroplasty* 33, 3238–3245. doi: 10.1016/j.arth.2018.05.042

Li, H., Xu, C., Hao, L., Chai, W., Jun, F., and Chen, J. (2021). The concordance between preoperative aspiration and intraoperative synovial fluid culture results: intraoperative synovial fluid re-cultures are necessary whether the preoperative aspiration culture is positive or not. *BMC Infect. Dis.* 21, 1018. doi: 10.1186/s12879-021-06721-4

Lisowska-Myjak, B., Żytyńska-Daniluk, J., and Skarżyńska, E. (2016). Concentrations of neutrophil-derived proteins in meconium and their correlations. *biomark. Med.* 10, 819–829. doi: 10.2217/bmm-2016-0034

Malhotra, R., and Morgan, D. (2004). Role of core biopsy in diagnosing infection before revision hip arthroplasty. *J. Arthroplasty* 19, 78–87. doi: 10.1016/S0883-5403(03)00453-4

McNally, M., Sousa, R., Wouthuyzen-Bakker, M., Chen, A. F., Soriano, A., Vogely, H. C., et al. (2021). The EBJIS definition of periprosthetic joint infection. *Bone Joint J.* 103-B, 18–25. doi: 10.1302/0301-620X.103B1.BJJ-2020-1381.R1

Moojen, D. J. F., Zwiers, J. H., Scholtes, V. A. B., Verheyen, C. C. P. M., and Poolman, R. W. (2014). Similar success rates for single and multiple debridement surgery for acute hip arthroplasty infection. *Acta Orthop* 85, 383–388. doi: 10.3109/17453674.2014.927729

Omar, M., Windhagen, H., Krettek, C., and Ettinger, M. (2021). Noninvasive diagnostic of periprosthetic joint infection by urinary peptide markers: a preliminary study. *J. Orthop Res.* 39, 339–347. doi: 10.1002/jor.24913

Osmon, D. R., Berbari, E. F., Berendt, A. R., Lew, D., Zimmerli, W., Steckelberg, J. M., et al. (2013). Diagnosis and management of prosthetic joint infection: clinical practice guidelines by the infectious diseases society of America. *Clin. Infect. Dis.* 56, e1–e25. doi: 10.1093/cid/cis803

Page, M. J., McKenzie, J. E., Bossuyt, P. M., Boutron, I., Hoffmann, T. C., Mulrow, C. D., et al. (2021). The PRISMA 2020 statement: an updated guideline for reporting systematic reviews. *Syst. Rev.* 10, 89. doi: 10.1186/s13643-021-01626-4

Parvizi, J., and Gehrke, T. (2014). Definition of periprosthetic joint infection. *J. Arthroplasty* 29, 1331. doi: 10.1016/j.arth.2014.03.009

Parvizi, J., Tan, T. L., Goswami, K., Higuera, C., Della Valle, C., Chen, A. F., et al. (2018). The 2018 definition of periprosthetic hip and knee infection: an evidence-based and validated criteria. *J. Arthroplasty* 33, 1309–1314.e2. doi: 10.1016/j.arth.2018.02.078

Parvizi, J., Zmistowski, B., Berbari, E. F., Bauer, T. W., Springer, B. D., Della Valle, C. J., et al. (2011). New definition for periprosthetic joint infection: from the workgroup of the musculoskeletal infection society. *Clin. Orthop Relat. Res.* 469, 2992–2994. doi: 10.1007/s11999-011-2102-9

Peel, T. N., Dowsey, M. M., Buising, K. L., Liew, D., and Choong, P. F.M. (2013). Cost analysis of debridement and retention for management of prosthetic joint infection. *Clin. Microbiol. Infect.* 19, 181–186. doi: 10.1111/j.1469-0691.2011.03758.x

Renz, N., Yermak, K., Perka, C., and Trampuz, A. (2018). Alpha defensin lateral flow test for diagnosis of periprosthetic joint infection: not a screening but a confirmatory test. *J. Bone Joint Surg. Am.* 100, 742–750. doi: 10.2106/JBJS.17.01005

Rodriguez-Merchan, E. C. (2018). Preoperative aspiration culture (PAC) for the diagnosis of infection in a prosthetic knee joint. *Arch. Bone Jt Surg.* 6, 342–345.

Rupp, M., Lau, E., Kurtz, S. M., and Alt, V. (2020). Projections of primary TKA and THA in Germany from 2016 through 2040. *Clin. Orthop Relat. Res.* 478, 1622–1633. doi: 10.1097/CORR.0000000000001214

Rüwald, J. M., Randau, T. M., Hilgers, C., Masson, W., Irsen, S., Eymael, R. L., et al. (2020). Extracellular vesicle isolation and characterization from periprosthetic joint synovial fluid in revision total joint arthroplasty. *J. Clin. Med.* 9 (2), 516. doi: 10.3390/jcm9020516

Saleh, K. J., Clark, C. R., Sharkey, P. F., Goldberg, V. M., Rand, J. A., Brown, G. A., et al. (2003). Modes of failure and preoperative evaluation. *J. Bone Joint Surg. Am.* 85-A Suppl 1, S21–S25. doi: 10.2106/00004623-200300001-00006

Sallai, I., Marton, N., Szatmári, A., Kittel, Á., Nagy, G., Buzás, E. I., et al. (2022). Activated polymorphonuclear derived extracellular vesicles are potential biomarkers of periprosthetic joint infection. *PloS One* 17, e0268076. doi: 10.1371/journal.pone.0268076

Schäfer, P., Fink, B., Sandow, D., Margull, A., Berger, I., Frommelt, L., et al. (2008). Prolonged bacterial culture to identify late periprosthetic joint infection: a promising strategy. *Clin. Infect. Dis.* 47, 1403–1409. doi: 10.1086/592973

Sigmund, I. K., Luger, M., Windhager, R., and McNally, M. A. (2022). Diagnosing periprosthetic joint infections : a comparison of infection definitions: EBJIS 2021, ICM 2018, and IDSA 2013. *Bone Joint Res.* 11, 608–618. doi: 10.1302/2046-3758.119.BJR-2022-0078.R1

Sigmund, I. K., Puchner, S. E., and Windhager, R. (2021). Serum inflammatory biomarkers in the diagnosis of periprosthetic joint infections. *Biomedicines* 9, 1128. doi: 10.3390/biomedicines9091128

Stríz, I., and Trebichavský, I. (2004). Calprotectin - a pleiotropic molecule in acute and chronic inflammation. *Physiol. Res.* 53, 245–253. doi: 10.33549/physiolres.930448

Vergara, A., Fernández-Pittol, M. J., Muñoz-Mahamud, E., Morata, L., Bosch, J., Vila, J., et al. (2019). Evaluation of lipocalin-2 as a biomarker of periprosthetic joint infection. *J. Arthroplasty* 34, 123–125. doi: 10.1016/j.arth.2018.09.047

Wang, C., Wang, Q., Li, R., Qin, J., Song, L., Zhang, Q., et al. (2019). LTF, PRTN3, and MNDA in synovial fluid as promising biomarkers for periprosthetic joint infection: identification by quadrupole orbital-trap mass spectrometry. *J. Bone Joint Surg. Am.* 101, 2226–2234. doi: 10.2106/JBJS.18.01483

Warren, J., Anis, H. K., Bowers, K., Pannu, T., Villa, J., Klika, A. K., et al. (2021). Diagnostic utility of a novel point-of-Care test of calprotectin for periprosthetic joint infection after total knee arthroplasty: a prospective cohort study. *J. Bone Joint Surg. Am.* 103, 1009–1015. doi: 10.2106/JBJS.20.01089

Warren, J. A., Klika, A. K., Bowers, K., Colon-Franco, J., Piuzzi, N. S., and Higuera, C. A. (2022). Calprotectin lateral flow test: consistent across criteria for ruling out periprosthetic joint infection. *J. Arthroplasty* 37, 1153–1158. doi: 10.1016/j.arth.2022.01.082

Whiting, P. F., Rutjes, A. W. S., Westwood, M. E., Mallett, S., Deeks, J. J., Reitsma, J. B., et al. (2011). QUADAS-2: a revised tool for the quality assessment of diagnostic accuracy studies. *Ann. Intern. Med.* 155, 529–536. doi: 10.7326/0003-4819-155-8-201110180-00009

Wildeman, P., Rolfson, O., Söderquist, B., Wretenberg, P., and Lindgren, V. (2021). What are the long-term outcomes of mortality, quality of life, and hip function after prosthetic joint infection of the hip? a 10-year follow-up from Sweden. *Clin. Orthop Relat. Res.* 479, 2203–2213. doi: 10.1097/CORR.0000000000001838

Williams, J. L., Norman, P., and Stockley, I. (2004). The value of hip aspiration versus tissue biopsy in diagnosing infection before exchange hip arthroplasty surgery. *J. Arthroplasty* 19, 582–586. doi: 10.1016/j.arth.2003.11.011

Wyatt, M. C., Beswick, A. D., Kunutsor, S. K., Wilson, M. J., Whitehouse, M. R., and Blom, A. W. (2016). The alpha-defensin immunoassay and leukocyte esterase colorimetric strip test for the diagnosis of periprosthetic infection: a systematic review and meta-analysis. *J. Bone Joint Surg. Am.* 98, 992–1000. doi: 10.2106/JBJS.15.01142

Yee, D. K. H., Chiu, K. Y., Yan, C. H., and Ng, F. Y. (2013). Review article: joint aspiration for diagnosis of periprosthetic infection. *J. Orthop Surg. (Hong Kong)* 21, 236–240. doi: 10.1177/230949901302100225

Yermak, K., Karbysheva, S., Perka, C., Trampuz, A., and Renz, N. (2019). Performance of synovial fluid d-lactate for the diagnosis of periprosthetic joint infection: a prospective observational study. *J. Infect.* 79, 123–129. doi: 10.1016/j.jinf.2019.05.015

Yi, P. H., Cross, M. B., Moric, M., Sporer, S. M., Berger, R. A., and Della Valle, C. J. (2014). The 2013 frank stinchfield award: diagnosis of infection in the early postoperative period after total hip arthroplasty. *Clin. Orthop Relat. Res.* 472, 424–429. doi: 10.1007/s11999-013-3089-1

frontiers | Frontiers in Cellular and Infection Microbiology

TYPE Original Research
PUBLISHED 17 July 2023
DOI 10.3389/fcimb.2023.1187543

OPEN ACCESS

EDITED BY
Chaofan Zhang,
First Affiliated Hospital of Fujian Medical University, China

REVIEWED BY
Erivan S. Ramos-Junior,
Augusta University, United States
Ning Hu,
First Affiliated Hospital of Chongqing Medical University, China

*CORRESPONDENCE
Mincheng Lu
luminchengcheng@smu.edu.cn
Xianrong Zhang
xianrongzh@smu.edu.cn
Bin Yu
yubin@smu.edu.cn

†These authors have contributed equally to this work and share first authorship

RECEIVED 16 March 2023
ACCEPTED 29 June 2023
PUBLISHED 17 July 2023

CITATION
Lu M, He R, Li C, Liu Z, Chen Y, Yang B, Zhang X and Yu B (2023) Apolipoprotein E deficiency potentiates macrophage against *Staphylococcus aureus* in mice with osteomyelitis via regulating cholesterol metabolism.
Front. Cell. Infect. Microbiol. 13:1187543.
doi: 10.3389/fcimb.2023.1187543

Apolipoprotein E deficiency potentiates macrophage against *Staphylococcus aureus* in mice with osteomyelitis via regulating cholesterol metabolism

Mincheng Lu[1,2*†], Ruiyi He[1,2†], Chao Li[1,2], Zixian Liu[1,2], Yuhui Chen[1,2], Bingsheng Yang[1,2], Xianrong Zhang[1,2*] and Bin Yu[1,2*]

[1]Division of Orthopedics and Traumatology, Department of Orthopedics, Nanfang Hospital, Southern Medical University, Guangzhou, Guangdong, China, [2]Guangdong Provincial Key Laboratory of Bone and Cartilage Regenerative Medicine, Nanfang Hospital, Southern Medical University, Guangzhou, Guangdong, China

Introduction: *Staphylococcus aureus* (*S. aureus*) osteomyelitis causes a variety of metabolism disorders in microenvironment and cells. Defining the changes in cholesterol metabolism and identifying key factors involved in cholesterol metabolism disorders during *S. aureus* osteomyelitis is crucial to understanding the mechanisms of *S. aureus* osteomyelitis and is important in designing host-directed therapeutic strategies.

Methods: In this study, we conducted *in vitro* and *in vivo* experiments to define the effects of *S. aureus* osteomyelitis on cholesterol metabolism, as well as the role of Apolipoprotein E (ApoE) in regulating cholesterol metabolism by macrophages during *S. aureus* osteomyelitis.

Results: The data from GSE166522 showed that cholesterol metabolism disorder was induced by *S. aureus* osteomyelitis. Loss of cholesterol from macrophage obtained from mice with *S. aureus* osteomyelitis was detected by liquid chromatography-tandem mass spectrometry(LC-MS/MS), which is consistent with Filipin III staining results. Changes in intracellular cholesterol content influenced bactericidal capacity of macrophage. Subsequently, it was proven by gene set enrichment analysis and qPCR, that ApoE played a key role in developing cholesterol metabolism disorder in *S. aureus* osteomyelitis. ApoE deficiency in macrophages resulted in increased resistance to *S. aureus*. ApoE-deficient mice manifested abated bone destruction and decreased bacteria load. Moreover, the combination of transcriptional analysis, qPCR, and killing assay showed that ApoE deficiency led to enhanced cholesterol biosynthesis in macrophage, ameliorating anti-infection ability.

Conclusion: We identified a previously unrecognized role of ApoE in *S. aureus* osteomyelitis from the perspective of metabolic reprogramming. Hence, during treating *S. aureus* osteomyelitis, considering cholesterol metabolism as a potential therapeutic target presents a new research direction.

KEYWORDS

Apolipoprotein E, Staphylococcus aureus, osteomyelitis, infection, cholesterol metabolism, macrophages

1 Introduction

Osteomyelitis, an infection of bone tissue and bone marrow caused primarily by microbial pathogens, is becoming an increasingly serious health problem. Since the 1970s, there have been less improvement in surgical techniques to reduce the incidence of osteomyelitis, resulting in a continued slow increase in the rate of infection in the hip and knee after open fracture surgery, reaching 5-33%, and 1-4% after arthroplasty (Acharya et al., 2013; Metsemakers et al., 2018; Schwarz et al., 2019). *S. aureus* and coagulase-negative staphylococci account for two-thirds of all osteomyelitis pathogens, with *S. aureus* being the most common single pathogen (Masters et al., 2022). The bone destruction observed during osteomyelitis suggests that *S. aureus* utilizes a dynamic nutrient environment inside the host, as host consumption and release of nutrients are altered by widespread cell death and inflammation (Potter et al., 2020).

Macrophages rely on pattern recognition receptors (PRRs) and other similar receptors to recognize pathogen-associated molecular patterns (PAMPs) (Ozinsky et al., 2000; Takeda et al., 2003). Rapid recognition of foreign factors leads to the production of pro-inflammatory cytokines and chemokines, phagocytosis, reactive oxygen species (ROS), and recruitment of other immune cells to the site of infection (Wynn et al., 2013). Macrophages can rapidly reprogram their metabolic state to promote inflammation and effector function (Hubler and Kennedy, 2016; Russell et al., 2019). However, *S. aureus* can lead to a metabolic reprogramming disorder in macrophages. Fumarate, which is itself a glycolytic inhibitor (Soh et al., 2020), induces epigenetic changes in macrophages that promote trained immunity, enhancing cytokine production (Berends et al., 2019). Furthermore, increased *fumC* expression caused by *S. aureus* results in lower levels of fumarate during infection of human macrophage-like cells (THP-1 cells) and peripheral blood mononuclear cells (PBMCs) (Raineri et al., 2022). *In vivo*, fumarate degradation by *S. aureus* results in diminished protection from a secondary staphylococcal challenge and promoted recurrent infection in a mouse model of skin infection (Raineri et al., 2022). *S. aureus* biofilms stimulate a metabolic bias in recruited macrophage and monocyte, favoring oxidative phosphorylation (OXPHOS) over glycolysis and facilitating their anti-inflammatory activity and biofilm persistence. These immune cells have anti-inflammatory properties including IL-10 and arginase production (Archer et al., 2011). Furthermore, it has been shown that exposure to fermentation supernatant of *S. aureus* results in chondrocyte degeneration, and further investigation indicates that, in response to fermentation supernatant of *S. aureus*, NF-κB signaling activation is coupled with increased cholesterol metabolism to stimulate catabolic factors in chondrocytes (Wang et al., 2022). However, the relationship between cholesterol metabolism and macrophages during *S. aureus* osteomyelitis remains uninvestigated.

Apolipoprotein E (ApoE) is a 35 kDa glycoprotein that belongs to a class of cellular proteins involved in lipid metabolism, which has an important role in cholesterol efflux and reverse cholesterol transport (Miao et al., 2023). Increasing studies have shown that ApoE is not only involved in cardiovascular disease, but also in degenerative disease, viral infection, and tumors (Tenger and Zhou, 2003; Zhu et al., 2012; Hui et al., 2022; Gao et al., n.d.). Based on these studies, it is worth investigating the role of ApoE in *S. aureus* osteomyelitis.

In the present study, we found that *S. aureus* osteomyelitis results in cholesterol loss from macrophage and alteration in intracellular cholesterol content affects bactericidal capacity of macrophage. We also identified ApoE as a core gene and ApoE deficiency attenuates *S. aureus* osteomyelitis infection both *in vivo* and *in vitro*. Mechanically, ApoE deficiency potentiates macrophage resistance to *S. aureus* osteomyelitis via regulating cholesterol metabolism. Our study reveals the role of ApoE in *S. aureus* osteomyelitis, suggesting that reprogramming of cholesterol metabolism is an essential host defense strategy against *S. aureus* osteomyelitis.

2 Materials and methods

2.1 Animals

C57BL/6 wild-type(WT)mice were purchased from the Experimental Animal Center, Southern Medical University (Guangzhou, China), and Ruisiyuan Biotechnology Co., Ltd (Zhaoqing, China). ApoE KO(*Apoe*$^{-/-}$) mice were purchased from Ruisiyuan Biotechnology Co., Ltd (Zhaoqing, China). All mice were housed in facility with a 12 h light/dark cycle, 24 ± 2°C room temperature, and ad libitum access to water and food.

2.2 Preparation of bacteria

S. aureus was isolated from a patient with chronic osteomyelitis, and methicillin-sensitive *S. aureus* was identified using PHOENIX 100 (Becton, Dickinson Microbiology Systems, USA). A frozen stock of *S. aureus* strains was routinely grown on tryptic soy broth (TSB) with shaking at 180 rpm at 37°C for 16-18h and collected by centrifugation at 3,000 rpm for 10 min. The bacterial pellets were washed and resuspended in phosphate-buffered saline (PBS). The concentration of *S. aureus* was adjusted to an optical density (OD) of 0.5 at 600 nm, approximately equal to $1x10^8$ CFU/mL. According to different experimental requirements, *S. aureus* bacteria liquid was diluted to different concentrations.

2.3 Cell culture

A total of $5x10^5$ L929 cells were seeded in 50mL DMEM growth medium containing 10% fetal bovine serum in a 75 cm^2 flask for 7 days without changing medium. After 7 days, the supernatant was collected as macrophage colony-stimulation factor.

For isolation of bone marrow derived macrophages (BMDMs), bone marrow cells were flushed out from tibias and femurs of 8–10-week-old C57BL/6 male mice. Erythrocytes were lysed by red blood cell lysing buffer (Cat.PH1594, Phygene) for 3 min at 4 °C. Next, the pellets were resuspended, after centrifugation, in BMDM growth medium (DMEM growth medium containing 10% fetal bovine serum and 25% L929 fibroblast supernatant) with 1% penicillin and streptomycin and incubated at 37°C and 5% CO2.

2.4 Filipin III staining

Filipin III (Cat.70440, Cayman) was dissolved in ethanol to reach a final concentration of 5 mg/mL. Cells were fixed with 4% paraformaldehyde (PFA) and stained with 50 mg/mL Filipin III for 30-min at room temperature. The emission and excitation of Filipin III was at 340-380 and 385-470nm, respectively. The images were captured with Zeiss LSM980 confocal microscope using a 40x objective.

2.5 Modified implant-associated osteomyelitis mouse model

To prepare infected implants, *S. aureus* bacteria liquid was diluted to 1 x 10^6 CFU/mL. Sterile self-tapping screws (1.5 × 1.0 mm) were placed into the diluted bacteria liquid and shaken at 20 rpm for 10-15 min. Next, the self-tapping screws were transferred to an incubator at 37 °C for 10 min. After desiccation, the infected self-tapping screws were placed on ice for subsequent use. Prior to surgery, mice were anesthetized by intraperitoneal injection of tribromoethanol (125 mg/kg of body weight). After the right hind leg was shaved followed by disinfection with iodine, mice were placed in the supine position and a 5 mm incision was made on the lateral side of the leg. The third trochanter of femur was exposed by blunt separation of the muscles, and a canal was created by drilling distally into the marrow. Next, the infected self-tapping screw, described above, was drilled into the bone along the canal, with care not to penetrate the contralateral cortex of the femur. Finally, the incision was closed with a 5-0 suture. Protocols for animal experiments were approved by the Animal Care and Use Committee at Nanfang Hospital, Southern Medical University.

2.6 Flow sorting

By day 7 after infection, implanted femurs were harvested, and a single-cell suspension of bone marrow was prepared after passing through a 70-μm cell strainer (15-1070, Biologix). Red blood cells were lysed (Cat.PH1594, Phygene) before cells were counted. After being incubated with anti-mouse-CD16/CD32 (E-AB-F0997A, Elabscience) to block non-specific antibody staining, cells were incubated with a mixture of mouse-specific cell surface antibodies on ice, including anti-F4/80-PE (E-AB-F0995D, Elabscience) and anti-CD11b-APC (E-AB-F1081E, Elabscience). After two rounds of washing in fluorescence-activated cell sorting (FACS) buffer, samples were run on a flow cytometer (COULTER MoFlo XDP, BECKMAN, USA). The $CD11b^+F4/80^+$ cells were defined as macrophages and collected for further analysis.

2.7 Cholesterol measurement by LC-MS/MS based metabolomics approach

See Supplementary Material for a detailed description.

2.8 Phagocytosis assay

Mature BMDMs were detached by Accutase (Cat.00-4555-56, Invitrogen), centrifuged, and resuspended at $2×10^5$ cells/well in a 24-well tissue culture plate with antibiotic-free BMDM growth medium. For phagocytosis assay, the cells were incubated for 30 min at 37°C at a multiplicity of infection (MOI) of 10 using bacterial suspensions in PBS. After 30 min, BMDMs were washed using PBS, followed by lysis with Triton X-100 (0.1%). Lysis was serially diluted in PBS, and dilutions were spot-plated onto agar plate. After overnight incubation at 37°C, the CFUs of *S. aureus* were recorded as a measure of phagocytosis.

2.9 Intracellular killing assay

For intracellular killing assay, following infection for 30 min, BMDMs were washed and treated for 1 h with gentamicin (50 μg/mL) and lysozyme (2 μg/mL). After extracellular bactericidal process, BMDMs were cultured with a fresh medium containing antibiotics (1% penicillin/streptomycin) in the presence or absence of Simvastatin (HY-17502, MCE) or water-soluble cholesterol (HY-

N0322A, MCE), or Avasimibe (HY-13215, MCE), or Terbinafine (HY-17395A, MCE). After 12 h treatment, the cells were lysed with 0.1% Triton X-100, and CFUs were counted to determine the intracellular killing rate.

2.10 Micro-computed tomography (micro-CT) imaging

Operated femurs were dissected free of soft tissue and self-tapping screw, fixed overnight in 4% paraformaldehyde, and analyzed by a high-resolution micro-CT (skyscan 1176, Bruker, Belgium). The scan was performed at an isotropic voxel size of 9 μm, a voltage of 50 kVp, a current of 200 μA and an integration time of 400 ms. Images were reconstructed and analyzed using software (NRecon, CTan, Bruker, Belgium). The region of interest (ROI) was defined as the 75-165 slices of proximal tibia bone starting from the growth plate. Structural parameters including bone volume fraction (BV/TV), bone mineral density (BMD), trabecular number (Tb.N), trabecular thickness (Tb.Th), and trabecular separation (Tb. Sp) were calculated.

2.11 Histological analysis

By day 7 after infection, mice were euthanized by cervical dislocation and perfused intracardially with 4% paraformaldehyde. The implanted femurs were harvested and fixed in 4% paraformaldehyde at 4°C overnight. After demineralization in 10% EDTA for 10 days, samples were processed and embedded in paraffin. Coronal sections of 4-μm thickness were cut and stained with hematoxylin and eosin. Smeltzer's scoring methods (Smeltzer et al., 1997) were used to evaluate the histopathological changes by two blinded observers. Each section was assigned a score according to the sum of intraosseous acute inflammation (0–4), intraosseous chronic inflammation (0–4), periosteal inflammation (0–4), and bone necrosis (0–4). To detect bacterial burden in bone, Gram staining was performed on deparaffinized and rehydrated sections using a Gram Stain Kit (Modified Brown & Brenn) (Cat.BBS-2, Seytek).

2.12 Isolation of bone marrow and bone marrow supernatant

By day 7 after infection, mice were euthanized by cervical dislocation. The implanted femurs were harvested and the self-tapping screws were removed. The femurs were then placed in 0.5 ml bottomless microtubes that funneled into 1.5 ml Eppendorf microcentrifuge tubes. The nested tubes with bone were spun for 9 s at 13,000 x g to acquire bone marrow pellets. The pellets were resuspended in 450 μl red blood cell lysis buffer (Cat.PH1594, Phygene) and centrifuged at 500 × g for 3 min at 4°C. A volume of 400 μl of separated middle layer was collected as bone marrow supernatant for further analysis. The pellets were resuspended in 400 μl PBS and centrifuged at 500 x g for 3 min. After centrifugation, the pellets were collected for RNA-seq analysis.

2.13 Blood lipid measurement

A volume of 0.5 ml blood was collected from mice to extract serum, and serum total cholesterol (TC), serum triglycerides (TG), serum high-density lipoprotein cholesterol (HDL-C), serum low-density lipoprotein cholesterol (LDL-C), were determined by an automatic biochemical analyzer (BS330, Mindray, China).

2.14 RNA isolation and quantitative real-time PCR

Total RNA of BMDMs was extracted using RNA Purification kit (B0004DP, EZBioscience) according to manufacturer instructions. Reverse transcription into cDNA was performed using Evo Moloney Murine Leukemia Virus RT Premix (AG11706,Accurate Biology). Quantitative real-time PCR was performed using SYBR Green (AG11702, Accurate Biology) on QuantStudio5 (Applied Biosystems, USA) according to manufacturer protocol. The PCR primers are shown in (Table S2). The Beta-Actin genes were used as internal control. The relative amount of each gene was calculated using the $2^{-\Delta\Delta CT}$ method.

2.15 RNA preparation and transcriptome sequencing

See Supplementary Material for a detailed description.

2.16 Differential expression analysis

The DESeq2 R package (1.22.1) was used for differential expression analysis. The resulting *P*-values were adjusted using Benjamini and Hochberg's approach to control for false-discovery rate. For dataset GSE166522, genes with an adjusted *P*-value < 0.05 and | log2 (fold change) | value > 0.5 were recognized as differentially expressed genes (DEGs). For expression analysis between WT and *Apoe*$^{-/-}$ mice with or without *S. aureus* osteomyelitis, genes with an adjusted *P*-value < 0.05 and | log2 (fold change) | value >1 were recognized as DEGs.

2.17 Gene set enrichment analysis (GSEA) and leading-edge analysis

Cholesterol metabolism gene sets were selected through the Molecular Signatures Database (MsigDB). The collection of cholesterol metabolism gene sets was comprised of 93 gene sets (Table S1). The gene expression data of 14-day groups from

GSE166522 was for GSEA, and the enriched gene sets ($P < 0.01$, FDR < 0.25) on *S. aureus* osteomyelitis group were continued to perform a leading-edge analysis. All analyses were performed using GSEA software (version 4.2.3).

2.18 Statistical analysis

Statistical analysis was performed using SPSS 26.0 software (IBM SPSS 26.0, SPSS Inc.). For comparisons between two groups (parametric data), Student's t-test was applied. Mann-Whitney U-test was used for nonparametric data. For multigroup comparisons, one-way analysis of variance (ANOVA), with LSD (equal variance assumed) or Dunnett T3 test (equal variance not assumed), was used. All data are expressed as mean ± SEM.

3 Result

3.1 *S. aureus* induces loss of cholesterol in macrophages in the infected-bone of mice

In order to determine whether cholesterol metabolism was affected in the bone of *S. aureus* osteomyelitis mice, we analyzed the expression of cholesterol metabolism genes (CMGs) (Xiao et al., 2020) in femur with *S. aureus* osteomyelitis from GSE166522 (Lin

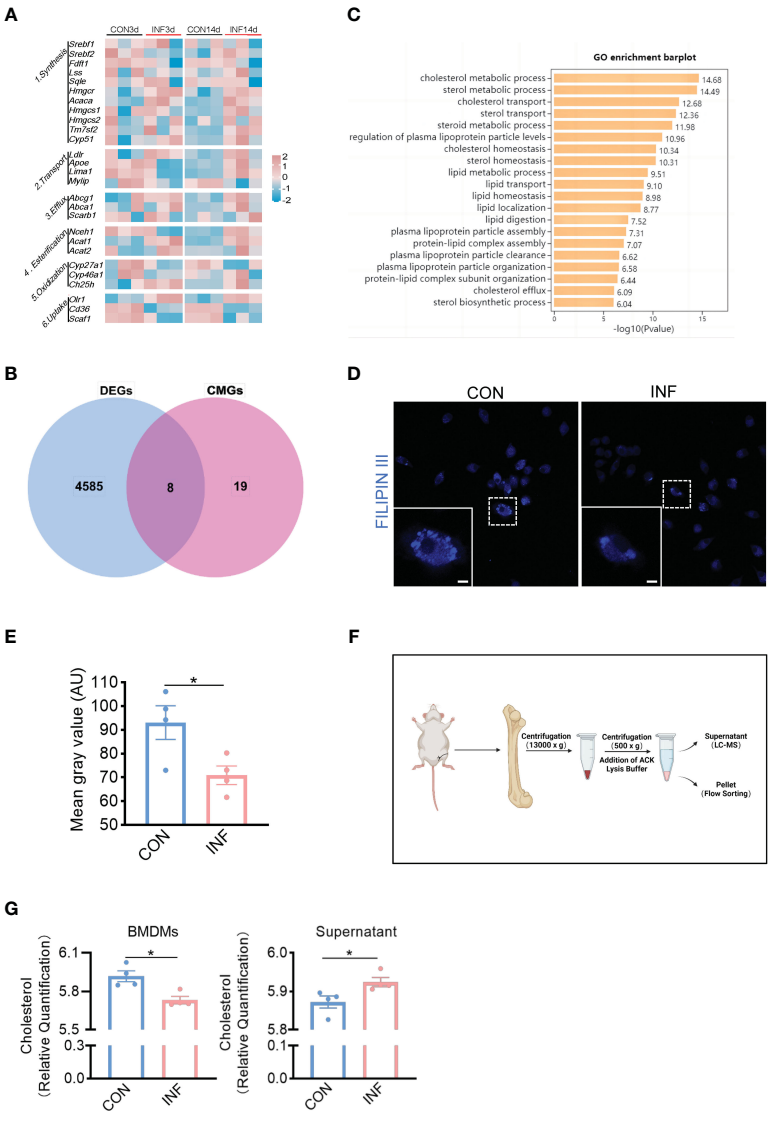

FIGURE 1
S. aureus induces loss of cholesterol in macrophages in the infected-bone of mice. **(A)** Heatmap showing relative expression of CMGs in *S. aureus* infected femur on day 3 and 14 post-infection. **(B)** Venn diagram showing number of differentially expressed CMGs on day 14 post-infection. **(C)** GO enrichment analysis of differentially expressed CMGs on day 14 post-infection. **(D)** Representative images of Filipin III staining in BMDMs infected with S. aureus for 12 hours. Scale bar was 5μm. **(E)** Fluorescence intensity result of Filipin III staining. **(F)** Schematic of the isolation of bone marrow and bone marrow supernatant. Images were created with BioRender.com. **(G)** Cholesterol content in $CD11b^{+}F4/80^{+}$ macrophages and supernatant from *S. aureus* osteomyelitis mice and controls. n = 4/group. Data are presented as mean ± SEM. Two-tailed Student's t-test was used. $*P < 0.05$.

et al., 2021). Compared to CMGs by day 3 post-infection, the differential expression of CMGs by day 14 post-infection was more pronounced (Figure 1A). Differentially expressed CMGs were chosen among differentially expressed genes by day 14 post-infection, followed by GO (Gene Ontology) enrichment analysis (Figure 1B). The differentially expressed CMGs were significantly enriched in a variety of cholesterol metabolism pathways (Figure 1C), indicating cholesterol metabolism might be altered during the pathogenesis of *S. aureus* osteomyelitis.

We then sought to determine the relationship between cholesterol content of macrophages and *S. aureus* osteomyelitis. The Filipin III results showed that *S. aureus* infection of BMDMs for 12 hours resulted in cholesterol loss (Figures 1D, E). Before detecting changes in the cholesterol content of BMDMs *in vivo*, we modified the establishment of mice model with *S. aureus* osteomyelitis on the basis of a previous method (Lin et al., 2021) (Figure S1A), and the histochemical staining results showed that the modified protocol was practicable and stable (Figures S1B,C). The modified protocol was similar to the clinical way of internal fixation. Moreover, it eliminated the injection of *S. aureus* during establishment and facilitated the removal of implant. Subsequently, we isolated the bone marrow macrophages and bone marrow supernatant from mice with S. aureus osteomyelitis by day 7 after operation (Figure 1F). Using a liquid chromatography-tandem mass spectrometry (LC-MS/MS)–based metabolomics approach, we assessed the impact of S. aureus osteomyelitis on cholesterol content of CD11b+F4/80+ macrophages and supernatant. S. aureus osteomyelitis led to decreased population of CD11b+F4/80+ macrophages (Figure S2A), increased cholesterol content of supernatant, and reduced cholesterol content of CD11b +F4/80+ macrophages (Figure 1G). Together, these data suggest that S. aureus osteomyelitis induces cholesterol content modulation in infected femur, which leads to diminished cholesterol content of infected macrophages.

3.2 ApoE is the key factor in cholesterol metabolism disorder during *S. aureus* osteomyelitis

Based on the results mentioned above, we hypothesized that the amount of intracellular cholesterol could influence the killing function of macrophages. We used Simvastatin, a competitive inhibitor of HMG-CoA reductase, that prevents cholesterol biosynthesis (Corsini et al., 1999). Comparing to control, Simvastatin significantly reduces the killing potency of infected BMDMs (Figures 2A, B). On the other hand, bactericidal function of BMDMs was upregulated under the treatment with water-soluble cholesterol (Figures 2C, D). In addition, we used Avasimibe, an acyl coenzyme A-cholesterol acyltransferase inhibitor, that relatively enhances cholesterol content via blocking the conversion of cholesterol to cholesterol esterase (Ohshiro et al., 2011). We noted that Avasimibe treatment enhance bactericidal activity of BMDMs upon *S. aureus* infection (Figures 2E, F). Overall, these findings indicate that regulating intracellular cholesterol could alter bactericidal capacity of macrophages against *S. aureus*.

Furthermore, to validate the key factor in cholesterol metabolism disorder during *S. aureus* osteomyelitis, the gene expression data of 14-day groups from GSE166522 was for GSEA, and we continued to perform a leading-edge analysis of the significantly enriched gene sets ($P < 0.01$, FDR < 0.25) on *S. aureus* osteomyelitis group, identifying the core driver (Figure 2G). The result of leading-edge analysis showed that ApoE was associated with the largest number of enriched gene sets (Figure 2H), and we found that expression of ApoE increased by day 14 post-infection, despite expression levels of ApoE comparable to control by day 3 post-infection (Figure 2I). We therefore assessed the expression of ApoE in BMDMs after stimulation of *S. aureus in vitro*. The qPCR results revealed, compared to control, a small, but significant, elevation of mRNA expression of ApoE in infected BMDMs (Figure 2J). We then isolated BMDMs from ApoE knockout ($Apoe^{-/-}$) mice to examine the impact of ApoE deficiency on the function of macrophages in response to *S. aureus* infection. The ApoE deficiency led to increased cholesterol content (Figure 2K), as well as enhanced phagocytosis and bactericidal rate of BMDMs (Figures 2L–O), indicating that ApoE deficiency may affect innate immune functions of macrophages via regulation of cholesterol metabolism.

3.3 ApoE deficiency ameliorates bacterial burden and bone destruction in mice with *S. aureus* osteomyelitis

To confirm the role of blocking ApoE against *S. aureus* osteomyelitis, we then developed *S. aureus* osteomyelitis models in wild-type (WT) mice and ApoE knockout ($Apoe^{-/-}$) mice. Before the establishment of mice models with *S. aureus* osteomyelitis, we confirmed that ApoE deficiency has no significant effect on the bone mass of 8-week-old male mice fed normal chow (Figure S3A). By day 7 after operation, several lipid parameters indicated that, though ApoE deficiency elevated total cholesterol (TC), total triglyceride (TG), and low-density lipoprotein (LDL) contents in $Apoe^{-/-}$ mice, *S. aureus* had no significant effect on lipid profile of infected-femurs of mice regardless of the presence or absence of ApoE (Figures 3A–D). We observed a considerable amount of Gram staining in the bone marrow of WT mice with *S. aureus* osteomyelitis, whereas sparse Gram staining could be noted in $Apoe^{-/-}$ mice (Figure 3E). Micro-CT data confirmed the protective role of ApoE deficiency against *S. aureus*-induced of bone destruction. $Apoe^{-/-}$ mice showed improved trabecular bone in the distal femur and reduced cortical bone loss in the implant area compared with WT mice (Figure 4A). The higher bone volume fraction (BV/TV) and bone mineral density (BMD) was associated with an increased trabecular number (Tb.N) and reduced trabecular separation (Tb.Sp) (Figures 4C–G). Consistent with the micro-CT results, histological staining and scores showed smaller areas of abscesses and decreased bone destruction in $Apoe^{-/-}$ mice relative to WT mice (Figures 4B, H). These data suggest that blocking ApoE might promote bacterial clearance and hinder bone destruction.

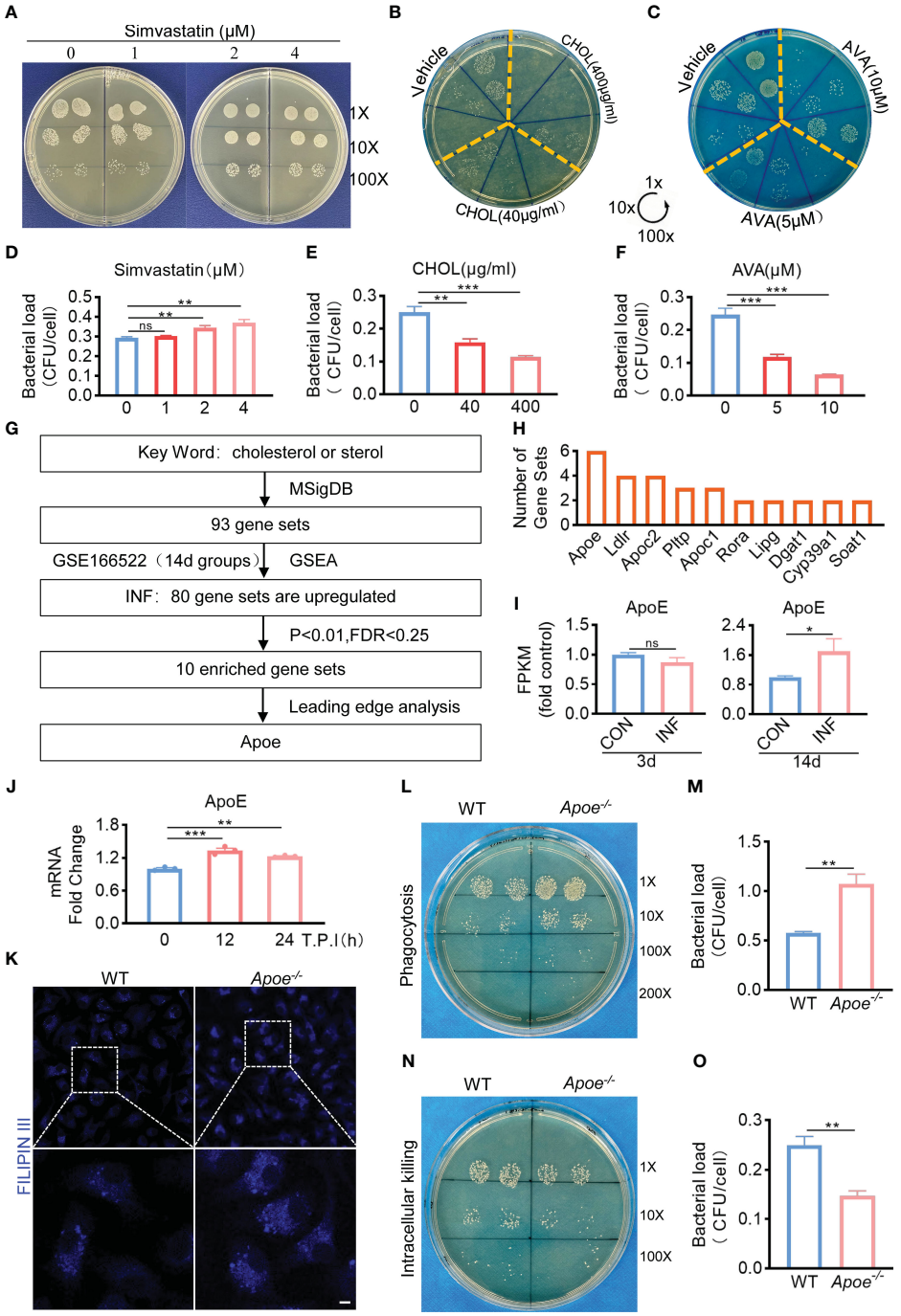

FIGURE 2
ApoE is the key factor in cholesterol metabolism disorder during *S. aureus* osteomyelitis. **(A-F)** Representative images **(A–C)** and quantification **(D– F)** of CFUs of *S. aureus* for the bactericidal assay. BMDMs were infected with *S. aureus* (MOI = 10) for 30 min. After extracellular bacteria were removed, cells were treated with Simvastatin, water-soluble cholesterol (CHOL), Avasimibe (AVA) for 12 h. n = 3/group. **(G)** Flowchart of collection of cholesterol metabolism gene sets, gene set enrichment analysis, screening for significantly enriched gene sets and leading-edge analysis. **(H)** The result of leading-edge analysis. **(I)** Normalized gene expression of ApoE in mice at day 3 or 14 after *S. aureus* osteomyelitis from GSE166522.n=3/group. **(J)** Quantification of mRNA expression of ApoE in BMDMs infected with *S. aureus* at an MOI of 10 for 12h and 24h. n = 3/group. **(K)** Representative images of Filipin III staining in WT or *Apoe*$^{-/-}$ BMDMs. Scale bar was 10μm. **(L, M)** Representative images **(L)** and quantification **(M)** of CFUs of *S. aureus* for the phagocytosis assay. WT or *Apoe*$^{-/-}$ BMDMs were infected with *S. aureus* (MOI = 10) for 30 min. n = 3/group. **(N, O)** Representative images **(N)** and quantification **(O)** of CFUs of *S. aureus* for the bactericidal assay. WT or *Apoe*$^{-/-}$ BMDMs were infected with *S. aureus* (MOI = 10) for 30 min. After extracellular bacteria were removed, cells were treated for 12 h. n = 3/group. Data are presented as mean ± SEM. One-way ANOVA with Tukey's test **(D-F, J)** and two-tailed Student's t-test **(I, M, O)** were used. *:$P < 0.05$, **:$P < 0.01$, ***:$P < 0.001$. "ns" means "not statistically significant".

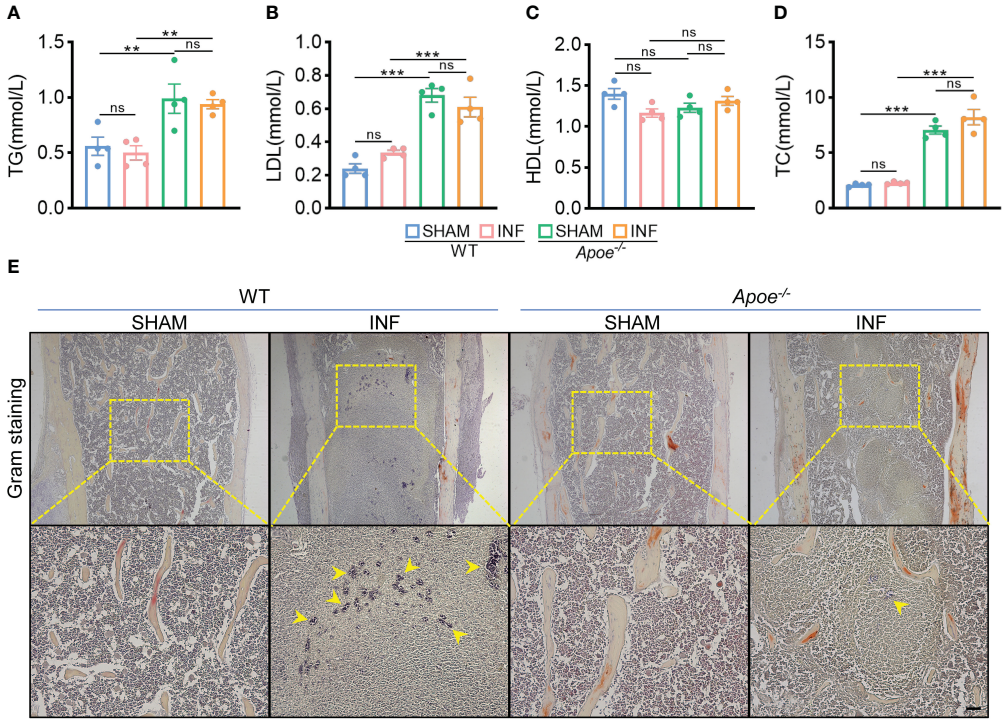

FIGURE 3
ApoE deficiency mitigates bacterial load in mice with *S. aureus* osteomyelitis. **(A–D)** Total triglyceride **(A)**, low-density lipoprotein **(B)**, high-density lipoprotein **(C)**, and total cholesterol content **(D)** of WT or *Apoe*$^{-/-}$ mice with or without *S. aureus* osteomyelitis. n = 4/group. **(E)** Representative images of gram staining of femurs in WT or *Apoe*$^{-/-}$ mice with or without *S. aureus* osteomyelitis. Yellow arrows indicate *S. aureus*. Scale bar was 100um.Data are presented as mean ± SEM. One-way ANOVA with Tukey's test were used. **:$P < 0.01$, ***:$P < 0.001$. "ns" means "not statistically significant".

3.4 ApoE deficiency mediates macrophage resistance to *S. aureus* osteomyelitis via regulation of cholesterol metabolism.

To explore how ApoE functions in the regulation of cholesterol metabolism during *S. aureus* osteomyelitis, we performed transcriptome analysis of the WT and *Apoe*$^{-/-}$ femur bone marrow using high-throughput sequencing. The principal component analysis result showed that ApoE deficiency caused some degree of gene expression variation between WT and *Apoe*$^{-/-}$ mice, but the effect of *S. aureus* infection on gene expression dispersion was more significant, suggesting, at the transcriptional level, ApoE affects the outcome of *S. aureus* osteomyelitis (Figure 5A). Because previous studies reported that ApoE is related to cholesterol efflux (Getz and Reardon, 2018), we conjectured that ApoE may influence cholesterol efflux in infected macrophages. However, the GSEA results showed that cholesterol biosynthesis gene sets were strongly enriched in *Apoe*$^{-/-}$ mice with *S. aureus* osteomyelitis (Figure 5B). Beyond this, bone marrow supernatant from mice with *S. aureus* osteomyelitis had an elevated level of cholesterol content and an upregulated mRNA expression of ATP-binding cassette transporter A1 (ABCA1), a critical transporter for cholesterol efflux, was detected in *S. aureus*-infected BMDMs,independent of the presence of the ApoE (Figures 5C–G). On the other hand, the expression of cholesterol biosynthesis genes showed a significant increase in *Apoe*$^{-/-}$ mice with *S. aureus* osteomyelitis, including Squalene Epoxidase (SQLE), Lanosterol Synthase (LSS), Cytochrome P450 Family 51 Subfamily (CYP51), 24-Dehydrocholesterol Reductase (DHCR24) (Figures 5C, F). We then detected the expression of these genes in BMDMs *in vitro*, and qPCR results were consistent with transcriptome analysis (Figure 5H). We observed that these upregulated cholesterol biosynthesis genes are in the pathway form squalene to lanosterol and assumed that killing capacity of *Apoe*$^{-/-}$ BMDMs would be impaired via blocking this pathway. We used SQLE inhibitor, Terbinafine, that prevents the conversion of squalene to lanosterol (Nowosielski et al., 2011). In comparison to control, the killing ability of ApoE-deleted BMDMs was reduced under Terbinafine treatment (Figures 6A, B), as well as induction of the cholesterol biosynthesis genes SQLE, LSS, and DHCR24 (Figure 6C). Overall, these findings indicate that the mechanism behind ApoE deficiency ameliorating macrophage resistance to *S. aureus* osteomyelitis is not only through augmentation of intracellular cholesterol caused by ApoE knockout, but also through reducing cholesterol loss via enhanced cholesterol biosynthesis.

4 Discussion

Cholesterol, a fat-like substance, is the main steroidal compound in mammals and plays a vital role in basic cellular life activities. Some bacterial pathogens rely on the host cell for a sizable percentage of their growth requirements and possess sophisticated mechanisms to manipulate the host cell to obtain essential nutrients. One of the targeted host cell factors is cholesterol.

10.3389/fcimb.2023.1187543

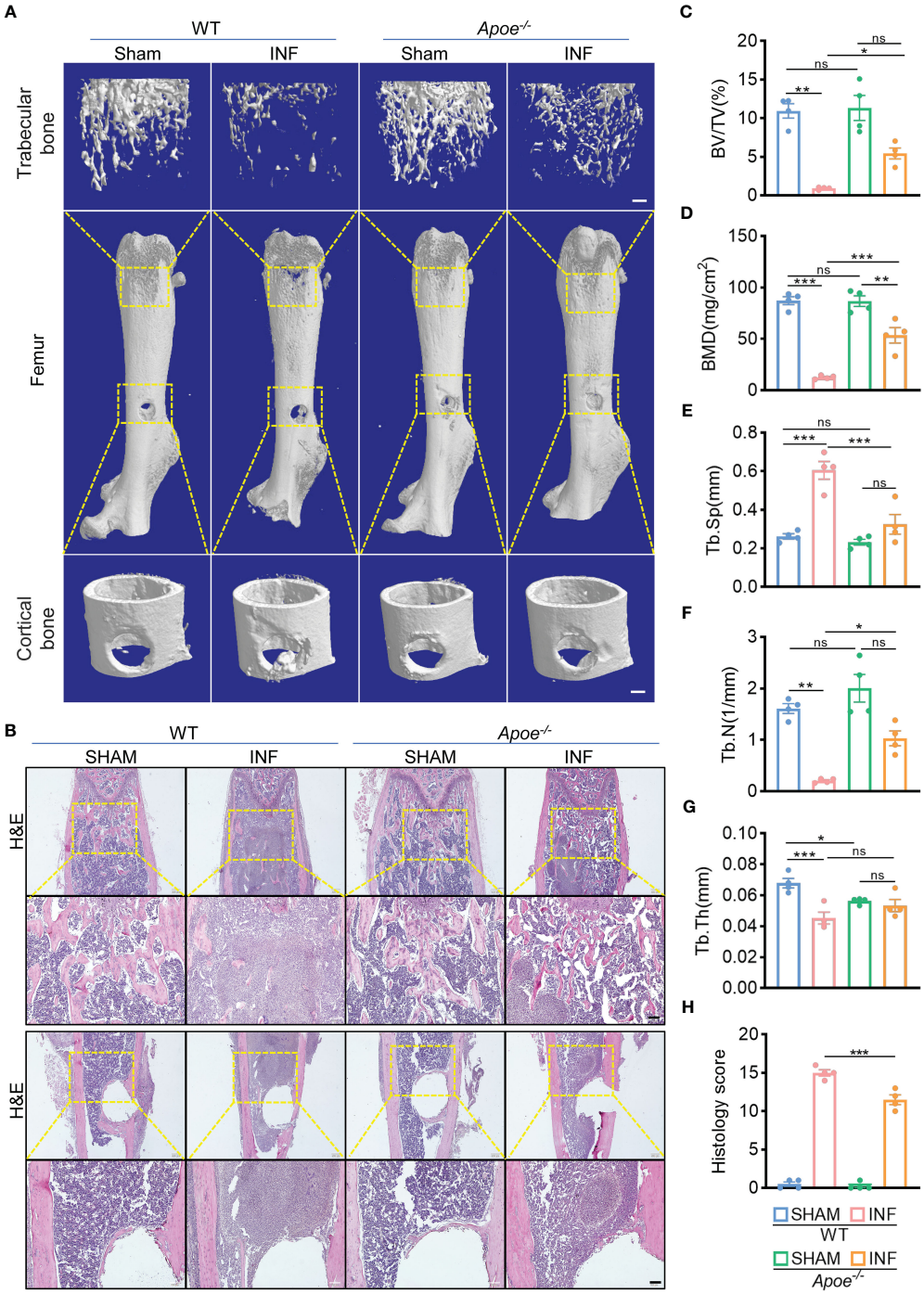

FIGURE 4
ApoE deficiency alleviates bone destruction in mice with *S. aureus* osteomyelitis. **(A)** Representative 3D images of femurs in WT or *Apoe*$^{-/-}$ mice with or without *S. aureus* osteomyelitis. Scale bar was 200um. **(B)** Representative images of H&E staining of femurs in WT or *Apoe*$^{-/-}$ mice with or without *S. aureus* osteomyelitis. Scale bar was 100um. **(C–G)** Quantitative analysis of trabecular bone fraction (BV/TV) **(C)**, bone mineral density (BMD) **(D)**, trabecular separation (Tb. Sp) **(E)**, trabecular number (Tb. N) **(F)**, and trabecular thickness (Tb.Th) **(G)** of the femur from WT or *Apoe*$^{-/-}$ mice with or without *S. aureus* osteomyelitis. n = 4/group. **(H)** Quantitative analysis of histopathological changes using Smeltzer's scoring method. n = 4/group. Data are presented as mean ± SEM. One-way ANOVA with Tukey's test were used. *:$P < 0.05$, **:$P < 0.01$, ***:$P < 0.001$. "ns" means "not statistically significant".

Pathogenic bacteria target cholesterol not only to gain entry to host cells, but also to hijack host cell signaling pathways favorable for intracellular survival (Samanta et al., 2017). *Chlamydia pneumoniae* (*C. pneumoniae*) infection decreased cholesterol efflux by downregulating expression of ABCA1 in A549 lung epithelial cell lines (Korhonen et al., 2013). Experimental measurement of cholesterol efflux to ApoA-1 showed a 50% decrease in *C. pneumoniae*-infected THP-1 macrophage-like foam cells compared to uninfected or heat-killed bacteria-infected cells. Further, *C. pneumoniae* appeared to downregulate host

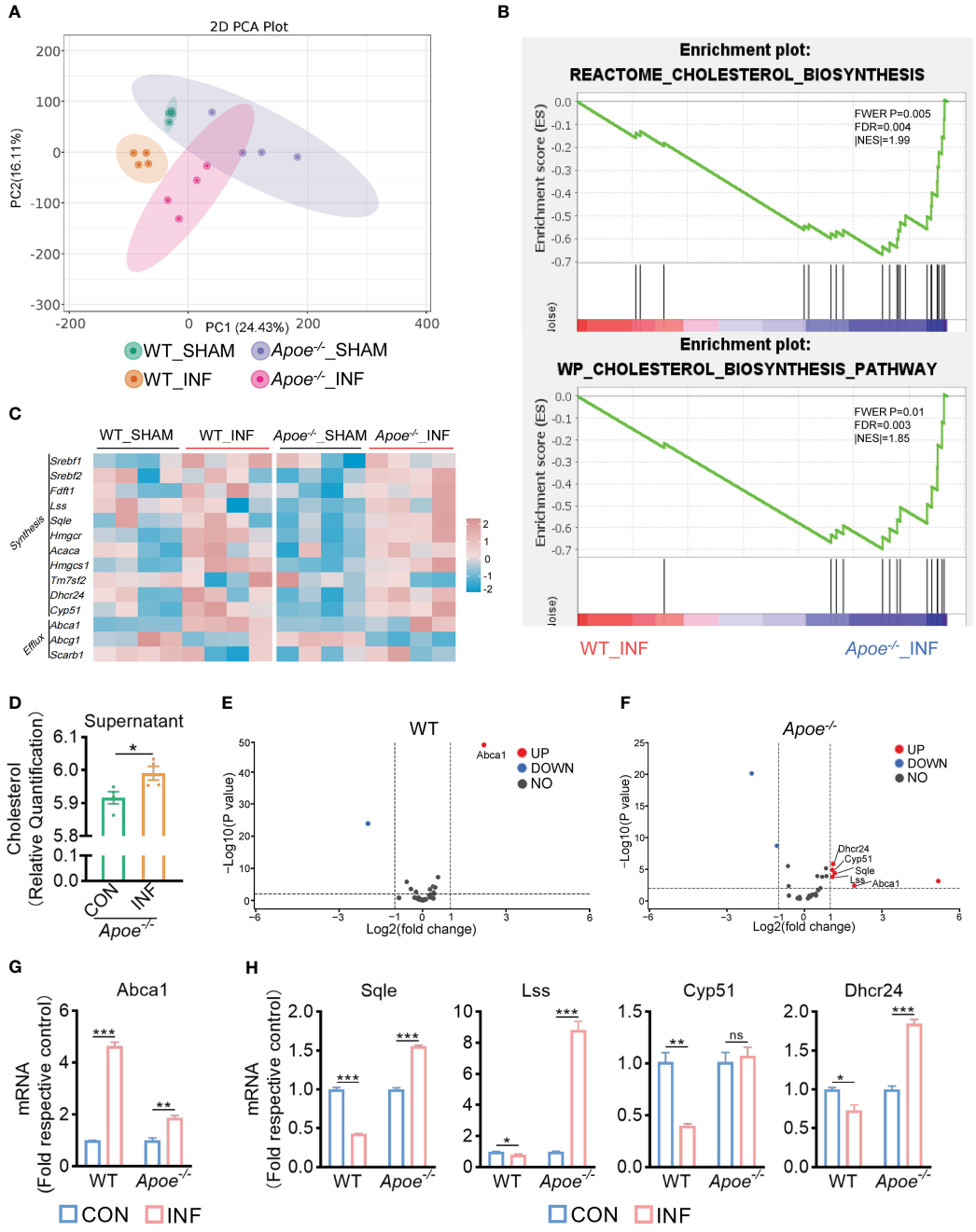

FIGURE 5
ApoE deficiency enhances cholesterol biosynthesis after *S. aureus* osteomyelitis. **(A)** Principal component analysis result. n = 4/group. **(B)** GSEA results showing the cholesterol biosynthesis pathway significantly enriched in *Apoe*$^{-/-}$ mice compared with WT mice, under *S. aureus* osteomyelitis conditions. **(C)** Heatmap showing relative expression of cholesterol efflux and cholesterol biosynthesis genes in femur bone marrow of WT and *Apoe*$^{-/-}$ mice with or without *S. aureus* osteomyelitis. **(D)** Cholesterol content in supernatant from *Apoe*$^{-/-}$ mice with or without *S. aureus* osteomyelitis. n = 4/group. **(E)** Volcano plot showing relative expression of CMGs in femur bone marrow of WT mice with or without *S. aureus* osteomyelitis. **(F)** Volcano plot showing relative expression of CMGs in femur bone marrow of *Apoe*$^{-/-}$ mice with or without *S. aureus* osteomyelitis. **(G)** mRNA expression of ABCA1 of WT or *Apoe*$^{-/-}$ BMDMs stimulated by *S. aureus* for 6h. n = 3/group. **(H)** mRNA expression of SQLE, LSS, CYP51, and DHCR24 of WT or *Apoe*$^{-/-}$ BMDMs stimulated by *S. aureus* for 12h. n = 3/group. Data are presented as mean ± SEM. One-way ANOVA with Tukey's test **(G, H)** and two-tailed Student's t-test **(D)** were used. *:$P < 0.05$, **:$P < 0.01$, ***:$P < 0.001$. "ns" means "not statistically significant".

cholesterol efflux by increasing microRNA miR-33 levels, which is produced from the SREBP intron, and downregulates ABCA1 (Zhao et al., 2014). *Coxiella burnetii* (*C. burnetii*) differentially regulated ApoE and APOC gene expression in THP-1 macrophages (Ren et al., 2003). In addition, a genome-wide RNA interference screen in HeLa cells revealed that siRNA depletion of apolipoproteins involved in lipid transport, affected the total number of *C. burnetii* parasitophorous vacuoles (McDonough et al., 2013). Although research on the association between *S. aureus* and cholesterol metabolism of macrophages is limited,

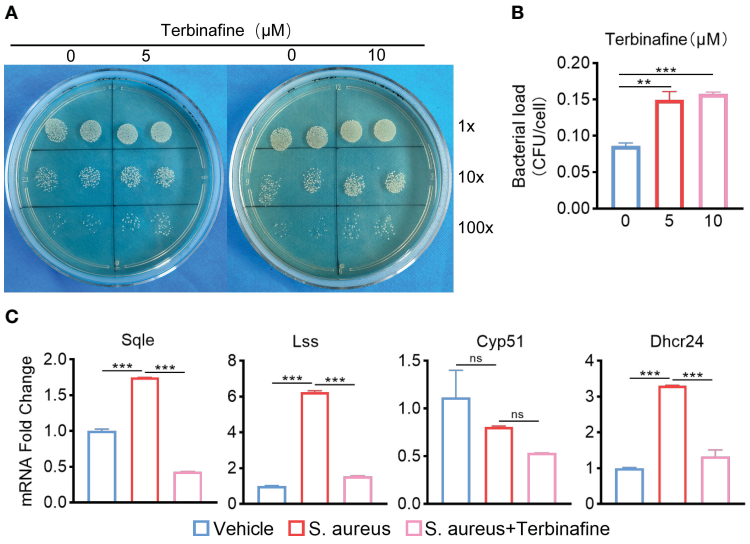

FIGURE 6
Terbinafine impairs the bactericidal capacity of *Apoe*$^{-/-}$ BMDMs via blocking cholesterol biosynthesis. **(A, B)** Representative images **(A)** and quantification **(B)** of CFUs of *S. aureus* for the bactericidal assay. *Apoe*$^{-/-}$ BMDMs were infected with *S. aureus* (MOI = 10) for 30 min. After extracellular bacteria were removed, cells were treated with Terbinafine for 12 h. n = 3/group. **(C)** mRNA expression of SQLE, LSS, CYP51, and DHCR24 of *Apoe*$^{-/-}$ BMDMs stimulated by *S. aureus* for 12h, in the presence or absence of Terbinafine (10μM). n = 3/group. Data are presented as mean ± SEM. One-way ANOVA with Tukey's test were used. **:$P < 0.01$, ***:$P < 0.001$. "ns" means "not statistically significant".

previous study reported that fermentation supernatant of *S. aureus* resulted in chondrocyte degeneration through NF-κB signaling activation coupled with increased cholesterol metabolism, stimulating catabolic factors in chondrocytes (Q et al., 2022). Our data show the enhanced cholesterol efflux and subsequent cholesterol loss in bone marrow macrophages of mice with *S. aureus* osteomyelitis. Moreover, cholesterol is associated with inflammation, polarization, and mitochondrial-derived reactive oxygen species(mtROS) (Sheedy et al., 2013; O'Rourke et al., 2022), which are critical for anti-bacterial activity of macrophages (West et al., 2011; Galli and Saleh, 2021).We assume that cholesterol loss of macrophage induced by *S. aureus* infection could impair bactericidal capacity of macrophages via the switch of macrophages toward M2 polarization or decreased generation of mtROS, promoting *S. aureus* survival. Thus, modulation of cholesterol metabolism in macrophages might be one way to alleviate *S. aureus* osteomyelitis, based on our present data.

ApoE was initially described as a lipid transport protein and major ligand for LDL receptors with a role in cholesterol metabolism and cardiovascular disease. ApoE deficiency is associated with decreased catabolism of atherogenic lipoproteins, favoring hypercholesterolemia and atherosclerosis development (Zhang et al., 1992). Recent studies showed that ApoE is involved in the pathogenesis of infection and tumor development. For example, ApoE is required for infectious viral particle production of Hepatitis C virus (HCV) (Gong and Cun, 2019). ApoE KO mice exhibit increased susceptibility to influenza A virus infection and severe disease pathology than WT mice, because ApoE-deleted cells exhibit an increased surface distribution of IAV receptor sialic acid via increased membrane cholesterol (Gao et al., 2022). In contrast, ApoE KO mice had significantly lower herpes simplex virus-1 concentrations in the nervous system than WT mice (Burgos et al., 2006). Additionally, ApoE inhibits HIV infection by directly interacting with HIV gp160 and suppresses Env expression (Siddiqui et al., 2018). On the other hand, single-cell transcriptomics of cholangiocarcinoma and anti-CSF1R–treated tumors, identified a unique granulocytic myeloid-derived suppressor cell (G-MDSCs) subset, ApoE G-MDSCs, with abundant expression of ApoE in the vehicle-treated tumors and marked ApoE downregulation with tumor-associated tumor blockade (Loeuillard et al., 2020). ApoE activation has been linked to enhanced MDSC apoptosis and consequent tumor regression (Tavazoie et al., 2018). Moreover, *Apoe*$^{-/-}$ mice exhibited higher resistance toward the development of three types of carcinomas as compared to wild-type mice and had greater responses to αPD-1 (anti-PD-1) immunotherapy (Hui et al., 2022). Our observation that ApoE knockout enhances innate immune function of BMDMs and ameliorates bone infection and destruction in mice with *S. aureus* osteomyelitis. Further transcriptome analyses and *in vitro* experiments evaluate how ApoE deficiency enhances cholesterol biosynthesis to inhibit cholesterol loss, mediating macrophage resistance to *S. aureus* osteomyelitis. Though ApoE is mostly linked to cholesterol efflux and reverse cholesterol transport, it is reported that astrocytic ApoE vectors a variety of microRNAs (miRNAs) that specifically silence genes involved in neuronal cholesterol biosynthesis (Li et al., 2021). However, we cannot exclude the possibility that ApoE may affect the pathogenesis of *S. aureus* osteomyelitis through other mechanisms.

Although we found that ApoE deficiency could improve macrophage bacterial clearance in *S. aureus* osteomyelitis, there are

some limitations in our study. First, we did not use myeloid specific ApoE knockout mice to further verify the mechanism of ApoE action in macrophages. Second, it remains to be determined how *S. aureus* may induce activation of ApoE in bone marrow macrophages, as well as the downstream mechanisms by which alteration in intracellular cholesterol content affects bactericidal capacity of macrophages. Third, whether ApoE mediates the suppressed bactericidal activity of macrophages against other bacterial species deserves further investigation.

In conclusion, our data demonstrate mice bone with *S. aureus* osteomyelitis has a reduced level of cholesterol in macrophages, and regulation of cholesterol metabolism could alter the bactericidal capacity of macrophages. We also identified ApoE as a key factor and established that ApoE deficiency functions as a protective factor against *S. aureus* osteomyelitis via regulating cellular cholesterol metabolism.

Data availability statement

The datasets presented in this study can be found in online repositories. The names of the repository/repositories and accession number(s) can be found below: https://www.ncbi.nlm.nih.gov/geo/ , GSE227521.

Ethics statement

The animal study was reviewed and approved by The Animal Care and Use Committee at Nanfang Hospital, Southern Medical University.

Author contributions

Conceptualization, BY, XZ, and ML. Bioinformatic analysis, ML and CL. Mouse experiments, ML, RH, CL, ZL, YC, and BSY. *In vitro* experiments, ML, CL, and ZL. Statistical analysis, ML and RH. Original draft, ML. Figure preparation, RH and ML. Critical revision of the manuscript, XZ. All authors contributed to the article and approved the submitted version.

Funding

This study was supported by the National Natural Science Foundation of China (82272517), and Science and Technology Project of Guangzhou (202201011339).

Acknowledgments

We gratefully acknowledge all individuals who participated in the study. The author, Lu, is especially grateful to Luoxiaohan Li, for her support and understanding during the experiment and hopes that she can accompany him forever.

Conflict of interest

The authors declare that the research was conducted in the absence of any commercial or financial relationships that could be construed as a potential conflict of interest.

Publisher's note

Supplementary material

The Supplementary Material for this article can be found online at: https://www.frontiersin.org/articles/10.3389/fcimb.2023.1187543/full#supplementary-material

References

Acharya, S., Soliman, M., Egun, A., and Rajbhandari, S. M. (2013). Conservative management of diabetic foot osteomyelitis. *Diabetes Res. Clin. Pract.* 101, e18–e20. doi: 10.1016/j.diabres.2013.06.010

Archer, N. K., Mazaitis, M. J., Costerton, J. W., Leid, J. G., Powers, M. E., and Shirtliff, M. E. (2011). Staphylococcus aureus biofilms: properties, regulation, and roles in human disease. *Virulence.* 2, 445–459. doi: 10.4161/viru.2.5.17724

Berends, E. T. M., Zheng, X., Zwack, E. E., Ménager, M. M., Cammer, M., Shopsin, B., et al. (2019). Staphylococcus aureus impairs the function of and kills human dendritic cells via the LukAB toxin. *mBio.* 10, e01918–e01918. doi: 10.1128/mBio.01918-18

Burgos, J. S., Ramirez, C., Sastre, I., and Valdivieso, F. (2006). Effect of apolipoprotein e on the cerebral load of latent herpes simplex virus type 1 DNA. *J. Virol.* 80, 5383–5387. doi: 10.1128/JVI.00006-06

Corsini, A., Bellosta, S., Baetta, R., Fumagalli, R., Paoletti, R., and Bernini, F. (1999). New insights into the pharmacodynamic and pharmacokinetic properties of statins. *Pharmacol. Ther.* 84, 413–428. doi: 10.1016/S0163-7258(99)00045-5

Galli, G., and Saleh, M. (2021). Immunometabolism of macrophages in bacterial infections. *Front. Cell Infect. Microbiol.* 10. doi: 10.3389/fcimb.2020.607650

Gao, P., Ji, M., Liu, X., Chen, X., Liu, H., Li, S., et al. (2022). Apolipoprotein e mediates cell resistance to influenza virus infection. *Sci. Adv.* 8, eabm6668. doi: 10.1126/sciadv.abm6668

Getz, G. S., and Reardon, C. A. (2018). Apoprotein e and reverse cholesterol transport. *Int. J. Mol. Sci.* 19, 3479. doi: 10.3390/ijms19113479

Gong, Y., and Cun, W. (2019). The role of ApoE in HCV infection and comorbidity. *Int. J. Mol. Sci.* 20, 2037. doi: 10.3390/ijms20082037

Hubler, M. J., and Kennedy, A. J. (2016). Role of lipids in the metabolism and activation of immune cells. *J. Nutr. Biochem.* 34, 1–7. doi: 10.1016/j.jnutbio.2015.11.002

Hui, B., Lu, C., Li, H., Hao, X., Liu, H., Zhuo, D., et al. (2022). Inhibition of APOE potentiates immune checkpoint therapy for cancer. *Int. J. Biol. Sci.* 18, 5230–5240. doi: 10.7150/ijbs.70117

Korhonen, J. T., Olkkonen, V. M., Lahesmaa, R., and Puolakkainen, M. (2013). ABC-Cassette transporter 1 (ABCA1) expression in epithelial cells in chlamydia pneumoniae infection. *Microbial Pathogenesis.* 61–62, 57–61. doi: 10.1016/j.micpath.2013.05.006

Li, X., Zhang, J., Li, D., He, C., He, K., Xue, T., et al. (2021). Astrocytic ApoE reprograms neuronal cholesterol metabolism and histone-acetylation-mediated memory. *Neuron.* 109, 957–970.e8. doi: 10.1016/j.neuron.2021.01.005

Lin, Y., Su, J., Wang, Y., Xu, D., Zhang, X., and Yu, B. (2021). mRNA transcriptome analysis of bone in a mouse model of implant-associated staphylococcus aureus osteomyelitis. *Infect. Immun.* 89, e00814–e00820. doi: 10.1128/IAI.00814-20

Loeuillard, E., Yang, J., Buckarma, E., Wang, J., Liu, Y., Conboy, C., et al. (2020). Targeting tumor-associated macrophages and granulocytic myeloid-derived suppressor cells augments PD-1 blockade in cholangiocarcinoma. *J. Clin. Invest.* 130, 5380–5396. doi: 10.1172/JCI137110

Masters, E. A., Ricciardi, B. F., Bentley, K. L., de, M., Moriarty, T. F., Schwarz, E. M., et al. (2022). Skeletal infections: microbial pathogenesis, immunity and clinical management. *Nat. Rev. Microbiol.* 20, 385–400. doi: 10.1038/s41579-022-00686-0

McDonough, J. A., Newton, H. J., Klum, S., Swiss, R., Agaisse, H., and Roy, C. R. (2013). Host pathways important for coxiella burnetii infection revealed by genome-wide RNA interference screening. *mBio.* 4, e00606–e00612. doi: 10.1128/mBio.00606-12

Metsemakers, W. J., Kuehl, R., Moriarty, T. F., Richards, R. G., Verhofstad, M. H. J., Borens, O., et al. (2018). Infection after fracture fixation: current surgical and microbiological concepts. *Injury.* 49, 511–522. doi: 10.1016/j.injury.2016.09.019

Miao, G., Zhuo, D., Han, X., Yao, W., Liu, C., Liu, H., et al. (2023). From degenerative disease to malignant tumors: insight to the function of ApoE. *Biomedicine Pharmacotherapy.* 158, 114127. doi: 10.1016/j.biopha.2022.114127

Nowosielski, M., Hoffmann, M., Wyrwicz, L. S., Stepniak, P., Plewczynski, D. M., Lazniewski, M., et al. (2011). Detailed mechanism of squalene epoxidase inhibition by terbinafine. *J. Chem. Inf Model.* 51, 455–462. doi: 10.1021/ci100403b

Ohshiro, T., Matsuda, D., Sakai, K., Degirolamo, C., Yagyu, H., Rudel, L. L., et al. (2011). Pyripyropene a, an acyl–coenzyme a: cholesterol acyltransferase 2–selective inhibitor, attenuates hypercholesterolemia and atherosclerosis in murine models of hyperlipidemia. *ATVB.* 31, 1108–1115. doi: 10.1161/ATVBAHA.111.223552

O'Rourke, S. A., Neto, N. G. B., Devilly, E., Shanley, L. C., Fitzgerald, H. K., Monaghan, M. G., et al. (2022). Cholesterol crystals drive metabolic reprogramming and M1 macrophage polarisation in primary human macrophages. *Atherosclerosis.* 352, 35–45. doi: 10.1016/j.atherosclerosis.2022.05.015

Ozinsky, A., Underhill, D. M., Fontenot, J. D., Hajjar, A. M., Smith, K. D., Wilson, C. B., et al. (2000). The repertoire for pattern recognition of pathogens by the innate immune system is defined by cooperation between toll-like receptors. *Proc. Natl. Acad. Sci. U S A.* 97, 13766–13771. doi: 10.1073/pnas.250476497

Potter, A. D., Butrico, C. E., Ford, C. A., Curry, J. M., Trenary, I. A., Tummarakota, S. S., et al. (2020). Host nutrient milieu drives an essential role for aspartate biosynthesis during invasive staphylococcus aureus infection. *Proc. Natl. Acad. Sci. U S A.* 117, 12394–12401. doi: 10.1073/pnas.1922211117

Raineri, E. J. M., Altulea, D., and van Dijl, J. M. (2022). Staphylococcal trafficking and infection-from "nose to gut" and back. *FEMS Microbiol. Rev.* 46, fuab041. doi: 10.1093/femsre/fuab041

Ren, Q., Robertson, S. J., Howe, D., Barrows, L. F., and Heinzen, R. A. (2003). Comparative DNA microarray analysis of host cell transcriptional responses to infection by coxiella burnetii or chlamydia trachomatis. *Ann. N Y Acad. Sci.* 990, 701–713. doi: 10.1111/j.1749-6632.2003.tb07447.x

Russell, D. G., Huang, L., and VanderVen, B. C. (2019). Immunometabolism at the interface between macrophages and pathogens. *Nat. Rev. Immunol.* 19, 291–304. doi: 10.1038/s41577-019-0124-9

Samanta, D., Mulye, M., Clemente, T. M., Justis, A. V., and Gilk, S. D. (2017). Manipulation of host cholesterol by obligate intracellular bacteria. *Front. Cell. Infect. Microbiol.* 7. doi: 10.3389/fcimb.2017.00165

Schwarz, E. M., Parvizi, J., Gehrke, T., Aiyer, A., Battenberg, A., Brown, S. A., et al. (2019). 2018 international consensus meeting on musculoskeletal infection: research priorities from the general assembly questions. *J. Orthop Res.* 37, 997–1006. doi: 10.1002/jor.24293

Sheedy, F. J., Grebe, A., Rayner, K. J., Kalantari, P., Ramkhelawon, B., Carpenter, S. B., et al. (2013). CD36 coordinates NLRP3 inflammasome activation by facilitating intracellular nucleation of soluble ligands into particulate ligands in sterile inflammation. *Nat. Immunol.* 14, 812–820. doi: 10.1038/ni.2639

Siddiqui, R., Suzu, S., Ueno, M., Nasser, H., Koba, R., Bhuyan, F., et al. (2018). Apolipoprotein e is an HIV-1-inducible inhibitor of viral production and infectivity in macrophages. *PloS Pathog.* 14, e1007372. doi: 10.1371/journal.ppat.1007372

Smeltzer, M. S., Thomas, J. R., Hickraon, S. G., Skinner, R. A., Nelson, C. L., Griffith, D., et al. (1997). Characterization of a rabbit model of staphylococcal osteomyelitis. *J. Orthopaedic Res.* 15, 414–421. doi: 10.1002/jor.1100150314

Soh, K. Y., Loh, J. M. S., and Proft, T. (2020). Cell wall-anchored 5'-nucleotidases in gram-positive cocci. *Mol. Microbiol.* 113, 691–698. doi: 10.1111/mmi.14442

Takeda, K., Kaisho, T., and Akira, S. (2003). Toll-like receptors. *Annu. Rev. Immunol.* 21, 335–376. doi: 10.1146/annurev.immunol.21.120601.141126

Tavazoie, M. F., Pollack, I., Tanqueco, R., Ostendorf, B. N., Reis, B. S., Gonsalves, F. C., et al. (2018). LXR/ApoE activation restricts innate immune suppression in cancer. *Cell.* 172, 825–840.e18. doi: 10.1016/j.cell.2017.12.026

Tenger, C., and Zhou, X. (2003). Apolipoprotein e modulates immune activation by acting on the antigen-presenting cell. *Immunology.* 109, 392–397. doi: 10.1046/j.1365-2567.2003.01665.x

Wang, Q., Huang, J., Li., S., Zhang, Y., Sun., R., Ren., J., et al. (2022). Fermentation supernatant of staphylococcus aureus drives catabolism in chondrocytes via NF-κB signaling mediated increase of cholesterol metabolism. *Exp. Cell Res.* 410(1):112952. doi: 10.1016/j.yexcr.2021.112952

West, A. P., Brodsky, I. E., Rahner, C., Woo, D. K., Erdjument-Bromage, H., Tempst, P., et al. (2011). TLR signalling augments macrophage bactericidal activity through mitochondrial ROS. *Nature.* 472, 476–480. doi: 10.1038/nature09973

Wynn, T. A., Chawla, A., and Pollard, J. W. (2013). Macrophage biology in development, homeostasis and disease. *Nature.* 496, 445–455. doi: 10.1038/nature12034

Xiao, J., Li, W., Zheng, X., Qi, L., Wang, H., Zhang, C., et al. (2020). Targeting 7-dehydrocholesterol reductase integrates cholesterol metabolism and IRF3 activation to eliminate infection. *Immunity.* 52, 109–122.e6. doi: 10.1016/j.immuni.2019.11.015

Zhang, S. H., Reddick, R. L., Piedrahita, J. A., and Maeda, N. (1992). Spontaneous hypercholesterolemia and arterial lesions in mice lacking apolipoprotein e. *Science.* 258, 468–471. doi: 10.1126/science.1411543

Zhao, G., Mo, Z.-C., Tang, S.-L., Ouyang, X.-P., He, P., Lv, Y., et al. (2014). Chlamydia pneumoniae negatively regulates ABCA1 expression via TLR2-nuclear factor-kappa b and miR-33 pathways in THP-1 macrophage-derived foam cells. *Atherosclerosis.* 235, 519–525. doi: 10.1016/j.atherosclerosis.2014.05.943

Zhu, Y., Nwabuisi-Heath, E., Dumanis, S. B., Tai, L. M., Yu, C., Rebeck, G. W., et al. (2012). APOE genotype alters glial activation and loss of synaptic markers in mice. *Glia.* 60, 559–569. doi: 10.1002/glia.22289

frontiers | Frontiers in Cellular and Infection Microbiology

TYPE Original Research
PUBLISHED 03 August 2023
DOI 10.3389/fcimb.2023.1220456

OPEN ACCESS

EDITED BY
Hongyi Shao,
Beijing Jishuitan Hospital, China

REVIEWED BY
Andreas G. Tsantes,
National and Kapodistrian University of Athens, Greece
Yang Lv,
Peking University Third Hospital, China

*CORRESPONDENCE
Mingxing Tang
Tangmingxing2018@163.com

RECEIVED 10 May 2023
ACCEPTED 20 July 2023
PUBLISHED 03 August 2023

CITATION
Xu D, Hu X, Zhang H, Gao Q, Guo C, Liu S, Tang B, Zhang G, Zhang C and Tang M (2023) Analysis of risk factors for deep vein thrombosis after spinal infection surgery and construction of a nomogram preoperative prediction model. *Front. Cell. Infect. Microbiol.* 13:1220456. doi: 10.3389/fcimb.2023.1220456

Analysis of risk factors for deep vein thrombosis after spinal infection surgery and construction of a nomogram preoperative prediction model

Dongcheng Xu[1,2], Xiaojiang Hu[1,2], Hongqi Zhang[1,2], Qile Gao[1,2], Chaofeng Guo[1,2], Shaohua Liu[1,2], Bo Tang[1,2], Guang Zhang[1,2], Chengran Zhang[1,2] and Mingxing Tang[1,2]*

[1]Department of Spine Surgery and Orthopaedics, Xiangya Hospital, Central South University, Changsha, China, [2]China for Geriatric Disorders, Xiangya Hospital, Central South University, Changsha, China

Objective: To investigate the differences in postoperative deep venous thrombosis (DVT) between patients with spinal infection and those with non-infected spinal disease; to construct a clinical prediction model using patients' preoperative clinical information and routine laboratory indicators to predict the likelihood of DVT after surgery.

Method: According to the inclusion criteria, 314 cases of spinal infection (SINF) and 314 cases of non-infected spinal disease (NSINF) were collected from January 1, 2016 to December 31, 2021 at Xiangya Hospital, Central South University, and the differences between the two groups in terms of postoperative DVT were analyzed by chi-square test. The spinal infection cases were divided into a thrombotic group (DVT) and a non-thrombotic group (NDVT) according to whether they developed DVT after surgery. Pre-operative clinical information and routine laboratory indicators of patients in the DVT and NDVT groups were used to compare the differences between groups for each variable, and variables with predictive significance were screened out by least absolute shrinkage and operator selection (LASSO) regression analysis, and a predictive model and nomogram of postoperative DVT was established using multi-factor logistic regression, with a Hosmer- Lemeshow goodness-of-fit test was used to plot the calibration curve of the model, and the predictive effect of the model was evaluated by the area under the ROC curve (AUC).

Result: The incidence of postoperative DVT in patients with spinal infection was 28%, significantly higher than 16% in the NSINF group, and statistically different from the NSINF group ($P < 0.000$). Five predictor variables for postoperative DVT in patients with spinal infection were screened by LASSO regression, and plotted as a nomogram. Calibration curves showed that the model was a good fit. The AUC of the predicted model was 0.8457 in the training cohort and 0.7917 in the validation cohort.

Conclusion: In this study, a nomogram prediction model was developed for predicting postoperative DVT in patients with spinal infection. The nomogram included five preoperative predictor variables, which would effectively predict the likelihood of DVT after spinal infection and may have greater clinical value for the treatment and prevention of postoperative DVT.

KEYWORDS

spine, infection, deep vein thrombosis, risk factors, predictive model, LASSO, nomogram, mNGS (metagenomic next-generation sequencing)

1 Introduction

Spinal infection is a rare disease. Its incidence rate is 0.001% ~0.004% and its estimated mortality rate ranges between 2 and 4% (Duarte and Vaccaro, 2013). In recent years, the incidence rate and mortality rate of spinal infection is on the rise (Babic and Simpfendorfer, 2017; Sato et al., 2019). The main reason of spinal infection is the colonization of pathogens in the spine, and its pathogens mainly include various bacteria and viruses. Diagnosis of spinal infection is mainly based on clinical symptoms and signs, laboratory tests and imaging examinations. Routine microbial culture as direct evidence for infection diagnosis is the gold standard for diagnosis of spinal infection (Urrutia and Bono, 2022). Antibiotics are the main treatment for spinal infection. Surgical treatment should be used for patients with severe illness and no significant improvement (Herren et al., 2017; Scheyerer et al., 2022).

Deep venous thrombosis (DVT) is a well-known and feared surgical complication, as well as a leading cause of death. The incidence of venous thrombosis following spinal surgery varies between 0.31% and 31%. DVT may result in substantial morbidity, poor quality of life, and even death. It may also lead to increased medical costs and a considerable financial burden on individuals and their families (Wang and Wu, 2022). Studies have showed that risk factors for venous thrombosis following spinal surgery are associated with high age, female, spinal fusion, big volume blood loss patients, operation time, and hypertension, diabetes, and walking issue. A series of risk prediction models for deep venous thrombosis after surgery for patients with spinal surgery and fracture (Cheng et al., 2022; Hu et al., 2022; Yan et al., 2022).

Recently, the association between infection and venous thrombosis has long been recognized (Colling et al., 2021). Systemic or localized infections increase the risk of thrombosis about 2~20 times and are independent risk factors for thromboembolic diseases (Beristain-Covarrubias et al., 2019). Neutrophils, monocytes, and platelets interact with each other and the endothelium in host defense and also play critical roles in the formation of venous thromboembolism (Beristain-Covarrubias et al., 2019; Colling et al., 2021). However, clinical research on thrombosis after spinal infection surgery has not received much attention yet. It is generally believed that the incidence of thrombosis should be higher than that of a single spinal surgery or infection. Study has showed that patients with spine infections requiring irrigation and débridement may be at considerably increased risk for DVT. Lambrechts MJ et al. found that 14.3% of patients undergoing spine irrigation and débridement with subsequent peripherally inserted central catheter (PICC) placement developed postoperative DVT (Lambrechts et al., 2022). In this study, we compared the incidence of DVT after surgery for spinal infection, analysed the risk factors for DVT after surgery for spinal infection, screened the predictor variables by LASSO regression and developed a predictive model for the prediction of postoperative DVT in patients with spinal infection.

2 Method

2.1 Study subjects

314 cases of spinal infection from January 2016 to December 2021 were collected from Xiangya Hospital of Central South University; 314 cases of non-infected spinal disease from January 2016 to December 2021 were randomly selected from Xiangya Hospital of Central South University. The spinal infection cases included 126 cases tested by metagenomic next-generation sequencing (mNGS). Ethical approval: Institutional ethics review board approval was obtained (IRB#: 201303232). This study was approved by the Ethics Committee of Xiangya Hospital Central South University.

2.1.1 Inclusion criteria

Inclusion criteria for spinal infection cases: (1) complete clinical information, including gender, age and temperature; (2) routine preoperative laboratory indices; (3) patients treated surgically; (4) lesion specimens identified as pathogenic microbial infections by pathological examination, bacterial culture and staining, DNA testing of Mycobacterium tuberculosis flora and macrogenome sequencing; (5) postoperative vascular ultrasound results of both lower limbs.

Inclusion criteria for non-infected spinal disease cases: (1) complete clinical information, including gender and age; (2)

patients were treated surgically; (3) patients did not have infectious diseases or signs of infection (e.g. fever, elevated blood count, etc.); (4) postoperative vascular ultrasound findings in both lower limbs.

2.1.2 Exclusion criteria

Patients meeting the following criteria will be excluded: (1) patients with infections elsewhere in the body; (2) patients with previous bleeding disorders (e.g. haemophilia, thrombocytopenic purpura, etc.) or vascular disorders (e.g. varicose veins, thrombophlebitis, etc.) (Boender et al., 2016; Chang et al., 2018); (3)Patients treated with preoperative anticoagulation or antiplatelet drugs; (4) patients with preoperative tests suggestive of DVT; (5) patients with critical multi-organ failure; (6) patients with malignancies (Falanga et al., 2013; Falanga et al., 2015).

2.2 Research methods

2.2.1 Pathogenic microbial detection methods

One of the following diagnostic criteria can be met: (1) pathological examination of the spinal lesion suggests a spinal infection (including inflammatory lesions, septicemia, etc.); (2) bacterial culture or staining of the spinal lesion detects bacteria or fungi (Berbari et al., 2015); (3) mNGS of the spinal lesion (Xu et al., 2022): high quality sequences are screened by FastQC software, removing sequences with connectors, low quality bases and too short (<50bp) sequences. BowtiE2 was used for inter-sequence comparison and to remove host-associated reads. The processed sequences were compared with the Guangzhou Sage pathogenic microbial database for BWA analysis to obtain the number of detected sequences of pathogenic microorganisms; (4) positive spinal lesions for Mycobacterium tuberculosis cluster DNA detection (Xpert MTB/RIF) (Dorman et al., 2018).

2.2.2 Routine laboratory test result data collection

Patient's preoperative platelet (PLT), plateletcrit (PCT), prothrombin time (PT), activeated partial thromboplastin time (APTT), international normalized ratio (INR), D-dimer (DD), white blood cell (WBC), red blood cell (RBC), hemoglobin (HGB), neutrophil (Neut), lymphocyte (Lymph), eosinophil (EO), basophil (BASO), monocyte (Mono), neutrophil% (Neut%), lymphocyte% (Lymph%), basophil% (BASO%), eosinophil% (EO %), monocyte% (Mono%), red blood cell distribution width (RDW), mean platelet volume (MPV), total protein (TP), albumin (A), globulin (G), albumin to globulin ratio (A/G), alanine transaminase (ALT), aspartate transaminase (AST), blood urea nitrogen (BUN), creatinine (Cr), triglyceride (TG), cholesterol (Chol), high density lipoprotein (HDL), low density lipoprotein (LDL), glucose (GLU), erythrocyte sedimentation rate (ESR), C-reactive protein (CRP), procalcitonin (PCT).

2.2.3 DVT diagnostic criteria

The diagnosis was confirmed on the basis of postoperative vascular ultrasound findings in both lower limbs (Lim et al., 2018).

2.3 Statistical methods

Measures that conformed to a normal distribution were described using the mean ± standard deviation and t-tests for two independent samples were used for comparisons between groups. Measures that did not conform to a normal distribution were described using the median and percentile, and comparisons between groups were made using a non-parametric test. The chi-square test was used for inter-group comparisons of the count data. Predictors were screened using the least absolute shrinkage and operator selection (LASSO) regression technique, and postoperative D-dimer prediction models and column line plots (nomograms) were developed using multifactorial logistic regression. The calibration curve of the model was plotted using the Hosmer-Lemeshow goodness-of-fit test. The predictive effect of the model was evaluated by calculating the area under the ROC curve (AUC). 60% of spinal infection cases were randomly selected as the training set and the remaining spinal infection cases were included in the validation set for internal validation of the prediction model. Statistical analyses and image plotting were performed using R software (version 4.2.2; R Foundation for Statistical Computing, Vienna, Austria) and differences were considered statistically significant when $p<0.05$.

3 Result

A total of 314 cases of all patients with spinal infection (SINF) and 314 cases of randomly selected patients with non-infected spinal disease (NSINF) who met the inclusion criteria and were admitted to Xiangya Hospital of Central South University from 1 January 2016 to 31 December 2021 were included in the study. The general data of patients in the SINF and NSINF groups are analysed in Table 1. There was no statistical difference in age and gender between the SINF and NSINF, The results of the chi-square test for

TABLE 1 Characteristics of the clinical data of each group of patients.

Variables	SINF (n=314)	NSINF (n=314)	p value
Age, years	55 (46.25, 64)	54 (46, 63)	0.453
Gender, n (%)			0.936
female	132 (42)	133 (42)	
male	182 (58)	181 (58)	

postoperative DVT between the SINF and NSINF groups are shown in Table 2. There was a significant difference in the incidence of postoperative DVT between the two groups ($p < 0.000$), and the incidence of postoperative DVT was significantly higher in SINF than in NSINF.

The SINF consisted of 126 cases tested by mNGS, including 110 bacterial infections (including 28 tuberculosis infections and 9 brucellosis infections), 6 fungal infections, 5 viral infections, 2 rickettsial infections, 1 mycoplasma infection and 2 undetected cases. See Supplementary Information for specific microbial species.

The SINF cases were divided into a thrombotic group (DVT) and a non-thrombotic group (NDVT) based on postoperative lower limb vascular ultrasound findings. There were 89 patients in the DVT and 225 patients in the NDVT. The general data and each preoperative serological index of the two groups are shown in Table 3. The two groups differed in Age, T, PCT, Plateletcrit, MPV, A, AG and APTT ($p<0.05$). In this study, univariate ROC curves were plotted by these variables (Figure 1A) and their AUC results were plotted (Figure 1B).

In this study, five non-zero coefficient variables (Figure 2), including Plateletcrit, MPV, APTT, T and Age, were selected from 40 variables in patients with spinal infection by LASSO regression, and the corresponding postoperative DVT prediction model was developed by multifactorial logistic regression analysis based on these five variables. In this study, a nomogram of postoperative DVT in patients with spinal infection (Figure 3) was constructed based on the prediction model, and the results of the prediction model were presented visually to facilitate the preoperative assessment of patients with spinal infection.

The Hosmer-Lemeshow goodness of fit test (Figure 4A) shows a good fit between the nomogram predicted probabilities and the actual probabilities. This indicates that there is no deviation from a perfect fit between the predicted and observed values. In addition, this study plotted the ROC curve for the model, which had an AUC of 0.8457 (Figure 4B) in the training cohort and 0.7917 (Figure 4C) in the validation cohort.

4 Discussion

In this study, a clinical prediction model for postoperative DVT in patients with spinal infection was developed using LASSO regression and visualised by nomogram. The nomogram had five preoperative predictor variables including Plateletcrit, MPV, APTT, T and Age. The goodness of fit test shows a good fit between the nomogram predicted probabilities and the actual probabilities. In addition, the ROC curve of the model was plotted in this study. Its AUC was 0.8457 in the training cohort and 0.7917 in the validation cohort. The prediction model nomogram showed good preoperative predictive ability and clinical value.

In recent years, with the progression of an ageing population and the misuse of antibiotics, there has been an upward trend in the incidence of spinal infections (Babic and Simpfendorfer, 2017; Dunn and Ben Husien, 2018), particularly with various drug-resistant bacterial infections, leading to an increased probability of serious complications. Patients with spinal infections who experience spinal bone destruction often experience skeletal related events (SREs) such as severe bone pain, pathological fractures, spinal cord compression and hypercalcaemia. Surgical treatment is usually required in this case. DVT is one of the most common complications of surgery and one of the most common causes of death in surgical patients (Blitzer and Eisenstein, 2021). Numerous studies have shown that the incidence of postoperative venous thromboembolism is significantly higher in surgical patients than preoperatively (Zhang et al., 2021; Jiang et al., 2022). Patients undergoing spinal surgery are more likely to develop postoperative DVT due to the need for prolonged bed rest after surgery, as evidenced by the study by Hengyan Zhang et al. (2021). The occurrence of postoperative DVT in patients has been associated with several preoperative factors, such as advanced age and infection. Studies have shown that infection is an important factor influencing the development of DVT, and that the dysfunction of haemostasis and vascular barrier dysfunction caused by infection promotes thrombosis (Colling et al., 2021). In this study, 314 SINF and 314 NSINF cases were included. There were no significant differences between SINF and NSINF in terms of age and gender, while there were statistically significant differences in terms of postoperative DVT. Therefore, for patients with spinal infection, the likelihood of postoperative DVT would be significantly increased.

This study included 126 cases that were tested for mNGS. The 2018 guidelines of the Infectious Diseases Society of America and the American Society for Microbiology continue to use microbiological culture of spinal lesions as a criterion for laboratory diagnosis of spinal infections (Miller et al., 2018). However, studies have shown that positive microbial cultures of spinal infection lesions are low (Zhang et al., 2023), making it difficult to meet clinical diagnostic needs, and the long culture period for some microorganisms (e.g. Mycobacterium tuberculosis) may lead to delays in treatment. mNGS is extremely sensitive and

TABLE 2 Results of the chi-square test analysis of postoperative DVT for each group of patients.

Group	DVT, n (%)		Total	χ^2	p value
	positive	negative			
SINF group	89 (28)	225 (72)	314	14.053	< 0.000
NSINF group	50 (16)	264 (84)	314		
Total	139 (22)	489 (78)	628		

10.3389/fcimb.2023.1220456

TABLE 3 Univariate analysis of patients and variables for spinal infection cases.

Variables	Total (n = 314)	NDVT (n = 225)	DVT (n = 89)	p value
Gender, n (%)				0.983
female	132 (42)	94 (42)	38 (43)	
male	182 (58)	131 (58)	51 (57)	
Age, years	55 (46.25, 64)	53 (44, 63)	60 (53, 69)	< 0.001
T, °C	36.6 (36.5, 36.8)	36.5 (36.5, 36.8)	36.6 (36.6, 36.9)	< 0.001
WBC, 10^9/L	6.25 (4.8, 7.7)	6.3 (5, 7.7)	6.2 (4.5, 7.7)	0.146
RBC, 10^12/L	4.07 ± 0.6	4.08 ± 0.63	4.06 ± 0.51	0.836
HGB, g/L	117 (106.25, 132)	117 (105, 132)	119 (108, 133)	0.249
PLT, 10^9/L	241 (188.25, 310.75)	253 (190, 323)	225 (184, 277)	0.046
Neut, 10^9/L	4 (3, 5.4)	4 (3, 5.5)	3.8 (2.9, 5)	0.339
Lymph, 10^9/L	1.31 (1, 1.79)	1.4 (1, 1.7)	1.3 (0.9, 1.8)	0.332
EO, 10^9/L	0.1 (0.08, 0.2)	0.1 (0.08, 0.2)	0.1 (0.1, 0.2)	0.566
BASO, 10^9/L	0 (0, 0.03)	0 (0, 0.03)	0 (0, 0.02)	0.328
Mono, 10^9/L	0.5 (0.4, 0.7)	0.5 (0.4, 0.7)	0.5 (0.4, 0.7)	0.917
Neut%, %	65.85 (58.82, 72.1)	66 (58.3, 72.5)	65.6 (60.5, 70.9)	0.855
Lymph%, %	21.65 (16.72, 27.6)	21.8 (16.8, 27.9)	21.5 (16.7, 26.3)	0.486
BASO%, %	0.5 (0.3, 0.7)	0.5 (0.3, 0.6)	0.5 (0.3, 0.7)	0.325
EO%, %	1.8 (0.9, 3.2)	1.7 (0.9, 3.1)	2 (1.1, 3.3)	0.27
Mono%, %	8.8 (7.2, 10.5)	8.8 (6.8, 10.5)	8.8 (7.6, 10.3)	0.27
RDW, %	13.8 (12.9, 14.8)	13.8 (12.9, 14.9)	14.1 (13.1, 14.7)	0.266
Plateletcrit*, %	0.2 (0.16, 0.26)	0.22 (0.17, 0.28)	0.17 (0.14, 0.2)	< 0.001
MPV, fL	8.35 (7.52, 9.5)	8.71 (7.76, 9.9)	7.81 (6.8, 8.35)	< 0.001
TP, g/L	69.83 ± 6.72	70.26 ± 6.77	68.73 ± 6.52	0.066
A, g/L	36.86 ± 4.47	37.43 ± 4.48	35.4 ± 4.12	< 0.001
G, g/L	32.4 (28.6, 36.9)	32.7 (28, 36.9)	31.8 (29.3, 36.9)	0.773
A/G	1.15 (0.97, 1.31)	1.2 (1, 1.4)	1.07 (0.91, 1.29)	0.029
ALT, U/L	17.8 (11.4, 28.25)	17.9 (11.9, 28.6)	17.3 (10.3, 27.7)	0.296
AST, U/L	21.1 (16.8, 29.7)	21 (17.1, 30.3)	21.6 (16.5, 27)	0.424
BUN, mmol/L	4.85 (3.81, 6.12)	4.68 (3.81, 5.98)	5 (3.82, 6.35)	0.333
Cr, mmol/L	72 (61, 82.2)	72 (61, 82.2)	72.4 (62, 82.2)	0.430
TG, mmol/L	1.23 (0.88, 1.65)	1.23 (0.86, 1.68)	1.25 (0.95, 1.62)	0.729
Chol, mmol/L	4.26 (3.6, 5.07)	4.21 (3.58, 4.94)	4.36 (3.7, 5.14)	0.299
HDL, mmol/L	1.02 (0.86, 1.21)	1.02 (0.87, 1.2)	1.01 (0.85, 1.23)	0.706
LDL, mmol/L	2.68 (2.25, 3.24)	2.67 (2.2, 3.25)	2.73 (2.32, 3.19)	0.491
GLU, mmol/L	5.19 (4.77, 5.8)	5.23 (4.74, 5.88)	5.16 (4.8, 5.61)	0.446
PT, s	12.8 (12, 13.7)	12.7 (12, 13.7)	12.9 (12, 13.7)	0.695
APTT, s	32.6 (29.2, 36.35)	32.9 (29.4, 36.9)	31.2 (28.7, 35.3)	0.044
INR	1.02 (0.96, 1.09)	1.02 (0.96, 1.09)	1.02 (0.96, 1.09)	0.951
DD, mg/L	0.3 (0.17, 0.54)	0.3 (0.17, 0.52)	0.29 (0.19, 0.57)	0.493

(Continued)

TABLE 3 Continued

Variables	Total (n = 314)	NDVT (n = 225)	DVT (n = 89)	p value
ESR, mm/h	70.5 (40.25, 103.75)	70 (38, 105)	71 (51, 102)	0.561
CRP, mg/L	17.3 (6.65, 41.88)	17.3 (6.57, 42.2)	17.5 (6.81, 37.4)	0.755
Procalcitonin**, n (%)				0.337
negative	226 (72)	158 (70)	68 (76)	
positive	88 (28)	67 (30)	21 (24)	

*Plateletcrit (PCT) and Procalcitonin (PCT) have the same abbreviation, so their full names are used in this study.
**The Procalcitonin is defined as a count data because there are multiple clinical assays with different normal values between methods.

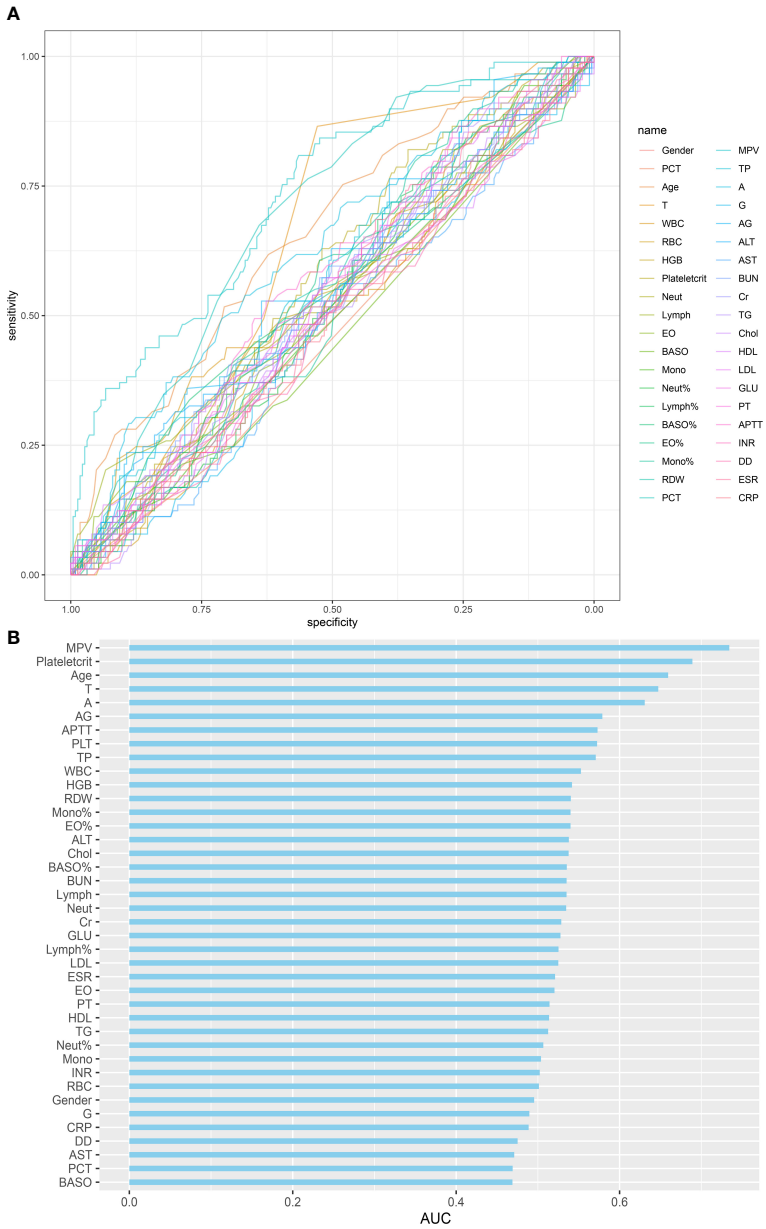

FIGURE 1
Single variables on DVT predictive capability: **(A)** ROC curve of single variables on DVT prediction; **(B)** AUC of single variables for DVT prediction.

10.3389/fcimb.2023.1220456

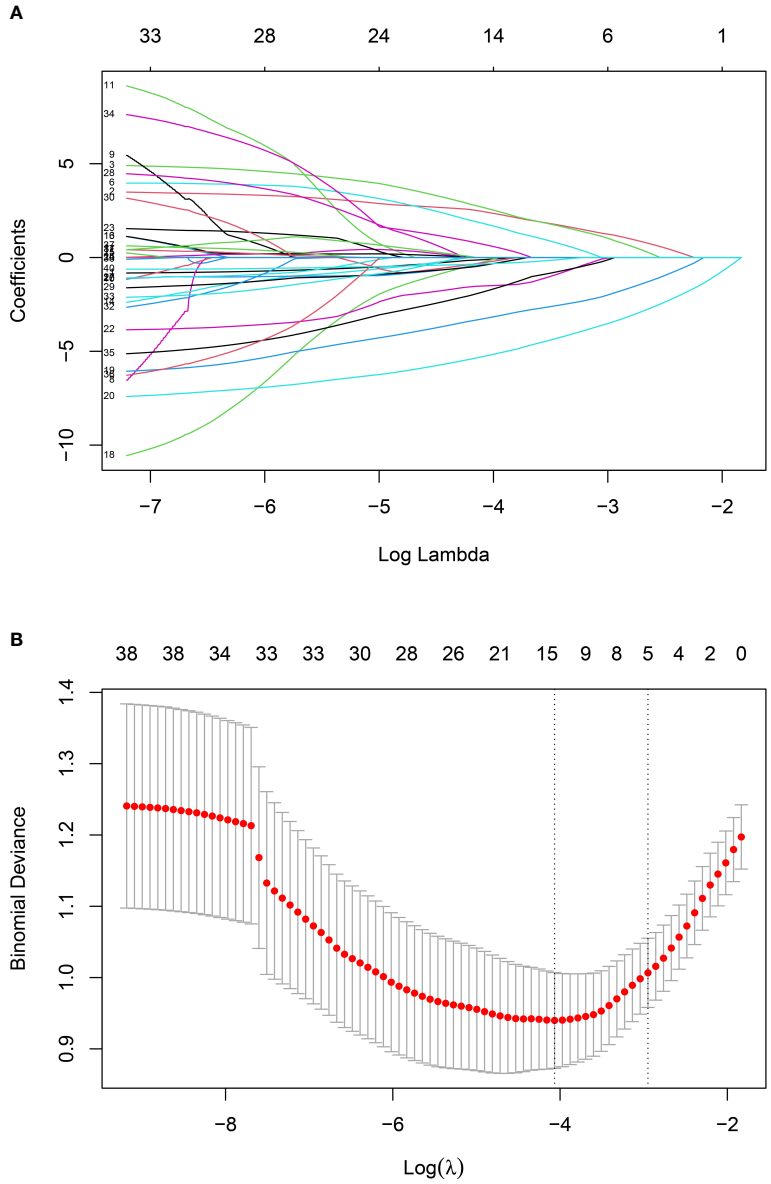

FIGURE 2
Screening variables by LASSO regression: **(A)** LASSO regression model graph. In this study, five non-zero coefficients were screened using Lambda.min as the criterion.; **(B)** Lambda (adjustment parameter) was obtained by cross-validated LASSO regression. The left dashed line is Lambda at minimum error (Lambda.min), the right dashed line is Lambda at standard error (Lambda.1-SE).

specific for the detection of pathogenic microorganisms (Zhang et al., 2023), and with advances in technology, a rapid 50-minute median time mNGS assays (Gu et al., 2021). Therefore, mNGS may become an effective clinical tool for accurate and rapid diagnosis of infections.

In this study, a total of 314 patients with spinal infections were included. They were divided into 89 cases of DVT and 225 cases of NDVT according to the results of the vascular ultrasound of both lower limbs. univariate analysis of 40 preoperative data from both groups showed significant differences in Age, T, PLT, Plateletcrit, MPV, A, AG and APTT. By plotting ROC curves and calculating AUC, we found that all individual variables did not show significant value for predicting DVT (AUC < 0.75), suggesting that a single variable is difficult to accurately predict the likelihood of postoperative DVT. Therefore, to more accurately predict postoperative DVT, this study used LASSO regression to screen out five variables, including Plateletcrit, MPV, APTT, T and Age, and construct a DVT prediction model by logistic regression. The model achieved an AUC of 0.8457 in the training cohort and 0.7917 in the validation cohort, indicating that the model has relatively good predictive value. The fitted curves also showed a good fit. This study found that a decrease in preoperative Plateletcrit, MPV and APTT levels predicted an increased likelihood of DVT in patients postoperatively, while an increase in T and Age predicted an increased likelihood of DVT in patients postoperatively.

Marina Panova-Noeva et al. observed that MPV was lower in cases where thrombosis occurred compared to controls (Panova-Noeva et al., 2020), a phenomenon that has been validated in other

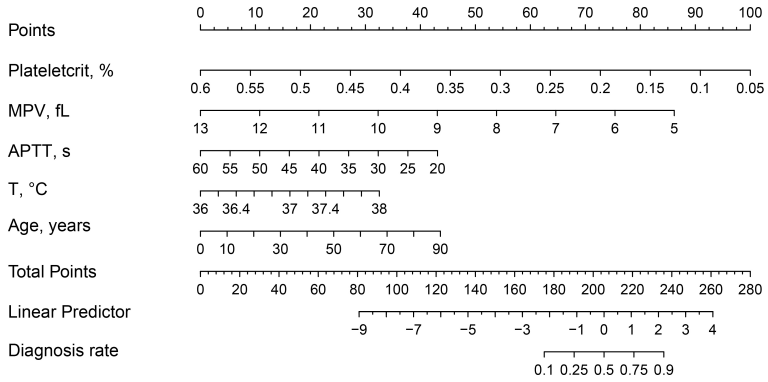

FIGURE 3
Nomogram and scoring method for postoperative DVT in patients with spinal infection. The corresponding score (top line) is found according to the value of each predictor variable (the line after each variable), then the values of the individual scores are summed to obtain the total score, and the corresponding predicted probability is based on the total score(bottom line).

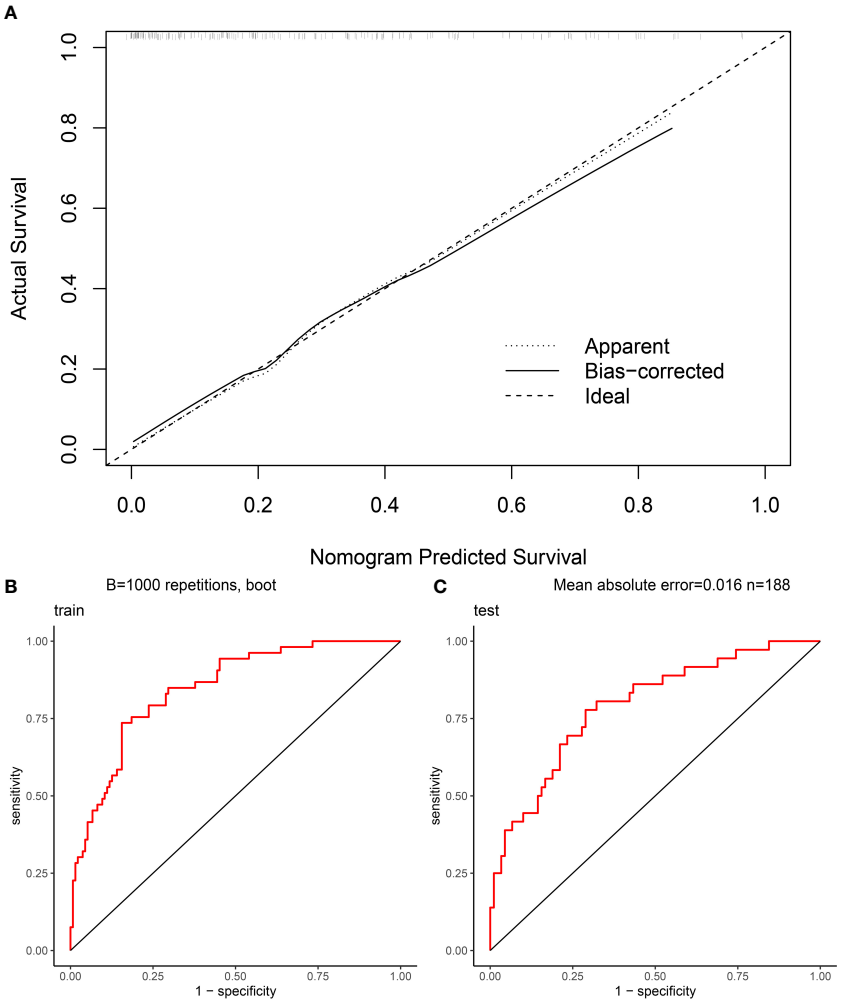

FIGURE 4
Evaluation of nomogram clinical prediction model: **(A)** Calibration curve of the model; **(B)** ROC curve of the model for the training cohort, and its AUC was 0.8457; **(C)** ROC curve of the model for the validation cohort, and its AUC was 0.7917.

studies on thrombosis (Lippi et al., 2016; Braester et al., 2021). In infectious diseases, MPV levels can help to indicate the onset of inflammation. For example, in cases of acute appendicitis, MPV levels were significantly lower than in controls (Fan et al., 2017). Plateletcrit, which is the percentage of platelet volume in peripheral blood to whole blood volume, is the product of PLT and MPV, and decreased levels of Plateletcrit have been suggested to be associated with sepsis and poor prognosis in systemic inflammatory diseases in established studies (Sayed et al., 2020; Yardımcı et al., 2021). Shortening of APTT as an indicator of coagulation is usually indicative of a hypercoagulable state, and APTT light transmission waveform analysis is currently used by some investigators as a tool to detect infection and assess its prognosis (Chopin et al., 2006). The correlation between fever and infection has been well documented (Lu et al., 2015), and clinically, in non-serious patients, an increase in temperature is also often indicative of the onset or exacerbation of infection. A clinical trial has shown that fever is common in patients with DVT and has a worse prognosis (Barba et al., 2011). Advanced age is known to be an independent risk factor for thrombosis (Abad Rico et al., 2010). Recent studies have also shown that age has shown greater value in the diagnosis and prediction of DVT. Kelly Broen et al. used age-adjusted DD, and the adjusted DD threshold showed higher specificity and negative predictive value for the exclusion diagnosis of DVT (Broen et al., 2016). Jian Xiang Wu et al. used a similar approach and used age-adjusted-DD for preoperative DVT screening (Wu et al., 2021). Advanced age is also a risk factor for various infectious diseases, and studies have shown that the risk of urinary tract and surgical site infections will increase with age (Cheadle, 2006; Tandogdu and Wagenlehner, 2016). The morbidity and mortality of sepsis also increases significantly with age (Kingren et al., 2021). A large number of previous studies as well as clinical practice have shown that DD is highly sensitive for the diagnosis of DVT exclusion and guidelines published by the American Society of Hematology have identified DD as a preferred screening indicator for thrombosis (Lim et al., 2018). However, in the present study, we observed that preoperative DD levels did not show good predictive value for postoperative DVT in patients with spinal infections. We speculate that this may be related to the short half-life of DD. However, whether this phenomenon exists in other diseases still needs to be verified by more studies.

In the existing study, we noted that Xin Yan et al. predicted the risk of postoperative DVT progression in patients undergoing spinal surgery by plotting a nomogram, and they eventually screened five preoperative and intraoperative indicators, which included the time of surgery (Yan et al., 2022). Unlike their study, firstly, the present study included a large number of cases for calculation in patients with spinal infection, making the nomogram more relevant. Secondly, the present study included more routine preoperative serological indicators, which made it easier for clinicians to assess. Of course, there are differences in the outcomes we predict, with the present study predicting the occurrence rather than progression of DVT. Kimon Bekelis et al. analysed several risk factors for postoperative complications of spinal surgery, including DVT, and presented them in the form of an odds ratio (OR) (Bekelis et al., 2014). However, they did not present the predictive model visually, and in this respect, nomogram showed a greater advantage. In addition, we note that several studies have explored new methods for the diagnosis and prediction of DVT. A pilot study has shown that patients with musculoskeletal tumors can be defined as hypercoagulable by preoperative thromboelastography. And patients with a preoperative defined hypercoagulable state are more likely to develop DVT postoperatively (Sabharwal et al., 2023). Andreas G Tsantes et al. analyzed preoperative and postoperative rotational thromboelastometry parameters in patients with malignant bone tumors. Their accuracy for postoperative thrombus prediction was found to be significantly better than that of DD (Tsantes et al., 2023). Another study on rotational thromboelastometry analyzed data from patients with hip fractures and found a number of abnormal rotational thromboelastometry abnormalities associated with the development of venous thromboembolism (VTE), with preoperative clot formation time showing good performance in detecting symptomatic VTE (Tsantes et al., 2021). A study on spinal fractures analyzed risk factors for preoperative DVT, which included DD, and the adjusted optimal threshold for DD was 1.08ug/ml (Ma et al., 2021).

In this study, clinical data were retrospectively collected from patients undergoing surgery for spinal infection in Hunan Province, but there are geographical differences in the incidence of spinal infection, for example, Mycobacterium tuberculosis infection may be related to regional economic level and climatic environment (European Centre for Disease Prevention and Control and WHO Regional Office for Europe, 2022). Therefore, the applicability of this prediction model to other regions still needs further validation. This is a retrospective study and due to the absence of some preoperative data, this study excluded some indicators, such as height and weight, which may have value for preoperative prediction of DVT. Therefore, we intend to conduct further prospective studies based on this study to improve the accuracy of preoperative prediction of DVT.

5 Conclusion

In this study, a nomogram was developed to predict postoperative DVT in patients with spinal infection. The nomogram includes five preoperative predictor variables, which will effectively predict the likelihood of DVT after surgery. This nomogram is valuable in predicting postoperative DVT and will help clinicians to decide whether early intervention is needed based on the preoperative prediction results and the patient's specific situation.

Data availability statement

The raw data supporting the conclusions of this article will be made available by the authors, without undue reservation.

Ethics statement

The studies involving humans were approved by Ethics Committee of Xiangya Hospital Central South University. The studies were conducted in accordance with the local legislation and institutional requirements. The ethics committee/institutional review board waived the requirement of written informed consent for participation from the participants or the participants' legal guardians/next of kin because All subjects signed a consent form.

Author contributions

DX and MT designed research, performed research, analyzed data, and wrote the paper. XH, HZ, QG, CG and SL developed the idea for the study. XH, BT, GZ and CZ collected the data. All authors contributed to the article and approved the submitted version.

Acknowledgments

A special thanks to Xiangya Medical Big Data of Central South University.

Conflict of interest

The authors declare that the research was conducted in the absence of any commercial or financial relationships that could be construed as a potential conflict of interest.

Publisher's note

All claims expressed in this article are solely those of the authors and do not necessarily represent those of their affiliated organizations, or those of the publisher, the editors and the reviewers. Any product that may be evaluated in this article, or claim that may be made by its manufacturer, is not guaranteed or endorsed by the publisher.

Supplementary material

The Supplementary Material for this article can be found online at: https://www.frontiersin.org/articles/10.3389/fcimb.2023.1220456/full#supplementary-material

References

Abad Rico, J. I., Llau Pitarch, J. V., and Rocha, E. (2010). Overview of venous thromboembolism. *Drugs* 70 (Suppl 2), 3–10. doi: 10.2165/1158583-S0-000000000-00000

Babic, M., and Simpfendorfer, C. S. (2017). Infections of the spine. *Infect. Dis. Clin. North Am.* 31 (2), 279–297. doi: 10.1016/j.idc.2017.01.003

Barba, R., Di Micco, P., Blanco-Molina, A., Delgado, C., Cisneros, E., Villalta, J., et al. (2011). Fever and deep venous thrombosis. Findings from the RIETE registry. *J. Thromb. Thrombolysis* 32 (3), 288–292. doi: 10.1007/s11239-011-0604-7

Bekelis, K., Desai, A., Bakhoum, S. F., and Missios, S. (2014). A predictive model of complications after spine surgery: the National Surgical Quality Improvement Program (NSQIP) 2005-2010. *Spine J.* 14 (7), 1247–1255. doi: 10.1016/j.spinee.2013.08.009

Berbari, E. F., Kanj, S. S., Kowalski, T. J., Darouiche, R. O., Widmer, A. F., Schmitt, S. K., et al. (2015). Infectious diseases society of America. 2015 infectious diseases society of America (IDSA) clinical practice guidelines for the diagnosis and treatment of native vertebral osteomyelitis in adults. *Clin. Infect. Dis.* 61 (6), e26–e46. doi: 10.1093/cid/civ482

Beristain-Covarrubias, N., Perez-Toledo, M., Thomas, M. R., Henderson, I. R., Watson, S. P., and Cunningham, A. F. (2019). Understanding infection-induced thrombosis: lessons learned from animal models. *Front. Immunol.* 10, 2569. doi: 10.3389/fimmu.2019.02569

Blitzer, R. R., and Eisenstein, S. (2021). Venous thromboembolism and pulmonary embolism: strategies for prevention and management. *Surg. Clin. North Am.* 101 (5), 925–938. doi: 10.1016/j.suc.2021.06.015

Boender, J., Kruip, M. J., and Leebeek, F. W. (2016). A diagnostic approach to mild bleeding disorders. *J. Thromb. Haemost.* 14 (8), 1507–1516. doi: 10.1111/jth.13368

Braester, A., Stemer, G., Khouri, S., Raviv, B., and Barhoum, M. (2021). Is there a predictive value of high mean platelet volume in early diagnosis of venous thromboembolism? *Isr. Med. Assoc. J.* 23 (10), 635–638.

Broen, K., Scholtes, B., and Vossen, R. (2016). Predicting the need for further thrombosis diagnostics in suspected DVT is increased by using age adjusted D-dimer values. *Thromb. Res.* 145, 107–108. doi: 10.1016/j.thromres.2016.08.011

Chang, S. L., Huang, Y. L., Lee, M. C., Hu, S., Hsiao, Y. C., Chang, S. W., et al. (2018). Association of varicose veins with incident venous thromboembolism and peripheral artery disease. *JAMA* 319 (8), 807–817. doi: 10.1001/jama.2018.0246

Cheadle, W. G. (2006). Risk factors for surgical site infection. *Surg. Infect. (Larchmt)* 7 (Suppl 1), S7–11. doi: 10.1089/sur.2006.7.s1-7

Cheng, X., Lei, X., Wu, H., Luo, H., Fu, X., Gao, Y., et al. (2022). Development and validation of a predictive nomogram for preoperative deep vein thrombosis (DVT) in isolated calcaneal fracture. *Sci. Rep.* 12 (1), 5923. doi: 10.1038/s41598-022-10002-8

Chopin, N., Floccard, B., Sobas, F., Illinger, J., Boselli, E., Benatir, F., et al. (2006). Activated partial thromboplastin time waveform analysis: a new tool to detect infection? *Crit. Care Med.* 34 (6), 1654–1660. doi: 10.1097/01.CCM.0000217471.12799.1C

Colling, M. E., Tourdot, B. E., and Kanthi, Y. (2021). Inflammation, infection and venous thromboembolism. *Circ. Res.* 128 (12), 2017–2036. doi: 10.1161/CIRCRESAHA.121.318225

Dorman, S. E., Schumacher, S. G., Alland, D., Nabeta, P., Armstrong, D. T., King, B., et al. (2018). Xpert MTB/RIF Ultra for detection of Mycobacterium tuberculosis and rifampicin resistance: a prospective multicentre diagnostic accuracy study. *Lancet Infect. Dis.* 18 (1), 76–84. doi: 10.1016/S1473-3099(17)30691-6

Duarte, R. M., and Vaccaro, A. R. (2013). Spinal infection: state of the art and management algorithm. *Eur. Spine J.* 22 (12), 2787–2799. doi: 10.1007/s00586-013-2850-1

Dunn, R. N., and Ben Husien, M. (2018). Spinal tuberculosis: review of current management. *Bone Joint J.* 100-B (4), 425–431. doi: 10.1302/0301-620X.100B4.BJJ-2017-1040.R1

European Centre for Disease Prevention and Control and WHO Regional Office for Europe. (2022). *Tuberculosis Surveillance and Monitoring in Europe 2022 – 2020 Data.* (Copenhagen: WHO Regional Office for Europe and Stockholm: European Centre for Disease Prevention and Control), Licence: CC BY 3.0 IGO.

Falanga, A., Marchetti, M., and Russo, L. (2015). The mechanisms of cancer-associated thrombosis. *Thromb. Res.* 135 (Suppl 1), S8–S11. doi: 10.1016/S0049-3848(15)50432-5

Falanga, A., Marchetti, M., and Vignoli, A. (2013). Coagulation and cancer: biological and clinical aspects. *J. Thromb. Haemost.* 11 (2), 223–233. doi: 10.1111/jth.12075

Fan, Z., Zhang, Y., Pan, J., and Wang, S. (2017). Acute appendicitis and mean platelet volume: A systemic review and meta-analysis. *Ann. Clin. Lab. Sci.* 47 (6), 768–772.

Gu, W., Deng, X., Lee, M., Sucu, Y. D., Arevalo, S., Stryke, D., et al. (2021). Rapid pathogen detection by metagenomic next-generation sequencing of infected body fluids. *Nat. Med.* 27 (1), 115–124. doi: 10.1038/s41591-020-1105-z

Herren, C., Jung, N., Pishnamaz, M., Breuninger, M., Siewe, J., and Sobottke, R. (2017). Spondylodiscitis: diagnosis and treatment options. *Dtsch Arztebl Int.* 114 (51-52), 875–882. doi: 10.3238/arztebl.2017.0875

Hu, J. S., Huang, C. B., Mao, S. M., Fang, K. H., Wu, Z. Y., and Zhao, Y. M. (2022). Development of a nomogram to predict surgical site infection after closed comminuted calcaneal fracture. *BMC Surg.* 22 (1), 313. doi: 10.1186/s12893-022-01735-4

Jiang, X. X., Li, X. Y., Zhang, J., Wang, X. X., and Lin, C. Q. (2022). A nomogram model can predict the risk of venous thromboembolism in postoperative patients with gynecological Malignancies. *Int. J. Gynaecol. Obstet.* 158 (3), 689–699. doi: 10.1002/ijgo.14061

Kingren, M. S., Starr, M. E., and Saito, H. (2021). Divergent sepsis pathophysiology in older adults. *Antioxid Redox Signal.* 35 (16), 1358–1375. doi: 10.1089/ars.2021.0056

Lambrechts, M. J., Fried, T., D'Antonio, N. D., Karamian, B. A., Bodnar, J. G., Somers, S., et al. (2022). Is deep vein thrombosis chemoprophylaxis indicated after spinal irrigation and débridement? *World Neurosurg.* 168, e278–e285. doi: 10.1016/j.wneu.2022.09.111

Lim, W., Le Gal, G., Bates, S. M., Righini, M., Haramati, L. B., Lang, E., et al. (2018). American Society of Hematology 2018 guidelines for management of venous thromboembolism: diagnosis of venous thromboembolism. *Blood Adv.* 2 (22), 3226–3256. doi: 10.1182/bloodadvances.2018024828

Lippi, G., Buonocore, R., and Cervellin, G. (2016). The mean platelet volume is decreased in patients diagnosed with venous thromboembolism in the emergency department. *Semin. Thromb. Hemost.* 42 (6), 632–635. doi: 10.1055/s-0036-1571335

Lu, X., Jin, J., Lin, J., Qian, W., and Weng, X. (2015). Course of fever and potential infection after total joint replacement. *Knee Surg. Sports Traumatol Arthrosc.* 23 (6), 1870–1876. doi: 10.1007/s00167-014-3098-y

Ma, J., Du, P., Qin, J., Zhou, Y., Liang, N., Hu, J., et al. (2021). Incidence and risk factors predicting deep venous thrombosis of lower extremity following spinal fractures. *Sci. Rep.* 11 (1), 2441. doi: 10.1038/s41598-021-82147-x

Miller, J. M., Binnicker, M. J., Campbell, S., Carroll, K. C., Chapin, K. C., Gilligan, P. H., et al. (2018). A guide to utilization of the microbiology laboratory for diagnosis of infectious diseases: 2018 update by the infectious diseases society of America and the American society for microbiology. *Clin. Infect. Dis.* 67 (6), 813–816. doi: 10.1093/cid/ciy584

Panova-Noeva, M., Wagner, B., Nagler, M., Koeck, T., Ten Cate, V., Prochaska, J. H., et al. (2020). Comprehensive platelet phenotyping supports the role of platelets in the pathogenesis of acute venous thromboembolism - results from clinical observation studies. *EBioMedicine* 60, 102978. doi: 10.1016/j.ebiom.2020.102978

Sabharwal, S., Jalloh, H. B., Levin, A. S., and Morris, C. D. (2023). What proportion of patients with musculoskeletal tumors demonstrate thromboelastographic markers of hypercoagulability? A pilot study. *Clin. Orthop. Relat. Res.* 481 (3), 553–561. doi: 10.1097/CORR.0000000000002314

Sato, K., Yamada, K., Yokosuka, K., Yoshida, T., Goto, M., Matsubara, T., et al. (2019). RESEARCH GROUP FOR SPINE AND SPINAL CORD DISORDERS (HONNEKAI). Pyogenic spondylitis: clinical features, diagnosis and treatment. *Kurume Med. J.* 65 (3), 83–89. doi: 10.2739/kurumemedj.MS653001

Sayed, S. Z., Mahmoud, M. M., Moness, H. M., and Mousa, S. O. (2020). Admission platelet count and indices as predictors of outcome in children with severe Sepsis: a prospective hospital-based study. *BMC Pediatr.* 20 (1), 387. doi: 10.1186/s12887-020-02278-4

Scheyerer, M. J., Herren, C., Kühne, C., Neufang, J., Pieroh, P., and von der Höh, N. H. (2022). Surgical treatment strategies for pyogenic spondylodiscitis of the thoracolumbar spine. *Z. Orthop. Unfall.* 160 (6), 621–628. doi: 10.1055/a-1527-7939

Tandogdu, Z., and Wagenlehner, F. M. (2016). Global epidemiology of urinary tract infections. *Curr. Opin. Infect. Dis.* 29 (1), 73–79. doi: 10.1097/QCO.0000000000000228

Tsantes, A. G., Loukopoulou, I., Papadopoulos, D. V., Trikoupis, I. G., Sokou, R., Tsante, K. A., et al. (2023). Fibrinolysis shutdown and elevated D-dimer levels have high prognostic capacity for postoperative thromboembolic complications in patients with bone tumors. *J. Thromb. Thrombolysis* 55 (3), 536–544. doi: 10.1007/s11239-023-02787-w

Tsantes, A. G., Papadopoulos, D. V., Trikoupis, I. G., Tsante, K. A., Mavrogenis, A. F., Koulouvaris, P., et al. (2021). Rotational thromboelastometry findings are associated with symptomatic venous thromboembolic complications after hip fracture surgery. *Clin. Orthop Relat. Res.* 479 (11), 2457–2467. doi: 10.1097/CORR.0000000000001832

Urrutia, J., and Bono, C. M. (2022). Update on the diagnosis and management of spinal infections. *Instr. Course Lect.* 71, 439–449.

Wang, S., and Wu, L. (2022). Risk factors for venous thrombosis after spinal surgery: A systematic review and meta-analysis. *Comput. Math Methods Med.* 2022, 1621106. doi: 10.1155/2022/1621106

Wu, J. X., Qing, J. H., Yao, Y., Chen, D. Y., and Jiang, Q. (2021). Performance of age-adjusted D-dimer values for predicting DVT before the knee and hip arthroplasty. *J. Orthop. Surg. Res.* 16 (1), 82. doi: 10.1186/s13018-020-02172-w

Xu, L., Zhou, Z., Wang, Y., Song, C., and Tan, H. (2022). Improved accuracy of etiological diagnosis of spinal infection by metagenomic next-generation sequencing. *Front. Cell Infect. Microbiol.* 12, 929701. doi: 10.3389/fcimb.2022.929701

Yan, X., Huang, K., Jia, M., Yang, J., Zhang, P., He, Y., et al. (2022). Construction and verification of a nomogram predicting the risk of preoperative deep vein thrombosis progression after elective spine surgery. *Clin. Neurol. Neurosurg.* 222, 107439. doi: 10.1016/j.clineuro.2022.107439

Yardımcı, A. C., Yıldız, S., Ergen, E., Ballı, H., Ergene, E., Guner, Y. S., et al. (2021). Association between platelet indices and the severity of the disease and mortality in patients with COVID-19. *Eur. Rev. Med. Pharmacol. Sci.* 25 (21), 6731–6740. doi: 10.26355/eurrev_202111_27118

Zhang, H., Weng, H., Yu, K., and Qiu, G. (2021). Clinical risk factors and perioperative hematological characteristics of early postoperative symptomatic deep vein thrombosis in posterior lumbar spinal surgery. *Spine (Phila Pa 1976).* 46 (19), E1042–E1048. doi: 10.1097/BRS.0000000000003963

Zhang, G., Zhang, H., Hu, X., Xu, D., Tang, B., Tang, M., et al. (2023). Clinical application value of metagenomic next-generation sequencing in the diagnosis of spinal infections and its impact on clinical outcomes. *Front. Cell Infect. Microbiol.* 13, 1076525. doi: 10.3389/fcimb.2023.1076525

frontiers | Frontiers in Cellular and Infection Microbiology

TYPE Original Research
PUBLISHED 20 September 2023
DOI 10.3389/fcimb.2023.1243290

OPEN ACCESS

EDITED BY
Nahed Ismail,
University of Illinois Chicago, United States

REVIEWED BY
Anna Benini,
University of Verona, Italy
Haiyang Wu,
Tianjin Medical University, China

*CORRESPONDENCE
Ji-Ying Chen
chenjiying_301@163.com
Chi Xu
zhenyunale@163.com

RECEIVED 20 June 2023
ACCEPTED 23 August 2023
PUBLISHED 20 September 2023

CITATION
Li Z, Maimaiti Z, Yang F, Fu J, Li Z-Y, Hao L-B, Chen J-Y and Xu C (2023) Incidence, associated factors, and outcomes of acute kidney injury following placement of antibiotic bone cement spacers in two-stage exchange for periprosthetic joint infection: a comprehensive study.
Front. Cell. Infect. Microbiol. 13:1243290.
doi: 10.3389/fcimb.2023.1243290

Incidence, associated factors, and outcomes of acute kidney injury following placement of antibiotic bone cement spacers in two-stage exchange for periprosthetic joint infection: a comprehensive study

Zhuo Li[1,2], Zulipikaer Maimaiti[2], Fan Yang[1,2], Jun Fu[2,3], Zhi-Yuan Li[2,3], Li-Bo Hao[2,3], Ji-Ying Chen[1,2,3]* and Chi Xu[2,3]*

[1]School of Medicine, Nankai University, Tianjin, China, [2]Department of Orthopedics, The First Medical Center, Chinese PLA General Hospital, Beijing, China, [3]Department of Orthopedics, The Fourth Medical Center, Chinese PLA General Hospital, Beijing, China

Background: Two-stage exchange with placement of antibiotic cement spacer (ACS) is the gold standard for the treatment of chronic periprosthetic joint infection (PJI), but it could cause a high prevalence of acute kidney injury (AKI). However, the results of the current evidence on this topic are too mixed to effectively guide clinical practice.

Methods: We retrospectively identified 340 chronic PJI patients who underwent the first-stage exchange with placement of ACS. The Kidney Disease Improving Global Outcomes guideline was used to define postoperative AKI. Multivariate logistic analysis was performed to determine the potential factors associated with AKI. Furthermore, a systematic review and meta-analysis on this topic were conducted to summarize the knowledge in the current literature further.

Results: In our cohort, the incidence of AKI following first-stage exchange was 12.1%. Older age (per 10 years, OR= 1.509) and preoperative hypoalbuminemia (OR= 3.593) were independent predictors for postoperative AKI. Eight AKI patients progressed to chronic kidney disease after 90 days. A meta-analysis including a total of 2525 PJI patients showed the incidence of AKI was 16.6%, and AKI requiring acute dialysis was 1.4%. Besides, host characteristics, poor baseline liver function, factors contributing to acute renal blood flow injury, and the use of nephrotoxic drugs may be associated with the development of AKI. However, only a few studies supported an association between antibiotic dose and AKI.

Conclusion: AKI occurs in approximately one out of every six PJI patients undergoing first-stage exchange. The pathogenesis of AKI is multifactorial, with hypoalbuminemia could be an overlooked associated factor. Although the need

for acute dialysis is uncommon, the fact that some AKI patients will develop CKD still needs to be taken into consideration.

KEYWORDS

periprosthetic joint infection, antibiotic bone cement spacer, acute kidney injury, incidence, associated factors, outcome

1 Introduction

Periprosthetic joint infection (PJI) is a catastrophic complication after total joint arthroplasty (TJA), with incidence rates ranging from 0.5% to 2% (Edwards et al., 2009; Namba et al., 2013). It takes a tremendous toll on patients' physical and mental health, often putting them at a higher risk of death, and adding a heavy financial burden to the healthcare system (Kurtz et al., 2008; Zmistowski et al., 2013; Premkumar et al., 2021). A two-stage exchange involving the placement of a high-dose antibiotic-loaded cement spacer (ACS) supplemented with intravenous or oral pathogen-sensitive antibiotics is the standard approach for treating chronic PJI (Cha et al., 2015; Charette and Melnic, 2018). This technique has proven effective, with studies reporting reliable eradication of infection and long-term prevention of reinfection (Haleem et al., 2004; Engesaeter et al., 2011; Cooper and Della Valle, 2013; Puhto et al., 2014).

However, the most commonly used antibiotics in two-stage exchange, such as aminoglycosides and vancomycin, are highly nephrotoxic (Humes, 1988; Rybak et al., 1990). The systemic absorption of high-dose antibiotics in ACS, especially when combined with intravenous antibiotics, anesthetic drugs, and surgical procedures, could increase the risk of acute kidney injury (AKI). Given that AKI is associated with an acute demand for dialysis, prolonged hospital stays, and increased mortality, there is an urgent need to deepen clinicians' understanding of AKI (Luu et al., 2013; Theil et al., 2021; Valenzuela et al., 2022).

The incidence of AKI following placement of ACS in two-stage exchange varies considerably in the literature (Geller et al., 2017; Berliner et al., 2018; Edelstein et al., 2018; Yadav et al., 2018; Theil et al., 2021; Dagneaux et al., 2021a; Dagneaux et al., 2021b; Valenzuela et al., 2022), ranging from 0% to 33.3% (Springer et al., 2004; Hsieh et al., 2006; Gooding et al., 2011; Theil et al., 2021). Luu et al. (2013) performed a preliminary systematic review of 544 patients, showing an AKI incidence of 4.8%. However, their major limitation was that AKI was not the primary endpoint in most included studies, and the definition of AKI was unclear. These may result in a significant underestimation of the incidence of AKI, even lower than the incidence of approximately 6.3% following primary TJA (Thongprayoon et al., 2019). In addition, a North American study reported that AKI developed in 3.4% of 2147 patients for aseptic reasons, and the incidence of AKI may be significantly higher in PJI patients (Yadav et al., 2018). Furthermore, although some recent studies attempted to explore potential risk factors for AKI following first-stage exchange, they often provided fragmented and conflicting knowledge (Menge et al., 2012; Geller et al., 2017; Berliner et al., 2018; Yadav et al., 2018; Theil et al., 2021; Valenzuela et al., 2022). Information regarding renal outcomes after AKI is also very limited.

Overall, the results of the current evidence on this topic were too mixed to effectively guide clinical practice. We therefore conducted a retrospective institutional study and a systematic literature review to summarize the evidence on the incidence, associated factors, and outcomes of AKI after placement of ACS in two-stage exchange.

2 Materials and methods

2.1 Study population

The retrospective study was conducted at a national high-volume PJI treatment center. After the Institutional Review Board's approval, we retrospectively reviewed our institution's two-stage revision database. Four hundred and sixteen patients with suspected PJI underwent the first-stage resection between January 2007 and August 2020 were identified. We excluded 15 patients who did not meet the International Consensus Meeting (ICM) 2018 criteria (Shohat et al., 2019), and sixty-one patients with missing laboratory test data. Three hundred and forty patients were included in the final cohort, and the flow chart for the enrolment of PJI patients is shown in Figure 1.

2.2 Two-stage exchange technique

Institutional-based surgical approaches performed by high-volume surgeons were applied to all patients. The first-stage resection consists primarily of removing the infected prosthesis, thorough debridement, and placement of an articulating or static ACS. An ACS was made by intraoperatively mixing bone cement (pre-mixed with gentamicin) with additional antibiotic powder (e.g. vancomycin). As a general rule, 4g of antibiotic powder was impregnated in every 40g of bone cement. Postoperative pathogen-sensitive antibiotics were administered systemically based on cultures from joint aspirations. If the cultures were negative, broad-spectrum antibiotics such as vancomycin would be administered. After retaining the spacer for at least eight weeks,

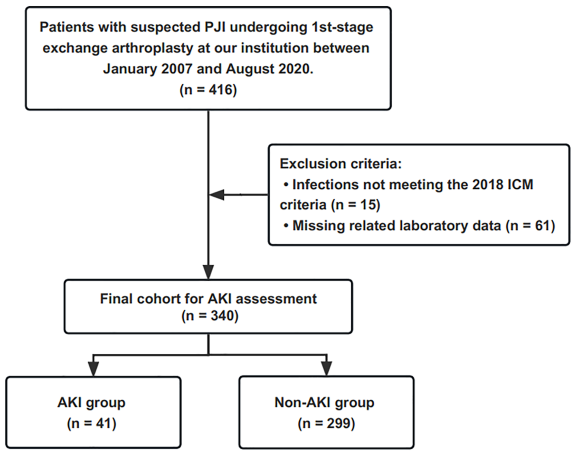

FIGURE 1
This flowchart demonstrates how patients are identified for inclusion in the final cohort. PJI, periprosthetic joint infection; ICM, International Consensus Meeting; AKI, acute kidney injury.

patients underwent a second-stage reimplantation if they were assessed as clear of infection.

2.3 Clinical data extraction

Two investigators independently reviewed the patient's medical records, surgical notes, and medical orders to extract clinical information associated with the development of AKI. Variables included: age, sex, Body Mass Index (BMI), type of antibiotics (administered for at least three days), comorbidities, type of pathogen, and laboratory values of blood urea nitrogen (BUN), blood uric acid (BUA), serum albumin, C-reactive protein (CRP), erythrocyte sedimentation rate (ESR), serum creatinine (SCr) and hemoglobin. The most recent preoperative SCr value was defined as the baseline. According to the care routine of our institution, patients were monitored for SCr levels on postoperative days 1, 3, 5, and 7, and these SCr values were extracted to assess the onset of AKI.

The baseline characteristics of the 340 PJI patients in the final cohort are summarized in Table 1. The patients were (60.1 ± 13.2) years old, and 50.0% were men with a mean BMI of (25.2 ± 3.8) kg/m2. The most common primary diagnosis was osteoarthritis (115/340, 33.8%).

2.4 Study outcomes

The diagnosis of AKI was based on the Kidney Disease Improving Global Outcomes (KDIGO) clinical practice guideline. It was proposed in 2012 and was a refinement of the Risk, Injury, Failure, Loss, and End-stage renal disease (RIFLE) criteria and the Acute Kidney Injury Network (AKIN) criteria (Khwaja, 2012). Due to the lack of information on urine output, only SCr levels were used to evaluate AKI. Briefly, an increase in SCr level of 0.3 mg/dL within 48 hours after surgery, or an increase in SCr level of more than 1.5 times the patient's preoperative baseline SCr level within one week, was diagnosed as AKI. Moreover, we further investigated whether AKI patients progressed to chronic kidney disease (CKD) (≥90 days).

2.5 Systematic review and meta-analysis

Moreover, a systematic literature search of the EMBASE, Pubmed, and Cochrane Database of Systematic Reviews was conducted in October 2022 to assess AKI's incidence and relevant factors following the first-stage exchange. The keywords included terms related to "acute kidney injury," "acute renal failure," "periprosthetic joint infection," "acute dialysis," "two-stage exchange," and "spacer," with specific search strategies shown in Supplementary Table 1. The above eligibility criteria covered all original reports dealing with two-stage exchange arthroplasty and postoperative AKI, and they all reported a definition of diagnosed AKI. We further considered observational studies, clinical trials, and case series with AKI following the first-stage exchange as the primary outcome and for which incidence or risk factors were reported. Three independent researchers reviewed the titles and abstracts of the publications to determine their suitability. Additionally, references in the key publications were reviewed to supplement the document collection further. A structured spreadsheet was created to collect the following information: title, first author's name, study year, country, study design, sample size, antibiotic information, the definition of AKI, incidence of AKI, and associated factors for AKI.

2.6 Statistical analysis

The study cohort was divided into AKI and non-AKI groups, and descriptive statistics were performed. Continuous variables were presented as mean ± standard deviation (SD) and compared using the t-test. Categorical data were presented as frequencies and percentages and compared using chi-square or Fisher's exact test. We first performed a univariate logistic regression analysis for all variables (continuous variables are converted to categorical variables via receiver operating characteristic curves) to assess the relationship between baseline patient characteristics and AKI. Variables with P values <0.1 were further included in multifactorial logistic regression analysis to identify independent predictors of AKI. All logistic regression analyses reported adjusted odds ratios (ORs) and 95% confidence intervals (CIs). The above statistical analyses were performed by SPSS 25.0. P<0.05 was considered to indicate statistical significance.

Comprehensive Meta-Analysis V3 software was used to perform the meta-analysis. Adjusted point estimates were consolidated using a generic inverse variance method of DerSimonian and Laird (1986). The random-effects model was used to pool AKI incidence. The I^2 statistic was adopted to assess the heterogeneity of included studies, with less than 50% of I^2 considered low heterogeneity, 51% to 75% moderate heterogeneity, and greater than 76% high heterogeneity. The publication bias was evaluated by funnel plot and Egger test.

10.3389/fcimb.2023.1243290

TABLE 1 Baseline Demographic Details.

Characteristics	Total	AKI Group (N=41)	Non-AKI (N=299)	P
Age, years	60.1 ± 13.2	66.3 ± 10.1	59.2 ± 13.4	**0.001**
Sex				0.868
Man	170 (50.0)	20 (48.8)	150 (50.2)	
Woman	170 (50.0)	21 (51.2)	149 (49.8)	
Joint				0.854
Hip	187 (55)	22 (52.7)	165 (55.2)	
Knee	153 (45)	19 (47.2)	134 (44.8)	
BMI, kg/m^2	25.2 ± 3.8	25.4 ± 3.8	25.1 ± 3.7	0.663
Asian race	340 (100)	41 (100)	299 (100)	–
Smoking	30 (8.8)	3 (7.3)	27 (9.0)	0.717
Primary Diagnosis				0.195
Osteoarthritis	115 (33.8)	18 (43.9)	97 (32.4)	
ONFH	85 (25.0)	10 (24.4)	75 (25.1)	
DDH	5 (1.5)	2 (4.9)	3 (1.0)	
Inflammatory arthritis	20 (5.9)	1 (2.4)	19 (6.4)	
Fracture	74 (21.8)	7 (17.1)	67 (22.4)	
Others	41 (12.1)	3 (7.3)	38 (12.7)	
Comorbidities				
Cardiovascular Disease	42 (12.4)	7 (17.1)	35 (11.7)	0.327
Kidney Disease	11 (3.2)	3 (7.3)	8 (2.7)	0.456
Diabetes	45 (13.2)	9 (22.0)	36 (12.0)	0.079
Number of Prior Surgery	1.6 ± 1.0	1.5 ± 0.8	1.6 ± 1.1	0.298
Presence of a Sinus Tract	132 (38.8)	17 (41.5)	115 (38.5)	0.711
History of Infected Surgery	191 (56.2)	21 (51.2)	170 (56.9)	0.495
Preoperative biomarkers				
Serum Creatinine, umol/L	63.2 ± 16.2	61.7 ± 15.1	63.4 ± 16.4	0.530
Hemoglobin, g/L	123.0 ± 15.9	121.6 ± 13.6	123.2 ± 16.2	0.560
Serum Albumin, g/L	38.5 ± 4.1	36.6 ± 3.8	38.7 ± 4.1	**0.002**
BUN, mmol/L	5.1 ± 1.7	5.1 ± 1.9	5.1 ± 1.7	0.857
BUA, µmol/L	301.7 ± 86.3	282.4 ± 81.8	304.4 ± 86.7	0.127
C-reactive Protein, mg/dL	2.4 ± 2.5	2.7 ± 2.1	2.4 ± 2.6	0.386
ESR, mm/h	42.6 ± 26.3	51.2 ± 27.0	41.4 ± 26.1	**0.025**

The numbers in brackets are standard deviations for continuous variables and percentages for categorical variables. AKI, acute kidney injury; BMI, body mass index; ONFH, osteonecrosis of the femoral head; DDH, developmental dysplasia of the hip; BUN, blood urea nitrogen; BUA, blood uric acid; ESR, erythrocyte sedimentation rate.
P values with statistical significance are highlighted in bold.
"-" means not applicable.

3 Results

3.1 Incidence of AKI following the first-stage exchange

In our study cohort, 41 patients (12.1%) developed AKI within the first seven days postoperatively. Compared to the non-AKI group, patients in the AKI group were significantly older (Table 1, 66.3 ± 10.1 vs. 59.2 ± 13.4, P= 0.01), had significantly lower serum albumin levels (36.6 ± 3.8 g/L vs. 38.7 ± 4.1 g/L, P= 0.002), and higher ESR levels (51.2 ± 27.0 mm/h vs. 41.4 ± 26.1 mm/h, P= 0.025). There were no significant differences between the two groups in terms of sex, BMI, joint, primary diagnosis, the presence of a sinus tract, number of prior open surgery, comorbidities, preoperative hemoglobin, BUN, BUA, SCr, and CRP levels. We also did not observe differences between the two groups regarding pathogenic organisms, with *coagulase-negative staphylococcus* being the most common (Table 2). Besides, the two groups had no differences in the type of spacer-loaded or systemically administered antibiotics (Table 3). Patients in the AKI group had higher SCr during the first week postoperatively than those in the non-AKI group (Table 4, P< 0.001). The highest SCr level was seen on the third postoperative day.

3.2 Associated factors of AKI

As shown in Table 5, the univariate logistic regression analysis identified older age, diabetes, ESR > 40 mm/h, and hypoalbuminemia as potential predictors. Older age (per additional 10 years, OR= 1.509; 95%CI, 1.072-2.119; P= 0.019) and hypoalbuminemia (OR= 3.593; 95%CI, 1.688-7.650; P= 0.001) remained significant predictors in the multifactorial logistic model.

3.3 Renal outcomes

No patient had acute dialysis needs during hospitalization. Nine AKI patients were diagnosed with CKD after 90 days, eight of whom did not suffer from pre-existing renal disease. Five patients with CKD were applied renal preservation therapy for more than one month and none of them were readmitted for CKD.

3.4 Systematic review and meta-analysis

Apart from our study, 13 studies (Hsieh et al., 2009; Jung et al., 2009; Menge et al., 2012; Reed et al., 2014; Aeng et al., 2015; Geller et al., 2017; Berliner et al., 2018; Edelstein et al., 2018; Yadav et al., 2018; Theil et al., 2021; Dagneaux et al., 2021a; Dagneaux et al., 2021b; Valenzuela et al., 2022) comprising additional 2185 PJI patients undergoing first-stage exchange were included in the meta-analysis of associated AKI incidence (Table 6). The pooled estimated incidence of AKI was 16.6% (95% CI: 12.5%-21.9%, I^2 = 79%, Figure 2A) and the incidence of AKI requiring dialysis was 1.4% (95% CI: 0.5%-4.1%, I^2 = 70%, Figure 2B). There was no significant publication bias in the meta-analysis assessing the incidence of AKI (Funnel plot was shown in Supplementary Figure 1, P for Egger test = 0.08).

Reported related factors for AKI in PJI patients undergoing first-stage exchange are demonstrated in Table 6. The identified factors include demographic characteristics such as age (Yadav et al., 2018; Theil et al., 2021) and BMI (Geller et al., 2017); factors affecting renal perfusions such as hypovolemia (Dagneaux et al., 2021a; Dagneaux et al., 2021b), acute atrial fibrillation (Rybak et al., 1990; Haleem et al., 2004) and low baseline hemoglobin levels (Aeng et al., 2015; Berliner et al., 2018; Theil et al., 2021); poorer baseline renal function such as a history of chronic renal disease (Dagneaux et al., 2021a; Dagneaux et al., 2021b; Valenzuela et al., 2022) and higher creatinine levels (Aeng et al., 2015); and the use of specific medications such as nonsteroidal anti-inflammatory drugs (NSAIDs) (Edwards et al., 2009) and angiotensin-converting enzyme inhibitors (ACEIs) (Reed et al., 2014). A few studies have also reported on the potential impact of the type or dose of antibiotics (Menge et al., 2012; Reed et al., 2014; Dagneaux et al., 2021a).

4 Discussion

Despite the widespread use of two-stage exchange arthroplasty in the management of chronic PJI, data on acute kidney injury

TABLE 2 Pathogen Data.

Identified Microorganisms	AKI Group (N=41)	Non-AKI (N=299)	*P*
Staphylococcus aureus	6 (14.6)	40 (13.4)	0.825
Coagulase-negative Staphylococcus	15 (36.6)	127 (42.5)	0.473
Streptococcus	0 (0)	17 (5.7)	0.117
Entoococcus	3 (7.3)	16 (5.4)	0.607
Gram-Negative Bacteria	2 (4.9)	28 (9.4)	0.342
Fungi	1 (2.4)	12 (4.0)	0.622
Others	2 (4.9)	20 (6.7)	0.658
Mixed	3 (7.3)	46 (15.4)	0.168
Negative	14 (34.1)	79 (26.4)	0.298

Numbers in brackets are percentages. AKI, acute kidney injury.

TABLE 3 Antibiotics Administered.

Systemic (Intravenous or Oral) Antibiotics	AKI Group (N=41)	Non-AKI (N=299)	*P*
Vancomycin	10 (24.4)	49 (16.4)	0.205
Quinolones	13 (31.7)	91 (30.4)	0.868
Linezolid	5 (12.2)	55 (18.4)	0.329
Rifapentine	6 (14.6)	46 (15.4)	0.900
Third-Generation Cephalosporin	1 (2.4)	20 (6.7)	0.289
Meropenem	0 (0)	8 (2.7)	0.289
Fluconazole/Voriconazole	1 (2.4)	12 (4.0)	0.622
Others	5 (12.2)	20 (6.7)	0.341
Antibiotics Added in Spacer			
Vancomycin	36 (87.8)	279 (93.3)	0.205
Meropenem/Imipenem	14 (34.1)	143 (47.8)	0.099
Others	8 (19.5)	51 (17.1)	0.841

Numbers in brackets are percentages. AKI, acute kidney injury.

(AKI) following placement of antibiotic-loaded ACS are limited and the results are mixed. Our results indicated the incidence of AKI following first-stage exchange was 12.1% in our large retrospective cohort; a meta-analysis including total 2525 PJI patients demonstrated an AKI incidence of 16.6%. In addition to the identified demographic characteristics, factors contributing to acute renal blood flow impairment, and the use of several medications, hypoalbuminemia may be a new potential factor associated with the development of AKI. Although the need for acute dialysis is uncommon when AKI occurs, approximately 20% of AKI patients still progress to CKD.

4.1 Incidence of AKI

The incidence of AKI following first-stage revision reported in the literature varies substantially at present, which may be explained by differences in the definition of AKI and the spacer technique (Luu et al., 2013; Dagneaux et al., 2021a; Dagneaux et al., 2021b). Our meta-analysis showed an incidence of 16.6% for AKI defined by standard criteria, which is three to four times higher than those following primary total joint arthroplasty (Thongprayoon et al., 2019; Yayac et al., 2021). This incidence is of greater concern to clinicians and is higher than the incidence of AKI after major abdominal surgery (approximately 13.4% (O'Connor et al., 2016)). A slightly lower incidence of AKI was observed in our cohort, which may be due to the fact that the patients were younger. Meanwhile, the incidence of AKI varied across races and our study is the first to report the incidence of AKI in Asians in a large PJI cohort. Reports from other areas have shown that black patients tend to have a higher risk of AKI than white patients, and Asians also have a relatively low incidence of AKI (Hassan and Balogun, 2022). However, black patients with AKI would have a lower in-hospital mortality rate (Hassan et al., 2021). The association between race and AKI in PJI remains unknown, but warrants further investigation to improve prognosis.

Previous studies reporting AKI after revision surgery for aseptic reasons were scarce. Yadav A et al (Yadav et al., 2018). evaluated 2147 patients using to the RIFLE criteria and found the incidence of AKI to be 3.4%, which is similar to the incidence of primary TJA. The present evidence further revealed the hazardous nature of PJI, and its associated renal burden should be of additional concern.

4.2 Associated factors of AKI

The natural question for surgeons is: "What can be modified intraoperatively to reduce the development of AKI?" Our results

TABLE 4 Trends of Creatinine in the First Seven Days Postoperatively.

SCr, umol/L	Total	AKI	Non-AKI	*P*
Baseline	63.2	61.7	63.4	0.530
POD1	65.0	83.8	62.4	<0.001
POD3	68.5	90.6	65.3	<0.001
POD5	66.0	85.7	63.3	<0.001
POD7	67.0	88.9	64.1	<0.001

SCr, Serum creatinine; AKI, acute kidney injury, POD, postoperative day.

TABLE 5 Logistic Regression Model for Acute Kidney Injury.

Variables	Univariate		Multivariate	
	OR (95% CI)	*P*	OR (95% CI)	*P*
Older Age (per 10 years)	1.692 (1.219-2.367)	0.002	1.509 (1.072-2.119)	0.019
Diabetes	2.055 (0.907-4.653)	0.084	1.541 (0.646-3.673)	0.329
ESR > 40 mm/h	2.163 (1.101-4.250)	0.025	1.375 (0.662-2.856)	0.394
Hypoalbuminemia	4.843 (2.380-9.858)	<0.001	3.593 (1.688-7.650)	0.001

ESR, erythrocyte sedimentation rate; OR, odds ratio; CI, confidence interval.

revealed that hypoalbuminemia was an independent predictor of AKI following the first-stage exchange (OR= 3.593; *P*= 0.001). To our knowledge, this is the first study to assess the association between hypoalbuminemia and AKI in the field of arthroplasty. One previous study showed that hypoalbuminemia rather than systemic inflammatory response syndrome was a predictor of AKI in the intensive care unit (ICU) setting (OR=2.17) (Chawla et al., 2005). Another meta-analysis including surgical and ICU patients demonstrated that hypoalbuminemia was an independent risk factor for AKI (OR= 2.34) and AKI-related death (OR= 2.47) (Wiedermann et al., 2010). Our results further suggested that routine preoperative measurement of serum albumin may help to identify PJI patients with a higher risk of developing AKI. The next key question is whether this potential association may provide a rationale for changes in clinical management. As a surrogate indicator of malnutrition, hypoalbuminemia has been proven to be strongly associated with failure of a two-stage exchange protocol (Green et al., 2023). Some factors may confound this proposed association, such as a high systemic inflammatory state, poor lifestyle habits such as smoking, and chronic wasting disease, which may accompany hypoalbuminemia. The present study did not evaluate the effect of these factors on hypoalbuminemia (Poston and Koyner, 2019; An et al., 2021; Li et al., 2022). However, the current data could give us more sufficient evidence to help patients restore normal serum albumin levels preoperatively. However, this issue will only be better addressed if serum albumin causally improves clinical outcomes rather than acting as a simple marker for pathological processes.

The renoprotective effect of albumin was mediated by scavenging reactive oxygen species, preventing oxidative damage, and binding and delivering protective lysophosphatidic acid (Wiedermann et al., 2010). In a recent study, Angerett NR et al (Angerett et al., 2022). reduced the incidence of AKI after TJA from 6.71% to 4.15% by implementing a perioperative renal protocol. The present study may offer a new perspective to improve this protocol by correcting perioperative serum albumin levels.

Advanced age was associated with a higher risk of AKI in our cohort, which is consistent with previous results (Yadav et al., 2018; Theil et al., 2021). Similarly, a recent retrospective study of 390,382 patients showed a progressive increase in the incidence of postoperative AKI with age (Privratsky et al., 2023).

Additionally, a systematic review revealed that the presence of AKI was multifactorial, with acute renal blood flow impairment, poorer baseline renal function, and the use of nephrotoxic drugs as potentially important factors. Hypovolemia and acute renal blood flow impairment could lead to insufficient renal blood perfusion, resulting in prerenal acute kidney injury. Besides, perioperative improvement of patient blood volume to protect the kidneys is now actively advocated (Goren and Matot, 2015). These results are understandable and underline the importance of improving renal perfusion and restricting nephrotoxic drug regimens in high-risk patients. Future exploration of the availability of nephroprotective protocols in PJI patients is warranted. Notably, despite considerable effort, only a few studies have confirmed the association of type or dose of antibiotics with AKI, while more studies have not proven such an association. A noteworthy example was the large single-center study by Dagneaux L et al, which found that the risk of postoperative AKI in the TKA revision cohort was associated with increased vancomycin or aminoglycoside concentrations in the spacer (Dagneaux et al., 2021a), whereas AKI after THA septic revision could not be attributed to the type, dose or concentration of antibiotics given in the spacer or intravenously (Dagneaux et al., 2021b). The rationale for this phenomenon was still not clear. Possible reasons were as follows: firstly, there was a high degree of heterogeneity between studies, as the type and dose of antibiotics were often adjustable, resulting in differentiated results; secondly, these data indicated that the pathogenesis of AKI following first-stage exchange was multifactorial, with host-related factors likely to play an even more critical role, whereas the available evidence suggested that the administration of nephrotoxic antibiotics within reasonable doses (less than 8 g/40 g cement (Li et al., 2023)) may not significantly increase the risk of AKI.

4.3 Renal outcomes

The incidence of AKI requiring acute dialysis following first-stage exchange reported in the literature varies widely. The results of our cohort were similar to those of Dagneaux L et al (Dagneaux et al., 2021a; Dagneaux et al., 2021b), indicating that almost no patients required dialysis during hospitalization. However, another study reported a 3.7% dialysis requirement rate (Theil et al., 2021). This variation may be caused by the different indications for dialysis across institutions. Long-term renal outcomes after AKI remain unclear. In our cohort, 20% of AKI patients without pre-existing renal disease developed CKD after 90 days. Previous studies have reported progression to CKD in approximately 2-4% of patients with normal renal function, accounting for 15%-60% of patients

TABLE 6 Systematic Review of AKI Following the First-Stage Exchange.

Study	Country	Design	Number of Patients (Male%)	Average Age (Years)	Spacer Retained	Systemic Antibiotics Used	AKI Definition	Incidence	Related Factors
Dagneaux et al., 2021a	USA	Cohort	227 (55)	65	15 weeks	Vancomycin (42%) cefazolin 51 (19.9%) ceftriaxone (16.8%)	KDIGO guidelines	10.1%	Postoperative fluid depletion and/or hypovolemia, acute atrial fibrillation, and CKD
Dagneaux et al., 2021a	USA	Cohort	424 (53)	67	11 weeks	Vancomycin (40%) cefazolin 51 (23%) ceftriaxone (13%)	KDIGO guidelines	19.1%	Hypertension, perioperative hypovolemia, CKD, acute atrial fibrillation, and higher concentrations of vancomycin or aminoglycosides in ACS
Theil et al., 2021	Germany	Cohort	285 (48)	–	13 weeks	Vancomycin, aminopenicillins, and linezolid	KDIGO guidelines	33.3%	Age and baseline SCr
Yadav et al., 2018	USA	Cohort	197 (54)	66	–	Cefazolin and vancomycin	RIFLE criteria	28.9%	Age and CCI
Edelstein et al., 2018	USA	Prospective cohort	37 (60)	67	8 weeks	Culture-directed intravenous antibiotics	RIFLE criteria	27.0%	–
Berliner ZP et al., 2017	USA	Cohort	74 (53)	67	–	–	A greater than 50% rise in SCr to a value of at least 1.4 mg/dL	14.9%	Lower baseline hemoglobin
Aeng et al., 2015	Canada	Prospective cohort	50 (54)	66	–	Cephalosporins, vancomycin, and rifampin	A greater than 50% rise in SCr within the first 7 days	20.0%	ACS premanufactured with gentamicin, administration of blood transfusions and NSAIDs postoperatively
Geller et al., 2017	USA	Cohort	247 (48)	64	–	Vancomycin (45%), daptomycin (21%), cefazolin (18%)	KDIGO guidelines	26.3%	Higher BMI, lower baseline hemoglobin level, and existence of a comorbid condition
Jung et al., 2009	Germany	Cohort	82 (52)	70	13 weeks	Primarily vancomycin and rifampicin	A greater than 50% rise in SCr	6.1%	–
Menge et al., 2012	USA	Cohort	84 (45)	63	–	–	A greater than 50% rise in SCr to a value of at least 1.4 mg/dL	16.7%	Dose of vancomycin or tobramycin in the ACS
Valenzuela et al., 2022	USA	RCT	66 (54)	68	–	Culture-targeted IV antibiotics	KDIGO guidelines	22.7%	Preoperative CKD
Reed et al., 2014	USA	Cohort	313	–	–	Primarily vancomycin, piperacillin/tazobactam	A SCr increase of 0.5 mg/dL or 50%	8.3%	ACE inhibitor exposure; piperacillin-tazobactam exposure
Hsieh et al., 2009	China	Cohort	99 (61)	–	–	1st-gen cephalosporin and gentamicin, else based on cultures and sensitivities	A SCr increase of 0.5 mg/dL or 50%	5.1%	–

AKI, acute kidney injury; SCr, serum creatinine; BMI, body mass index; ACS, antibiotic-loaded cement spacer; CKD, chronic kidney disease; CCI, Charlson comorbidity index; KDIGO, Kidney Disease: Improving Global Outcomes; RIFLE, risk, injury, failure, loss, end stage kidney disease; RCT, randomized controlled trial; ACE, angiotensin converting enzyme; NSAIDs, nonsteroidal anti-inflammatory drugs.
"-" means not applicable.

10.3389/fcimb.2023.1243290

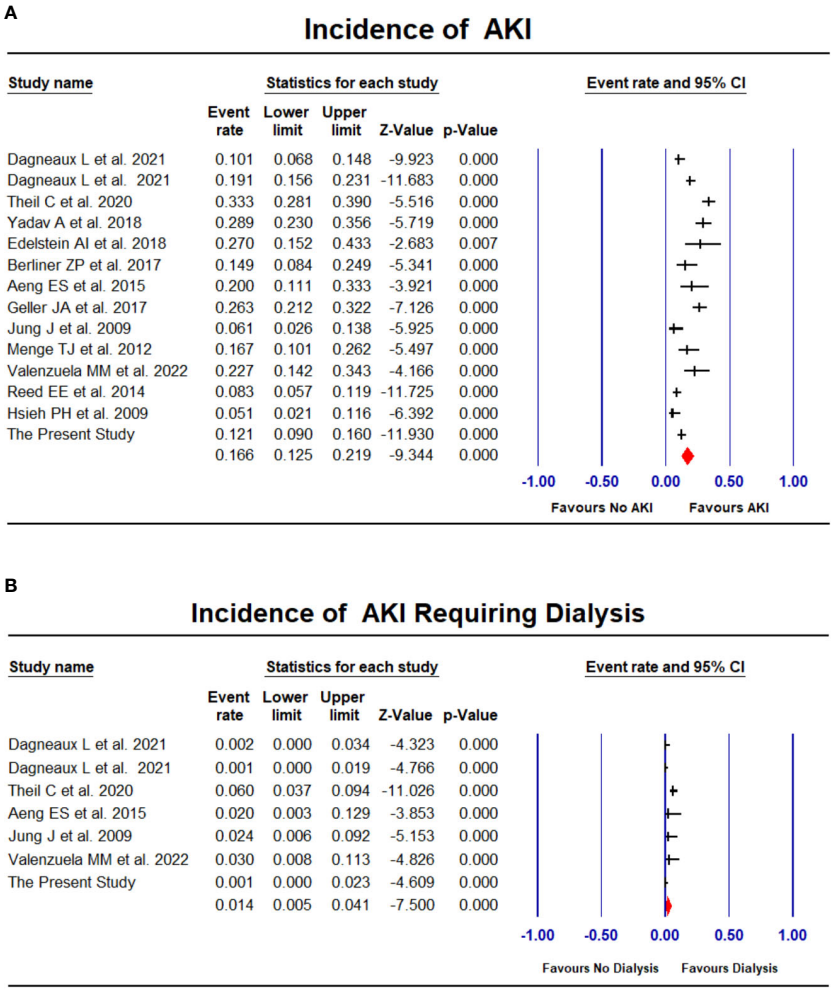

FIGURE 2
Forest plots of the included studies assessing incidence of AKI **(A)** and AKI requiring dialysis **(B)**.

with AKI (Dagneaux et al., 2021a; Dagneaux et al., 2021b). These findings should be interpreted with caution as relevant data are scarce.

4.4 Limitations

Several limitations in present study are worth mentioning. Firstly, the design was retrospective, and certain biases of retrospective study are inherent. Secondly, limited by the unavailability of data, the impact of perioperative fluid management, antibiotic dose, and anesthetic factors on AKI could not be assessed in our cohort. However, as an updated systematic review of the current topic, we summarized the present research evidence and illustrated the multifactorial nature of AKI pathogenesis. One point of interest was the association between antibiotic dose and AKI. We found only a few publications supporting that a higher antibiotic dose in two-stage revision may lead to the development of AKI, however, we were not able to further evaluate the relationship between antibiotic dose and AKI in our cohort. Future, more thorough studies could investigate this issue. Thirdly, the studies included in the meta-analysis were heterogeneous in terms of patient characteristics, surgical technique, and AKI diagnosis. Future studies based on large-scale databases are still needed. Fourthly, the incidence of AKI is probably underestimated, as information about novel AKI biomarkers and urine volume were lacking and some patients may be discharged before they meet the AKI criteria. Approximately 10% of patients in our cohort were discharged within 7 days postoperatively, but their AKI prevalence was not significantly reduced (4/34). Furthermore, although we found an association between preoperative hypoalbuminemia and AKI, this conclusion is still preliminary, and future prospective studies with close renal monitoring are warranted. However, given that this association has been demonstrated in a variety of other diseases, clinicians should be vigilant in such patients.

5 Conclusions

In conclusion, a meta-analysis including 2525 PJI patients indicated the incidence of AKI following first-stage exchange was

16.6%. Current evidence suggested that the pathogenesis of AKI is multifactorial, including host characteristics, factors contributing to acute renal blood flow injury, and the use of nephrotoxic drugs. Hypoalbuminemia may be a novel factor associated with AKI development. Although the need for acute dialysis in the case of AKI is uncommon, the fact that some AKI patients will develop CKD still needs to be taken into consideration. Further high-quality studies are needed to investigate approaches to improve the occurrence and progression of AKI.

Data availability statement

The original contributions presented in the study are included in the article/Supplementary Material. Further inquiries can be directed to the corresponding author.

Ethics statement

The studies involving humans were approved by Chinese PLA General Hospital Ethics Committee. The studies were conducted in accordance with the local legislation and institutional requirements. The ethics committee/institutional review board waived the requirement of written informed consent for participation from the participants or the participants' legal guardians/next of kin because retrospective study, which was approved by the Ethics Committee.

Author contributions

ZL provided idea. ZM, ZL, JF, and L-BH analyzed the data and performed the experiments. ZL, ZM, and FY wrote the manuscript. CX and J-YC assisted in revising the manuscript. CX and J-YC gave important guidance and analysis in the review process. All authors contributed to the article and approved the submitted version.

Conflict of interest

The authors declare that the research was conducted in the absence of any commercial or financial relationships that could be construed as a potential conflict of interest.

Publisher's note

Supplementary material

The Supplementary Material for this article can be found online at: https://www.frontiersin.org/articles/10.3389/fcimb.2023.1243290/full#supplementary-material

References

Aeng, E. S., Shalansky, K. F., Lau, T. T., Zalunardo, N., Li, G., Bowie, W. R., et al. (2015). Acute kidney injury with tobramycin-impregnated bone cement spacers in prosthetic joint infections. *Ann. Pharmacother.* 49 (11), 1207–1213. doi: 10.1177/1060028015600176

An, X., Wang, J., Shi, W., Ma, R., Li, Z., Lei, M., et al. (2021). The effect of passive smoking on early clinical outcomes after total knee arthroplasty among female patients. *Risk Manag Healthc Policy.* 14, 2407–2419. doi: 10.2147/RMHP.S309893

Angerett, N. R., Yevtukh, A., Ferguson, C. M., Kahan, M. E., Ali, M., and Hallock, R. H. (2022). Improving postoperative acute kidney injury rates following primary total joint arthroplasty. *J. Arthroplasty.* 37 (8S), S1004–S1009. doi: 10.1016/j.arth.2021.12.019

Berliner, Z. P., Mo, A. Z., Porter, D. A., Grossman, J. M., Hepinstall, M. S., Cooper, H. J., et al. (2018). In-hospital acute kidney injury after TKA revision with placement of an antibiotic cement spacer. *J. Arthroplasty.* 33 (7S), S209–S212. doi: 10.1016/j.arth.2017.11.050

Cha, M. S., Cho, S. H., Kim, D. H., Yoon, H. K., Cho, H. S., Lee, D. Y., et al. (2015). Two-stage total knee arthroplasty for prosthetic joint infection. *Knee Surg. Relat. Res.* 27 (2), 82–89. doi: 10.5792/ksrr.2015.27.2.82

Charette, R. S., and Melnic, C. M. (2018). Two-stage revision arthroplasty for the treatment of prosthetic joint infection. *Curr. Rev. Musculoskelet Med.* 11 (3), 332–340. doi: 10.1007/s12178-018-9495-y

Chawla, L. S., Abell, L., Mazhari, R., Egan, M., Kadambi, N., Burke, H. B., et al. (2005). Identifying critically ill patients at high risk for developing acute renal failure: a pilot study. *Kidney Int.* 68 (5), 2274–2280. doi: 10.1111/j.1523-1755.2005.00686.x

Cooper, H. J., and Della Valle, C. J. (2013). The two-stage standard in revision total hip replacement. *Bone Joint J.* 95-B (11 Suppl A), 84–87. doi: 10.1302/0301-620X.95B11.32906

Dagneaux, L., Limberg, A. K., Osmon, D. R., Leung, N., Berry, D. J., and Abdel, M. P. (2021a). Acute kidney injury when treating periprosthetic joint infections after total knee arthroplasties with antibiotic-loaded spacers: incidence, risks, and outcomes. *J. Bone Joint Surg. Am.* 103 (9), 754–760. doi: 10.2106/JBJS.20.01825

Dagneaux, L., Limberg, A. K., Osmon, D. R., Leung, N., Berry, D. J., and Abdel, M. P. (2021b). Renal toxicity associated with resection and spacer insertion for chronic hip PJI. *J. Arthroplasty.* 36 (9), 3289–3293. doi: 10.1016/j.arth.2021.04.012

DerSimonian, R., and Laird, N. (1986). Meta-analysis in clinical trials. *Control Clin. Trials.* 7 (3), 177–188. doi: 10.1016/0197-2456(86)90046-2

Edelstein, A. I., Okroj, K. T., Rogers, T., Della Valle, C. J., and Sporer, S. M. (2018). Nephrotoxicity after the treatment of periprosthetic joint infection with antibiotic-loaded cement spacers. *J. Arthroplasty.* 33 (7), 2225–2229. doi: 10.1016/j.arth.2018.02.012

Edwards, J. R., Peterson, K. D., Mu, Y., Banerjee, S., Allen-Bridson, K., Morrell, G., et al. (2009). National Healthcare Safety Network (NHSN) report: data summary for 2006 through 2008, issued December 2009. *Am. J. Infect. Control.* 37 (10), 783–805. doi: 10.1016/j.ajic.2009.10.001

Engesaeter, L. B., Dale, H., Schrama, J. C., Hallan, G., and Lie, S. A. (2011). Surgical procedures in the treatment of 784 infected THAs reported to the Norwegian Arthroplasty Register. *Acta Orthop.* 82 (5), 530–537. doi: 10.3109/17453674.2011.623572

Geller, J. A., Cunn, G., Herschmiller, T., Murtaugh, T., and Chen, A. (2017). Acute kidney injury after first-stage joint revision for infection: risk factors and the impact of antibiotic dosing. *J. Arthroplasty.* 32 (10), 3120–3125. doi: 10.1016/j.arth.2017.04.054

Gooding, C. R., Masri, B. A., Duncan, C. P., Greidanus, N. V., and Garbuz, D. S. (2011). Durable infection control and function with the PROSTALAC spacer in two-stage revision for infected knee arthroplasty. *Clin. Orthop Relat. Res.* 469 (4), 985–993. doi: 10.1007/s11999-010-1579-y

Goren, O., and Matot, I. (2015). Perioperative acute kidney injury. *Br. J. Anaesth.* 115 Suppl 2, ii3–i14. doi: 10.1093/bja/aev380

Green, C. C., Valenzuela, M. M., Odum, S. M., Rowe, T. M., Springer, B. D., Fehring, T. K., et al. (2023). Hypoalbuminemia predicts failure of two-stage exchange for chronic periprosthetic joint infection of the hip and knee. *J. Arthroplasty* 38 (7), 1363–1368. doi: 10.1016/j.arth.2023.01.012

Haleem, A. A., Berry, D. J., and Hanssen, A. D. (2004). Mid-term to long-term followup of two-stage reimplantation for infected total knee arthroplasty. *Clin. Orthop Relat. Res.* 428, 35–39. doi: 10.1097/01.blo.0000147713.64235.73

Hassan, M. O., and Balogun, R. A. (2022). The effects of race on acute kidney injury. *J. Clin. Med.* 11 (19), 5822. doi: 10.3390/jcm11195822

Hassan, M. O., Owoyemi, I., Abdel-Rahman, E. M., Ma, J. Z., and Balogun, R. A. (2021). Association of race with in-hospital and post-hospitalization mortality in patients with acute kidney injury. *Nephron* 145 (3), 214–224. doi: 10.1159/000511405

Hsieh, P. H., Chang, Y. H., Chen, S. H., Ueng, S. W., and Shih, C. H. (2006). High concentration and bioactivity of vancomycin and aztreonam eluted from Simplex cement spacers in two-stage revision of infected hip implants: a study of 46 patients at an average follow-up of 107 days. *J. Orthop Res.* 24 (8), 1615–1621. doi: 10.1002/jor.20214

Hsieh, P. H., Huang, K. C., Lee, P. C., and Lee, M. S. (2009). Two-stage revision of infected hip arthroplasty using an antibiotic-loaded spacer: retrospective comparison between short-term and prolonged antibiotic therapy. *J. Antimicrob. Chemother.* 64 (2), 392–397. doi: 10.1093/jac/dkp177

Humes, H. D. (1988). Aminoglycoside nephrotoxicity. *Kidney Int.* 33 (4), 900–911. doi: 10.1038/ki.1988.83

Jung, J., Schmid, N. V., Kelm, J., Schmitt, E., and Anagnostakos, K. (2009). Complications after spacer implantation in the treatment of hip joint infections. *Int. J. Med. Sci.* 6 (5), 265–273. doi: 10.7150/ijms.6.265

Khwaja, A. (2012). KDIGO clinical practice guidelines for acute kidney injury. *Nephron Clin. Pract.* 120 (4), c179–c184. doi: 10.1159/000339789

Kurtz, S. M., Lau, E., Schmier, J., Ong, K. L., Zhao, K., and Parvizi, J. (2008). Infection burden for hip and knee arthroplasty in the United States. *J. Arthroplasty.* 23 (7), 984–991. doi: 10.1016/j.arth.2007.10.017

Li, Z., Maimaiti, Z., Li, Z. Y., Fu, J., Hao, L. B., Xu, C., et al. (2022). Moderate-to-severe malnutrition identified by the controlling nutritional status (CONUT) score is significantly associated with treatment failure of periprosthetic joint infection. *Nutrients* 14 (20), 4433. doi: 10.3390/nu14204433

Li, Z., Xu, C., and Chen, J. (2023). Articulating spacers: what are available and how to utilize them? *Arthroplasty* 5 (1), 22. doi: 10.1186/s42836-023-00167-6

Luu, A., Syed, F., Raman, G., Bhalla, A., Muldoon, E., Hadley, S., et al. (2013). Two-stage arthroplasty for prosthetic joint infection: a systematic review of acute kidney injury, systemic toxicity and infection control. *J. Arthroplasty* 28 (9), 1490–8.e1. doi: 10.1016/j.arth.2013.02.035

Menge, T. J., Koethe, J. R., Jenkins, C. A., Wright, P. W., Shinar, A. A., Miller, G. G., et al. (2012). Acute kidney injury after placement of an antibiotic-impregnated cement spacer during revision total knee arthroplasty. *J. Arthroplasty* 27 (6), 1221–7.e1-2. doi: 10.1016/j.arth.2011.12.005

Namba, R. S., Inacio, M. C., and Paxton, E. W. (2013). Risk factors associated with deep surgical site infections after primary total knee arthroplasty: an analysis of 56,216 knees. *J. Bone Joint Surg. Am.* 95 (9), 775–782. doi: 10.2106/JBJS.L.00211

O'Connor, M. E., Kirwan, C. J., Pearse, R. M., and Prowle, J. R. (2016). Incidence and associations of acute kidney injury after major abdominal surgery. *Intensive Care Med.* 42 (4), 521–530. doi: 10.1007/s00134-015-4157-7

Poston, J. T., and Koyner, J. L. (2019). Sepsis associated acute kidney injury. *BMJ* 364, k4891. doi: 10.1136/bmj.k4891

Premkumar, A., Kolin, D. A., Farley, K. X., Wilson, J. M., McLawhorn, A. S., Cross, M. B., et al. (2021). Projected economic burden of periprosthetic joint infection of the hip and knee in the United States. *J. Arthroplasty* 36 (5), 1484–1489.e3. doi: 10.1016/j.arth.2020.12.005

Privratsky, J. R., Fuller, M., Raghunathan, K., Ohnuma, T., Bartz, R. R., Schroeder, R., et al. (2023). Postoperative acute kidney injury by age and sex: A retrospective cohort association study. *Anesthesiology* 138 (2), 184–194. doi: 10.1097/ALN.0000000000004436

Puhto, A. P., Puhto, T. M., Niinimaki, T. T., Leppilahti, J. I., and Syrjala, H. P. (2014). Two-stage revision for prosthetic joint infection: outcome and role of reimplantation microbiology in 107 cases. *J. Arthroplasty.* 29 (6), 1101–1104. doi: 10.1016/j.arth.2013.12.027

Reed, E. E., Johnston, J., Severing, J., Stevenson, K. B., and Deutscher, M. (2014). Nephrotoxicity risk factors and intravenous vancomycin dosing in the immediate postoperative period following antibiotic-impregnated cement spacer placement. *Ann. Pharmacother.* 48 (8), 962–969. doi: 10.1177/1060028014535360

Rybak, M. J., Albrecht, L. M., Boike, S. C., and Chandrasekar, P. H. (1990). Nephrotoxicity of vancomycin, alone and with an aminoglycoside. *J. Antimicrob. Chemother.* 25 (4), 679–687. doi: 10.1093/jac/25.4.679

Shohat, N., Bauer, T., Buttaro, M., Budhiparama, N., Cashman, J., Della Valle, C. J., et al. (2019). Hip and knee section, what is the definition of a periprosthetic joint infection (PJI) of the knee and the hip? Can the same criteria be used for both joints?: proceedings of international consensus on orthopedic infections. *J. Arthroplasty.* 34 (2S), S325–S327. doi: 10.1016/j.arth.2018.09.045

Springer, B. D., Lee, G. C., Osmon, D., Haidukewych, G. J., Hanssen, A. D., and Jacofsky, D. J. (2004). Systemic safety of high-dose antibiotic-loaded cement spacers after resection of an infected total knee arthroplasty. *Clin. Orthop Relat. Res.* 427), 47–51. doi: 10.1097/01.blo.0000144476.43661.10

Theil, C., Riegel, R. F., Gosheger, G., Schwarze, J., Schmidt-Braekling, T., and Moellenbeck, B. (2021). Acute renal failure after the first stage of a 2-stage exchange for periprosthetic joint infection. *J. Arthroplasty.* 36 (2), 717–721. doi: 10.1016/j.arth.2020.08.028

Thongprayoon, C., Kaewput, W., Thamcharoen, N., Bathini, T., Watthanasuntorn, K., Salim, S. A., et al. (2019). Acute kidney injury in patients undergoing total hip arthroplasty: A systematic review and meta-analysis. *J. Clin. Med.* 8 (1):66. doi: 10.3390/jcm8010066

Valenzuela, M. M., Odum, S. M., Griffin, W. L., Springer, B. D., Fehring, T. K., and Otero, J. E. (2022). High-dose antibiotic cement spacers independently increase the risk of acute kidney injury in revision for periprosthetic joint infection: A prospective randomized controlled clinical trial. *J. Arthroplasty.* 37 (6S), S321–S326. doi: 10.1016/j.arth.2022.01.060

Wiedermann, C. J., Wiedermann, W., and Joannidis, M. (2010). Hypoalbuminemia and acute kidney injury: a meta-analysis of observational clinical studies. *Intensive Care Med.* 36 (10), 1657–1665. doi: 10.1007/s00134-010-1928-z

Yadav, A., Alijanipour, P., Ackerman, C. T., Karanth, S., Hozack, W. J., and Filippone, E. J. (2018). Acute kidney injury following failed total hip and knee arthroplasty. *J. Arthroplasty.* 33 (10), 3297–3303. doi: 10.1016/j.arth.2018.06.019

Yayac, M., Aman, Z. S., Rondon, A. J., Tan, T. L., Courtney, P. M., and Purtill, J. J. (2021). Risk factors and effect of acute kidney injury on outcomes following total hip and knee arthroplasty. *J. Arthroplasty.* 36 (1), 331–338. doi: 10.1016/j.arth.2020.07.072

Zmistowski, B., Karam, J. A., Durinka, J. B., Casper, D. S., and Parvizi, J. (2013). Periprosthetic joint infection increases the risk of one-year mortality. *J. Bone Joint Surg. Am.* 95 (24), 2177–2184. doi: 10.2106/JBJS.L.00789

frontiers | Frontiers in Cellular and Infection Microbiology

TYPE Review
PUBLISHED 03 October 2023
DOI 10.3389/fcimb.2023.1275086

OPEN ACCESS

EDITED BY
Chaofan Zhang,
First Affiliated Hospital of Fujian Medical University, China

REVIEWED BY
Erivan S. Ramos-Junior,
Augusta University, United States
Anna Benini,
University of Verona, Italy

*CORRESPONDENCE
Yuanchen Ma
mayuanchen@gdph.org.cn
Zhantao Deng
dengzhantao@gdph.org.cn
Feng-Juan Lyu
44238553@qq.com

†These authors have contributed equally to this work

RECEIVED 09 August 2023
ACCEPTED 05 September 2023
PUBLISHED 03 October 2023

CITATION
Xie Y, Peng Y, Fu G, Jin J, Wang S, Li M, Zheng Q, Lyu F-J, Deng Z and Ma Y (2023) Nano wear particles and the periprosthetic microenvironment in aseptic loosening induced osteolysis following joint arthroplasty.
Front. Cell. Infect. Microbiol. 13:1275086.
doi: 10.3389/fcimb.2023.1275086

Nano wear particles and the periprosthetic microenvironment in aseptic loosening induced osteolysis following joint arthroplasty

Yu Xie[1,2†], Yujie Peng[1,2†], Guangtao Fu[1], Jiewen Jin[3], Shuai Wang[1], Mengyuan Li[1], Qiujian Zheng[1], Feng-Juan Lyu[4*], Zhantao Deng[1*] and Yuanchen Ma[1*]

[1]Department of Orthopedics, Guangdong Provincial People's Hospital (Guangdong Academy of Medical Sciences), Southern Medical University, Guangzhou, China, [2]Shantou University Medical College, Shantou, China, [3]Department of Endocrinology, The First Affiliated Hospital of Sun Yat-sen University, Guangzhou, China, [4]The Sixth Affiliated Hospital, School of Medicine, South China University of Technology, Guangzhou, China

Joint arthroplasty is an option for end-stage septic arthritis due to joint infection after effective control of infection. However, complications such as osteolysis and aseptic loosening can arise afterwards due to wear and tear caused by high joint activity after surgery, necessitating joint revision. Some studies on tissue pathology after prosthesis implantation have identified various cell populations involved in the process. However, these studies have often overlooked the complexity of the altered periprosthetic microenvironment, especially the role of nano wear particles in the etiology of osteolysis and aseptic loosening. To address this gap, we propose the concept of the "prosthetic microenvironment". In this perspective, we first summarize the histological changes in the periprosthetic tissue from prosthetic implantation to aseptic loosening, then analyze the cellular components in the periprosthetic microenvironment post prosthetic implantation. We further elucidate the interactions among cells within periprosthetic tissues, and display the impact of wear particles on the disturbed periprosthetic microenvironments. Moreover, we explore the origins of disease states arising from imbalances in the homeostasis of the periprosthetic microenvironment. The aim of this review is to summarize the role of relevant factors in the microenvironment of the periprosthetic tissues, in an attempt to contribute to the development of innovative treatments to manage this common complication of joint replacement surgery.

KEYWORDS

microenvironment, homeostatic imbalance, joint prothesis, joint arthroplasty, aseptic loosening

1 Introduction

Septic arthritis occurs when bacteria invade the joint cavity, resulting in the infection of joint cavity and joint function impairment. Joint arthroplasty is an option for end-stage septic arthritis combined with successful control of infection by anti-biotic medications. It is also the surgical option for end-stage hip and knee arthritis due to developmental anomaly, degenerative changes, or autoimmune diseases. This surgical procedure replaces part of the arthritic joint with a plastic, metal, or ceramic prosthesis, aiming to restore normal joint function and improve patients' quality of life. The evolution of joint replacement techniques has come a long way since the first artificial hip prosthesis was implanted in 1891, using ivory femoral heads (Trebše and Mihelič, 2012), with millions of patients benefiting from this procedure (Katti, 2004; Huang et al., 2012; Singh et al., 2019).

Despite the advances in the biomaterials and improved biocompatibility over the years, complications such as osteolysis persist due to the inevitable release of wear particles (Kapadia et al., 2015; Hodges et al., 2021). The National Joint Registry database records millions of annual primary joint replacement surgeries, with approximately 4-6% requiring joint revision after 10 years, and the revision rate increases over time. Aseptic loosening, characterized by the unexplained loosening of the joint prosthesis without mechanical causes or infection, is the leading cause of joint revision, accounting for over 30% of revision surgeries. Consequently, tens of thousands of individuals undergo revision arthroplasty each year. Understanding the pathogenesis following joint arthroplasty is crucial for the prevention and treatment of these complications (Sadoghi et al., 2013).

Current studies on tissue pathology after prosthesis implantation have identified various cell populations involved in the process, including osteoblasts, osteoclasts, osteocytes, fibroblasts, macrophages, and inflammatory cells. However, there is a paucity of literature describing the interaction between these cells and the altered periprosthetic microenvironment. The periprosthetic microenvironment is a highly intricate environment comprising various cells and extracellular matrix components that work together to maintain microenvironmental homeostasis. Nano wear particles, which is the result of continuous and intense wear of the artificial joint, is a major contributor to the periprosthetic microenvironment and plays an important role in the development of post-implantation inflammation and aseptic loosening.

In this review, we first recall the histological changes occurred after prosthetic implantation, then summarize the cellular changes in the periprosthetic microenvironment, and further put a focus on the disturbance of nano wear particles of the metal implants on the periprosthetic microenvironment. In the last, we also look into cell-cell interactions after prosthetic implantation. Furthermore, we examine previous studies on the mechanisms associated with post-implantation prostheses to gain a better understanding of the changes occurring in the periprosthetic tissue microenvironment and the mechanisms underlying complications. The aim of this review is to summarize the role of relevant factors in the microenvironment of the periprosthetic tissues, and the mechanisms underlying cell-cell and cell-environment interactions caused by imbalances in the periprosthetic tissue microenvironment, therefore contributing to the development of innovative treatments.

2 Histological changes after prosthetic implantation

2.1 Remodeling of the periprosthetic tissue

The normal joint structure consists of bone, cartilage, and the synovial joint (Wright et al., 1973). After joint arthroplasty, the new composition of the joint includes bone, prosthesis, synovial joint, its newly formed synovial tissue, and joint synovial fluid (Athanasou, 2002) (Figure 1). The bone undergoes a series of healing processes, including inflammation, hematoma formation, reparative tissue formation, callus formation, and bone remodeling and maturation (Gallo et al., 2013). Cartilage repair may also occur, but the rate and extent of repair can vary and may not occur in all cases.

In the immediate aftermath of surgery, the body responds to the surgical trauma and the presence of the foreign object (the prosthesis) with an acute inflammatory response. This response involves the accumulation of fluid and immune cells around the prosthesis. Hematoma formation is a natural outcome of this inflammation and plays a vital role in the bone healing process. It occurs when blood leaks from damaged blood vessels and accumulates in the surrounding tissue, providing growth factors and a barrier between the prosthesis and the surrounding tissues. Subsequently, reparative tissue, also known as granulation tissue, forms around the implant. This tissue consists of fibroblasts and blood vessels and acts as a scaffold for new bone formation. Over time, the reparative tissue becomes calcified and forms a callus, which provides support to the surrounding bone. In the final phase of bone healing, the callus undergoes remodeling and maturation. This process allows the bone to regain its original strength and structure while integrating the prosthesis into the surrounding bone. Eventually, the artificial joint replaces the original joint as part of the joint (Athanasou, 2002).

Following the removal of chronically inflamed synovial tissue during joint replacement surgery, over time residual synovial tissue and regenerated synovial tissue form a new synovial component, which contains a lining layer and a sub-lining layer. The synovium is composed of highly vascularized and fibrotic connective tissue infiltrated by macrophages and dendritic cells. The regenerated synovial tissue covers the implant and serves as a smooth gliding surface for joint movement. Periprosthetic pseudomembranes are often observed in pathological states such as aseptic loosening, indicating a poor prognosis for prosthetic implantation (Konttinen et al., 2001; Kung et al., 2015). The combined synovial and periprosthetic membranes are referred to as the "synovial-like interface membrane" (SLIM). The synovial fluid produced by the new synovial tissue contains hyaluronic acid, lubricin, and various phosphatidylcholines, with protein and phospholipid concentration

10.3389/fcimb.2023.1275086

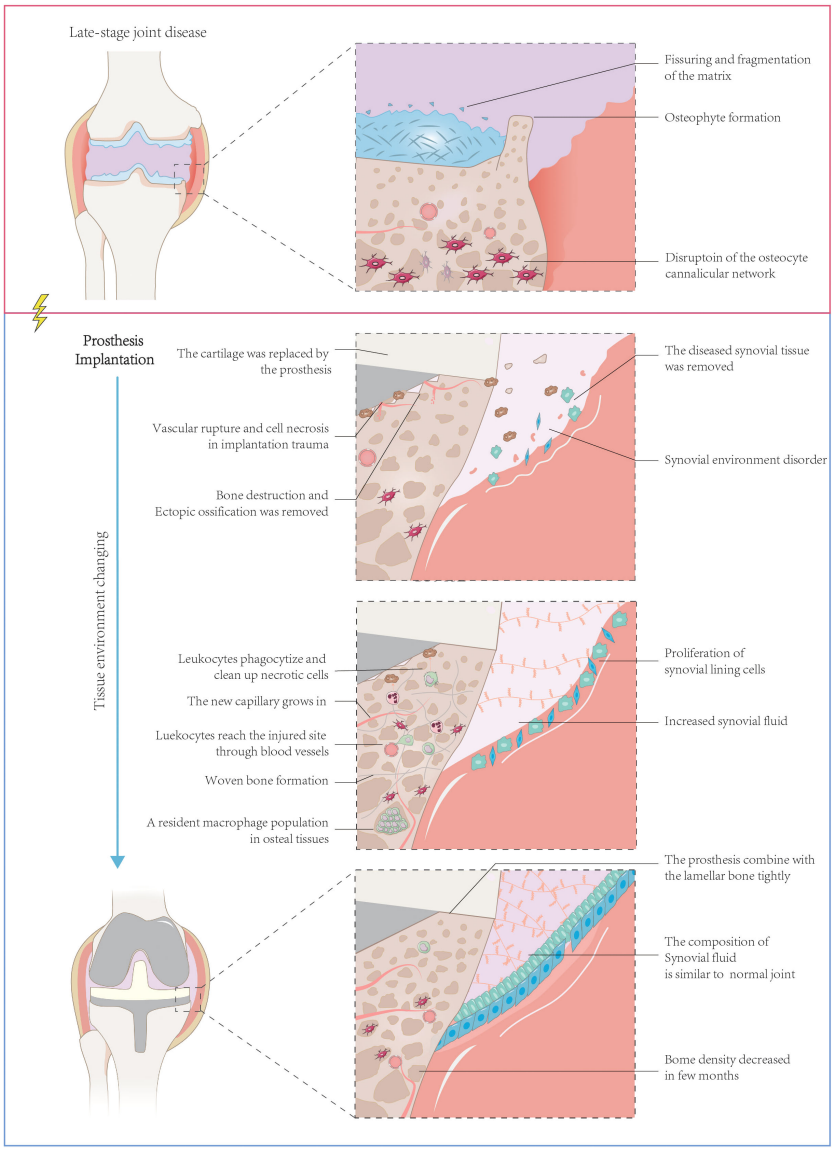

FIGURE 1
Structure of the artificial joint structure and sequential changes after prosthesis implantation. Artificial joint implantation for end-stage joint disease involves a process of removing damaged cartilage, synovial tissue, and osteophytes, followed by implanting a prosthesis composed of bone and artificial elements. The initial removal leads to joint tissue trauma and potential tissue necrosis, along with diminished synovial function. The body's reparative processes subsequently get triggered, which involves phagocytosing necrotic tissue, forming woven bone, regrowing microvessels, and repairing synovial tissue, and increasing synovial fluid production. Over time, the prosthesis tightly integrates with the bone, although a decrease in bone density may occur post-implantation. Despite this, synovial function is ultimately restored, and the composition of synovial fluid in the artificial joint mirrors that of a normal one.

levels comparable to normal synovial fluid. However, the concentration of hyaluronic acid decreases, reducing fluid viscosity and increasing the risk of joint abrasion (Mazzucco et al., 2004).

2.2 Appearance of nano wear particles after prosthetic implantation

Elderly patients undergo a significant number of gait cycles per year, ranging from 500,000 to 1 million (Goodman et al., 2014). This continuous and intense wear action exerts strain on the artificial joint, resulting in the generation of wear particles, referred to as prosthetic debris. These wear particles are dispersed throughout the joint fluid along the bone-implant interface (Schmalzried et al., 1992; Revell, 2008). The quantity, size, and origin of these particles influence the extent of bone loss and the number and depth of resorption sites (Saleh et al., 2004; Goodman, 2007). Furthermore, the presence of wear particles in the periprosthetic microenvironment can induce the accumulation of inflammatory cells, leading to bone destruction and disruption of the microenvironment (Jacobs et al., 2006).

2.3 The onset of aseptic loosening

When the equilibrium of the prosthetic microenvironment is disrupted by factors such as wear particles, it can give rise to the development of disease states, notably aseptic loosening, where the rate of particle accumulation can surpass the body's ability to maintain microenvironmental balance, resulting in periprosthetic osteolysis (PPOL) (Shanbhag et al., 1994; Maloney and Smith, 1996; Shanbhag et al., 2002). Aseptic loosening often accompanies periprosthetic osteolysis and an inflammatory response. Additionally, it stands as a significant reason for revision arthroplasty (Maradit Kremers et al., 2015; Singh et al., 2019). Therefore, although significant advancements have been made in prosthetic materials, it remains crucial to prolong the lifespan of prosthetics and minimize particle production to mitigate the risk of aseptic loosening (Couto et al., 2020).

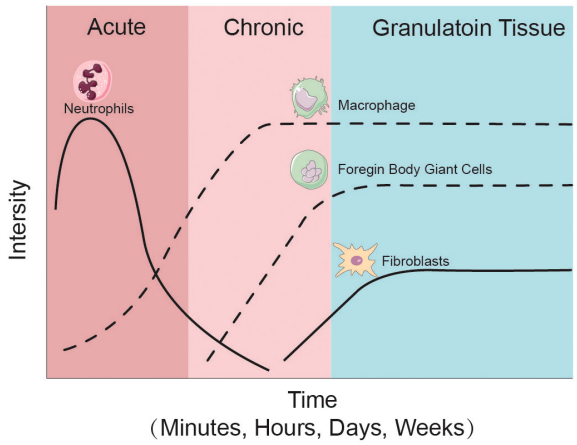

FIGURE 2
Cellular changes after joint implantation. During the initial phase of prosthesis implantation, neutrophils, as representatives of the acute inflammatory response, are the first to enter the cellular repair response at the site of injury, followed by macrophages and foreign body giant cells as representative cells of the chronic response in the prosthetic microenvironment. At the same time the repair of new capillaries and fibrous tissues gradually proceeds and eventually granulation tissue is formed.

3 The cellular periprosthetic microenvironment after prosthetic implantation

The microenvironment refers to the extracellular matrix (ECM) and cells that surround and support target cells. In the context of arthroplasty and prosthesis implantation, the microenvironment encompasses the prosthesis itself, released wear particles, bone-forming lineage cells, immune cells, fibroblasts, and the ECM, which forms a complex network structure that influences the behavior of cells within the microenvironment and plays a crucial role in maintaining homeostasis (Buckley et al., 2021). Here we first analyze the cellular components in the periprosthetic microenvironment, which include immune cells, osteogenic lineage cells forming the joint, and other cells associated with tissue repair processes.

3.1 Activation of immune cells in the periprosthetic microenvironment

Various types of immune cells respond to prosthetic implantation. Leukocytes, such as neutrophils and monocytes, migrate from the vascularized tissue to the site of damage during the acute inflammatory response, as illustrated in Figure 2 and Figure 3A. As illustrated in Figure 2, neutrophils release proteases, lysozymes, and reactive radicals in the form of extracellular traps (NETs). This process contributes to opsonization, clearance, and scavenging at the implant site (Jhunjhunwala et al., 2015; Jorch and Kubes, 2017). However, neutrophils appear transiently and are subsequently replaced by macrophages. Prolonged accumulation of neutrophils after a metal implant may indicate a potential adverse reaction to the metal implant (Grammatopoulos et al., 2016). Mast cells also participate in the acute inflammatory response to the implant by releasing histamine, which recruits macrophages to the implant site by inducing the expression of adhesion molecules on endothelial cells (Zdolsek et al., 2007). Simultaneously, macrophages produce IL-1α, IL-1β, and TGFβ, which recruit aggregates of neutrophils (St. Pierre et al., 2010; Akbar et al., 2012). Macrophages can originate from resident macrophages in bone or differentiate from monocytes in blood vessels. They play a crucial role in clearing the debris at injury site during the subsequent inflammatory response. Eosinophils and dendritic cells are also observed in the acute inflammatory response. Dendritic cells play a role in inducing and programming T cells, while the specific role of eosinophils remains unclear (Keselowsky and Lewis, 2017).

In the adaptive immune response triggered by prostheses, particularly metal implants, lymphocytes, including T cells and B cells, play a crucial role in the normal biological response to the implant (U.S. Food and Drug Administration, 2019). CD4+ T helper cells (Th) exhibit diverse functional responses to different metal components, including proliferation, expansion, and expression of phenotypic markers associated with activation. Tregs cells promote wound healing by inhibiting the aggregation of inflammatory cells and macrophages (Nosbaum et al., 2016; Revell et al., 2016; Markel et al., 2018). CD8+ T cells can be detected in the vicinity of the prosthetic implant, although their involvement in the implant response remains uncertain (Hallab et al., 2012). Histological evidence finds abundant number of T cells in failed implant tissues. However, the presence of T cells near an implant does not necessarily indicate a maladaptive response (Hasegawa et al., 2016; Paukkeri et al., 2016). The response of B cells to implants is not yet fully understood, but their role in prosthetic implantation may involve B cell-mediated type I, II, and III hypersensitivity reactions. Signs of B cell activation have been observed in failed implants (Mittal et al., 2013).

3.2 Activation of osteogenic lineage cells after prosthetic implantation

The trauma caused by prosthetic implantation disrupts bone homeostasis and activates MSCs as well as osteogenic lineage cells, including osteocytes and osteoblasts, leading to new bone formation. As illustrated in Figure 3B, MSCs are present in the bone marrow stroma, periosteum, and local microvascular walls, which can differentiate into osteoblasts. During the process of bone formation, MSCs are stimulated by cytokines to differentiate into the osteoblast lineage, resulting in the formation of collagen fibers and bone-like tissue composed of mesenchymal cells, pre-osteoblasts, and osteoblasts (Marco et al., 2005; Kuzyk and Schemitsch, 2011). Osteoblasts play a vital role in bone deposition and implant osseointegration. They are primarily responsible for the synthesis of most bone matrix components, regulation of bone mineralization, and provide the foundation for the growth of new bone tissue. Consequently, osteoblasts play a critical role in postoperative implant osseointegration. Osteoclasts are also involved in implant osseointegration and normal bone remodeling. Activation of osteoclasts leads to bone resorption, followed by the activation of osteoblasts and mineralization of new bone tissue (Zhang et al., 2020). Eventually, a new balance is established in bone regeneration and osteolysis. Osteoblasts that are surrounded by the newly generated bone extracellular matrix differentiate into osteocytes, which constitute the majority of cells within the bone and contribute to maintaining bone homeostasis through their involvement in matrix synthesis, regulation of cytokines, and other functions (Pajarinen et al., 2017).

3.3 Alterations in other cells during prosthetic implantation

Fibroblasts and endothelial cells play crucial roles in tissue repair following prosthesis implantation (Figure 3C). Fibroblasts migrate to the injury site within 2-10 days of implantation. They contribute to tissue repair by producing ECM, especially type I and type III collagen. Simultaneously, proliferating endothelial cells facilitate the formation of new blood vessels, promoting the development of granulation tissue at the injury site. Over time, the granulation tissue gradually diminishes along with fibroblasts,

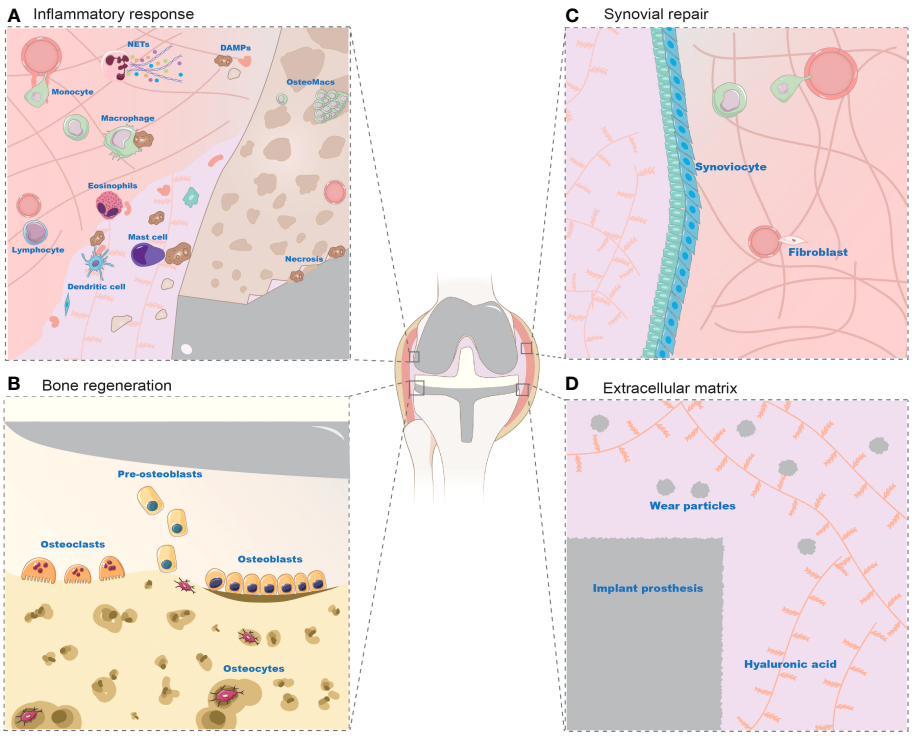

FIGURE 3
Cell changes in periprosthetic environment after prosthesis implantation. **(A)**: Inflammatory Response Post-Implantation **(B)**: Bone Regeneration Post-Implantation **(C)**: Synovial Repair Post-Implantation **(D)**: Extracellular Matrix Post-Implantation The prosthetic microenvironment comprises cells and extracellular matrix, playing roles in inflammatory response, bone regeneration, and synovial repair. Cells like neutrophils, monocytes, eosinophils, mast cells, dendritic cells, and lymphocytes contribute to the inflammatory response. Neutrophils are the first to converge on the damaged area, eliminating DAMPs (necrotic cells and bone debris) via NETs (extracellular traps). Monocytes migrate to the prosthetic microenvironment, differentiating into macrophages to phagocytose necrotic cells, alongside tissue-resident macrophages. However, the exact mechanisms of eosinophils, mast cells, dendritic cells, and lymphocytes are not fully elucidated. During bone regeneration, mesenchymal stem cells differentiate into osteoblasts to stimulate osteogenesis. Osteoblasts subsequently encapsulated by bone form osteocytes, while osteoclasts are responsible for bone resorption. The synovial membrane consists of synovial-like and fibroblast-like cells, with macrophages aiding in its regeneration and endothelial cells participating in tissue repair. The extracellular matrix, largely studied in the context of wear particles, is an inevitable byproduct in the prosthetic microenvironment, dispersing within the synovial fluid and tissue areas of the joint.

leaving behind a collagenous scar. M2 Macrophages also play a role in this process by secreting growth factors that stimulate fibroblasts and endothelial progenitor cells, as well as guiding ECM remodeling (Krafts, 2010). Additionally, fibroblasts may contribute to the pathological process of bone resorption through the secretion of pro-inflammatory factors (Koreny et al., 2006).

Post implantation, the synovial membrane consists of a thin layer of cells containing macrophage-like synoviocytes and fibroblast-like synoviocytes, and ECM similar to that of a normal joint. The regeneration capacity of synovial tissue are postulated to be originated from local synovial mesenchymal stem cells (MSCs). MSCs is the precursor for mesenchymal lineage (Huang et al., 2011; Lv et al., 2014), which harbor in many tissue sources (Lv et al., 2012) and become the key cell type for tissue regeneration in recent years (Leung et al., 2014; Deng et al., 2020; Qi et al., 2020; Chen et al., 2022). Some literature also suggests that synovial MSCs may manifest as fibroblast-like synoviocytes (Kung et al., 2015; Li et al., 2019; Li et al., 2020).

4 The disturbance of nano wear particles on the periprosthetic microenvironment

A persistent low-grade chronic inflammation could be triggered by nano wear particles surrounding the prosthesis to cause aseptic loosening (Marmotti et al., 2020). As depicted in Figures 3D, Figure 4, wear particles exhibit resistance to enzymatic degradation and are not readily absorbed by the body, leading to their accumulation in the periprosthetic microenvironment. The persistent chronic foreign body reaction diminishes local bone formation and augments osteolysis, ultimately culminating in aseptic loosening.

4.1 Nano wear debris induces inflammation in aseptic loosening

Wear particles primarily activate an innate immune response dominated by macrophages, with the involvement of monocytes, mast cells, and dendritic cells, as illustrated in Figure 4C. However, there is still ongoing debate regarding the involvement of lymphocytes in the process of aseptic loosening.

Osteoclasts and tissue-resident macrophages are recognized as the initial cells that encounter wear debris (Lenz et al., 2009; Goodman and Ma, 2010; Smith et al., 2010; Lin et al., 2015). Upon activation, these cells produce pro-inflammatory cytokines and chemokines, which attract monocytes and dendritic cells and amplify the overall inflammatory response. Following the presence of wear particles in the periprosthetic environment, resident macrophages surrounding the prosthesis identify the foreign body through sensing, chemotaxis, phagocytosis, and adaptive stimulation (Medzhitov, 2008). The magnitude of the macrophage

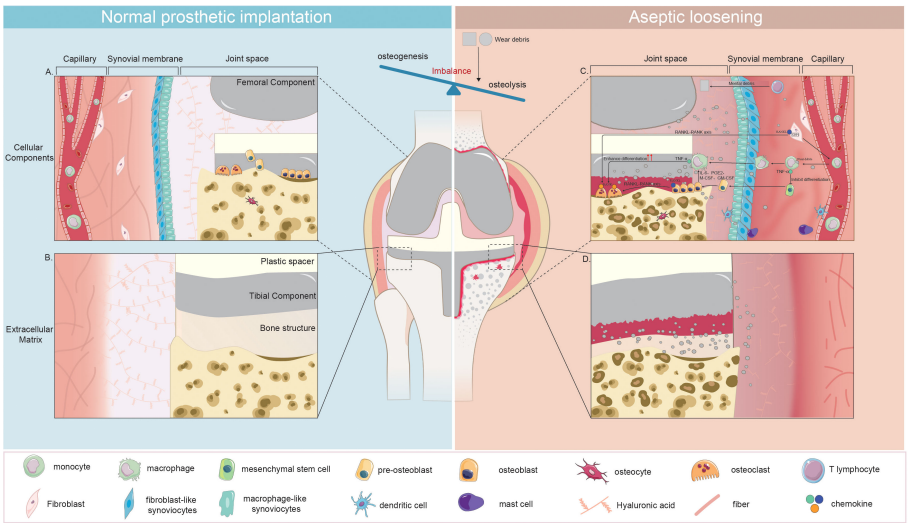

FIGURE 4
Disruption of Microenvironment Homeostasis in Joint Prosthesis: Cellular and Extracellular Changes Leading to Aseptic Loosening. **(A)**: Cellular Components Post-Implantation with homeostaisis **(B)**: Extracellular Matrix Post-Implantation with homeostaisis **(C)**: Changes in Cellular Components during Aseptic Loosening **(D)**: Changes in Extracellular Matrix during Aseptic Loosening Following implantation, the microenvironment within the joint prosthesis initially attains stability. This is evidenced by the harmonious presence of diverse cell types, including osteoblasts, osteoclasts, osteocytes, synovial cells, and fibroblasts and the establishment of a steady extracellular matrix that includes the prosthesis, bone, and synovium. However, this state of balance is disrupted when aseptic loosening begins. This process initiates as wear particles trigger the differentiation of monocytes into macrophages. The macrophages that form from this differentiation process not only attract additional macrophages but also inhibit the differentiation of osteoblasts by releasing cytokines such as TNF-α. Concurrently, fibroblasts stimulate increased activity in osteoclasts via the RANKL-RANK axis. These changes lead to an overall increase in osteoclast activity and a suppression of osteogenesis. The response also includes participation from mast cells and dendritic cells. In addition, it is suggested that T lymphocytes participate in this process when metal wear particles are generated. The culmination of these alterations results in bone destruction, a roughened surface of the prosthesis, and an increase in synovial inflammation, all of which contribute to aseptic loosening.

response is intensified by larger abrasive particles. When particles are small (<10 μm), individual macrophages and foreign body macrophages can effectively adhere to and phagocytose them. For particles that cannot be efficiently phagocytosed by individual macrophages or foreign body macrophages (20-100 μm), macrophages can fuse together to form multinucleated macrophages or multinucleated foreign body macrophages that surround or isolate large particles, eventually resulting in the formation of foreign body granulomas (Nich et al., 2013). Granulomas comprise histiocytes, fibroblasts, and multinucleated foreign body giant cells (Shen et al., 2006), while monocytes continue to differentiate into macrophages, participating in the reaction during this process.

Current hypotheses propose that wear particle-engulfing macrophages exhibit an MΦ phenotype, and wear particles induce the polarization of macrophages into a pro-inflammatory M1 phenotype. This, in turn, promotes osteoclast maturation, leading to increased bone resorption and periprosthetic osteolysis (Mandelin et al., 2004; Masui et al., 2004; Sabokbar et al., 2015; O'Brien et al., 2016) (Figure 5). Simultaneously, macrophages cause further macrophage aggregation through the release of pro-inflammatory cytokines, such as interleukin 1α (IL1-α), IL1-β, tumor necrosis factor α (TNF-α), IL-6, IL-1, growth factors such as macrophage colony-stimulating factor-1), and chemokines such as macrophage inflammatory protein-1 α (MIP-1a) and monocyte chemoattractant protein-1 (MCP-1) (Gibon et al., 2017). Other macrophages, not activated by phagocytosis, undergo polarization through membrane receptor interactions by toll-like receptor 4 (TLR4), CD11b, CD14, wherein TLR4 is induced to activate the nuclear factor kappa-B (NF-κB) pathway primarily via the adapter protein myeloid differentiation primary response gene 88 (MyD88) or directly through the interferon regulatory Factor 3 (IRF3) pathway, resulting in cytokine release. Our previous study revealed a significant downregulation of sirtuin 1 (SIRT1) in macrophages stimulated by metal nanoparticles via the NF-κB pathway (Deng et al., 2017a). Following activation, an increased number of macrophages contribute to an enhanced osteolytic effect (Akira et al., 2001; Tuan et al., 2008). Moreover, macrophages also play a role in fibrosis and attempt tissue repair and restoration. During this phase, M2 phenotype macrophages exhibit an anti-inflammatory function by releasing cytokines (IL-4, IL-10, IL-13), regulating ongoing tissue damage, isolating granuloma-like structures, and attempting to isolate nondegradable materials (Mosser and Edwards, 2008; Purdue, 2008; Sun et al., 2021).

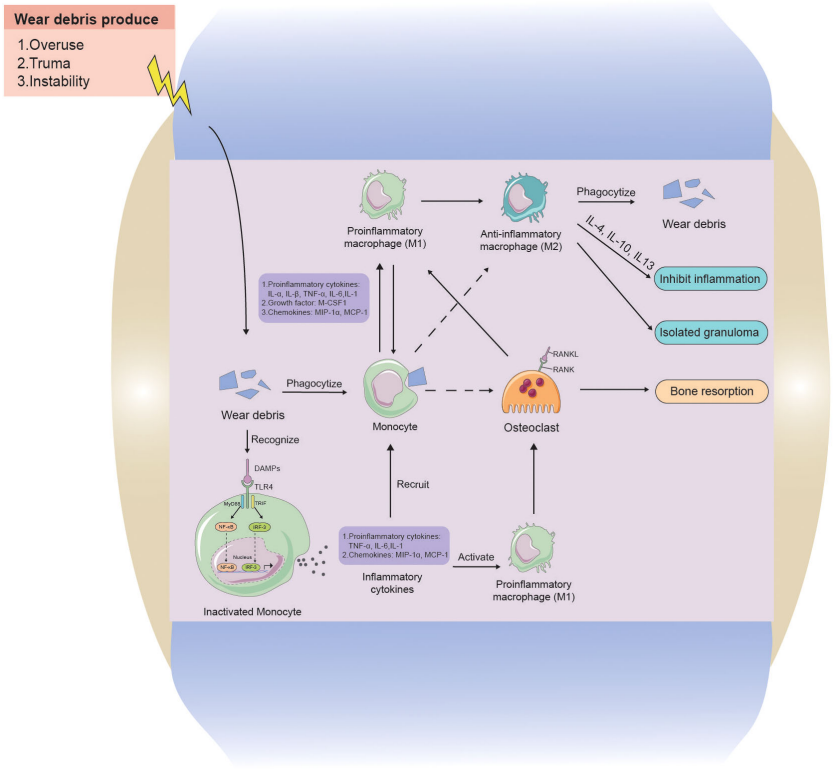

FIGURE 5
The interaction between wear particles and macrophages in aseptic loosening. Wear particles of artificial joint prosthesis are often released into the prosthetic microenvironment because of overuse, Instability, and trauma factors. Monocytes can swallow wear particles, and when wear particles are swallowed by phagocytes, they will aggravate inflammation by releasing pro-inflammatory cytokines, chemokines, and M-CSF1 to activate M1 phenotype macrophages and promote the release of more inflammatory factors. Whereas osteoclast growth increases, causing increased osteolysis. Monocytes can also recognize stimulatory signals from wear particles through cell contact and release cytokines to further recruit more macrophages, while activating macrophages, causing more osteolysis. M2 phenotype macrophages and M1 phenotype macrophages can interconvert, with M2 phenotype anti-inflammatory macrophages phagocytosing wear particles to lyse and releasing cytokines to inhibit inflammation, as well as encapsulating granulomas to isolate inflammatory lesions.

Infiltration of mast cells (Solovieva et al., 1996; Qiu et al., 2005) and dendritic cells (Kou and Babensee, 2010; Vaculová et al., 2018) can be observed in the periprosthetic microenvironment during aseptic loosening (Figure 4C). However, the mechanisms behind their involvement remain poorly understood. Concerning the effect of wear particles on dendritic cells (DCs), *in vitro* exposure to ultra-high-molecular-weight polyethylene (UHWMP) particles has demonstrated that wear particles can stimulate major histocompatibility complex (MHC) II expression and IL-12 production by activating TLR1/2 on the surface of DCs (Maitra et al., 2008). Furthermore, the inability of DCs to digest wear particles following phagocytosis leads to lysosome rupture and the release of histone proteases S and proteases B into the cytoplasm, triggering activation of pattern recognition receptors (PRRs) such as the NLR family pyrin domain containing 3 (NLRP3) inflammasome. This activation results in the release of IL-18 and IL-1β from the cells into the extracellular environment. In turn, these cytokines contribute to extracellular matrix lysis, the onset of periprosthetic inflammation, and bone resorption, ultimately leading to the development of osteolysis (Maitra et al., 2009).

Based on current literature, it has been established that lymphocytes play a crucial role in the development of aseptic lymphocyte-dominated vasculitis-associated lesion (ALVAL) in response to wear particle stimulation. However, the role of lymphocytes in aseptic loosening induced by wear particles remains controversial. Some studies have observed a greater aggregation of CD3+ T cells, particularly in metal-on-metal prostheses, in pathological tissue specimens (Hercus and Revell, 2001; Hopf et al., 2017). Conversely, other studies have reported lower levels of T cells in osteolysis tissue and the absence of cytokine release associated with T cells (Li et al., 2001). Furthermore, no significant increase in Th1, Th2, and CD3+ T cells was observed in osteolytic tissue compared to non-osteolytic tissue (Arora et al., 2003; Dapunt et al., 2014). Based on the available literature, it can be presumed that lymphocytes may not play a significant role in aseptic loosening. Existing studies, which are limited by small sample sizes, have primarily reported an increase in T lymphocytes in metal implants, potentially due to the coexistence of ALVAL. Therefore, further investigation is necessary to clarify the role of lymphocytes in aseptic loosening.

4.2 Impact of wear particles on bone forming lineage cells

The impact of wear particles on bone-forming lineage cells (MSCs, osteoblasts, osteocytes) is crucial in the osteolysis process within the prosthesis microenvironment in aseptic loosening (Figure 4C).

An increasing number of studies have demonstrated that wear particles not only activate macrophages and osteoclasts, leading to increased bone resorption, but also cause significant damage to MSCs. This damage prevents osteoblast differentiation and impairs bone formation, reducing cell viability and impairing the production of mineralized bone matrix (Goodman et al., 2006; O'Neill et al., 2013; Ebert et al., 2021). Animal experiments and cellular studies have revealed that wear particles inhibit MSCs' osteogenic differentiation, induce the production of pro-inflammatory cytokines such as IL-1β, IL-6, and TNF-α, upregulate receptor activator of nuclear factor-kappa B ligand (RANKL), and decrease osteoprotegerin (OPG) (Cai et al., 2013; Jiang et al., 2013). In response to titanium (Ti) particles, impaired MSCs activity and osteogenic differentiation depend on the phagocytosis of Ti particles. Additionally, granulocyte-macrophage colony stimulating factor (GM-GSF) disrupts cytoskeletal organization and induces MSCs to secrete IL-8 and GM-CSF, further reducing cell viability and osteogenic differentiation similar to the effects of phagocytosis of Ti particles (Okafor et al., 2006; Haleem-Smith et al., 2011). Although several signaling pathways have been observed to have adverse effects on MSCs due to wear particles, such as the NF-κB signaling pathway adversely affecting osteogenic differentiation (Lin et al., 2014), reduced involvement of the Wnt/β-actin signaling pathway in MSC differentiation to osteogenesis (Wang et al., 2016) and activation of the extracellular regulated protein kinases (ERK) signaling pathway (Lee et al., 2011), the number of studies on this topic is limited, and the signaling pathways involved in the inhibition of MSC differentiation induced by wear particles remain poorly understood.

Simultaneously, wear particles stimulate MSCs to express metalloproteinases through multiple signaling pathways. These metalloproteinases can cleave the collagen-rich, mineralized ECM of bone (Chen et al., 2018). Consequently, when matrix metalloproteinases are overexpressed and attach to the surface of the bone-prosthetic tissue, they can degrade the bone matrix and exacerbate periprosthetic osteolysis (Takei et al., 2004; Jonitz-Heincke et al., 2016).

Osteoblasts primarily interact with wear particles through phagocytosis, involving the internalization of the particles (Chiu et al., 2009, 5; Vermes et al., 2016). They also engage in non-phagocytic interactions with the particles (Granchi et al., 2003; Vermes et al., 2006). When particles enter the cytoplasm of osteoblasts, attachment to different cells causes swelling of intracellular organelles and rupture of cell membranes. Furthermore, particles can lead to DNA damage and activate DNA repair mechanisms, although no particles have been observed within the nucleus (Lee et al., 2013; Ribeiro et al., 2016). When particles attach to actin fibers, they significantly disrupt the cytoskeletal structure of osteoblasts, impeding cell function (Saldaña and Vilaboa, 2009; Lee et al., 2011; Lee et al., 2013). Our study has shown that the expression of SIRT1 is significantly downregulated in osteoblasts treated with particles. Additionally, particles can stimulate the production of inflammatory cytokines and induce apoptosis in osteoblasts through the NF-κB pathway (Deng et al., 2017b). Furthermore, our results suggest that the STAT/IL-6 pathway may mediate nanoparticle-induced inflammation and stimulate osteoclast formation (Deng et al., 2021). Moreover, particles inhibit the osteogenic differentiation of osteoblasts through the Wnt/β-catenin and bone morphogenic protein (BMP)/smad signaling pathways (Preedy et al., 2015; Nam et al., 2017; Sun et al., 2019). By secreting extracellular matrix (mainly type I collagen) and matrix metalloproteinases

along with their inhibitors such as tissue inhibitor of metalloproteinase (TIMP), osteoblasts wearing particles can inhibit the formation of type I precollagen through the NF-κB signaling (Roebuck et al., 2006; Vermes et al., 2006). This disruption also disturbs the balance between osteogenic matrix metalloproteinases and TIMP (Ma et al., 2006; Syggelos et al., 2013), resulting in decreased osseointegration and subsequent implant failure.

Osteoblasts reside in the mineralized matrix lumen and account for 90-95% of the cells in mineralized bone, with osteoclasts and osteocytes comprising only about 5% of the cells (Shiflett et al., 2019). In response to wear particle stimulation, osteoblasts shift from anabolic to catabolic, as evidenced by increased expression of catabolic markers such as cathepsin K and tartrate-resistant acid phosphatase (TRAP). This leads to periluminal remodeling, causing a significant increase in osteocyte lumen size (Atkins et al., 2009; Ormsby et al., 2016). Interestingly, according to Ormsby's study, osteoblast-induced bone loss in response to wear particles appears to be gender-specific, affecting only women (Ormsby et al., 2019).

4.3 Impact of wear particles on fibroblasts in the synovial membrane

The composition of the synovial membrane in aseptic loosening includes synovial tissue, regenerated synovial tissue, and the periprosthetic membrane between bone and cement or bone and implant, with fibroblasts comprising 70% of these components. During the dispersion of joint fluid along the bone-implant interface, wear particles can persist in the synovial membrane, leading to fibroblasts' involvement in wear particle-induced osteolysis (Rose et al., 2012). Wear particles can induce the expression of receptor activator of nuclear kappa-B (RANKL) in fibroblasts through various pathways, including the TLR-MyD88-RANKL pathway, the endoplasmic reticulum (ER) stress pathway, and the prostaglandin E2 (PGE2) receptor EP4 signaling pathway, thereby stimulating osteoblast differentiation (Tsutsumi et al., 2009; Wang et al., 2015; Li et al., 2018). However, it is important to note that this response may vary among patients.

5 Cell-cell interaction

To gain a better understanding of the complex periprosthetic environment and the interactions among different cell types involved in aseptic loosening, it is crucial to investigate cell communication. The periprosthetic environment encompasses osteogenic lineage cells and various immune cells, such as macrophages, osteoclasts, MSCs, osteoblasts, osteocytes, fibroblasts, mast cells, dendritic cells, and lymphocytes. Among these cell types, osteogenic lineage cells and immune cells play significant roles. Due to their spatial proximity, interactions between these cell types are inevitable, and studying these interactions could provide insights into the mechanisms underlying aseptic loosening (Okamoto et al., 2017). While much remains unknown, exploring cell-to-cell interactions studied in the context of osteolysis and other aspects of orthopedics could serve as a valuable starting point for future research aimed at developing new treatments.

5.1 Osteoimmunological interactions

Osteoimmunological interactions are essential for maintaining bone homeostasis and play a significant role in bone pathology, particularly in the process of aseptic loosening, where macrophages and osteoclasts dominate the innate immune response. Immune cells have the ability to influence osteoblastic lineage cells, and conversely, osteoblastic lineage cells may also regulate innate immunity in this process.

The proliferation, function and differentiation of MSCs could be affected by their local microenvironments (Huang et al., 2020). Studies exploring the interaction between macrophages and MSCs in aseptic loosening are still limited. Macrophages contribute to MSCs aggregation by secreting chemokines such as macrophage inflammatory protein 1 (MIP1α) and monocyte chemotactic protein-1 (MCP-1) (Huang et al., 2010). Furthermore, macrophages can inhibit the osteogenic differentiation of MSCs. In conditioned medium with Ti particles mimicking macrophage activation, macrophages induce the MSCs-mediated NF-κB signaling pathway in sclerostin via TNF-α. This inhibits Wnt and BMP signaling pathways, resulting in decreased runt-related Transcription Factor 2 (RUNX2) expression, alkaline phosphatase (ALP) activity, and bone mineralization in MSCs (Lee et al., 2012). On the contrary, particle-stimulated macrophages have been shown to stimulate MSCs to promote osteogenesis through IL-10 (Mahon et al., 2020). Recent studies have demonstrated that co-culturing MSCs with M2 macrophages promotes bone formation (Gao et al., 2021). Additionally, it has been observed that M1 macrophages inhibit the growth of MSCs, while M2 macrophages promote their growth (Lu et al., 2021). Therefore, it is possible that M1 macrophages inhibit osteogenic differentiation, whereas M2 macrophages promote bone formation in aseptic loosening.

Regarding the effect of MSCs on immune cells, it has been discovered that MSCs have an inhibitory effect on the inflammatory response. Blocking the secretion of the chemokine C-C-motif receptor (CCR1) in MSCs can lead to an increase in particles-induced osteolysis, suggesting that recruiting MSCs to inflamed areas helps limit inflammation and may contribute to bone regeneration (Gibon et al., 2012). Recent studies have also shown that MSCs can increase the ratio of M2/M1 cells, reducing bone resorption and enhancing bone formation (Shen et al., 2022; Kushioka et al., 2023). While MSCs primarily regulate adaptive immune responses in inflammatory diseases (Bernardo and Fibbe, 2013), an increasing number of studies indicate their crucial role in modulating innate immunity (Le Blanc and Mougiakakos, 2012). MSCs can induce macrophage polarization to an M2 anti-inflammatory phenotype through the paracrine secretion of PGE2, transforming growth factor β (TGF-β), indoleamine 2,3-dioxygenase (IDO), chemokine C-C motif ligand 2 (CCL2), and chemokine C-X-C Motif ligand 12 (CXCL12) (Pajarinen et al., 2017; Lu et al., 2021). Thus, MSCs may suppress the inflammatory

response by modulating the innate immune response in aseptic loosening.

Macrophages can aggregate in osteal tissues to form osteomas and are believed to play a crucial role in directing osteoblast function and mineralization. However, the interaction of site-specific macrophage populations with other cells has not been studied yet (Cho, 2015; Miron and Bosshardt, 2015). In the context of aseptic loosening, macrophages inhibit osteoblasts, leading to increased osteolysis. The release of cytokines, such as TNF-α, IL-6, IL-1β, and GM-CSF, stimulates the secretion of osteoblasts, including IL-6, PGE2, M-CSF, GM-CSF, MCP-1, and RANKL (Rodrigo et al., 2002; Vallés et al., 2008; Guo et al., 2013), which further recruit macrophages, increase osteoclast production, and inhibit osteoblast function. Osteoblasts can modulate the degree of inflammation in macrophages and regulate the macrophage response to particle stimulation through the release of soluble mediators. In an osteoblast-macrophage co-culture model, lower levels of TNF-α and IL-1β were detected, possibly due to the paracrine action of PGE2 from osteoblasts (Rodrigo et al., 2005). Furthermore, it has been found that when macrophages were co-cultured with osteoblasts, macrophages could produce lipoxin A4 (LXA4) to counteract polymethylmethacrylate (PMMA) induced cytokine production, and this production of LXA4 was only observed in the presence of osteoblasts (Li et al., 2009). These findings suggest that osteoblast-macrophage interactions contribute to the resolution of particle-induced inflammation.

Osteoclasts are the only cells in the body responsible for bone resorption and work together with osteoblasts to maintain the dynamic balance of bone metabolism. Osteoblasts interact with osteoclasts through secreted factors RANKL and osteoprotegerin (OPG). The binding of RANKL and RANK activates the NF-κB pathway, ultimately leading to osteoclast formation, while OPG serves as a decoy receptor for RANKL and negatively regulates osteogenesis. The ratio of RANKL/OPG determines the degree of osteoclast differentiation and function. Wear particles induce a shift from an anabolic phenotype to a catabolic phenotype in osteoblasts (Atkins et al., 2009), resulting in increased expression of cytokines mediating osteoclastogenesis (TNF-α, IL-1β, IL-6, IL-8, PGE2, M-CSF, MCP1, RANKL) and decreased OPG expression (Granchi et al., 2003; Pioletti and Kottelat, 2004; Atkins et al., 2009; Gordon, 2016). Recent studies have also identified a reverse signaling pathway of RANKL in osteoclast-osteoblast coupling, where osteoclasts promote osteoblast bone formation by secreting vesicular RANK and stimulating osteoblast differentiation. Signaling proteins and neurotrophins also play a significant role in the communication between osteoclasts and osteoblasts. Moreover, non-resorbing osteoclasts have been found to influence the function of osteoblasts under particle attack. Interestingly, recent research suggests that the intricate balance of bone homeostasis is maintained through communication between osteoblasts and osteoclasts using exosomes (Yuan et al., 2018). However, the roles of these interactions in aseptic loosening have not been studied extensively, and further research is needed to determine their importance.

The interaction between osteoclasts and MSCs is not well understood, but current research suggests that MSCs can regulate osteoclast activation and formation through paracrine secretion and the RANKL-RANK-OPG pathway. New studies have also shown that MSCs can inhibit osteoclasts, and stem cell exosomes can block osteoclast activation or differentiate into osteoblasts to regulate bone remodeling. BMSC derived exosomes have been demonstrated to activate osteogenesis and downregulate osteoclastogenesis through multiple pathways (Ma et al., 2022).

5.2 The interaction of fibroblasts with other cells

Apart from the interaction between immune cells and bone cells, limited research has been conducted on other types of cell-to-cell interactions within implant microenvironments. However, some evidence suggests that fibroblasts, when interacting with osteoclasts, also play a crucial role in maintaining microenvironment homeostasis in aseptic loosening. Studies have shown that fibroblasts in the periprosthetic environment can induce the differentiation of MSCs and peripheral blood mononuclear cells into mature osteoclasts, leading to local bone resorption or osteolysis through mechanisms involving RANKL and TNF-α (Sakai et al., 2002; Sabokbar et al., 2005). Recent research has found that fibroblasts can enhance osteoclast differentiation through X-box binding protein 1 (XBP1) mediated RANKL expression (Wang et al., 2017). Furthermore, fibroblasts on the bone surface can actively participate in bone resorption by degrading the bone matrix through the release of acidic components and bone-degrading enzymes, without the involvement of osteoclasts (Pap et al., 2003). In summary, fibroblasts can accelerate bone resorption around implants by promoting osteoclast differentiation and directly releasing bone-resorbing substances.

The role of osteoclasts in relation to fibroblasts has not been explored in the literature, and there is currently no available research on the interaction between osteogenic lineage cells and fibroblasts. The lack of literature on the interaction between osteoclasts and fibroblasts, as well as between osteoblasts and fibroblasts, highlights the need for further research in this area. Understanding the mechanisms underlying the interaction between these cell types may provide insight into the development and progression of aseptic loosening.

6 Conclusion

Aseptic loosening is a complex process involving biomaterials, host tissues, and the immune system. It is characterized by immune cell infiltration, cytokine production, osteoclast activation, bone resorption, and wear debris production. Factors such as long-term wear of the implant and disruption of microenvironment homeostasis contribute to aseptic loosening. Potential therapeutic targets include anti-inflammatory drugs, osteoclast inhibitors, and antioxidants, addressing chronic inflammation, bone resorption, and oxidative stress, respectively.

Despite the progress made in understanding aseptic loosening, current research mainly focuses on wear particle-induced cellular effects, while cell interactions and spatial distribution in the

prosthesis remain understudied. Therefore, future studies should concentrate on elucidating cell interactions using advanced technologies such as single-cell and spatial sequencing to uncover the complex relationships between various cell types and their functions in the microenvironment. Moreover, interdisciplinary collaboration among material scientists, biologists, and clinicians is essential for developing innovative solutions that bridge the gap between fundamental research and clinical applications.

Further research should investigate cellular interactions, spatial distribution in the microenvironment, and potential therapeutic targets, with the aim of developing a comprehensive understanding of the mechanisms underlying aseptic loosening. This knowledge will contribute to the development of innovative treatments that effectively prevent and manage this common complication of joint replacement surgery, ultimately improving patient outcomes and quality of life.

Author contributions

XY: Data curation, Formal Analysis, Investigation, Visualization, Writing – original draft. YP: Data curation, Investigation, Validation, Writing – review & editing. GF: Investigation, Validation, Writing – review & editing. JJ: Investigation, Writing – review & editing. SW: Investigation, Writing – review & editing. ML: Investigation, Writing – review & editing. QZ: Writing – review & editing, Funding acquisition, Supervision. FL: Funding acquisition, Writing – review & editing, Validation. ZD: Conceptualization, Funding acquisition, Project administration, Supervision, Writing – review & editing. YM: Conceptualization, Funding acquisition, Project administration, Supervision, Writing – review & editing.

Funding

This research was funded by the Natural Science Foundation of Guangdong Province (2022A1515011306, 2021A1515011008, 2023A1515010403), the Outstanding Young Talents Foundation of Guangdong Provincial People's Hospital (KJ012019091), NSFC Incubation Project of Guangdong Provincial People's Hospital (KY0120220031) and the Natural Science Foundation of China (82272552).

Conflict of interest

The authors declare that the research was conducted in the absence of any commercial or financial relationships that could be construed as a potential conflict of interest.

Publisher's note

References

Akbar, M., Fraser, A. R., Graham, G. J., Brewer, J. M., and Grant, M. H. (2012). Acute inflammatory response to cobalt chromium orthopaedic wear debris in a rodent air-pouch model. *J. R. Soc. Interface* 9, 2109–2119. doi: 10.1098/rsif.2012.0006

Akira, S., Takeda, K., and Kaisho, T. (2001). Toll-like receptors: critical proteins linking innate and acquired immunity. *Nat. Immunol.* 2, 675–680. doi: 10.1038/90609

Arora, A., Song, Y., Chun, L., Huie, P., Trindade, M., Smith, R. L., et al. (2003). 17-The role of the TH1 and TH2 immune responses in loosening and osteolysis of cemented total hip replacements. *J. Biomed. Mater. Res.* 64A, 693–697. doi: 10.1002/jbm.a.10200

Athanasou, N. A. (2002). The pathology of joint replacement. *Curr. Diagn. Pathol.* 8, 26–32. doi: 10.1054/cdip.2001.0092

Atkins, G. J., Welldon, K. J., Holding, C. A., Haynes, D. R., Howie, D. W., and Findlay, D. M. (2009). The induction of a catabolic phenotype in human primary osteoblasts and osteocytes by polyethylene particles. *Biomaterials* 30, 3672–3681. doi: 10.1016/j.biomaterials.2009.03.035

Bernardo, M. E., and Fibbe, W. E. (2013). Mesenchymal stromal cells: sensors and switchers of inflammation. *Cell Stem Cell* 13, 392–402. doi: 10.1016/j.stem.2013.09.006

Buckley, C. D., Ospelt, C., Gay, S., and Midwood, K. S. (2021). Location, location, location: how the tissue microenvironment affects inflammation in RA. *Nat. Rev. Rheumatol.* 17, 195–212. doi: 10.1038/s41584-020-00570-2

Cai, K., Hou, Y., Li, J., Chen, X., Hu, Y., Luo, Z., et al. (2013). Effects of titanium nanoparticles on adhesion, migration, proliferation, and differentiation of mesenchymal stem cells. *IJN* 8, 3619. doi: 10.2147/IJN.S38992

Chen, Y., Aiken, A., Saw, S., Weiss, A., Fang, H., and Khokha, R. (2018). TIMP loss activates metalloproteinase-TNFα-DKK1 axis to compromise wnt signaling and bone mass. *J. Bone Miner. Res.* 34, 182–194. doi: 10.1002/jbmr.3585

Chen, W., He, Z., Li, S., Wu, Z., Tan, J., Yang, W., et al. (2022). The effect of mesenchymal stem cells, adipose tissue derived stem cells, and cellular stromal vascular fraction on the repair of acute anal sphincter injury in rats. *Bioengineering* 9, 318. doi: 10.3390/bioengineering9070318

Chiu, R., Smith, K. E., Ma, G. K., Ma, T., Smith, R. L., and Goodman, S. B. (2009). Polymethylmethacrylate particles impair osteoprogenitor viability and expression of osteogenic transcription factors Runx2, osterix, and Dlx5. *J. Orthop. Res.* 28, 571–577. doi: 10.1002/jor.21035

Cho, S. W. (2015). Role of osteal macrophages in bone metabolism. *J. Pathol. Transl. Med.* 49, 102–104. doi: 10.4132/jptm.2015.02.02

Couto, M., Vasconcelos, D., Sousa, D., Sousa, B., Conceicao, F., Neto, E., et al. (2020). The mechanisms underlying the biological response to wear debris in periprosthetic inflammation. *Front. IN. MATERIALS.* 7. doi: 10.3389/fmats.2020.00274

Dapunt, U., Giese, T., Prior, B., Gaida, M. M., and Hänsch, G. M. (2014). Infectious versus non-infectious loosening of implants: activation of T lymphocytes differentiates between the two entities. *Int. Orthopaedics. (SICOT).* 38, 1291–1296. doi: 10.1007/s00264-014-2310-5

Deng, Z., Jin, J., Wang, S., Qi, F., Chen, X., Liu, C., et al. (2020). Narrative review of the choices of stem cell sources and hydrogels for cartilage tissue engineering. *Ann. OF. Trans. Med.* 8, 1598. doi: 10.21037/atm-20-2342

Deng, Z., Jin, J., Wang, Z., Wang, Y., Gao, Q., and Zhao, J. (2017a). The metal nanoparticle-induced inflammatory response is regulated by SIRT1 through NF-kappa B deacetylation in aseptic loosening. *Int. J. OF. NANOMED.* 12, 3617–3636. doi: 10.2147/IJN.S124661

Deng, Z., Wang, Z., Jin, J., Wang, Y., Bao, N., Gao, Q., et al. (2017b). SIRT1 protects osteoblasts against particle-induced inflammatory responses and apoptosis in aseptic prosthesis loosening. *Acta BIOMATERIALIA.* 49, 541–554. doi: 10.1016/j.actbio.2016.11.051

Deng, Z., Zhang, R., Li, M., Wang, S., Fu, G., Jin, J., et al. (2021). STAT3/IL-6 dependent induction of inflammatory response in osteoblast and osteoclast formation in nanoscale wear particle-induced aseptic prosthesis loosening. *BIOMATER. Sci.* 9, 1291–1300. doi: 10.1039/d0bm01256d

Ebert, R., Weissenberger, M., Braun, C., Wagenbrenner, M., Herrmann, M., Müller-Deubert, S., et al. (2021). Impaired regenerative capacity and senescence-associated secretory phenotype in mesenchymal stromal cells from samples of patients with aseptic joint arthroplasty loosening. *J. Orthopaedic. Res.* 40, 513–523. doi: 10.1002/jor.25041

Gallo, J., Goodman, S. B., Konttinen, Y. T., and Raska, M. (2013). Particle disease: Biologic mechanisms of periprosthetic osteolysis in total hip arthroplasty. *Innate. Immun.* 19, 213–224. doi: 10.1177/1753425912451779

Gao, Q., Rhee, C., Maruyama, M., Li, Z., Shen, H., Zhang, N., et al. (2021). The effects of macrophage phenotype on osteogenic differentiation of MSCs in the presence of polyethylene particles. *Biomedicines* 9, 499. doi: 10.3390/biomedicines9050499

Gibon, E., Córdova, L. A., Lu, L., Lin, T.-H., Yao, Z., Hamadouche, M., et al. (2017). The biological response to orthopedic implants for joint replacement. II: Polyethylene, ceramics, PMMA, and the foreign body reaction. *J. BioMed. Mater. Res. B.* 105, 1685–1691. doi: 10.1002/jbm.b.33676

Gibon, E., Yao, Z., Rao, A. J., Zwingenberger, S., Batke, B., Valladares, R., et al. (2012). Effect of a CCR1 receptor antagonist on systemic trafficking of MSCs and polyethylene particle-associated bone loss. *Biomaterials* 33, 3632–3638. doi: 10.1016/j.biomaterials.2012.02.003

Goodman, S. B. (2007). Wear particles, periprosthetic osteolysis and the immune system. *Biomaterials* 28, 5044–5048. doi: 10.1016/j.biomaterials.2007.06.035

Goodman, S. B., Konttinen, Y. T., and Takagi, M. (2014). Joint replacement surgery and the innate immune system. *J. Long. Term. Eff. Med. Implants.* 24, 253–257. doi: 10.1615/jlongtermeffmedimplants.2014010627

Goodman, S. B., and Ma, T. (2010). Cellular chemotaxis induced by wear particles from joint replacements. *Biomaterials* 31, 5045–5050. doi: 10.1016/j.biomaterials.2010.03.046

Goodman, S. B., Ma, T., Chiu, R., Ramachandran, R., and Lane Smith, R. (2006). Effects of orthopaedic wear particles on osteoprogenitor cells. *Biomaterials* 27, 6096–6101. doi: 10.1016/j.biomaterials.2006.08.023

Gordon, S. (2016). Phagocytosis: an immunobiologic process. *Immunity* 44, 463–475. doi: 10.1016/j.immuni.2016.02.026

Grammatopoulos, G., Munemoto, M., Inagaki, Y., Tanaka, Y., and Athanasou, N. A. (2016). The diagnosis of infection in metal-on-metal hip arthroplasties. *J. Arthroplasty.* 31, 2569–2573. doi: 10.1016/j.arth.2016.03.064

Granchi, D., Ciapetti, G., Amato, I., Pagani, S., Cenni, E., Savarino, L., et al. (2003). The influence of alumina and ultra-high molecular weight polyethylene particles on osteoblast–osteoclast cooperation. *Biomaterials* 25, 4037–4045. doi: 10.1016/j.biomaterials.2003.10.100

Guo, H. H., Yu, C. C., Sun, S. X., Ma, X. J., Yang, X. C., Sun, K. N., et al. (2013). Adenovirus-mediated siRNA targeting TNF-α and overexpression of bone morphogenetic protein-2 promotes early osteoblast differentiation on a cell model of Ti particle-induced inflammatory response in *vitro*. *Braz. J. Med. Biol. Res.* 46, 831–838. doi: 10.1590/1414-431X20133092

Haleem-Smith, H., Argintar, E., Bush, C., Hampton, D., Postma, W. F., Chen, F. H., et al. (2011). Biological responses of human mesenchymal stem cells to titanium wear debris particles. *J. Orthop. Res.* 30, 853–863. doi: 10.1002/jor.22002

Hallab, N. J., Caicedo, M., McAllister, K., Skipor, A., Amstutz, H., and Jacobs, J. J. (2012). Asymptomatic prospective and retrospective cohorts with metal-on-metal hip arthroplasty indicate acquired lymphocyte reactivity varies with metal ion levels on a group basis. *J. Orthop. Res.* 31, 173–182. doi: 10.1002/jor.22214

Hasegawa, M., Iino, T., and Sudo, A. (2016). Immune response in adverse reactions to metal debris following metal-on-metal total hip arthroplasty. *BMC Musculoskelet. Disord.* 17, 221. doi: 10.1186/s12891-016-1069-9

Hercus, B., and Revell, P. A. (2001). Phenotypic characteristics of T lymphocytes in the interfacial tissue of aseptically loosened prosthetic joints. *J. Mater. Sci. Mater. Med.* 12, 1063–1067. doi: 10.1023/a:1012806409544

Hodges, N. A., Sussman, E. M., and Stegemann, J. P. (2021). Aseptic and septic prosthetic joint loosening: Impact of biomaterial wear on immune cell function, inflammation, and infection. *Biomaterials* 278, 121127. doi: 10.1016/j.biomaterials.2021.121127

Hopf, F., Thomas, P., Sesselmann, S., Thomsen, M. N., Hopf, M., Hopf, J., et al. (2017). CD3+ lymphocytosis in the peri-implant membrane of 222 loosened joint endoprostheses depends on the tribological pairing. *Acta Orthopaedica.* 88, 642–648. doi: 10.1080/17453674.2017.1362774

Huang, S.-L., He, X.-J., and Wang, K.-Z. (2012). Joint replacement in China: progress and challenges. *Rheumatology* 51, 1525–1526. doi: 10.1093/rheumatology/kes077

Huang, S., Leung, V., Peng, S., Li, L., Lu, F. J., Wang, T., et al. (2011). Developmental definition of MSCs: new insights into pending questions. *Cell. Reprogramming.* 13, 465–472. doi: 10.1089/cell.2011.0045

Huang, Y.-C., Li, Z., Li, J., and Lyu, F.-J. (2020). Interaction between stem cells and the microenvironment for musculoskeletal repair. *Stem Cells Int.* 2020, 1–3. doi: 10.1155/2020/7587428

Huang, Z., Ma, T., Ren, P.-G., Smith, R. L., and Goodman, S. B. (2010). Effects of orthopedic polymer particles on chemotaxis of macrophages and mesenchymal stem cells. *J. BioMed. Mater. Res. A.* 94, 1264–1269. doi: 10.1002/jbm.a.32803

Jacobs, J. J., Hallab, N. J., Urban, R. M., and Wimmer, M. A. (2006). Wear particles. *J. Bone Joint Surg. Am.* 88, 99–102. doi: 10.2106/JBJS.F.00102

Jhunjhunwala, S., Aresta-DaSilva, S., Tang, K., Alvarez, D., Webber, M. J., Tang, B. C., et al. (2015). Neutrophil responses to sterile implant materials. *PloS One* 10, e0137550. doi: 10.1371/journal.pone.0137550

Jiang, Y., Jia, T., Gong, W., Wooley, P. H., and Yang, S.-Y. (2013). Effects of Ti, PMMA, UHMWPE, and Co-Cr wear particles on differentiation and functions of bone marrow stromal cells. *J. Biomed. Mater. Res.* 101, 2817–2825. doi: 10.1002/jbm.a.34595

Jonitz-Heincke, A., Lochner, K., Schulze, C., Pohle, D., Pustlauk, W., Hansmann, D., et al. (2016). Contribution of human osteoblasts and macrophages to bone matrix degradation and proinflammatory cytokine release after exposure to abrasive endoprosthetic wear particles. *Mol. Med. Rep.* 14, 1491–1500. doi: 10.3892/mmr.2016.5415

Jorch, S. K., and Kubes, P. (2017). An emerging role for neutrophil extracellular traps in noninfectious disease. *Nat. Med.* 23, 279–287. doi: 10.1038/nm.4294

Kapadia, B. H., Berg, R. A., Daley, J. A., Fritz, J., Bhave, A., and Mont, M. A. (2015). Periprosthetic joint infection. *Lancet* 387, 386–394. doi: 10.1016/S0140-6736(14)61798-0

Katti, K. S. (2004). Biomaterials in total joint replacement. *Colloids. Surfaces. B.: Biointerfaces.* 39, 133–142. doi: 10.1016/j.colsurfb.2003.12.002

Keselowsky, B. G., and Lewis, J. S. (2017). Dendritic cells in the host response to implanted materials. *Semin. Immunol.* 29, 33–40. doi: 10.1016/j.smim.2017.04.002

Konttinen, Y. T., Li, T.-F., Mandelin, J., Ainola, M., Lassus, J., Virtanen, I., et al. (2001). Hyaluronan synthases, hyaluronan, and its CD44 receptor in tissue around loosened total hip prostheses. *J. Pathol.* 194, 384–390. doi: 10.1002/1096-9896(200107)194:3<384::AID-PATH896>3.0.CO;2-8

Koreny, T., Tunyogi-Csapó, M., Gál, I., Vermes, C., Jacobs, J. J., and Glant, T. T. (2006). The role of fibroblasts and fibroblast-derived factors in periprosthetic osteolysis. *Arthritis Rheum.* 54, 3221–3232. doi: 10.1002/art.22134

Kou, P. M., and Babensee, J. E. (2010). Macrophage and dendritic cell phenotypic diversity in the context of biomaterials. *J. Biomed. Mater. Res.* 96A, 239–260. doi: 10.1002/jbm.a.32971

Krafts, K. P. (2010). Tissue repair. *Organogenesis* 6, 225–233. doi: 10.4161/org.6.4.12555

Kung, M., Markantonis, J., Nelson, S., and Campbell, P. (2015). The synovial lining and synovial fluid properties after joint arthroplasty. *Lubricants* 3, 394–412. doi: 10.3390/lubricants3020394

Kushioka, J., Toya, M., Shen, H., Hirata, H., Zhang, N., Huang, E., et al. (2023). Therapeutic effects of MSCs, genetically modified MSCs, and NFκB-inhibitor on chronic inflammatory osteolysis in aged mice. *J. Orthop. Res.* 41, 1004–1013. doi: 10.1002/jor.25434

Kuzyk, P. R. T., and Schemitsch, E. H. (2011). The basic science of peri-implant bone healing. *IJOO* 45, 108–115. doi: 10.4103/0019-5413.77129

Le Blanc, K., and Mougiakakos, D. (2012). Multipotent mesenchymal stromal cells and the innate immune system. *Nat. Rev. Immunol.* 12, 383–396. doi: 10.1038/nri3209

Lee, H. G., Hsu, A., Goto, H., Nizami, S., Lee, J. H., Cadet, E. R., et al. (2013). Aggravation of inflammatory response by costimulation with titanium particles and mechanical perturbations in osteoblast- and macrophage-like cells. *Am. J. Physiol-Cell. Ph.* 304, C431–C439. doi: 10.1152/ajpcell.00202.2012

Lee, H. G., Minematsu, H., Kim, K. O., Celil Aydemir, A. B., Shin, M. J., Nizami, S. A., et al. (2011). Actin and ERK1/2-CEBPβ signaling mediates phagocytosis-induced innate immune response of osteoprogenitor cells. *Biomaterials* 32, 9197–9206. doi: 10.1016/j.biomaterials.2011.08.059

Lee, S.-S., Sharma, A. R., Choi, B.-S., Jung, J.-S., Chang, J.-D., Park, S., et al. (2012). The effect of TNFα secreted from macrophages activated by titanium particles on osteogenic activity regulated by WNT/BMP signaling in osteoprogenitor cells. *Biomaterials* 33, 4251–4263. doi: 10.1016/j.biomaterials.2012.03.005

Lenz, R., Mittelmeier, W., Hansmann, D., Brem, R., Diehl, P., Fritsche, A., et al. (2009). Response of human osteoblasts exposed to wear particles generated at the interface of total hip stems and bone cement. *J. Biomed. Mater. Res.* 89A, 370–378. doi: 10.1002/jbm.a.31996

Leung, V. Y. L., Aladin, D. M. K., Lv, F., Tam, V., Sun, Y., Lau, R. Y. C., et al. (2014). Mesenchymal stem cells reduce intervertebral disc fibrosis and facilitate repair. *Stem Cells* 32, 2164–2177. doi: 10.1002/stem.1717

Li, N., Gao, J., Mi, L., Zhang, G., Zhang, L., Zhang, N., et al. (2020). Synovial membrane mesenchymal stem cells: past life, current situation, and application in bone and joint diseases. *Stem Cell Res. Ther.* 11, 381. doi: 10.1186/s13287-020-01885-3

Li, T. F., Santavirta, S., Waris, V., Lassus, J., Lindroos, L., Xu, J. W., et al. (2001). No lymphokines in T-cells around loosened hip prostheses. *Acta Orthop. Scand.* 72, 241–247. doi: 10.1080/00016470152846556

Li, F., Tang, Y., Song, B., Yu, M., Li, Q., Zhang, C., et al. (2019). Nomenclature clarification: synovial fibroblasts and synovial mesenchymal stem cells. *Stem Cell Res. Ther.* 10, 260. doi: 10.1186/s13287-019-1359-x

Li, D., Wang, H., Li, Z., Wang, C., Xiao, F., Gao, Y., et al. (2018). The inhibition of RANKL expression in fibroblasts attenuate CoCr particles induced aseptic prosthesis loosening via the MyD88-independent TLR signaling pathway. *Biochem. Biophys. Res. Commun.* 503, 1115–1122. doi: 10.1016/j.bbrc.2018.06.128

Li, G., Wu, P., Xu, Y., Yu, Y., Sun, L., Zhu, L., et al. (2009). The effect of Lipoxin A4 on the interaction between macrophage and osteoblast: possible role in the treatment of aseptic loosening. *BMC Musculoskelet. Disord.* 10, 57. doi: 10.1186/1471-2474-10-57

Lin, T.-H., Kao, S., Sato, T., Pajarinen, J., Zhang, R., Loi, F., et al. (2015). Exposure of polyethylene particles induces interferon-γ expression in a natural killer T lymphocyte and dendritic cell coculture system*in vitro*: A preliminary study. *J. Biomed. Mater. Res.* 103, 71–75. doi: 10.1002/jbm.a.35159

Lin, T.-H., Sato, T., Barcay, K. R., Waters, H., Loi, F., Zhang, R., et al. (2014). NF-κB decoy oligodeoxynucleotide enhanced osteogenesis in mesenchymal stem cells exposed to polyethylene particle. *Tissue Eng. Part A.* 21, 875–883. doi: 10.1089/ten.TEA.2014.0144

Lu, D., Xu, Y., Liu, Q., and Zhang, Q. (2021). Mesenchymal stem cell-macrophage crosstalk and maintenance of inflammatory microenvironment homeostasis. *Front. Cell Dev. Biol.* 9. doi: 10.3389/fcell.2021.681171

Lv, F., Lu, M., MC Cheung, K., YL Leung, V., and Zhou, G. (2012). Intrinsic properties of mesemchymal stem cells from human bone marrow, umbilical cord and umbilical cord blood comparing the different sources of MSC. *CSCR* 7, 389–399. doi: 10.2174/157488812804484611

Lv, F.-J., Tuan, R. S., Cheung, K. M. C., Leung, V. Y. L., Lv, F.-J., Tuan, R. S., et al. (2014). Concise review: the surface markers and identity of human mesenchymal stem cells. *Stem Cells* 32, 1408–1419. doi: 10.1002/stem.1681

Ma, G.-F., Ali, A., Verzijl, N., Hanemaaijer, R., TeKoppele, J., T. Konttinen, Y., et al. (2006). Increased collagen degradation around loosened total hip replacement implants. *Arthritis Rheum.* 54, 2928–2933. doi: 10.1002/art.22064

Ma, T.-L., Chen, J.-X., Ke, Z.-R., Zhu, P., Hu, Y.-H., and Xie, J. (2022). Targeting regulation of stem cell exosomes: Exploring novel strategies for aseptic loosening of joint prosthesis. *Front. Bioeng. Biotech.* 10. doi: 10.3389/fbioe.2022.925841

Mahon, O. R., Browe, D. C., Gonzalez-Fernandez, T., Pitacco, P., Whelan, I. T., Von Euw, S., et al. (2020). Nano-particle mediated M2 macrophage polarization enhances bone formation and MSC osteogenesis in an IL-10 dependent manner. *Biomaterials* 239, 119833. doi: 10.1016/j.biomaterials.2020.119833

Maitra, R., Clement, C. C., Crisi, G. M., Cobelli, N., and Santambrogio, L. (2008). Immunogenecity of modified alkane polymers is mediated through TLR1/2 activation. *PloS One* 3, e2438. doi: 10.1371/journal.pone.0002438

Maitra, R., Clement, C. C., Scharf, B., Crisi, G. M., Chitta, S., Paget, D., et al. (2009). Endosomal damage and TLR2 mediated inflammasome activation by alkane particles in the generation of aseptic osteolysis. *Mol. Immunol.* 47, 175–184. doi: 10.1016/j.molimm.2009.09.023

Maloney, W. J., and Smith, R. L. (1996). Periprosthetic osteolysis in total hip arthroplasty: the role of particulate wear debris. *Instr. Course. Lect.* 45, 171–182. doi: 10.2106/00004623-199509000-00022

Mandelin, J., Li, T. F., Liljeström, M., Kroon, M. E., Hanemaaijer, R., Santavirta, S., et al. (2004). 13-Imbalance of RANKL/RANK/OPG system in interface tissue in loosening of total hip replacement. *J. Bone Joint Surgery. Br. volume* 85-B, 1196–1201. doi: 10.1302/0301-620x.85b8.13311

Maradit Kremers, H., Larson, D. R., Crowson, C. S., Kremers, W. K., Washington, R. E., Steiner, C. A., et al. (2015). Prevalence of total hip and knee replacement in the United States. *J. Bone Joint Surgery-American. Volume* 97, 1386–1397. doi: 10.2106/JBJS.N.01141

Marco, F., Milena, F., Gianluca, G., and Vittoria, O. (2005). Peri-implant osteogenesis in health and osteoporosis. *Micron* 36, 630–644. doi: 10.1016/j.micron.2005.07.008

Markel, D. C., Bergum, C., Flynn, J., Jackson, N., Bou-Akl, T., and Ren, W. (2018). Relationship of blood metal ion levels and leukocyte profiles in patients with articular surface replacement metal-on-metal hip replacement. *Orthopedics* 41, e424–e431. doi: 10.3928/01477447-20180409-02

Marmotti, A., Messina, D., Cykowska, A., Beltramo, C., Bellato, E., Colombero, D., et al. (2020). Periprosthetic osteolysis: a narrative review. *J. Biol. Regul. Homeost. Agents* 34, 405–417. Congress of the Italian Orthopaedic Research Society.

Masui, T., Sakano, S., Hasegawa, Y., Warashina, H., and Ishiguro, N. (2004). Expression of inflammatory cytokines, RANKL and OPG induced by titanium, cobalt-chromium and polyethylene particles. *Biomaterials* 26, 1695–1702. doi: 10.1016/j.biomaterials.2004.05.017

Mazzucco, D., Scott, R., and Spector, M. (2004). Composition of joint fluid in patients undergoing total knee replacement and revision arthroplasty: correlation with flow properties. *Biomaterials* 25, 4433–4445. doi: 10.1016/j.biomaterials.2003.11.023

Medzhitov, R. (2008). Origin and physiological roles of inflammation. *Nature* 454, 428–435. doi: 10.1038/nature07201

Miron, R. J., and Bosshardt, D. D. (2015). OsteoMacs: Key players around bone biomaterials. *Biomaterials* 82, 1–19. doi: 10.1016/j.biomaterials.2015.12.017

Mittal, S., Revell, M., Barone, F., Hardie, D. L., Matharu, G. S., Davenport, A. J., et al. (2013). Lymphoid aggregates that resemble tertiary lymphoid organs define a specific pathological subset in metal-on-metal hip replacements. *PloS One* 8, e63470. doi: 10.1371/journal.pone.0063470

Mosser, D. M., and Edwards, J. P. (2008). Exploring the full spectrum of macrophage activation. *Nat. Rev. Immunol.* 8, 958–969. doi: 10.1038/nri2448

Nam, J.-S., Sharma, A. R., Jagga, S., Lee, D.-H., Sharma, G., Nguyen, L. T., et al. (2017). Suppression of osteogenic activity by regulation of WNT and BMP signaling during titanium particle induced osteolysis. *J. Biomed. Mater. Res.* 105, 912–926. doi: 10.1002/jbm.a.36004

Nich, C., Takakubo, Y., Pajarinen, J., Ainola, M., Salem, A., Sillat, T., et al. (2013). Macrophages-Key cells in the response to wear debris from joint replacements. *J. Biomed. Mater. Res.* 101, 3033–3045. doi: 10.1002/jbm.a.34599

Nosbaum, A., Prevel, N., Truong, H.-A., Mehta, P., Ettinger, M., Scharschmidt, T. C., et al. (2016). Cutting edge: regulatory T cells facilitate cutaneous wound healing. *J.I.* 196, 2010–2014. doi: 10.4049/jimmunol.1502139

O'Brien, W., Fissel, B. M., Maeda, Y., Yan, J., Ge, X., Gravallese, E. M., et al. (2016). RANK-independent osteoclast formation and bone erosion in inflammatory arthritis. *Arthritis Rheumatol.* 68, 2889–2900. doi: 10.1002/art.39837

Okafor, C. C., Haleem-Smith, H., Laqueriere, P., Manner, P. A., and Tuan, R. S. (2006). Particulate endocytosis mediates biological responses of human mesenchymal stem cells to titanium wear debris. *J. Orthopaedic. Res.* 24, 461–473. doi: 10.1002/jor.20075

Okamoto, K., Nakashima, T., Shinohara, M., Negishi-Koga, T., Komatsu, N., Terashima, A., et al. (2017). Osteoimmunology: the conceptual framework unifying the immune and skeletal systems. *Physiol. Rev.* 97, 1295–1349. doi: 10.1152/physrev.00036.2016

O'Neill, S., Queally, J., Devitt, B., Doran, P., and O'Byrne, J. (2013). The role of osteoblasts in peri-prosthetic osteolysis. *Bone Joint J.* 95B, 1022–1026. doi: 10.1302/0301-620X.95B8.31229

Ormsby, R. T., Cantley, M., Kogawa, M., Solomon, L. B., Haynes, D. R., Findlay, D. M., et al. (2016). Evidence that osteocyte perilacunar remodelling contributes to polyethylene wear particle induced osteolysis. *Acta Biomaterialia.* 33, 242–251. doi: 10.1016/j.actbio.2016.01.016

Ormsby, R. T., Solomon, L. B., Stamenkov, R., Findlay, D. M., and Atkins, G. J. (2019). Evidence for gender-specific bone loss mechanisms in periprosthetic osteolysis. *JCM* 9, 53. doi: 10.3390/jcm9010053

Pajarinen, J., Lin, T., Nabeshima, A., Jamsen, E., Lu, L., Nathan, K., et al. (2017). Mesenchymal stem cells in the aseptic loosening of total joint replacements. *J. Biomed. Mater. Res. Part A.* 105, 1195–1207. doi: 10.1002/jbm.a.35978

Pap, T., Claus, A., Ohtsu, S., Hummel, K. M., Schwartz, P., Drynda, S., et al. (2003). Osteoclast-independent bone resorption by fibroblast-like cells. *Arthritis Res. Ther.* 5, R163–R173. doi: 10.1186/ar752

Paukkeri, E.-L., Korhonen, R., Hämäläinen, M., Pesu, M., Eskelinen, A., Moilanen, T., et al. (2016). The inflammatory phenotype in failed metal-on-metal hip arthroplasty correlates with blood metal concentrations. *PloS One* 11, e0155121. doi: 10.1371/journal.pone.0155121

Pioletti, D. P., and Kottelat, A. (2004). The influence of wear particles in the expression of osteoclastogenesis factors by osteoblasts. *Biomaterials* 25, 5803–5808. doi: 10.1016/j.biomaterials.2004.01.053

Preedy, E. C., Perni, S., and Prokopovich, P. (2015). Cobalt, titanium and PMMA bone cement debris influence on mouse osteoblast cell elasticity, spring constant and calcium production activity. *RSC. Adv.* 5, 83885–83898. doi: 10.1039/c5ra15390e

Purdue, P. E. (2008). Alternative macrophage activation in periprosthetic osteolysis. *Autoimmunity* 41, 212–217. doi: 10.1080/08916930701694626

Qi, F., Deng, Z., Ma, Y., Wang, S., Liu, C., Lyu, F., et al. (2020). From the perspective of embryonic tendon development: various cells applied to tendon tissue engineering. *Ann. OF. Trans. Med.* 8, 131. doi: 10.21037/atm.2019.12.78

Qiu, J., Beckman, M. J., Qian, J., and Jiranek, W. (2005). Simultaneous labeling of mast cell proteases and protease mRNAs at the bone–implant interface of aseptically loosened hip implants. *J. Orthop. Res.* 23, 942–948. doi: 10.1016/j.orthres.2005.04.008

Revell, P. A. (2008). The combined role of wear particles, macrophages and lymphocytes in the loosening of total joint prostheses. *J. R. Soc Interface.* 5, 1263–1278. doi: 10.1098/rsif.2008.0142

Revell, P. A., Matharu, G. S., Mittal, S., Pynsent, P. B., Buckley, C. D., and Revell, M. P. (2016). Increased expression of inducible co-stimulator on CD4+ T-cells in the peripheral blood and synovial fluid of patients with failed hip arthroplasties. *Bone Joint Res.* 5, 52–60. doi: 10.1302/2046-3758.52.2000574

Ribeiro, A. R., Gemini-Piperni, S., Travassos, R., Lemgruber, L., C. Silva, R., Rossi, A. L., et al. (2016). Trojan-like internalization of anatase titanium dioxide nanoparticles by human osteoblast cells. *Sci. Rep.* 6, 23615. doi: 10.1038/srep23615

Rodrigo, A. M., Martínez, M. E., Saldaña, L., Vallés, G., Martínez, P., González-Carrasco, J. L., et al. (2002). Effects of polyethylene and α-alumina particles on IL-6 expression and secretion in primary cultures of human osteoblastic cells. *Biomaterials* 23, 901–908. doi: 10.1016/s0142-9612(01)00200-9

Rodrigo, A., Vallés, G., Saldaña, L., Rodríguez, M., Martínez, M. E., Munuera, L., et al. (2005). Alumina particles influence the interactions of cocultured osteoblasts and macrophages. *J. Orthop. Res.* 24, 46–54. doi: 10.1002/jor.20007

Roebuck, K. A., Vermes, C., Carpenter, L. R., Fritz, E. A., Narayanan, R., and Glant, T. T. (2006). Down-regulation of procollagen α1[I] messenger RNA by titanium particles correlates with nuclear factor κB (NF-κB) activation and increased rel A and NF-κB1 binding to the collagen promoter. *J. Bone Miner. Res.* 16, 501–510. doi: 10.1359/jbmr.2001.16.3.501

Rose, S. F., Weaver, C. L., Fenwick, S. A., Horner, A., and Pawar, V. D. (2012). The effect of diffusion hardened oxidized zirconium wear debris on cell viability and inflammation-An in *vitro* study. *J. Biomed. Mater. Res.* 100B, 1359–1368. doi: 10.1002/jbm.b.32704

Sabokbar, A., Itonaga, I., Sun, S. G., Kudo, O., and Athanasou, N. A. (2005). Arthroplasty membrane-derived fibroblasts directly induce osteoclast formation and osteolysis in aseptic loosening. *J. Orthop. Res.* 23, 511–519. doi: 10.1016/j.orthres.2004.10.006

Sabokbar, A., Mahoney, D. J., Hemingway, F., and Athanasou, N. A. (2015). Non-canonical (RANKL-independent) pathways of osteoclast differentiation and their role in musculoskeletal diseases. *Clinic. Rev. Allerg. Immunol.* 51, 16–26. doi: 10.1007/s12016-015-8523-6

Sadoghi, P., Liebensteiner, M., Agreiter, M., Leithner, A., Böhler, N., and Labek, G. (2013). Revision surgery after total joint arthroplasty: A complication-based analysis using worldwide arthroplasty registers. *J. Arthroplasty.* 28, 1329–1332. doi: 10.1016/j.arth.2013.01.012

Sakai, H., Jingushi, S., Shuto, T., Urabe, K., Ikenoue, T., Okazaki, K., et al. (2002). Fibroblasts from the inner granulation tissue of the pseudocapsule in hips at revision arthroplasty induce osteoclast differentiation, as do stromal cells. *Ann. Rheum. Dis.* 61 (12), 103–109. doi: 10.1136/ard.61.2.103

Saldaña, L., and Vilaboa, N. (2009). Effects of micrometric titanium particles on osteoblast attachment and cytoskeleton architecture. *Acta Biomaterialia.* 6, 1649–1660. doi: 10.1016/j.actbio.2009.10.033

Saleh, K. J., Thongtrangan, I., and Schwarz, E. M. (2004). Osteolysis: medical and surgical approaches. *Clin. Orthop. Relat. Res.* 427, 138–147. doi: 10.1097/01.blo.0000142288.66246.4d

Schmalzried, T. P., Jasty, M., and Harris, W. H. (1992). Periprosthetic bone loss in total hip arthroplasty. Polyethylene wear debris and the concept of the effective joint space. *J. Bone Joint Surg. Am.* 74, 849–863. doi: 10.2106/00004623-199274060-00006

Shanbhag, A. S., Bailey, H. O., Hwang, D.-S., Cha, C. W., Eror, N. G., and Rubash, H. E. (2002). Quantitative analysis of ultrahigh molecular weight polyethylene (UHMWPE) wear debris associated with total knee replacements. *J. Biomed. Mater. Res.* 53, 100–110. doi: 10.1002/(sici)1097-4636(2000)53:1<100::aid-jbm14>3.0.co;2-4

Shanbhag, A. S., Jacobs, J. J., Glant, T. T., Gilbert, J. L., Black, J., and Galante, J. O. (1994). Composition and morphology of wear debris in failed uncemented total hip replacement. *J. Bone Joint Surg. Br.* 76, 60–67. doi: 10.1302/0301-620X.76B1.8300684

Shen, Z., Crotti, T. N., McHugh, K. P., Matsuzaki, K., Gravallese, E. M., Bierbaum, B. E., et al. (2006). The role played by cell-substrate interactions in the pathogenesis of osteoclast-mediated periImplant osteolysis. *Arthritis Res. Ther.* 8, R70. doi: 10.1186/ar1938

Shen, H., Kushioka, J., Toya, M., Utsunomiya, T., Hirata, H., Huang, E. E., et al. (2022). Sex differences in the therapeutic effect of unaltered versus NFκB sensing IL-4 over-expressing mesenchymal stromal cells in a murine model of chronic inflammatory bone loss. *Front. Bioeng. Biotechnol.* 10. doi: 10.3389/fbioe.2022.962114

Shiflett, L. A., Tiede-Lewis, L. M., Xie, Y., Lu, Y., Ray, E. C., and Dallas, S. L. (2019). Collagen dynamics during the process of osteocyte embedding and mineralization. *Front. Cell Dev. Biol.* 7. doi: 10.3389/fcell.2019.00178

Singh, J. A., Yu, S., Chen, L., and Cleveland, J. D. (2019). Rates of total joint replacement in the United States: future projections to 2020–2040 using the national inpatient sample. *J. Rheumatol.* 46, 1134–1140. doi: 10.3899/jrheum.170990

Smith, R. A., Maghsoodpour, A., and Hallab, N. J. (2010). *In vivo* response to cross-linked polyethylene and polycarbonate-urethane particles. *J. BioMed. Mater. Res. A.* 93, 227–234. doi: 10.1002/jbm.a.32531

Solovieva, S. A., Ceponis, A., Konttinen, Y. T., Takagi, M., Suda, A., Eklund, K. K., et al. (1996). Mast cells in loosening of totally replaced hips. *Clin. Orthop. Relat. Res.* 322, 158–165. doi: 10.1097/00003086-199601000-00020

St. Pierre, C. A., Chan, M., Iwakura, Y., Ayers, D. C., Kurt-Jones, E. A., and Finberg, R. W. (2010). Periprosthetic osteolysis: Characterizing the innate immune response to titanium wear-particles. *J. Orthop. Res.* 28, 1418–1424. doi: 10.1002/jor.21149

Sun, Y., Li, J., Xie, X., Gu, F., Sui, Z., Zhang, K., et al. (2021). Macrophage-osteoclast associations: origin, polarization, and subgroups. *Front. Immunol.* 12. doi: 10.3389/fimmu.2021.778078

Sun, G., Yang, S., Ti, Y., Guo, G., Fan, G., Chen, F., et al. (2019). Influence of ceramic debris on osteoblast behaviors: an *in vivo* study. *Orthop. Surg.* 11, 770–776. doi: 10.1111/os.12496

Syggelos, S., Aletras, A., Smirlaki, I., and Skandalis, S. (2013). Extracellular matrix degradation and tissue remodeling in periprosthetic loosening and osteolysis: focus on matrix metalloproteinases, their endogenous tissue inhibitors, and the proteasome. *BioMed. Res. Int.* 2013, 1–18. doi: 10.1155/2013/230805

Takei, I., Takagi, M., Santavirta, S., Ida, H., Ishii, M., Ogino, T., et al. (2004). Messenger ribonucleic acid expression of 16 matrix metalloproteinases in bone-implant interface tissues of loose artificial hip joints. *J. Biomed. Mater. Res.* 52, 613–620. doi: 10.1002/1097-4636(20001215)52:4<613::aid-jbm5>3.0.co;2-8

Trebše, R., and Mihelič, A. (2012)Joint replacement: historical overview. In: *Infected total joint arthroplasty: the algorithmic approach* (London: Springer) (Accessed October 11, 2021).

Tsutsumi, R., Xie, C., Wei, X., Zhang, M., Zhang, X., Flick, L. M., et al. (2009). PGE2 signaling through the EP4 receptor on fibroblasts upregulates RANKL and stimulates osteolysis. *J. Bone Mineral. Res.* 24, 1753–1762. doi: 10.1359/jbmr.090412

Tuan, R. S., Lee, F. Y.-I., Konttinen, Y. T., Wilkinson, M. J., and Smith, R. L. (2008). What are the local and systemic biologic reactions and mediators to wear debris, and what host factors determine or modulate the biologic response to wear particles? *J. Am. Acad. Orthopaedic. Surgeons.* 16, S42–S48. doi: 10.5435/00124635-200800001-00010

U.S. Food and Drug Administration (2019) *Biological responses to metal implants - september 2019*. Available at: https://www.fda.gov/media/131150/download (Accessed August 4, 2023).

Vaculová, J., Hurník, P., Gallo, J., Žiak, D., and Motyka, O. (2018). Immunohistochemical detection of mast and dendritic cells in periprosthetic tissues of aseptically loosened total prostheses. *Acta Chir. Orthop. Traumatol. Cech.* 85, 351–358. doi: 10.55095/achot2018/060

Vallés, G., Gil-Garay, E., Munuera, L., and Vilaboa, N. (2008). Modulation of the cross-talk between macrophages and osteoblasts by titanium-based particles. *Biomaterials* 29, 2326–2335. doi: 10.1016/j.biomaterials.2008.02.011

Vermes, C., Chandrasekaran, R., Jacobs, J. J., Galante, J. O., Roebuck, K. A., and Glant, T. T. (2016). The effects of particulate wear debris, cytokines, and growth factors on the functions of MG-63 osteoblasts. *J. Bone Joint Surgery-American. Volume* 83, 201–211. doi: 10.2106/00004623-200102000-00007

Vermes, C., Roebuck, K. A., Chandrasekaran, R., Dobai, J. G., Jacobs, J. J., and Glant, T. T. (2006). Particulate wear debris activates protein tyrosine kinases and nuclear factor κB, which down-regulates type I collagen synthesis in human osteoblasts. *J. Bone Miner. Res.* 15, 1756–1765. doi: 10.1359/jbmr.2000.15.9.1756

Wang, Z., Liu, N., Shi, T., Zhou, G., Wang, Z., Gan, J., et al. (2015). ER stress mediates tiAl6V4 particle-induced peri-implant osteolysis by promoting RANKL expression in fibroblasts. *PloS One* 10, e0137774. doi: 10.1371/journal.pone.0137774

Wang, Z., Liu, N., Zhou, G., Shi, T., Wang, Z., Gan, J., et al. (2017). Expression of XBP1s in fibroblasts is critical for TiAl6 V4 particle-induced RANKL expression and osteolysis. *J. Orthop. Res.* 35, 752–759. doi: 10.1002/jor.23056

Wang, J., Tao, Y., Ping, Z., Zhang, W., Hu, X., Wang, Y., et al. (2016). Icariin attenuates titanium-particle inhibition of bone formation by activating the Wnt/β-catenin signaling pathway in *vivo* and in *vitro*. *Sci. Rep.* 6, 23827. doi: 10.1038/srep23827

Wright, V., Dowson, D., and Kerr, J. (1973). "The structure of joints. *International review of connective tissue research*,". Eds. D. A. Hall and D. S. Jackson (Elsevier), 105–125. doi: 10.1016/B978-0-12-363706-2.50009-X

Yuan, F.-L., Wu, Q., Miao, Z.-N., Xu, M.-H., Xu, R.-S., Jiang, D.-L., et al. (2018). Osteoclast-derived extracellular vesicles: novel regulators of osteoclastogenesis and osteoclast–osteoblasts communication in bone remodeling. *Front. Physiol.* 9. doi: 10.3389/fphys.2018.00628

Zdolsek, J., Eaton, J. W., and Tang, L. (2007). Histamine release and fibrinogen adsorption mediate acute inflammatory responses to biomaterial implants in humans. *J. Transl. Med.* 5, 31. doi: 10.1186/1479-5876-5-31

Zhang, L., Haddouti, E.-M., Welle, K., Burger, C., Kabir, K., and Schildberg, F. A. (2020). Local cellular responses to metallic and ceramic nanoparticles from orthopedic joint arthroplasty implants. *IJN. Volume* 15, 6705–6720. doi: 10.2147/IJN.S248848

frontiers | Frontiers in Cellular and Infection Microbiology

TYPE Case Report
PUBLISHED 04 January 2024
DOI 10.3389/fcimb.2023.1269352

OPEN ACCESS

EDITED BY
Chi Xu,
Chinese PLA General Hospital, China

REVIEWED BY
Jata Shankar,
Jaypee University of Information Technology, India
Iman Haghani,
Mazandaran University of Medical Sciences, Iran
Osvaldo Mazza,
Bambino GesùChildren's Hospital (IRCCS), Italy

*CORRESPONDENCE
Xiang Yin
20091997@qq.com

RECEIVED 29 July 2023
ACCEPTED 14 December 2023
PUBLISHED 04 January 2024

CITATION
Jin Y and Yin X (2024) *Aspergillus terreus* spondylodiscitis following acupuncture and acupotomy in an immunocompetent host: case report and literature review.
Front. Cell. Infect. Microbiol. 13:1269352.
doi: 10.3389/fcimb.2023.1269352

Aspergillus terreus spondylodiscitis following acupuncture and acupotomy in an immunocompetent host: case report and literature review

Yufei Jin and Xiang Yin*

Department of Spine Surgery, Daping Hospital, Army Medical University, Chongqing, China

Aspergillus terreus is a fungus responsible for various infections in human beings; however, spine involvement is uncommon. Herein, we report a case of *A. terreus* spondylodiscitis following acupuncture and acupotomy in an immunocompetent Chinese patient. Admission lumbar magnetic resonance imaging (MRI) revealed infection at the L4/5 level without significant vertebral destruction. After unsuccessful symptomatic and anti-tuberculosis treatments, *A. terreus* was identified through culture, microscopy of isolate, histological examination and VITEK system. Intravenous voriconazole was then given; however, the patient's spinal condition deteriorated rapidly, resulting in evident destruction of the L4/5 vertebral bodies. Surgeries including L4/5 intervertebral disc debridement, spinal canal decompression, posterior lumbar interbody fusion (PLIF) with allogeneic fibula ring fusion cages, and posterior pedicle screw fixation were then performed. Imaging findings at one-month and six-month follow-up suggested that the patient was successfully treated. This case highlighted two important points: firstly, although acupuncture and acupotomy are generally regarded as safe conservative treatments for pain management, they can still lead to complications such as fungal spinal infection. Therefore, vigilance is necessary when considering these treatments; secondly, PLIF with allogeneic fibula ring fusion cages may be beneficial for *A. terreus* spondylodiscitis patients with spinal instability.

KEYWORDS

***Aspergillus terreus*, spondylodiscitis, acupuncture, acupotomy, allogeneic fibula ring**

Introduction

Aspergillus terreus, a thermotolerant fungus belonging to the *Aspergillus* section *Terrei*, is commonly found in the environment. It can cause opportunistic infections, such as pneumonia (Modi et al., 2012), meningitis (Elsawy et al., 2015), endophthalmitis (Panigrahi et al., 2014), periprosthetic joint infection (Bartash et al., 2017), and cutaneous infection

(Ozer et al., 2009), in both immunocompetent and immunocompromised patients. Spondylodiscitis is a rare but devastating disease that primarily affects the intervertebral disc and the adjacent vertebral bodies. *A. terreus* spondylodiscitis is even rare, with only ten reported cases (Seligsohn et al., 1977; Glotzbach, 1982; Brown et al., 1987; Grandière-Perez et al., 2000; Park et al., 2000; Maman et al., 2015; Comacle et al., 2016; Sohn et al., 2019; Takagi et al., 2019; Vithiya et al., 2023). In this report, we present a rare case of *A. terreus* spondylodiscitis following acupuncture and acupotomy in an immunocompetent Chinese patient. It's worth noting that, posterior lumbar interbody fusion (PLIF) with allogeneic fibula ring fusion cages was firstly used to treat this kind of infectious spondylodiscitis.

Case description

In October 2019, a 58-year-old female presented to our hospital due to recurrent low back pain. One month prior to admission, the patient suffered severe low back pain after physical labor work, with limited movement and difficulty in squatting, which were relieved after acupuncture and acupotomy (also called needle knife) treatment in a local clinic. Remarkably, her low back pain symptoms recurred repeatedly later. Magnetic resonance imaging (MRI) examinations in outside hospital showed multiple conditions such as lumbar degeneration, hyperostosis, endplate inflammation, lumbar disc herniation, and deep back fasciitis. Her abnormal laboratory findings [(white blood cells of 10.19×10^9/L (normal range: 4-10×10^9/L), platelet count of 313×10^9/L (normal range: 100-300×10^9/L), lymphocyte percentage of 14.2% (normal range: 20-40%), neutrophil percentage of 79.9% (normal range: 50-70%), neutrophil count of 8.14×10^9/L (normal range: 1.8-6.3×10^9/L), C-reaction protein (CRP) of 36.4 mg/L (normal range: 0-10 mg/L), erythrocyte sedimentation rate (ESR) of 89 mm/h (normal range: 0-20 mm/h), alkaline phosphatase of 158.1 U/L (normal range: 50-135 U/L), and albumin of 35.4 g/L (normal range: 40-55 g/L)] were far from being under control after 6 days of levofloxacin treatment. The patient was then admitted to the rheumatology and immunology department of our hospital (Figure 1A).

On admission physical examination showed obvious tenderness to percussion, activity limitation, and euesthesia. Laboratory findings indicated elevated CRP of 29.8 mg/L, fibrinogen of 5.74 g/L, interleukin-6 (IL-6) of 630.07 pg/ml (normal range: 0-7 pg/ml), and ESR of 101.0 mm/h. Her albumin was 34.8 g/L. Lumbar MRI at our hospital revealed abnormalities in the L4/5 vertebral bodies, intervertebral disc and surrounding soft tissues (Figures 1B–E). After 10 days of unsuccessful symptomatic treatment with anti-inflammatory and analgesic drugs, the patient was then transferred to the spine surgery department of our hospital for further treatment. Laboratory tests consistently showed inflammation (CRP of 47.0 mg/L, neutrophil count of 6.45×10^9/L, IL-6 of 649.24 pg/ml, and ESR of 103.0 mm/h) and decrease in albumin (25.9 g/L), suggesting the possibility of tuberculosis infection. Thus, anti-tuberculosis treatment and strengthening nutrition intervention were given to the patient.

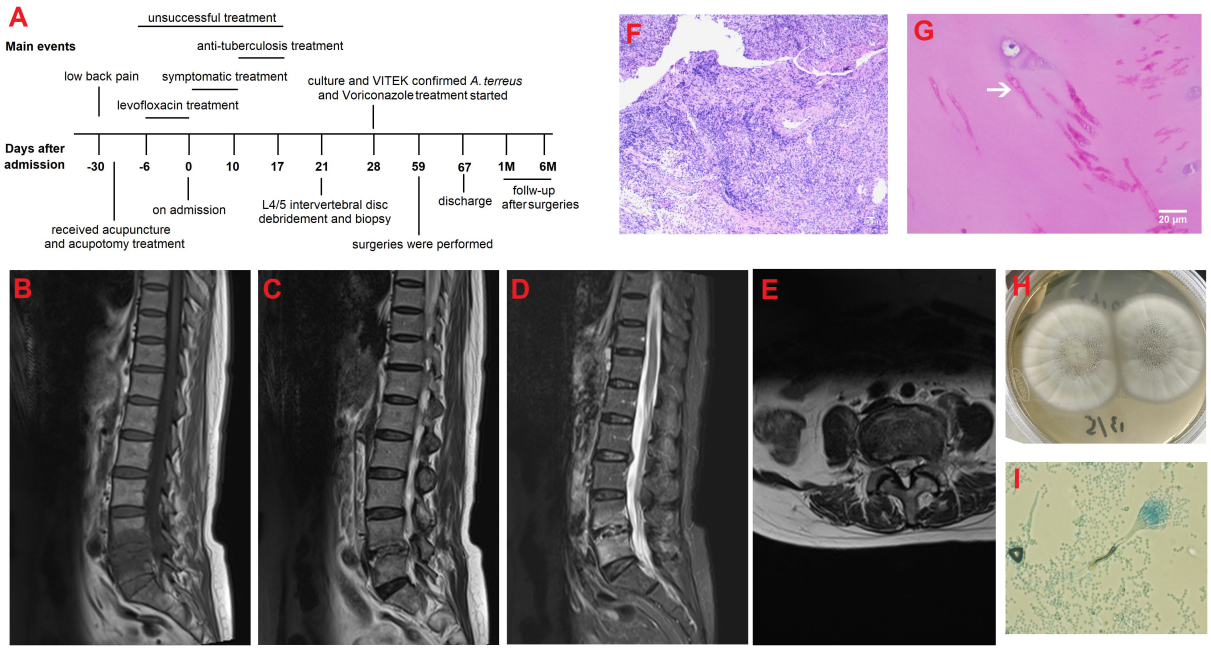

FIGURE 1
(A) The clinical timeline of the patient; **(B)** Lumbar sagittal T1-weighted MRI image at admission showed hypointensity of L4/5 vertebral bodies and intervertebral disc; **(C)** Lumbar sagittal T2-weighted image and **(D)** T2-weighted fat-suppression image at admission showed hyperintensity of L4/5 vertebral bodies and intervertebral disc; **(E)** Axial T2-weighted image at the level of L4/5 showed paravertebral soft tissue swelling and slight paraspinous abscess; **(F)** H&E staining showed massive inflammatory cells infiltration with some degree of purulent inflammation and necrosis (scale bar=20μm; magnification=10×); **(G)** Periodic acid–Schiff staining revealed septate fungal hyphae in the cartilage area; arrow indicates fungal hyphae (scale bar=20μm; magnification=40×); **(H)** Morphology features observed on the Sabouraud dextrose agar at 28°C after 5 days of incubation; and **(I)** Microscopic image of the subculture of the isolate following lactophenol cotton blue staining (magnification, 400×).

One week later, laboratory tests consistently showed inflammation (CRP of 37.0 mg/L, D dimer of 282.00 ug/L, white blood cells of 15.01×10^9/L, neutrophil percentage of 80.2%, and ESR of 92.0 mm/h) and decrease in albumin (35.3 g/L). The poor effects of anti-tuberculosis treatment indicated a former wrong diagnosis of tuberculosis infection.

Four days later, L4/5 intervertebral disc debridement was performed with the assistance of lateral transforaminal endoscope. Purulent tissues were noticed in the L4/5 intervertebral space during operation. L4/5 disk space materials were biopsied for culture and histological examination. The symptoms of low back pain were alleviated after operation but aggravated two days later. H&E staining showed massive inflammatory cells infiltration with some degree of purulent inflammation and necrosis (Figure 1F). Periodic acid–Schiff staining revealed septate fungal hyphae (Figure 1G). One week after operation, biopsy culture (Figure 1H) and microscopy of isolate (Figure 1I) revealed *A. terreus*, which was also identified in a subculture of the isolate using the VITEK matrix-assisted laser desorption ionization time of-flight mass spectrometry (MALDI-TOF MS) system (BioMe´rieux, France); in addition, her galactomannan (GM) testing of biopsy specimen was positive with a value of 0.35. Based on the culture, microscopy of isolate, histological examination and VITEK system results, the patient was diagnosed as *A. terreus* spondylodiscitis and intravenously treated with voriconazole at a loading dose of 300 mg every 12 h on Day-1 followed by 200 mg every 12 h.

Ten days after antifungal therapy, her inflammatory indictors (CRP of 11.78 mg/L, IL-6 of 69.77 pg/ml, white blood cells of 8.21×10^9/L, and ESR of 87 mm/h), low back pain and left lower limb pain were significantly improved than treatment before; however, repeated MRI and computerized tomography (CT) revealed aggravation of local vertebral destruction (Supplementary Figures 1A–G). Since her inflammation was alleviated after voriconazole treatment, conservative medical treatment was continued.

Twenty-four days after antifungal therapy, although her inflammatory indictors (CRP of 7.52 mg/L, IL-6 of 69.86 pg/ml, white blood cells of 8.21×10^9/L, and ESR of 29 mm/h) were further declined, her L4/5 vertebral bodies' destruction still existed (Figures 2A–H). One week later, surgeries including L4/5 intervertebral disc debridement, spinal canal decompression, PLIF with allogeneic fibula ring fusion cages, and posterior pedicle screw fixation were successfully performed under general anesthesia (Supplementary Figures 2A–H). Antifungal therapy was continued after surgeries. Eight days after surgeries, the patient's wound healed well and she was then discharged from our hospital. Imaging findings at one-month (Supplementary Figures 3A–H) and

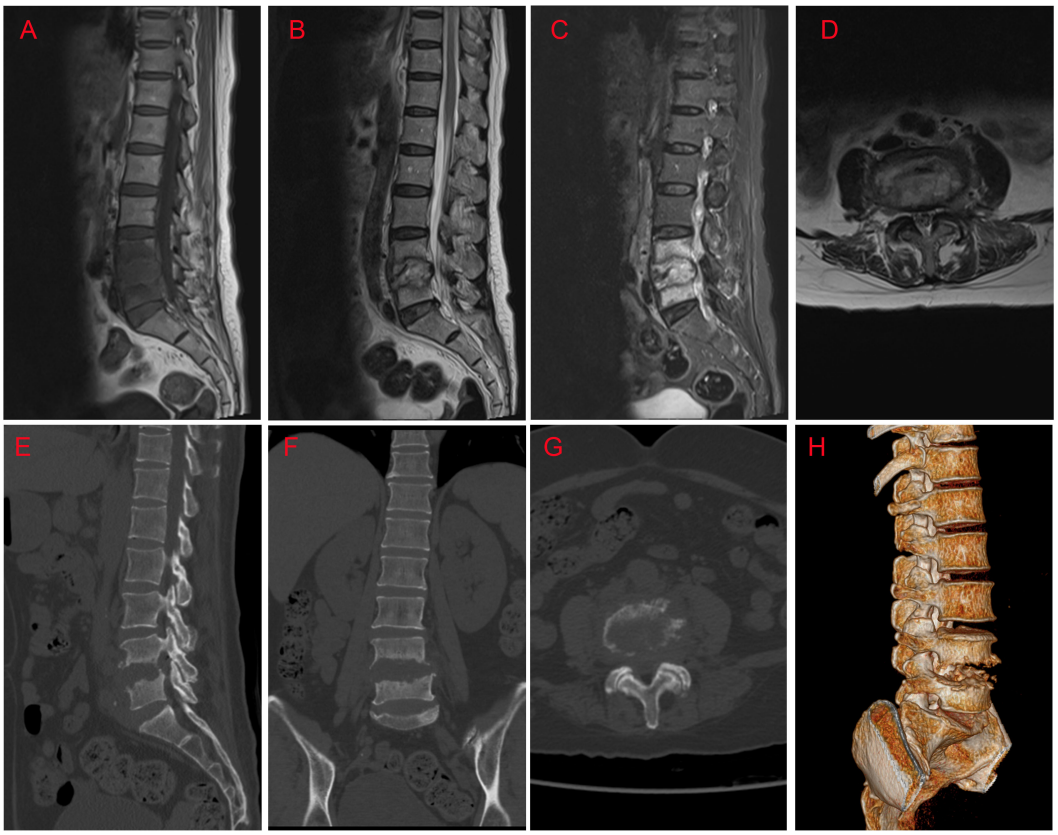

FIGURE 2
MRI and CT findings at approximately 24 days after antifungal therapy. **(A)** Sagittal T1-weighted image; **(B)** Sagittal T2-weighted image; **(C)** Sagittal T2-weighted fat-suppression image; **(D)** Axial T2-weighted image at the level of L4/5; **(E)** Sagittal CT image; **(F)** Coronal CT image; **(G)** Axial CT image; **(H)** Preoperative CT three-dimensional reconstruction image.

six-month (Figures 3A–I) follow-up demonstrated that the patient was successfully treated.

Discussion

A. terreus is a saprophytic fungus that found in a variety of habitats, such as soil, dust, and compost heaps. While it is known to cause different types of infections, spine involvement is uncommon. To the best of our knowledge, only ten cases of *A. terreus* spondylodiscitis have been reported in humans (Seligsohn et al., 1977; Glotzbach, 1982; Brown et al., 1987; Grandière-Perez et al., 2000; Park et al., 2000; Maman et al., 2015; Comacle et al., 2016; Sohn et al., 2019; Takagi et al., 2019; Vithiya et al., 2023). The clinical characteristics of these reported cases and the current case are summarized in Table 1. Briefly, *A. terreus* spondylodiscitis occurred predominantly in males (9/11, 81.8%), without an age preponderance (range from 12 to 74 years old). The infection affected lumbar spine in 5 cases (45.5%), thoracic spine in 4 cases (36.4%), lumbar and thoracic spine in one case (9.1%), and lumbar spine and sacral section in one case (9.1%). All patients experienced back pain (100%), while four cases (36.4%) also presented with fever. *A. terreus* spondylodiscitis can occur in both immunocompetent and immunocompromised hosts. Surprisingly, the majority of reviewed cases (7/11, 63.6%) in this study were immunocompetent patient. As for the antifungal therapy, amphotericin B (AmB) was used as monotherapy in 4 cases (36.4%) and voriconazole in 5 cases (45.5%). Both the combination of AmB and itraconazole and the combination of voriconazole and caspofungin was reported in 1 case (9.1%).

As we know, *A. terreus* can cause spine infection through three mechanisms: 1) contiguous spread from an adjacent site of infection; 2) hematogenous dissemination, and 3) direct inoculation (Comacle et al., 2016). Among all the reviewed cases, contiguous spread appears to be the predominant mode of transmission. In the four cases reported by Glotzbach et al.(Glotzbach, 1982), Grandie`re-Perez et al. (Grandière-Perez et al., 2000), Park et al. (Park et al., 2000), and Sohn et al.(Sohn et al., 2019), the infection may have resulted from contiguous spread from an adjacent site of infection. Moreover, in two cases reported by Seligsohn et al. (Seligsohn et al., 1977), and Brown et al. (Brown et al., 1987), the infection may have originated from hematogenous dissemination. It is worth mentioning that, with the exception of two cases that did not mention the mechanism of infection (Maman et al., 2015; Vithiya et al., 2023), in the remaining three cases (including the present case), direct inoculation might have been the contributing factor (Comacle et al., 2016; Takagi et al., 2019).

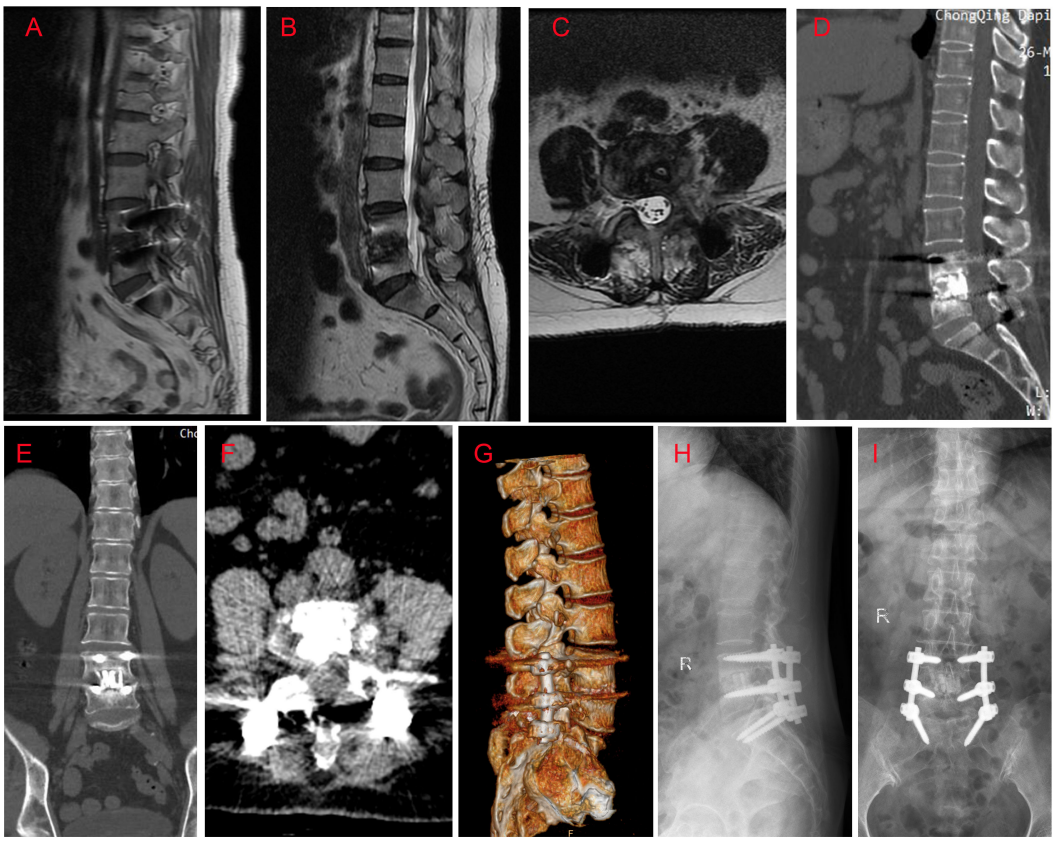

FIGURE 3
MRI, CT and X ray findings at six month follow-up. **(A)** Sagittal T1-weighted image; **(B)** Sagittal T2-weighted image; **(C)** Axial T2-weighted image at the level of L4/5; **(D)** Sagittal CT image; **(E)** Coronal CT image; **(F)** Axial CT image; **(G)** Lateral X ray image; **(H)** Anteroposterior X ray image; **(I)** CT three-dimensional reconstruction image. Imaging findings revealed that: the pedicle screws and cages were inserted in the right place, without cracked or displacement; there was no evidence of spinal infection; a certain level of L4/5 interbody fusion was observed.

TABLE 1 Clinical features of 11 reviewed *Aspergillus terreus* spondylodiscitis cases.

Author/year	Sex/ age	Location	Symptoms	Immune status	Probable mechanism of infection	Predisposing factor (s)	Antifungal therapy	Surgery	Outcome
Seligsohn et al., 1977	F/42	L1-2	Low back pain	Immunocompetent	Hematogenous	IV drug abuse, alcoholism, liver cirrhosis, back injury	AmB	No	Recovered
Glotzbach, 1982	M/71	L2-3	Low back pain, fever	NM	Contiguous	Aortofemoral bypass surgery	AmB	No	Died
Brown et al., 1987	M/30	T6-7	Thoracic back pain, fever	Immunocompetent	Hematogenous	IV drug abuse	AmB	Yes	Recovered
Grandière-Perez et al., 2000	M/40	L3-4	Low back pain	Immunocompromised	Contiguous	AML, IPA	AmB, Itra	Yes	Died because of AML
Park et al., 2000	M/37	L3-S1	Low back pain	Immunocompromised	Contiguous	ALL	AmB	Yes	Recovered
Maman et al., 2000	M/67	L1-2, T6-9	Back pain, fever	Immunocompetent	NM	NM	Vori	NM	NM
Comacle et al., 2016	M/20	T7-12	Back pain, weakness, weight loss, cough, fever	Immunocompetent	Direct inoculation	TB, motorbike accident	Vori, Casp	Yes	Vertebral sequelae
Takagi et al., 2019	M/74	T11-12	Back pain	Immunocompetent	Direct inoculation	Abdominal stab wound	Vori	Yes	Recovered
Sohn et al., 2019	M/12	L1-4	Back pain	Immunocompromised	Contiguous	aGVHD	Vori	No	Recovered
Vithiya et al., 2023	M/45	T9-12	Back pain	Immunocompetent	NM	NM	Vori	Yes	Recovered
The present case	F/58	L4-5	Low back pain	Immunocompetent	Direct inoculation	None	Vori	Yes	Recovered

L, lumbar; S, sacral; T, thoracic; IV, intravenous; AmB, amphotericin B; Itra, itraconazole; Casp, caspofungin; Vori, voriconazole; AML, acute myeloid leukemia; IPA, invasive pulmonary aspergillosis; ALL, acute lymphoblastic leukemia; TB, tuberculosis; aGVHD, acute graft versus host disease; NM, not mentioned.

10.3389/fcimb.2023.1269352

In the case reported by Comacle et al., the fungus infection possibly arose from direct inoculation after a motorbike accident (Comacle et al., 2016). Takagi et al. reported one case of spondylodiscitis that probablely occurred due to the direct inoculation of *A. terreus* after an abdominal penetrating injury (Takagi et al., 2019). Acupotomy is a treatment method that uses specially designed needle-scalpels, either reusable or disposable. It is similar to traditional acupuncture, but more invasive. In China and other countries, including Korea, acupuncture and acupotomy are commonly used conservative therapies for pain management (Zhang et al., 2017). Although these therapies are generally considered safe and effective, they can cause adverse events such as spinal infection (Bang & Lim, 2006; P. S. Kim & Hsu, 2004; Y. J. White, 2004; Kim et al., 2014; Tsai et al., 2020). For instance, Bang and Lim reported one case of paraplegia which was caused by spinal infection after acupuncture (Bang & Lim, 2006). Tsai et al. reported one case of cervical spinal epidural abscess following acupotomy, in which reusable materials were used (Tsai et al., 2020). In this case, the patient didn't have any predisposing conditions such as tuberculosis, intravenous drug use, diabetes mellitus, chronic obstructive pulmonary disease, or a history of laminectomy. Her past history was remarkable for receiving acupuncture and acupotomy in a local clinic to treat low back pain. She claimed that the needles and needle-scalpels used in acupuncture and acupotomy were reusable rather than disposable, which increased the possibility of infection. Following acupuncture and acupotomy, her symptoms recurred repeatedly and deteriorated rapidly after admission. Based on all above-mentioned information, we hypothesized the infection of this patient may have resulted from direct inoculation following acupuncture and acupotomy.

Since only few cases of *A. terreus* spondylodiscitis have been reported in human, the frequency of this condition is far from clear; however, we speculated that it may be underestimated because some cases may go undetected or misdiagnosed as tuberculosis due to shared clinical features and risk factors (Vithiya et al., 2023). Traditionally, the diagnosis of *A. terreus* is mainly based on cultures, microscopy, and/or histopathology. In some cases, VITEK MALDI-TOF MS method has been proven to be beneficial for the accurate diagnosis of *A. terreus* infection (Shin & Kim, 2021; Jing et al., 2022). Nevertheless, one thing we should keep in mind is that VITEK system has some limitations, such as limited ability of identification of rarely isolated species due to its narrow-spectrum database, which may lead to misidentification (Shin & Kim, 2021). Thus, a combination of VITEK and other methods, such as molecular sequencing and morphological evaluation, will contribute to more accurate diagnosis of *A. terreus*. In this case, the patient was diagnosed as *A. terreus* spondylodiscitis based on her culture, microscopy, histopathology, and VITEK system results.

The management of *A. terreus* spondylodiscitis can be challenging and often requires extended antifungal therapy, with or without surgical intervention. In the past, AmB was the preferred agent for the treatment of *A. terreus* spondylodiscitis; however, the clinical use of this drug in *A. terreus* infection has been limited because most isolates of *A. terreus* developed an intrinsic resistance against AmB (Posch et al., 2018; Vahedi Shahandashti & Lass-Flörl, 2019). Voriconazole is currently the preferred antifungal drug for treating *A. terreus* spondylodiscitis due to its broad antifungal coverage, favorable safety profile, and effective bone penetration. Conservative medical treatment may be sufficient for patients who only experience pain without significant spinal instability or neural compression; however, if these symptoms are present, surgical interventions such as debridement, spinal cord decompression, fusion, and fixation should be considered (Sohn et al., 2019). In this case, antifungal therapy alone was used after *A. terreus* was identified through culture. However, about one month later, the patient's spinal condition deteriorated rapidly, resulting in significant lumbar instability. To address this, a combination of antifungal therapy and surgical interventions were performed. Notably, PLIF combined with posterior pedicle screw fixation were performed in this case to promote spine interbody fusion. During PLIF, two allogeneic fibula ring fusion cages loaded with autologous bone fragments were inserted. The hollow fibular ring filled with autogenous bone fragments can not only increase the contact area of autogenous bone graft, but also improve the support strength of the fibular ring. In addition, the large effective support area matching the anatomical morphology of the end plate provides a good biological and mechanical environment for efficient bone fusion (Shi et al., 2013). After the procedures, the patient recovered well with good bone fusion. However, it is important to note that although the surgical treatment options, which involved PLIF with allogeneic fibula ring fusion cages, have shown promising outcomes in our patient, further evidence is required to support their widespread clinical use in treating this kind of infectious disease.

Conclusions

In this report, we present the first case of *A. terreus* spondylodiscitis following acupuncture and acupotomy in an immunocompetent Chinese patient. Although acupuncture and acupotomy are widely used in China as conservative treatments and are generally regarded as safe and effective, they can still lead to complications such as fungal spinal infection. Therefore, vigilance is necessary when considering these treatments. In addition, PLIF with allogeneic fibula ring fusion cages may be beneficial for *A. terreus* spondylodiscitis patients with spinal instability.

Data availability statement

The original contributions presented in the study are included in the article/Supplementary Material. Further inquiries can be directed to the corresponding author.

Ethics statement

The studies involving humans were approved by the ethics committee of Daping Hospital. The studies were conducted in accordance with the local legislation and institutional requirements. The participants provided their written informed consent to

participate in this study. Written informed consent was obtained from the individual(s) for the publication of any potentially identifiable images or data included in this article.

Author contributions

YJ: Conceptualization, Data curation, Investigation, Methodology, Project administration, Writing – original draft. XY: Conceptualization, Investigation, Methodology, Supervision, Visualization, Writing – original draft, Writing – review & editing.

Funding

The author(s) declare that no financial support was received for the research, authorship, and/or publication of this article.

Acknowledgments

The authors would like to thank the patient involved in this article.

Conflict of interest

The authors declare that the research was conducted in the absence of any commercial or financial relationships that could be construed as a potential conflict of interest.

Publisher's note

Supplementary material

The Supplementary Material for this article can be found online at: https://www.frontiersin.org/articles/10.3389/fcimb.2023.1269352/full#supplementary-material

References

Bang, M. S., and Lim, S. H. (2006). Paraplegia caused by spinal infection after acupuncture. *Spinal Cord* 44 (4), 258–259. doi: 10.1038/sj.sc.3101819

Bartash, R., Guo, Y., Pope, J. B., Levi, M. H., Szymczak, W., Saraiya, N., et al. (2017). Periprosthetic hip joint infection with Aspergillus terreus: A clinical case and a review of the literature. *Med. Mycol Case Rep.* 18, 24–27. doi: 10.1016/j.mmcr.2017.07.006

Brown, D. L., Musher, D. M., and Taffet, G. E. (1987). Hematogenously acquired Aspergillus vertebral osteomyelitis in seemingly immunocompetent drug addicts. *West J. Med.* 147 (1), 84–85.

Comacle, P., Le Govic, Y., Hoche-Delchet, C., Sandrini, J., Aguilar, C., Bouyer, B., et al. (2016). Spondylodiscitis due to Aspergillus terreus in an immunocompetent host: case report and literature review. *Mycopathologia* 181 (7-8), 575–581. doi: 10.1007/s11046-016-0007-6

Elsawy, A., Faidah, H., Ahmed, A., Mostafa, A., and Mohamed, F. (2015). Aspergillus terreus meningitis in immunocompetent patient: A case report. *Front. Microbiol.* 6. doi: 10.3389/fmicb.2015.01353

Glotzbach, R. E. (1982). Aspergillus terreus infection of pseudoaneurysm of aortofemoral vascular graft with contiguous vertebral osteomyelitis. *Am. J. Clin. Pathol.* 77 (2), 224–227. doi: 10.1093/ajcp/77.2.224

Grandière-Perez, L., Asfar, P., Foussard, C., Chennebault, J. M., Penn, P., and Degasne, I. (2000). Spondylodiscitis due to Aspergillus terreus during an efficient treatment against invasive pulmonary aspergillosis. *Intensive Care Med.* 26 (7), 1010–1011. doi: 10.1007/s001340051299

Jing, R., Yang, W. H., Xiao, M., Li, Y., Zou, G. L., Wang, C. Y., et al. (2022). Species identification and antifungal susceptibility testing of Aspergillus strains isolated from patients with otomycosis in northern China. *J. Microbiol. Immunol. Infect.* 55 (2), 282–290. doi: 10.1016/j.jmii.2021.03.011

Kim, P. S., and Hsu, W. (2004). Discitis in an adult following acupuncture treatment: a case report. *J. Can. Chiropr Assoc.* 48 (2), 132–136.

Kim, Y. J., Lee, J. Y., Kim, B. M., Kim, Y. M., and Min, S.-H. (2014). MRI findings on iatrogenic spinal infection following various pain management procedures. *J. Korean Soc. Radiol.* 71 (6), 296–303. doi: 10.3348/jksr.2014.71.6.296

Maman, E., Morin, A. S., Soussan, M., Coignard, H., Lortholary, O., and Fain, O. (2015). Multifocal bone aspergillosis by Aspergillus terreus in an apparently immunocompetent patient. *Presse Med.* 44 (10), 1064–1066. doi: 10.1016/j.lpm.2015.07.019

Modi, D. A., Farrell, J. J., Sampath, R., Bhatia, N. S., Massire, C., Ranken, R., et al. (2012). Rapid identification of Aspergillus terreus from bronchoalveolar lavage fluid by PCR and electrospray ionization with mass spectrometry. *J. Clin. Microbiol.* 50 (7), 2529–2530. doi: 10.1128/jcm.00325-12

Ozer, B., Kalaci, A., Duran, N., Dogramaci, Y., and Yanat, A. N. (2009). Cutaneous infection caused by Aspergillus terreus. *J. Med. Microbiol* 58 (Pt 7), 968–970. doi: 10.1099/jmm.0.007799-0

Panigrahi, P. K., Roy, R., Pal, S. S., Mukherjee, A., and Lobo, A. (2014). Aspergillus terreus endogenous endophthalmitis: report of a case and review of literature. *Indian J. Ophthalmol.* 62 (8), 887–889. doi: 10.4103/0301-4738.141065

Park, K. U., Lee, H. S., Kim, C. J., and Kim, E. C. (2000). Fungal discitis due to Aspergillus terreus in a patient with acute lymphoblastic leukemia. *J. Korean Med. Sci.* 15 (6), 704–707. doi: 10.3346/jkms.2000.15.6.704

Posch, W., Blatzer, M., Wilflingseder, D., and Lass-Flörl, C. (2018). Aspergillus terreus: Novel lessons learned on amphotericin B resistance. *Med. Mycol* 56 (suppl_1), 73–82. doi: 10.1093/mmy/myx119

Seligsohn, R., Rippon, J. W., and Lerner, S. A. (1977). Aspergillus terreus osteomyelitis. *Arch. Internal Med.* 137 (7), 918–920. doi: 10.1001/archinte.1977.03630190072018

Shi, W., Guo, C., and Zhou, Q. (2013). Biomechanical study of allogeneic fibula ring lumbar interbody fusion cage. *J. Third Mil Med. Univ* 35 (12), 1279–1305.

Shin, J. H., and Kim, S. H. (2021). Performance evaluation of VITEK MS for the identification of a wide spectrum of clinically relevant filamentous fungi using a Korean collection. *Ann Lab Med* 41, 2, 214–220. doi: 10.3343/alm.2021.41.2.214

Sohn, Y. J., Yun, J. H., Yun, K. W., Kang, H. J., Choi, E. H., Shin, H. Y., et al. (2019). Aspergillus terreus spondylodiscitis in an immunocompromised child. *Pediatr. Infect. Dis. J.* 38 (2), 161–163. doi: 10.1097/inf.0000000000002125

Takagi, Y., Yamada, H., Ebara, H., Hayashi, H., Kidani, S., Okamoto, S., et al. (2019). Aspergillus terreus spondylodiscitis following an abdominal stab wound: a case report. *J. Med. Case Rep.* 13 (1), 172. doi: 10.1186/s13256-019-2109-5

Tsai, S.-T., Huang, W.-S., Jiang, S.-K., and Liao, H.-Y. (2020). Cervical spinal epidural abscess following needle-knife acupotomy, with an initial presentation that mimicked an acute stroke: A case report. *Hong Kong J. Emergency Med.* 27 (2), 99–102. doi: 10.1177/1024907918790858

Vahedi Shahandashti, R., and Lass-Flörl, C. (2019). Antifungal resistance in Aspergillus terreus: A current scenario. *Fungal Genet. Biol.* 131, 103247. doi: 10.1016/j.fgb.2019.103247

Vithiya, G., Raja, S., Mariappan, M., and Rajendran, T. (2023). Case series of aspergillus spondylodiscitis from a tertiary care centre in India. *Indian J. Med. Microbiol.* 44, 100363. doi: 10.1016/j.ijmmb.2023.02.006

White, A. (2004). A cumulative review of the range and incidence of significant adverse events associated with acupuncture. *Acupunct Med.* 22 (3), 122–133. doi: 10.1136/aim.22.3.122

Zhang, B., Xu, H., Wang, J., Liu, B., and Sun, G. (2017). A narrative review of non-operative treatment, especially traditional Chinese medicine therapy, for lumbar intervertebral disc herniation. *Biosci. Trends* 11 (4), 406–417. doi: 10.5582/bst.2017.01199

Frontiers in
Cellular and Infection Microbiology

Investigates how microorganisms interact with their hosts

Explores bacteria, fungi, parasites, viruses, endosymbionts, prions and all microbial pathogens as well as the microbiota and its effect on health and disease in various hosts.

Discover the latest Research Topics

See more →

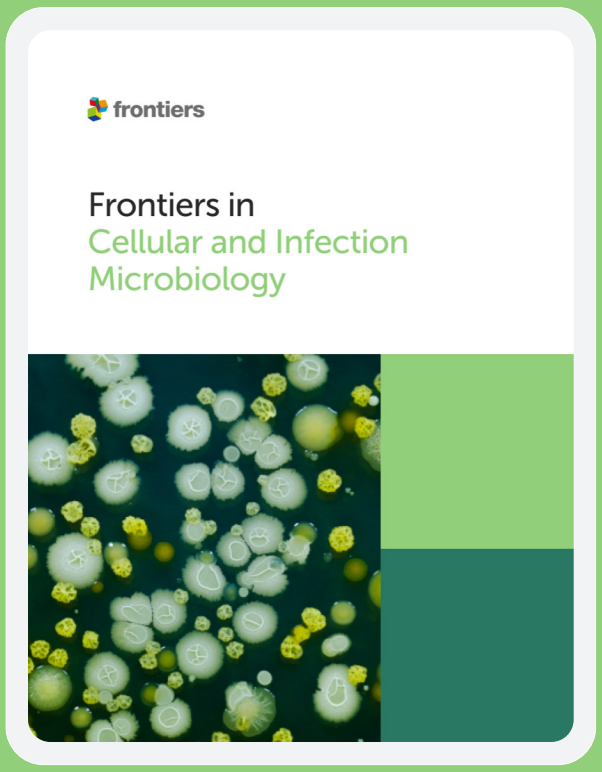

Frontiers

Avenue du Tribunal-Fédéral 34
1005 Lausanne, Switzerland
frontiersin.org

Contact us

+41 (0)21 510 17 00
frontiersin.org/about/contact